VASCULAR CALCIFICATION AS A RISK FACTOR FOR PERIPHERAL ARTERIAL DISEASE AND ITS EFFECTS ON ANGIOGENESIS

JOCELYNE MULANGALA

Lifelong Health Theme, South Australian Health and Medical Research Institute

University of Adelaide, School of Medicine, Discipline of Medicine

A thesis submitted in fulfilment of the requirements for the degree of

Doctor of Philosophy

November 2020

Table of Contents

ABSTRACT

Peripheral arterial disease (PAD) refers to the obstruction or blockage of arteries of the lower extremity vessels. PAD is characterised by accelerated arterial calcification and impairment in angiogenesis, both of which associate with adverse cardiovascular outcomes. The pathogenesis of lower extremity PAD remains poorly described but is regarded secondary to atherosclerosis due to fatty plaque build-up within the arterial wall. Despite the many clinical advances available to treat PAD, impairment in microcirculation continues to put patients at constant risk of ischemia; increasing their risk of developing limb amputations which subsequently affects their quality of life. Therapies for PAD are centred around alleviating stenosis and promoting tissue revascularization following ischemia, and while atherosclerosis is recognised as the main cause of PAD, acute or chronic limb ischemia may be the result of various other cardiovascular risk factors. Calcification is implicated as a contributor to PAD, but the mechanisms underlying this are not fully elucidated. Firstly, I sought to determine the effect of elevated calcium on ischemia-driven angiogenesis. Human coronary artery endothelial cells were cultured and incubated with calcification medium (CM) ($CaCl_2$ 2.7mM, Na_2PO_4 2.0mM) for 24h and conditioned to either normoxia or hypoxia. The Hindlimb ischemia model was used to assess the role of high calcium on ischemia-driven angiogenesis in vivo, on 8-week-old and 24-week-old mice, with high calcium levels ($OPG^{-/-}$) and wildtype (C57BL6/J, control) mice. Blood flow reperfusion was assessed by Laser Doppler Perfusion Imaging (LDPI). In vitro, CM upregulated mRNA expression of calcification inductive genes, *Bmp2* and *Runx2*. CM significantly decreased tubule formation in normoxia, with further reduction in hypoxia (13%); and reduced cell migration in normoxia alone. CM increased the expression of key angiogenic markers Hif-1α and Vegfa mRNA levels in normoxic conditions, which coincided with an increase in their protein expression in normoxia; and reduction in hypoxia. Incubation with CM reduced cell viability

and induced cell death in EC. 8-week-old $OPG^{-/-}$ mice showed elevated serum calcium levels and ALP activity, an important diagnostic marker of calcification. LDPI showed striking reductions in blood-flow reperfusion of 8-week $OPG^{-/-}$ mice compared to controls at day 14; which was further impaired in an aged cohort of mice, with a significant reduction in blood flow at day 10. Mechanistically, ischemic limbs of 8-week old $OPG^{-/-}$ mice showed significant upregulation HIF-1α and reduced CD31 neovessels. Clinical scoring revealed significantly worse outcomes for both limb function and tissue ischemia in the $OPG^{-/-}$ mice versus controls, assessed by Tarlov scores, with higher values indicating a worse outcome. Furthermore, to assess the effect of calcification milieu on inflammatory-driven angiogenesis, cells were stimulated with both CM and TNF-α in vitro to induce inflammation. Overall, CM had no additive effect in driving inflammatory-driven angiogenesis, with no effects on HIF-1α and VEGFA expression. CM however induced the expression of inflammatory markers ICAM, VCAM, MCP1 and NF- κB (P65) expression in treated cells compared to controls. When this was modelled in vivo using the peri-arterial femoral cuff placement, $OPG^{-/-}$ mice with high calcification milieu displayed no changes in angiogenic marker expression though displayed significantly elevated inflammatory-marker expression. This is the first demonstration that high-levels of calcium negatively regulates ischemia-driven angiogenesis. These findings have implications for the development of therapies that can suppress calcification in PAD.

DECLARATION

I certify that this work contains no material which has been accepted for the award of any other degree or diploma in my name in any university or other tertiary institution and, to the best of my knowledge and belief, contains no material previously published or written by another person, except where due reference has been made in the text. In addition, I certify that no part of this work will, in the future, be used in a submission in my name for any other degree or diploma in any university or other tertiary institution without the prior approval of the University of Adelaide and where applicable, any partner institution responsible for the joint award of this degree. I give permission for the digital version of my thesis to be made available on the web, via the University's digital research repository, the Library Search and also through web search engines, unless permission has been granted by the University to restrict access for a period of time.

I acknowledge the support I have received for my research through the provision of an Australian Government Research Training Program Scholarship.

Jocelyne Mulangala

Date: 16th November 2020

Signature:

ACKNOWLEDGEMENTS

Before I start, I would like to give all Praise and Glory to God for bringing me this far. Philippians 4:13 said "I can do all things through Christ which strengthens me".

Where do I even begin!! 5 years ago, I remember starting my summer research placement with no laboratory experience whatsoever. I remember sitting at my lab bench and spending weeks learning how to pipette water just so I could learn the technique. This PhD has challenged me emotionally, mentally, and physically; but as I reach the end of this chapter of my life, I am very grateful for the opportunities and experiences that my PhD has provided me with. After so many trials and tribulations, failures and being known as the girl who sings in the lab and cries at the microscope -it's hard to believe that I've finally PhinisheD!!

The completion of this thesis would not have been possible without the help of many people.

Firstly, to my principal supervisor Professor Stephen Nicholls, thank you for all the support and guidance you've given me throughout my studies. your passion for science and research is something that has always inspired me and I'm forever grateful to you for taking a chance and giving me the opportunity to work under your wing.

A heartfelt and sincere thank you to my co-supervisor, mentor and friend, Dr Belinda Di Bartolo. I couldn't have gotten through these past 4 years without you. From day one, you've always believed in me even when I failed to believe in myself. When I couldn't see the end in sight, when experiments failed and when I reached rock bottom, you were there constantly reminding and encouraging me to keep going. You've always supported me in all I do and have pushed me to be better so that I can achieve all my goals; and I wouldn't be the scientist I am today without you. I cannot thank you enough for all the support, guidance, and mentorship you've given me all these years, both PhD and life related. I am forever grateful to you, and I am truly blessed to have been taught by such an incredible supervisor like you. I owe this thesis to you and hope my work is a testimony of your excellent leadership.

I would also like to thank Mrs Julie Butters, Dr Joanne Tan, Dr Christina Bursill, Associate Professor Peter Psaltis, Dr Achini Vidanapathirana and Ms Louise Pitman, for all your technical support and encouragement throughout my time at SAHMRI.

I would like to extend a huge thank you to all Heart Health team members (Past and present) for all their support throughout my studies. In particular, Emma Akers, my PhD and calcification buddy and Benjamin Pullen, my tea

buddy; thank you both always checking me and for reminding me to stop “eye rolling” and for putting up with my dramatic sassy self all throughout my PhD journey. You have both been such troopers and I’m lucky to have shared my PhD journey with you both by my side. To my “Realest team” Jonar and Thira, thank you for always keeping it real and being there for me since our first days in honours! Y’all know what’s up!! A huge thank you to Emma Solly, for being the best hind-limb ischemia surgery buddy and Scicomm partner in crime; and for always lending a helping hand with experiments. To my personal doctor and western blot expert Nathan, thank you for the constant laughter; and for being brave enough to endure my eye-rolls and sass, your patience and calmness always amazed me especially in times of failed experiments. To my fashion partner in crime Zahra, thank you for always brightening my mornings and encouraging me every day. To the rest of the SAHMRI Heart Health family, Steve.J, Joey, Jarrad, Gianluca, Laura, Sanuja, Anna, Khalia, Sanuri, Thalia, Victoria, Jake, Lukah and Ayla; thank you all so much for making my time at SAHMRI an enjoyable and fun one! I’ll miss our HH quiz night wins and our daily lunch table chats!

To my amazing best friends, Panashe & Titchien, thank you both so much for your unwavering support and continuous encouragement throughout my studies. You have both played a huge part in pushing me to finish and get my thesis done and have always cheered me on even when I was stubborn and lazy. Thank you for enduring my constant complaining and for being the best friends a girl could ask for.

To my partner Duncan, you’ve been my pillar of strength all throughout my PhD and have endured the stress, highs and lows with me and I’m forever grateful for your support.

Last but not least, to my family, especially my parents Emmanuel and Vicky, thank you both for the endless love and support you’ve both shown me. You’ve instilled me with so much faith, patience and knowledge and I could not be here today without you both. To my beautiful sisters, Emelyne and Roselyne, you’ve been my amazing motivators throughout this whole PhD and I’m very thankful for all your encouraging words and prayers. To my brothers Marcellin, Ghyslain, and Herman C, thank you all for being the best team-players; and a big shoutout and thank you for my brother Ghyslain for always picking me up late on my late nights at SAHMRI and being my personal driver. I couldn’t have done this PhD without you all.

SCHOLARSHIP:

- Adelaide University Postgraduate Research Stipend

AWARDS:

1. Cardiac Society Australia New Zealand (CSANZ) Ralph Reader Finalist
2. 2020 Paul Dudley White International Scholar Award at Arteriosclerosis, Thrombosis, and Vascular Biology, Vascular Discovery Virtual Meeting
3. Australian Atherosclerosis Society 2019 (AAS) Travel Trust Award ($1500)
4. 2019 Paul Dudley White International Scholar Award at Scientific Sessions, American Heart Association (AHA), Philadelphia, Pennsylvania, USA
5. Australian Atherosclerosis Society (AAS) 2019 PhD Poster Winner ($500)
6. Australian Atherosclerosis Society (AAS) 2019 Travel Grant, Melbourne ($250
7. Florey Postgraduate Research Conference 2019: Executive Dean Faculty of Health and Medical Sciences Prize ($300)
8. Florey Postgraduate Research Conference 2019: Adelaide Medical School Prize ($200
9. Australian Vascular Biology Conference 2018 (Oral Presentation Finalist), Adelaide, SÁ
10. SAHMRI Research showcase 2018, People's Choice Award Winner ($500)
11. Australian Atherosclerosis Society Travel Grant (2017), NSW, Sydney ($150)
12. Australian Atherosclerosis Society 2017 (Oral Presentation Finalist), Sydney

ABSTRACTS & CONFERENCE PRESENTATIONS:

American Heart Association (AHA) Scientific Sessions	(E-Poster Oral Presentation) **Presenter: Ms Jocelyne Mulangala** Titled: High Calcium Impairs Ischemia-Driven Angiogenesis	November 2019, Philadelphia, Pennsylvania, USA
Australian Atherosclerosis Society (AAS)	(Poster) **Presenter: Ms Jocelyne Mulangala** **Titled:** High Calcium Impairs Ischemia-Driven Angiogenesis	**October 2019,** Melbourne, Victoria, Australia
SAHMRI Annual Scientific Meeting	(3 Minute Thesis Presentation) **Presenter: Ms Jocelyne Mulangala** **Titled:** It's Not That Crystal Clear!	**October 201**9 Adelaide, SA Australia
Florey Postgraduate Research Showcase	(Poster) **Presenter: Ms Jocelyne Mulangala** **Titled:** High Calcium Impairs Ischemia-Driven Angiogenesis	**September 201**9 Adelaide, SA Australia
Australian Society for Medical Research (ASMR)	(Poster) **Presenter: Ms Jocelyne Mulangala** **Titled:** High Calcium Impairs Ischemia-Driven Angiogenesis	**June 2019** Adelaide, SA Australia
Adelaide Faculty of Health & Medical Sciences 3 Minute Thesis Competition – Finals	(3 Minute Thesis Presentation) **Presenter: Ms Jocelyne Mulangala** **Titled:** It's Not That Crystal Clear! It's Not That Crystal Clear!	**August 2019** Adelaide, SA Australia
Heart Foundation Cardiovascular Research Showcase	(Poster) **Presenter: Ms Jocelyne Mulangala** **Titled:** Elevated calcium drives inflammatory-driven angiogenesis.	**November 2018,** Adelaide, SA, Australia
SAHMRI Annual Scientific Showcase	(Poster) **Presenter: Ms Jocelyne Mulangala** **Titled:** Elevated calcium drives inflammatory-driven angiogenesis.	**November 2018,** Adelaide, SA, Australia
Australian Atherosclerosis Society, Australian High Blood Pressure society and Australian Vascular Biology Society Joint Meeting 2018	(Oral Finalist Presentation) **Presenter: Ms Jocelyne Mulangala** **Titled:** Elevated calcium drives inflammatory-driven angiogenesis.	**November 2018,** Adelaide, SA, Australia
Florey Postgraduate Research Showcase	(Poster) **Presenter: Ms Jocelyne Mulangala** **Titled:** Elevated calcium drives inflammatory-driven angiogenesis.	**September 2018,** Adelaide, SA, Australia
Invited Speaker at Heart Health Seminars, SAHMRI	(Presentation) **Presenter: Ms Jocelyne Mulangala** **Titled:** Elevated calcium drives inflammatory-driven angiogenesis.	**August 31st 2018** Adelaide, SA Australia
Australian Society for Medical Research (ASMR)	(Presentation) **Presenter: Ms Jocelyne Mulangala** **Titled:** Elevated calcium regulates angiogenesis**.**	**June 2018** Adelaide, SA Australia

Australian Atherosclerosis Society (AAS)	(Oral Presentation Finalist) **Presenter: Ms Jocelyne Mulangala** **Titled:** Calcium regulates angiogenic marker expression in endothelial cells .	**October 2017** Sydney, NSW Australia
SAHMRI Annual Scientific Meeting	(Poster) **Presenter: Ms Jocelyne Mulangala** **Titled:** Calcium regulates angiogenic marker expression in endothelial cells.	**October 2017** Adelaide, SA Australia
Florey Postgraduate Research Showcase	(Poster) **Presenter: Ms Jocelyne Mulangala** **Titled:** Calcium dose dependently influences endothelial cell angiogenesis**.**	**September 2017** Adelaide, SA Australia
SAHMRI Heart Health Seminar Invited Guest Speaker	(presentation) **Presenter: Ms Jocelyne Mulangala** **Titled:** The role of vascular calcification on angiogenesis, and its clinical implications on peripheral artery disease and coronary artery disease.	**August 2017** Adelaide, SA, Australia
Australian Society for Medical Research (AAS)	(Presentation) **Presenter: Ms Jocelyne Mulangala** **Titled:** Role of Vascular Calcification in Angiogenesis. (presentation)	**June 2017** Adelaide, SA Australia

LIST OF TABLES

LIST OF FIGURES

LIST OF ABBREVIATIONS

ABI	**Ankle brachial index**
ACS	Acute coronary syndrome
AF	Atrial fibrillation
ALP	Alkaline phosphatase
ATP	Adenosine triphosphate
BMP2	Bone morphogenetic protein 2
CAD	Coronary artery disease
$CaCl_2$	Calcium Chloride
CLI	Chronic limb ischemia
CM	Calcification medium
CVD	Cardiovascular disease
EC	Endothelial cell
ECM	Extracellular matrix
eNOS	Endothelial nitric oxide synthase
ERK	Extracellular-signal regulated kinase
ESRD	End-stage renal disease
FGF	Fibroblast-growth factor
HIF-1a	Hypoxia inducible factor 1-alpha
HLI	Hind-limb ischemia
HRE	Hypoxia response element
HRP	Horseradish peroxidase
IC	Intermittent claudication
ICAM	Intracellular adhesion molecule

IκB	Inhibitor of kappa B
IFN	Interferon gamma
IKK	Inhibitor of kappa B kinase
IL	Interleukin
LDL	Low-density lipoprotein
LPS	Lipopolysaccharide
MAPK	Mitogen activated protein kinase
MCP-1	Monocyte chemoattractant protein 1
MGP	Matrix Gla protein
MMP	matrix metalloproteinases
mRNA	Messenger ribonucleic acid
MRI	Magnetic resonance imaging
MV	Matrix vesicles
$NaHPO_4$	Sodium Phosphate
NF-κB	Nuclear factor of kappa B
NO	Nitric oxide
NOS	Nitric oxide synthase
OCT	Optimal cutting temperature
OPG	osteoprotegerin
OPN	Osteopontin
PAD	Peripheral arterial disease
PBS	Phosphate-buffered saline
PI3K	Phosphoinositide 3-kinase
PDGF	Platelet-derived growth factor
PHD	Propyl-hydroxylase enzyme

PLC	Phospholipase C
qRT-PCR	Quantitative real-time polymerase chain reaction
RANK	Receptor-activator nuclear factor Kappa B
RANKL	Receptor-activator nuclear factor Kappa B ligand
RNA	Ribonucleic acid
Runx2	Runt-related transcription factor 2
SMC	Smooth muscle cell
TGF	Transforming growth factor
TNF	Tumour necrosis factor
TNFRSF	Tumour necrosis factor receptor superfamily
TRAIL	TNF-related apoptosis-inducing ligand
VC	Vascular calcification
VCAM	Vascular cell adhesion protein
VEGFA	Vascular endothelial growth factor
VEGFR2	Vascular endothelial growth factor receptor 2
VHL	Von-Hippel Lindau
VSMC	Vascular smooth muscle cell
WT	Wildtype

QUOTE

“There Is Nothing Permanent Except Change. The Only Constant Is Change “ - Heraclitus

CHAPTER 1:

INTRODUCTION

1. Introduction to Cardiovascular Diseases

Cardiovascular diseases (CVD) are the leading cause of death worldwide accounting for an estimated 31% of global deaths. CVD is the main cause of death in Australians, killing 1 person every 11 minutes[1]. According to the World Health Organisation (WHO), approximately 17.3 million people died from CVD in 2008, with predictions that around 23.6 million individuals will die from CVD, mainly heart disease by the year 2030[2]. The most common cause of CVD is atherosclerosis, or the accumulation of fatty plaques in the arterial wall which results in the narrowing of blood vessels. Atherosclerosis is a three pathology disease and is associated with coronary artery disease, peripheral arterial diseases and cerebrovascular disease[3].

1.1 Pathogenesis of Atherosclerosis

Atherosclerosis is a complex inflammatory process that occurs due to the accumulation of lipids within the artery wall. This occurs in large and medium-sized arteries and leads to ischemia of the heart, brain or extremities, which can ultimately lead to Myocardial Infarction (MI), stroke and peripheral vascular diseases[4]. In atherosclerotic plaques, vascular calcification (VC) can appear in two morphologies of either (1) micro or spotty early calcification and (2) macro or sheet like late-stage calcification[5]. Microcalcifications are said to be more inflammatory and may perpetuate inflammatory cycles leading to plaque instability. Conversely, macrocalcifications are thought to have plaque stabilizing properties[5]. Furthermore, VC in the form of spotty intimal microcalcifications is driven by numerous factors such as endothelial injury, increased generation of reactive oxygen species (ROS), the accumulation of oxidised lipids and apoptosis of vascular smooth

muscle cells (VSMCs), which provide a nidus for hydroxyapatite mineral deposition (site of mineralisation).

The initial step during atherosclerotic plaque development that leads to vascular endothelial inflammation is subendothelial deposition of low-density lipoprotein-cholesterol (LDL). LDL becomes modified to oxidized LDL (oxLDL) by various CVD risk factors due to an increase in oxidative stress within the vascular wall. oxLDL triggers the activation of NF-κB signalling, which promotes the expression of adhesion molecules including vascular cell adhesion molecule-1 (VCAM-1) and intercellular adhesion molecule-1 (ICAM-1), and other chemokines including monocyte chemoattractant protein (MCP1) and interleukin 8 (IL-8) on the vascular surface of endothelial cells[6] **(Figure 1.1 A)**. As a result, binding of VCAM-1 and ICAM-1 to their ligands α4: β1 and CD11a:CD18 on monocytes triggers the recruitment and transmigration of monocytes into the vascular wall. This results in the differentiation of monocytes into pro-atherogenic macrophages or foam cells, which are able to scavenge oxLDL and act to amplify the inflammatory process via the secretion of cytokines (IL-1β, IL-12, TNF-α) **Figure 1.1 B)** [6].

The inflammatory response is continued by further recruitment of monocytes, which eventually leads to intimal thickening and increases in plaque volume. This promotes neovascularization of the atherosclerotic lesions and the formation of fatty streaks, which are the earliest lesions seen in atherosclerosis. As the plaque develops and grows, this leads to the recruitment of additional cell types such as VSMCs, which undergo proliferation to stabilise the fibrous plaque **Figure 1.1 C)** [6]. As the inflammatory response is exacerbated, other inflammatory markers such as von Willebrand factor (vWF) and tissue factor (TF) are secreted, which stimulate fibrin deposition and platelet binding creating a pro-thrombotic

environment. Overtime, foam cells may undergo apoptosis resulting in the release of cell-debris and lipids, which result in the formation of a necrotic core **Figure 1.1 D)** [6].

Atherosclerosis is a systematic disease that is not limited to a single arterial territory and can affect arteries of different vascular beds simultaneously, with varying degree of progression. It is a is a widespread, chronic and progressive disease affecting larger to medium-sized arteries and commonly occurs in the brain (carotid, vertebral, and cerebral arteries, heart (coronary arteries disease) or in the lower extremities (the iliac and femoral arteries)[7]. Furthermore, its presence at different sites is associated with increased risk of development in other vascular beds. Therefore because of the systemic nature of the disease, treatment with statins, antiplatelet agents have proven beneficial, irrespective of the vascular bed affected. For the purpose of this thesis, atherosclerosis was investigated in the setting of peripheral arterial disease.

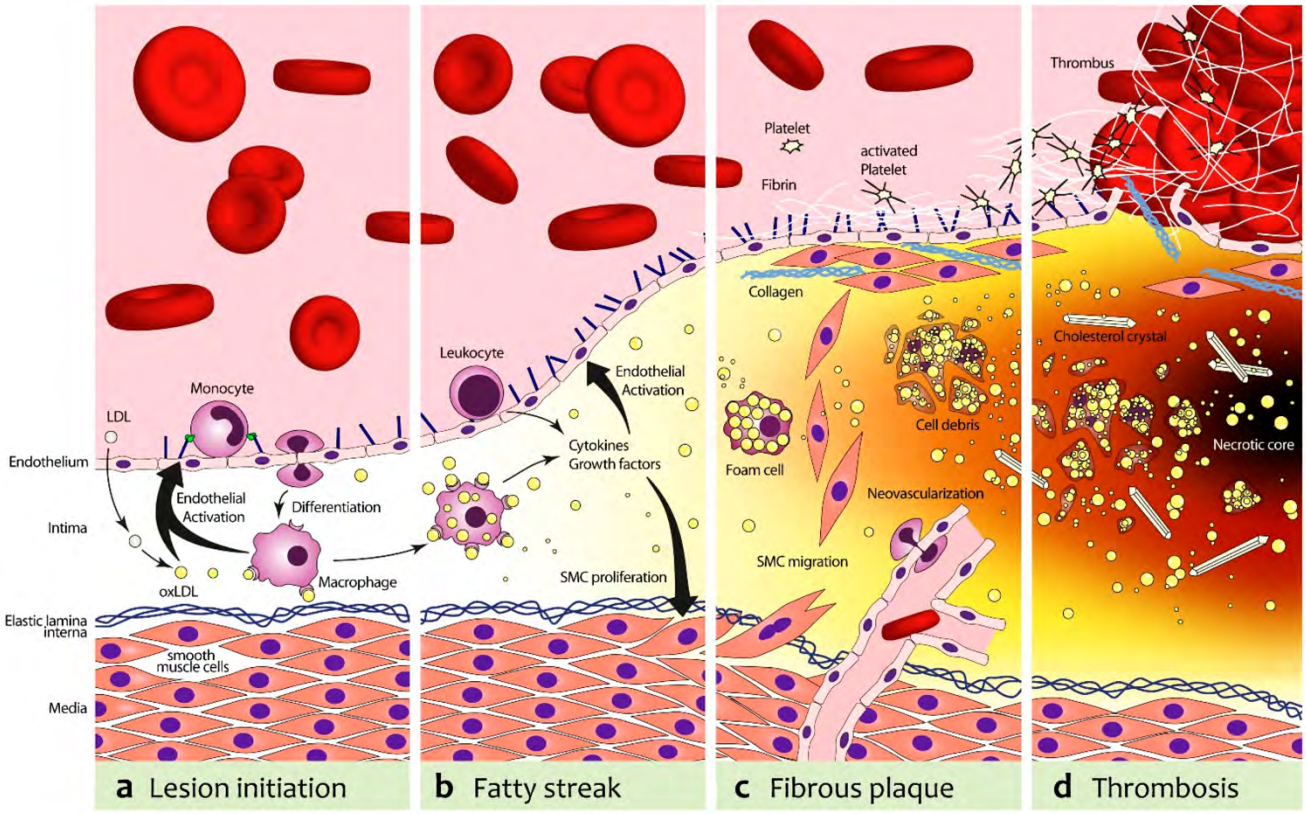

Figure1.1 1.1: Schematic representation of the pathophysiology of Atherosclerosis in PAD (Adapted from[6]).

(a) Low density lipoprotein-cholesterol (LDL) is deposited within the endothelium and undergoes oxidative modification to oxidized LDL (oxLDL, which stimulates endothelial cells (ECs) to express adhesion molecules VCAM-1 and chemokines (MCP1, IL-8). Monocytes are recruited into the vessel and undergo differentiation into pro-atherogenic macrophages; (b) Macrophages scavenge oxLDL and leukocytes are recruited into the vessel wall; (c) the increasing plaque volume promotes plaque neovascularization and recruitment and proliferation of SMCs which stabilize the fibrous plaque. A pro-thrombotic environment is created due to deposition of fibrin and activated platelets, with increased expression of tissue factor (TF) and von Willebrand factor (vWF); (d) foam cells may undergo apoptosis thereby release cell-debris and lipids, which result in the formation of a necrotic core.

1.2 Peripheral Arterial Disease (PAD)

Peripheral arterial disease (PAD) refers to the occlusion or narrowing of the arteries supplying blood to the lower extremities, exclusive of the coronary and cerebrovascular vessels[3]. It is a progressive occlusive disease and is the main macrovascular complication in type 2 diabetes; and is estimated to affect over 200 million adults worldwide[8, 9]. PAD is the leading cause of cardiovascular morbidity and mortality associated with limb loss[10-12] and is a major risk factor for MI (MI) [13]. Interestingly, the prevalence of PAD is 2.1 times that of patients with a history of MI[12], and has a similar relative risk as coronary artery patients and cerebrovascular disease patients[14]. The exact pathogenesis for PAD remains unclear, but it is generally regarded as secondary to atherosclerosis[15]. Patients with PAD often present with multilevel disease, characterised by fatty plaque build-up and high levels of diffused calcium deposits in the media of their peripheral arteries. Rupture of the atherosclerotic plaque in the arterial wall results in obstruction of blood flow thereby reducing perfusion to organs[16].

1.2.1 Pathophysiological Response to Atherosclerosis in PAD

PAD is primarily caused by atherosclerosis and is associated with thrombus formation within arteries of the lower limb that results to tissue ischemia. Atherosclerosis-induced PAD is a complex mechanism that involves numerous cell types, proteins, and pathways. The main cell types involved include ECs, VSMCs, fibroblasts, monocytes, resident stem cells, pericytes, platelets and an array of inflammatory cells[11].

1.2.2 Risk factors for PAD

PAD coexists with cardiovascular and vascular diseases[17]. The most recognised cause underlying PAD development is atherosclerosis[18]. Risk factors for PAD are parallel to those of atherosclerosis[14], including age (>50), smoking, diabetes mellitus, hypertension and dyslipidemia[19-21]. Age is the hallmark marker of PAD, and around 35% of adults aged 60-65 years of age show symptoms of intermittent claudication (the physical pain experienced upon walking)[17]. Disease severity is four-fold higher in PAD patients engaging in heavy smoking and two-fold with diabetes[17, 22]. Diabetes mellitus is associated with increased risk of PAD, as 1% increase in glycosylated haemoglobin correlates with a 25% increase for PAD[17]. Diabetic patients also face a 10 times greater risk of amputation than non-diabetic patients. Dyslipidaemia, defined as elevated levels of cholesterol within the body also contributes to PAD development.

1.2.3 Symptoms for PAD

The two most prevalent clinical manifestations of PAD are critical limb ischemia (CLI), and intermittent claudication (IC)[11]. Intermittent claudication (IC) is the earliest and most commonly observed symptom of PAD and refers to the physical symptoms of pain exerted in the lower limb muscles of both legs (calf) upon exercise and walking, which is rapidly relieved at rest [11, 12]. With IC patients, the severity of symptoms increases by 25%, with 5% of these patients facing limb amputation within 5 years [23]. CLI is the most severe and long-term clinical manifestation of PAD; that occurs due to hypoperfusion of the lower limbs and is commonly observed in diabetic patients[11, 19]. Patients suffering from CLI experience severe pain at rest, and present with ulcerations and gangrene formation in the foot with disease progression[11, 19]. However, unlike

claudication, CLI patients have a substantially increased risk of limb amputation and other fatal or non-fatal vascular events like MI and stroke[11,23,19]. Overal, PAD patients are highly affected and face difficulties performing daily activities, due to reduced functional capacity in their limbs. Therefore, treatment goals for PAD are critical to help alleviate these physical symptoms and increase the quality of life for all PAD sufferers [23].

1.2.4 Diagnosis for PAD

PAD patients who present with asymptomatic PAD are faced with a poor long-term prognosis, with a 15 times increase and a 10 year higher risk of mortality compared to non-PAD patients[23]. Currently, the gold standard diagnosis for documenting the presence and severity of lower extremity PAD is via two non-invasive doppler techniques using the Ankle Brachial pressure index (ABI) and Toe Brachial pressure index (TBI)[3, 15, 24].

ABI measures are used to illustrate how well blood is perfused in limbs and compares blood pressure readings between ankle pressure and brachial arm pressure. This is a quick and effective test that can be used to assess blood pressures in a 10-15 min time frame[24]. Normal ABI values range from 0.90 to 1.30, and ABI values of 0.50-0.85 are indicative of intermittent claudication in PAD patients[3, 24]. ABI values >0.30 can be seen in patients with resting claudication pain or gangrene[3, 24]. The efficiency of ABI testing however is reduced with the presence of calcified lower leg vessels as seen with type II diabetic or chronic kidney disease patients[3, 24]. This is because calcified vessels are less compliant, more rigid and incompressible, therefore raise ABI making blood pressure more difficult to detect. In such cases, TBI becomes useful as its more predictive of substantial arterial disease[3].

TBI pressures provide more definitive diagnosis for patients with rigid and noncompliant blood vessels. TBI measurements are performed similarly to ABI, where tiny blood pressure cuffs are placed around the toe, and blood pressure is measured using a photoplethysmograph (PPG) infrared light sensor; with TBI value of 0.8 or greater deemed normal. To enable proper diagnosis, following ABI and TBI readings, further confirmation is done via other imaging modalities including angiography, computed tomography (CT) and magnetic resonance imaging (MRI)[15].

1.2.5 Current Therapies and Treatments for PAD

Currently, treatment options for PAD are focused on revascularization techniques to alleviate vessel stenosis and occlusions; and to reduce the harmful effects of ischemia on the limb, and thus prevent secondary cardiovascular events such as MI and stroke[14, 25 15]. Long-term recurrent CLI in PAD patients may result in lower extremity revascularization, and thus these patients may require extensive treatment to alleviate stenosis. Current therapies used for PAD management are centred on a two-way approach, the first focused on reducing CVD risk factors followed by interventions such as pharmacotherapy, endovascular therapy, or surgery to reduce lower extremity symptoms[3, 11]. Exercise programs and other lifestyle modifications have also proven to be effective in reducing PAD symptoms in IC patients by reducing pain upon walking[11]. Other revascularisation therapies used to treat CLI include angioplasty or stenting and surgical bypass[13].

1.2.5.1 Lifestyle and Risk Factor Modification

Risk factor modification is key in the early treatment and prevention of PAD. This is centred on reducing risk factors that cause PAD such as diabetes, smoking, hypertension and hyperlipidaemia[24]. Studies have shown that smoking cessation reduces the progression and development of IC and critical limb ischemia in PAD patients[3, 26]. Physical activity is also important in managing PAD symptoms, and despite the pain caused by IC in these patients, studies have shown that walking was able to increase collateral circulation in patients suffering from IC[27] and also increased walking distance[28]. Overall, the treatment options for PAD are beneficial in reducing risk factors and for the development of other cardiovascular diseases; and to help increase quality of life of individuals. There is however the need to identify possible mechanisms of action in PAD that can be targeted for the development of new therapeutic strategies.

1.2.5.2 Pharmacotherapy

Therapeutic treatment strategies with medication to treat PAD-associated intermittent caludication are aimed to reduce pain and to increase walking distance in PAD patients[17]. These serve as secondary-preventative measures for reducing PAD-associated risk factors. There are numerous drugs that have been studied to treat PAD symptoms, with statins and anti-platelet therapy being mostly explored[3, 14]. Statins, mainly Simvastatin and Atorvastatin were found to have a 24% risk reduction rate for PAD[17]. Statins have also demonstrated reduced claudication in PAD patients[17]. In addition, the use PCSK9 inhibitors on top of high intensity statin medications have demonstrated significant benefits in lowering LDL cholesterol in PAD; as reported in the FOURIER large randomised controlled trial [29, 30].

Anti-platelet therapy is known to reduce the risk of adverse cardiovascular outcomes with CVD by approximately 25%[26]. Platelet therapy using acetylsalicylic acid demonstrated a 23% reduction in total mortality of CVD and MI[17]. Furthermore, aspirin is one of the most widely used and studied antiplatelet therapy drugs. The Clopidogrel versus Aspirin in Patients at Risk of Ischemic Events (CAPRIE) trial investigated the efficacy of clopidogrel and aspirin in reducing the primary outcome (cardiovascular mortality, MI, and stroke) in a subgroup of patients with symptomatic PAD. This study found that clopidogrel caused a 23.8% relative risk reduction in the primary outcome compared to aspirin therapy[31]. Furthermore, Rivaroxaban in the Cardiovascular Outcomes for People Using Anticoagulation Strategies (COMPASS) trial extends anti-thrombotic benefits in PAD[32].

1.2.5.3 Surgical

Endovascular procedures used in treating PAD are aimed to revascularise obstructed arteries[26]. Endoluminal stent placement and endarterectomy are minimally invasive procedures used to treat stenosis. These procedures utilize the femoral approach whereby catheters are inserted into the blocked artery; and are procedures have shown promising results for PAD treatment[17, 23]. Balloon angioplasty is another commonly used surgical procedure, which involves placing a tiny balloon at the vessel narrowing and expanding the balloon to open up the blockage[24, 26]. Stents are instruments made of expandable mesh wires that are inserted into the endothelium of the vessel and are left in situ to hold the blocked artery open and thus allow blood flow through the vessel. Atherectomy is a procedure that is often conducted following angioplasty, that is used to clear fatty plaques within occluded vessels using special devices attached onto the catheter that is placed within the vessel. This

is a procedure that is more beneficial for patients with heavily calcified plaques. The presence of calcification within the peripheral arteries is a major limiting factor for the treatment of PAD as observed in numerous clinical studies, this warrants for the development of more effective treatment options to treat PAD [33-37].

1.3 Current Angiogenic Therapies

Currently, there is a growing demand for the development of angiogenic therapies due to the high prevalence of ischemic diseases. Angiogenic therapies are aimed to augment physiological angiogenesis and suppress pathological inflammatory angiogenesis[38, 39]. Current anti-angiogenic therapies used for cancer pathologies and proliferative eye diseases have proven effective in randomised control trials[38]. Therapeutic stimulation is the most commonly used form of angiogenic therapy, that is aimed to increase blood flow reperfusion following ischemic insult to tissues in following MI, peripheral vascular diseases and in other cardiovascular conditions. While there are many different modes of therapeutic angiogenesis such cell transfer, the use of recombinant agents and gene therapy; majority of these treatment options are still in their infancy. Furthermore, despite the many clinical advances with these pro-angiogenic therapeutic agents, many patients remain refractory following treatment.

Therapeutic angiogenesis is aimed to enhance new blood vessel development via the administration of specific pro-angiogenic growth factors. The most commonly trialled agents to enhance angiogenesis involve the administration of recombinant pro-angiogenic growth factors such as fibroblast growth factors (FGF1/2) and other isoforms of VEGFA [40, 41, 42]. Clinical trials using recombinant $VEGFA_{165}$ have proven effective in one study were $VEGFA_{165}$ improved myocardial perfusion in patients who were not suitable for coronary

revascularization, whilst also increasing collateral density in these patients[42]. In another phase 1 clinical trial, recombinant VEGF caused improvement in myocardial perfusion at rest[43]. FGF administration was shown to stimulate the growth of dense capillary networks in the myocardium of patients with three-vessel coronary disease, which resulted in increased local blood supply to the tissues[44, 45].

However, these current anti-angiogenic agents remain ineffective as they cannot specifically target inflammatory-driven angiogenesis while preserving physiological angiogenesis. This results in several side effects of nausea, vomiting, reduced wound healing and other gastrointestinal perforations[42]. And while much focus is placed on the currently available risk factors for PAD, there is compelling clinical evidence to demonstrate the devastating effects of calcification on lower extremity revascularisation in PAD, and this is the main focus for this PhD.

1.4 Mechanisms of Neovascularization in PAD

Following occlusion, the body works to stimulate mechanisms to stimulate blood flow to the occluded site. In PAD, hypoxia is a potent inducer of angiogenesis and may occur due to compromised vascular supply to tissues following vascular occlusion. This triggers the expression of pro-angiogenic signalling cascades to drive neovascularisation. In response to ischemia, the body works to revascularize the affected tissues via activation of 3 macrovascular adaptation processes known as (1) angiogenesis, (2) vasculogenesis and (3) arteriogenesis[46-48].

1.4.1 Angiogenesis

Angiogenesis is described as the formation of new blood vessels due to sprouting of new capillary networks from pre-existing capillary beds[11, 19, 46, 49]. Angiogenesis is the hallmark physiological process that occurs postnatally and is involved in wound healing and repair, menstrual cycle and growth and development. It is also a very crucial process for tissue revascularization post-ischemia, in particularly following a MI, stroke and in peripheral vascular disease. Angiogenesis also occurs in pathological conditions such as tumour development and other cardiovascular diseases[11, 19, 50, 51].

1.4.2 Vasculogenesis

Vasculogenesis occurs in early stages of embryonic development and refers to de novo assembly of primary vascular plexus in the developing embryo from the differentiation of mesoderm-derived precursors known as angioblasts[38]. During vasculogenesis, primary vascular plexus is formed by differentiation mesoderm-derived angioblasts into endothelial cells. This process is primarily driven by pro-angiogenic factors VEGF and its receptors (VEGFR1 & VEGFR2), fibroblast growth factor (FGF), transforming growth factor (TGF) and angiopietin-1 and Tie-2[48]. VEGFA acts in a paracrine manner by binding to its receptor VEGFR2 on the surface of angioblasts to stimulate EC differentiation, which later results in the formation of primitive vascular cords, which later transform into new blood vessels by angiogenesis.

1.4.3 Arteriogenesis

Arteriogenesis describes the remodelling of pre-existing collateral arteries to increase tissue perfusion following vessel obstruction[11, 19,49].This process is primarily dependent on the presence of pre-existing vessels, and is the only process known to help reduce the effects of arterial occlusion[21, 52]. Arteriogenesis occurs outside of the affected area, and is primarily induced by an increase in shear stress [53]. Hemodynamically, arterioles are capable of becoming large conductance vessels that regulate sufficient blood flow following events of MI or limb ischemia. However, following stenosis or occlusion of a vessel, blood flow is redistributed towards the pre-existent artery with the lowest resistance. As a result, there is a 20-30x increase in blood flow through the pre-existent collateral artery, which is considered as shear stress[21, 53]. Endothelial cell activation is also thought to occur in response to shear stress. Activation of specific shear stress receptors on ECs induces an intracellular signalling cascade, which then regulates the recruitment of monocytes that differentiate into macrophages. This results in increased proliferation and migration of collateral arteries.

1.5 Blood vessels

Blood vessels consist of arteries, arterioles, capillaries, venules, and veins. Arteries are large blood vessels that carry oxygenated blood away from the heart to the cells, tissues, and organs. Veins however are responsible for carrying deoxygenated blood back to the heart. Arterioles are smaller branches of an artery that lead to form capillaries. Venules are small branches of a vein and serve as the connecting link between capillaries and veins. Capillaries are the smallest form of blood vessel in the body, and their main function is serving as an interconnecting network between arterioles and venules to allow for oxygen and waste exchange between the tissues and the blood, and they merge to form larger lymph vessels.

Blood vessels are comprised of three main distinct layers known as the tunics. The tunica intima is the innermost layer lining blood vessels and contains a monolayer of endothelial cells (ECs) which line the vessel and are surrounded by collagen-rich extracellular matrix (ECM), a protection scaffold for the vessel[54]. The middle layer or tunica media is mainly comprised of VSMCs and plays a key role in regulating blood vessel tone by contraction and dilation. The outermost layer is known as the tunica adventitia which consists of collagen-rich extracellular matrix and connective tissue and contains other cells such as macrophages as a defence mechanism against injury[54] (depicted in Figure 2).

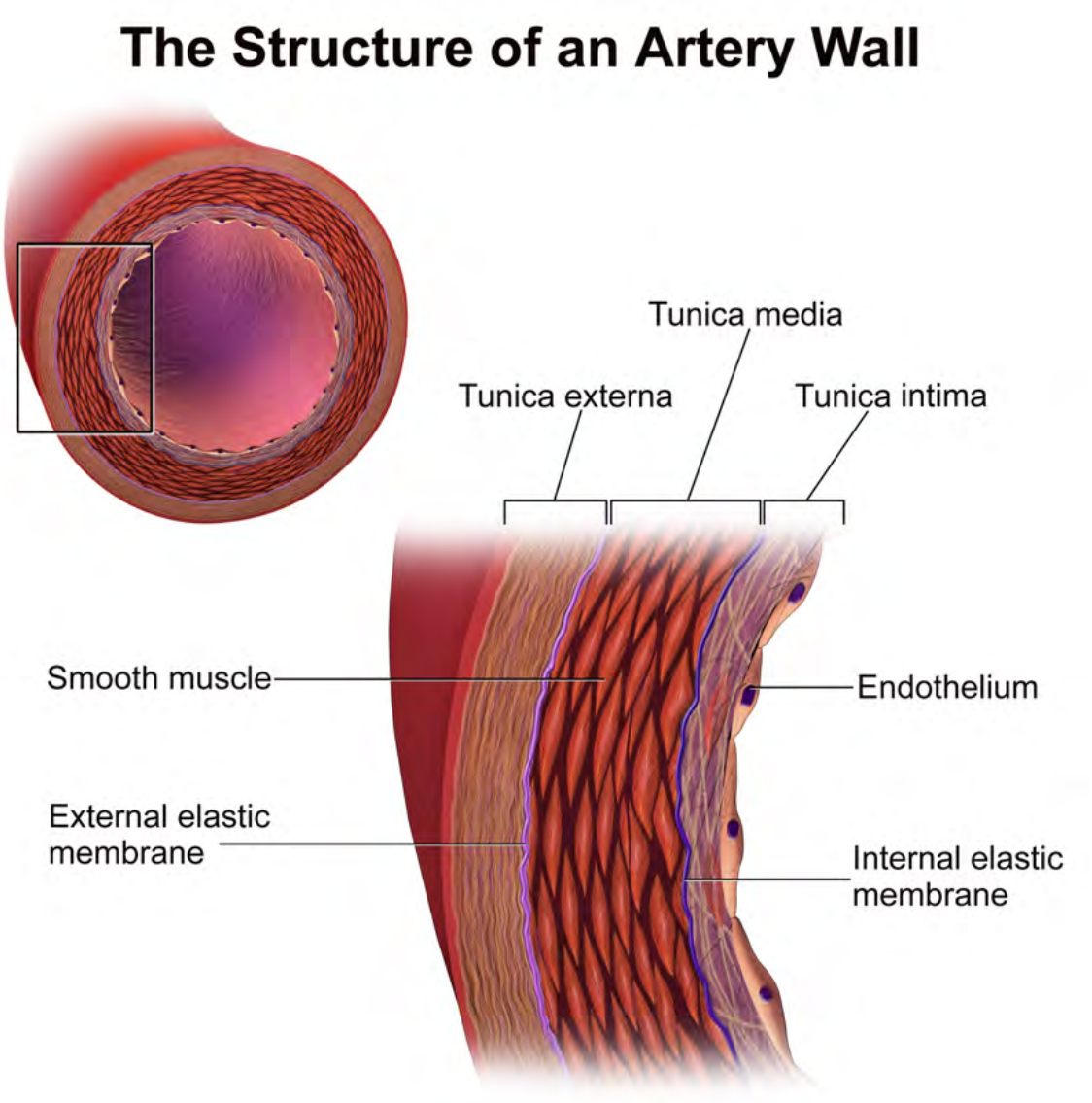

Figure 1.2: Schematic of the normal structure of blood vessels.

Tunica Media is the innermost layer lined by endothelial cells (ECs) Tunica media, consist of a layer of vascular smooth muscle cells (VSMC) for regulating vascular tone. The tunica externa is the outermost layer of blood vessels and is predominantly connective tissue consisting of blood vessels and immune cells. ***(Image adapted from:*** *Blausen.com staff (2014). "Medical gallery of Blausen Medical 2014". WikiJournal of Medicine* ***1****(2). DOI:10.15347/wjm/2014.010. ISSN 2002-4436.*

1.6 The Endothelium and Endothelial Disfunction

The endothelium lining the vascular system plays an important role in maintaining vascular homeostasis and serves as an inert barrier between the blood and vessel wall and separates blood from the VSMCS[55]. It contains a delicate monolayer of cells known as endothelial cells (ECs), which are the primary cells that line the vessel wall. These cells serve many functions such as regulating vascular tone, permeability and the angiogenic processes, proliferation, migration and apoptosis; whilst also mediating a range of reparative responses including inflammation which occurs in response to injury[56].

The main function of the endothelium is to protect against disease, and impairment of this leads to endothelial dysfunction. Endothelial dysfunction occurs due to changes in endothelial cell phenotype towards a proinflammatory and prothrombotic state within the vascular wall[57]. Impaired endothelial function has been suggested as an early characteristic of PAD and in particular diabetic vasculopathy and stage 1 chronic kidney disease [58]. ECs secrete a variety of factors which regulate vascular motor activity[14]**.** Additionally, studies have reported PAD patients experiencing reduced endothelial function in their limbs. This is most likely due to several mechanisms such as inflammation, reduced nitric oxide synthesis, oxidative stress and elevated levels of lipid serum[14]**.** Endothelial dysfunction is also known to exacerbate clinical symptoms of PAD, by interfering with arteriogenesis or the formation of collateral vessels[57]. Therefore**,** endothelial dysfunction is considered a key hallmark of vascular diseases such as PAD, and maintaining proper integrity of the endothelium is very important in preventing the occurrence of other cardiovascular-related diseases[59].

1.6.1 The Angiogenic Cascades

Endothelial cells are key initiators in blood vessel formation[60-62]. In adults, the process of angiogenesis is highly regulated by several stimulators and inhibitors of angiogenesis which create a delicate balance for blood vessel formation on inhibition[47]. Impairment of this balance is recognised as a key common feature underlying many pathological diseases including cancer, rhematoid aarthritis, type II diabetes mellitis and cardiovascular diseases where there is either excessive or insufficient blood vessel growth[47].

The angiogenic response is mainly triggered by hypoxia. The initial step is the release and binding of pro-angiogenic growth factors hypoxia-inducible factor (HIF-1α), which activates the transcription of vascular endothelial growth factor (VEGFA), resulting in VEGFA-mediated increase in vascular permeability **(Figure 1.3)**[21, 52]. VEGF transcription is also stimulated by other growth factors such as fibroblast growth factor (FGF-2) and platelet derived growth factor (PDGF) [21, 60]. This activates endothelial cells and promotes the release of various proteinases and enzymes, mostly matrix metalloproteinases which cause degradation of the extracellular basement membrane and thus causing alterations in the cell membrane structure and redistribution of intracellular adhesion molecules. This drives endothelial cell migration and proliferation that results in the formation and maturation of vascular tubes **(Figure 1.3)**[21 60].

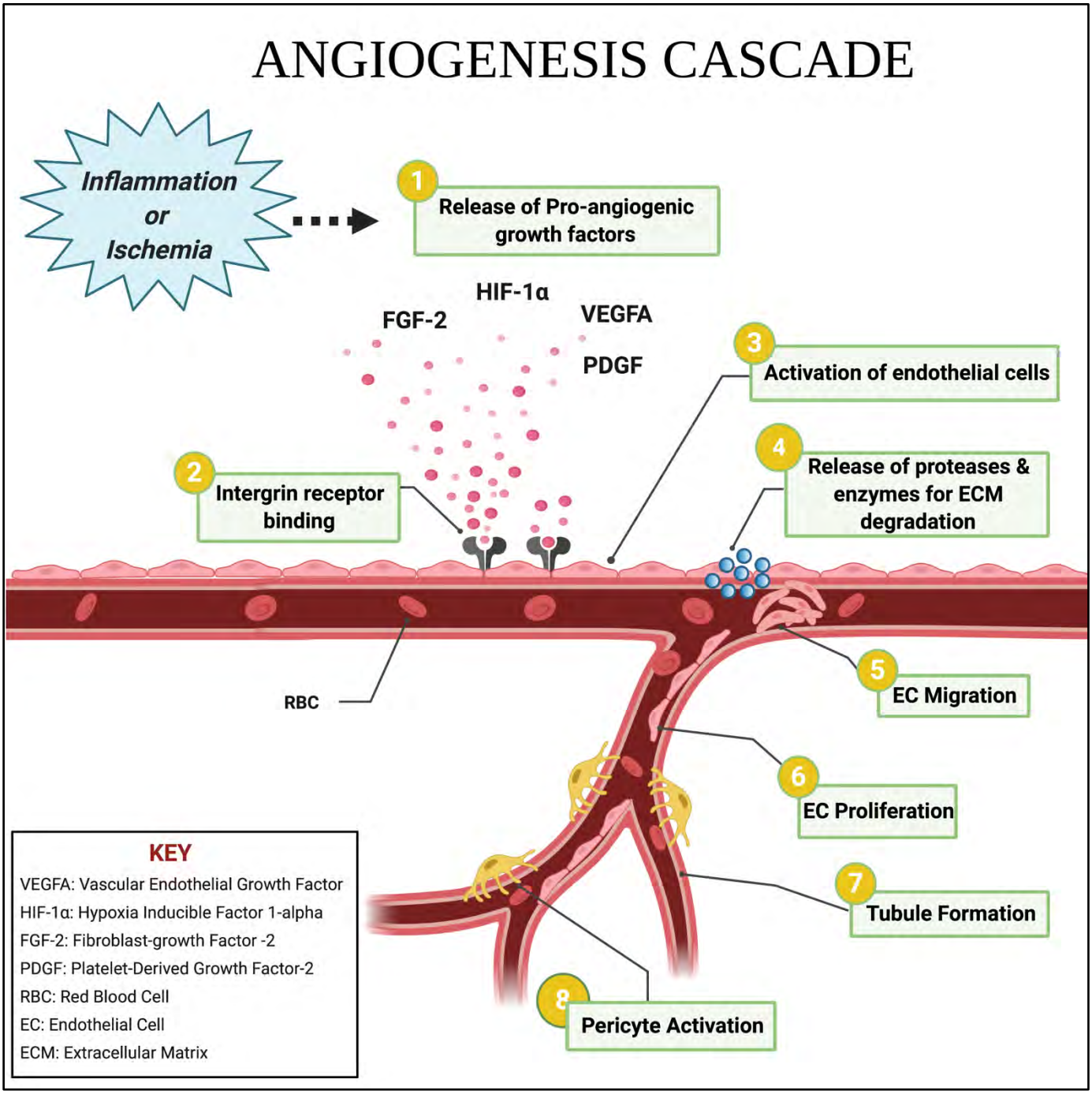

Figure 1.3: Schematic illustrating the angiogenic cascade in endothelial cells.

The main steps of the angiogenic pathway include the release and binding of pro-angiogenic factor, endothelial cell activation, extracellular matrix degradation, EC proliferation and migration which results in the formation of vascular tubes.

1.6.2 Angiogenesis Is Driven by Two Distinct Yet-overlapping Pathways

Angiogenesis is a multi-step process involving well define stages that are orchestrated by numerous growth factors, cellular events, cytokines and signalling cascades. Depending on the pathophysiological context, angiogenesis is regulated via two distinctly different yet overlapping pathways[63]. Ischemia-driven angiogenesis by HIF-1 α is primarily mediated by hypoxia[64]. Conversely, inflammatory-driven angiogenesis and is driven by NF-kB (P65) signalling pathway[65]. There is conditional regulation of angiogenesis by VEGF to regulate both ischemia-driven and inflammatory-driven angiogenesis. Notably, VEGF is an important stimulator of angiogenesis in both ischemia and inflammatory conditions; modulated by HIF-1α and NF-κB, respectively. VEGF is known to possess a response element for both NF-κB and HIF-1α in its promoter region; thus, allowing for conditional regulation via activation of both signalling pathways independently.

1.6.2.1 Ischemia-Driven Physiological Angiogenesis is Regulated Via the HIF-1α Signalling Pathway

Physiological-ischemia-driven angiogenesis is a crucial process for growth and development, wound healing and the menstrual cycle. This occurs post-ischemia and is triggered due to a chronic imbalance in oxygen supply to the tissues; resulting in a highly hypoxic environment; as seen following a myocardial infarct, and in disease states with vessel occlusion such as perivascular diseases[21, 66]. As a result, ischemia-driven angiogenesis is stimulated to induce neovascularisation of the ischemic tissue and thus restore blood flow in the affected area[67]. Reduced blood supply can also result due to imbalance between pro- and anti-angiogenic factors[67].

The molecular mechanism of ischemia-driven angiogenesis is regulated primarily via the hypoxia-inducible factor pathway (HIFs). HIFs form a heterodimer comprising of two subunits, HIF-1α and HIF-1β, which are regulated depending on the intracellular concentration of oxygen in the tissue[66]. There are two isoforms of HIFS, HIF-1α and proteins are regulated transcriptionally, the stability and activity of HIF-1α are reliant upon post-translational regulation[66].

In aerobic conditions when oxygen tissue supply is sufficient, HIF-1α is regulated within the cytosol by propyl hydroxylase domain proteins (PHD1, PHD2 and PHD3), which cause hydroxylation of the proline residues (Pro402, Pro564 on HIF-1α) and (Pro405, Pro531 on HIF-2α), situated within the oxygen-dependent degradation domain of an inducible α-subunit of HIFs[66, 67]. This therefore allows binding of the Von-Hippen Lindau (VHL) tumour suppressor protein, E3 ubiquitin ligase complex, which targets HIF-1α for ubiquitination and proteasomal degradation **(Figure 1.4)**[46, 67].

Conversely, under anaerobic conditions where there is depletion in intracellular oxygen concentration, the PI3K/Akt signalling pathway is activated, inducing of gene transcription of E3 ubiquitin ligases Siah 1 & Siah 2, which target and promote degradation of PHD enzymes, leading to HIF-1α stabilisation and accumulation **(Figure 1.4)**[66, 67]. As a result, this allows HIF-1α to be translocated into the nucleus where it complexes with the HIF-1β subunit and binds to the hypoxia response element (HRE). It then facilitates the expression of pro-angiogenic mediators such as VEGF and its receptors (VEGFR1 and VEGFR2), basic fibroblast growth factor (bFGF), angiopoietin, stromal derived-factor 1 (SDF-1 or CXCL12), platelet derived growth factor (PDGF) and matrix metalloproteinases (MMPs) [32,67]. As a result of these mechanistic interactions, these angiogenic factors stimulate endothelial cellular processes of proliferation, migration, extracellular matrix degradation and pericyte activation, leading to vessel wall maturation and the formation of new blood vessels[32,67].

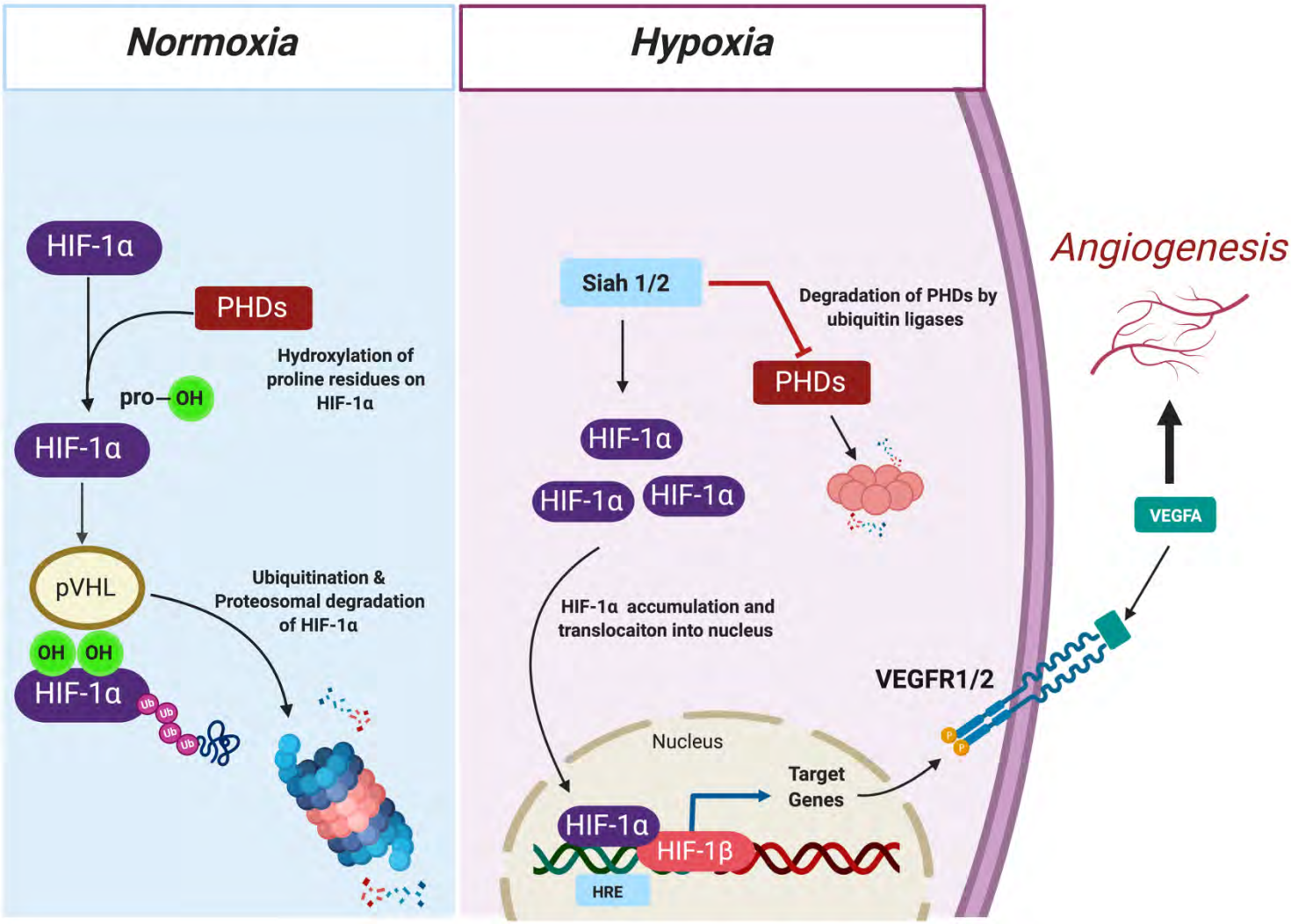

Figure 1.4: Mechanistic diagram for HIF-1α regulation during hypoxia-mediated angiogenesis. *Under normoxic conditions, PHD1-3 hydroxylates proline residues on HIF-1α allowing von Hippel-Lindau proteins to bind thereby targeting HIF-1α for ubiquitination and proteasomal degradation by The von Hippel-Lindau (VHL) complex. In hypoxia, low oxygen levels stimulate the increase of Siah ubiquitin ligases (Siah 1/2) which inhibit PHDs thus preventing HIF-1α from ubiquitination and degradation. This increases HIF-1α stability and allows it to accumulate and translocate into the nucleus where it complexes with HIF-1ß and bind to the hypoxia response element (HRE) driving angiogenic target genes such as VEGFA to bind to its receptor VEGFR2, thus driving an angiogenic response.*

1.6.2.2 Ischemia-Driven Angiogenesis and VEGFA Signalling

The VEGF family of ligands and receptors play a key role during angiogenesis and are regulated via the activation of HIF-1α. The VEGF family comprise of five members (VEGFA, VEGFB, VEGFC and VEGFD and placenta growth factor (PGF), and VEGFA is the most potent pro-angiogenic member of its family[68]. It is produced by endothelial cells following hypoxic stimulation and helps to regulate angiogenesis by controlling EC proliferation, apoptosis and migration which ultimately leads to the development of a vascular network[68]. It's important role in angiogenesis has been highlighted in murine gene knockout studies where mutations of a single VEGFA allele results in embryonic fatality[69]. VEGF are a family of ligands highly expressed under hypoxic conditions and regulate vascular permeability in inflammatory responses and other pathological diseases[60, 70].

Mechanistically, VEGFA binding to its receptor VEGFR-2 on endothelial cells causes phosphorylation and dimerization of the receptor, in turn activating multiple downstream signalling pathways **(Figure 1.5)**. These include the phosphatidylinositol 3'-kinase (PI3K/Akt), P38/mitogen-activated protein kinase (MAPK), and phospholipase C gamma (PLCγ)/MAPK pathways. Specifically, PI3K activation results in phosphorylation of Akt, promoting EC survival. Secondly, activation of P38 by Akt in turn activates MAPK signalling activation which regulates EC migration. Lastly, activation of PLCγ stimulates the activation of the ERK pathway, leading to EC proliferation. Ultimately, stimulation and activation of these pathways leads to EC proliferation, migration, and tubule formation **(Figure 1.5)**.

Other downstream signalling pathways that are also activated during angiogenesis following VEGFA signalling involve endothelial nitric oxide (eNOS). eNOS is located downstream of the HIF-1α-VEGFA pathway[71]. During hypoxia, eNOS produces nitric oxide

(NO) to help enhance EC proliferation, migration and to increase VEGFA expression; which ultimately increases angiogenesis **(Figure 1.5)**[72].

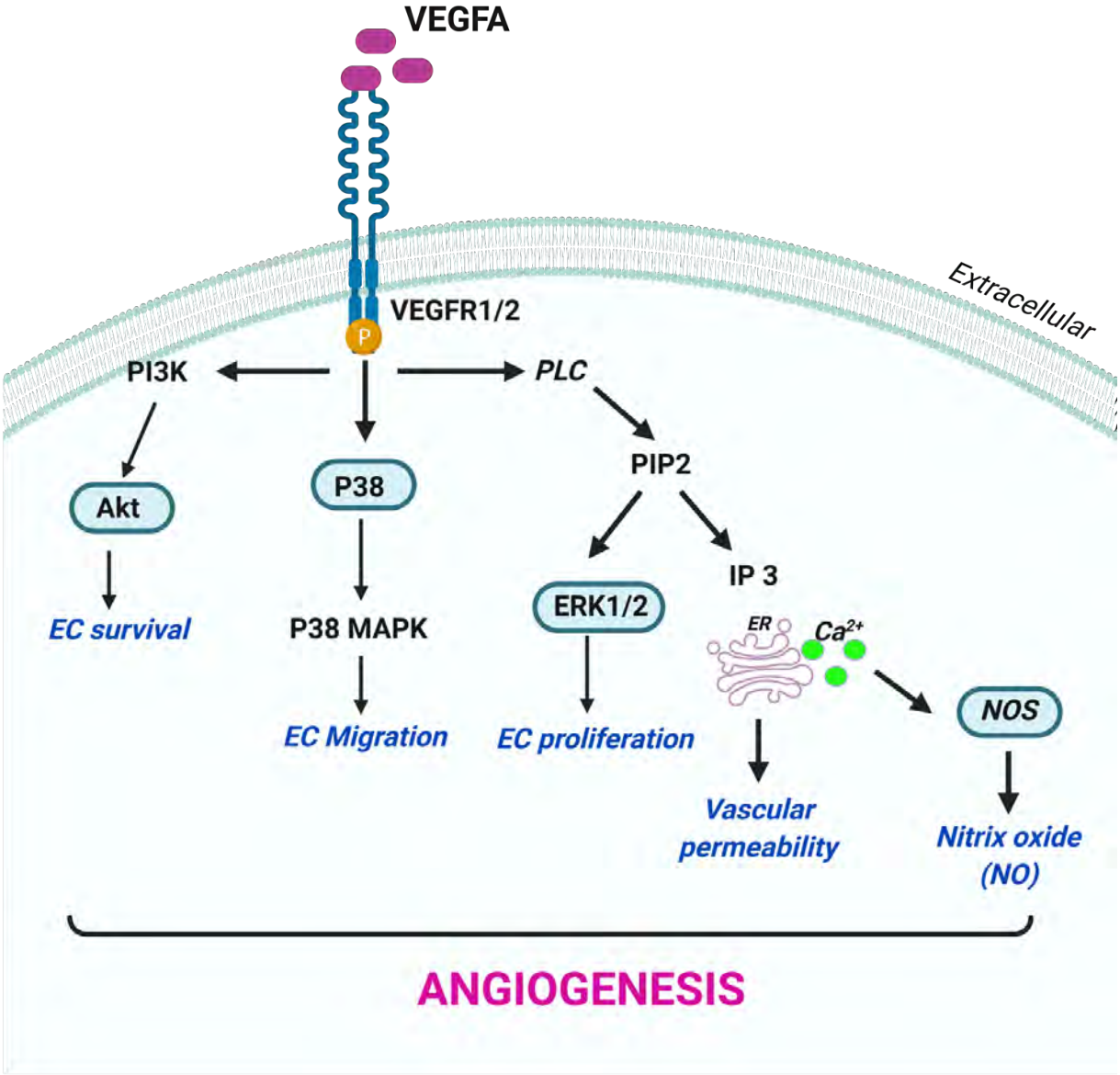

Figure 1.5: VEGFA Signalling Pathway

Binding of VEGFA to its receptor VEGFR2 results in dimerization which results to activation of multiple signalling pathways. PI3K stimulates subsequent activation of Akt phosphorylation which promotes endothelial cell survival. Activation of p38 leads to activation of P38 MAPK signalling, which promotes EC migration. VEGFA-VEGFR2 binding also results in activation of the PLC-y pathway that cleaves PIP2 to IP3, which results in activation downstream activation of ERK1/2 which regulates EC proliferation. This pathway also stimulates the release of calcium from the endoplasmic reticulum that results to increased vascular permeability. Calcium release is also responsible for the synthesis of nitric oxide from nitric oxide synthase.

1.6.2.3 Inflammatory-Driven Angiogenesis Is Regulated Via NF-κB Activation

Angiogenic regulation and homeostasis is importance for maintaining healthy physiological processes. During angiogenesis, there lies a delicate balance between pro-angiogenic and anti-angiogenic factor regulation, and disturbances in this can result in pathological forms of angiogenesis. Cases where this is increased include disease states of cancer, macular degeneration, rheumatoid arthritis, haemangioma and psoriasis[46,73]. Conversely, impairment or insufficient angiogenesis is commonly present in disease states such as diabetes, cardiovascular diseases, ischemic heart diseases and peripheral arterial disease[46,73]. Therefore, there is a crucial need for homeostasis to be maintained to prevent the occurrence of numerous pathological conditions.

In contrast to ischemia-driven angiogenesis, pathological angiogenesis is driven by inflammation. Inflammatory-driven angiogenesis may be triggered by direct or indirect stimulation[66]. Direct stimulation involves increased expression of inflammatory cytokines on ECs to regulate EC proliferation and migration, leading to angiogenesis[67]. In contrast, indirect stimulation involves the release and recruitment of macrophages to the inflamed site in response to an inflammatory stimulus, which then triggers the secretions of a host of pro-angiogenic factors including VEGFA, TNF-α, bFGF and interferon gamma (IFNγ) to promote angiogenesis[67]. Other key promoters of inflammatory driven angiogenesis include TNF-α, NF-κB, cell adhesion molecules (CAMs) including vascular cell adhesion molecule-1 (VCAM-1), intracellular adhesion molecule-1 (ICAM-1) and monocyte chemoattractant protein-1 (MCP1)[74].

The NF-κB pathway is regulated by two signalling pathways, the canonical or classical pathway and the non-canonical or alternative pathway; however inflammatory-driven angiogenesis is mainly driven by the canonical pathway[65, 66, 74]. Mechanistically, the

canonical pathway is activated by inflammatory stimulus such as TNF-α and interleukins. The NF-κB complex comprises of two subunits, P50 and P65. Under normal conditions, in response to an inflammatory stimulus, the IκB kinase (IKK) enzyme complex is activated and phosphorylated, which results in phosphorylation of the inhibitor of κB (IκB) proteins, specifically IκBα, which gets targeted for ubiquitination and subsequent proteasomal degradation. This results in sequestering and translocation of the NF-κB dimer P50/P65 into the cytosol, where it binds to the NF-κB response element thereby initiating the transcription of pro-angiogenic factors such as VEGFA, VCAM, ICAM, and matrix metalloproteinases (MMPs) **(Figure 1.6)**[65, 66, 74].

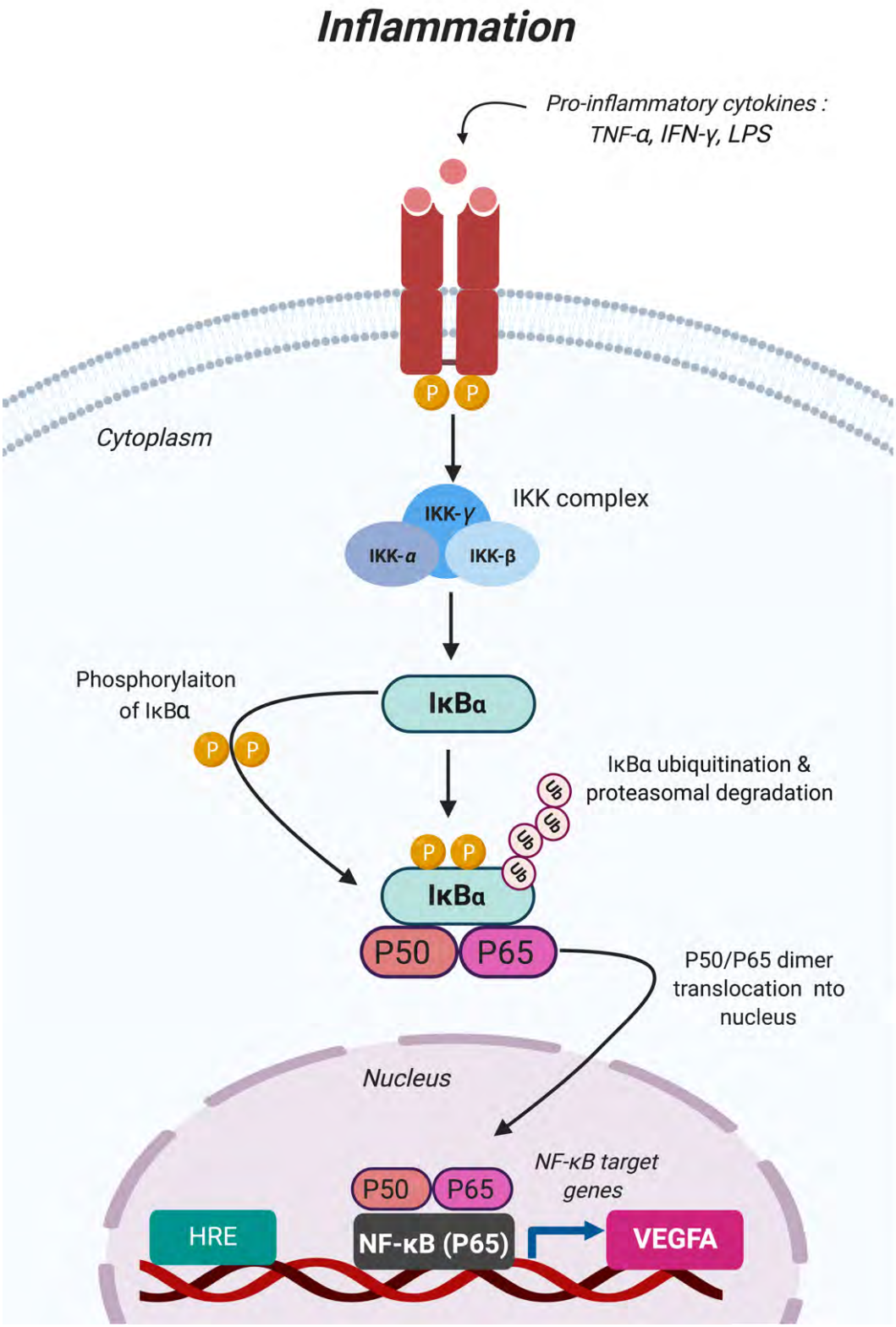

Figure 1.6: Schematic illustrating inflammatory-driven angiogenesis mediated by NF-kB signalling. *During inflammatory-driven angiogenesis, pro-inflammatory stimuli such as TNF-α, IFN-γ , or LPS stimulate phosphorylation of IκBα by the IKK complex, resulting in ubiquitination and proteasomal degradation of IκBα. This leads to translocation of the p50/p65 NF-κB dimer into the nucleus, where is binds to the NF-kB response element to activate the production of NF-KB target genes such as VEGFA to further drive the inflammatory response.*

1.6.3 Adhesion Molecules and Cytokines in Acute Inflammation

Adhesion molecules are a group of heterogeneous cell surface proteins that regulate cell-to-extracellular matrix interactions as well as cell-to-cell interactions[75]. These proteins are expressed by most cells and play important roles in the regulation of inflammatory responses within tissues. However, these proteins may also contribute to pathological inflammation by promoting chronic inflammatory processes as seen in atherosclerosis, type II diabetes and other CVDs[75].

1.6.3.1 Vascular Cell Adhesion Molecule 1 (VCAM-1)

VCAM-1 also known as CD106 (cluster of differentiation) is an immunoglobulin-like adhesion molecule that is constitutively expressed on blood cells including monocytes, lymphocytes, and eosinophils[76]. However unlike ICAM-1, VCAM-1 exhibits low expression on unstimulated ECs and thus its expression is profoundly stimulated by pro-inflammatory stimulus such as TNF-α, IL-1β, liposaccharides (LPS), oxidised LDL (oxLDL) and high glucose[77]. Its expression is also known to be upregulated and detected mainly at atherosclerotic-prone sites of the endothelium[75]. VCAM-1 expression is also known to be stimulated by NF-κB signalling. VCAM-1 functions by binding to $\alpha_4\beta_1$ integrin expressed on lymphocytes, monocytes, and eosinophils; thereby binding these cells to the endothelium during early atherogenesis and causing the arrest of rolling monocytes[77].

1.6.3.2 Intracellular Cell Adhesion Molecule 1 (ICAM-1)

ICAM-1 also known as CD54 (cluster of differentiation) is a transmembrane protein of the immunoglobulin superfamily that is constitutively expressed during physiological

conditions on endothelial cells; and is important in regulating adaptive and innate immune responses[76]. ICAM-1 expression is upregulated in response to inflammatory cytokines such as TNF-α, IL-1β, IL-6, interferon-γ and LPS[76]. ICAM-1 functions by binding to two integrins of the β2 family on the surface of leucocytes, including CD11a/CD18 and CD11b/CD18[75]. Furthermore, during an inflammatory response, ICAM-1 binding to its integrin triggers rolling and transmigration of leucocytes into the sub-endothelium[76]. ICAM-1 expression can also be regulated by transcription factors NF-κB (specifically the p65 subunit), as NF-κB is always required for its activation[75].

1.6.3.3 Monocyte Chemoattractant Protein (MCP1)

Chemokines are a sub-class of cytokines which are produced by the damaged endothelium and promote monocyte recruitment to the site of injury through chemotaxis[78]. MCP1 also known as CCL2 is a chemoattractant chemokine that is secreted by numerous cell types including endothelial cells, SMCs, fibroblasts, epithelial, smooth muscle, mesangial, monocytes and microglial cells[78]. MCP1 is highly expressed in atherosclerotic lesions and plays an important role for the recruitment of monocytes into the arterial wall during inflammatory responses[76]. MCP1 levels are also known to be elevated by SMCs, monocytes/macrophages within the activated vessel wall during inflammation. MCP1 is regulated transcriptionally by NF-κB signalling and by the mitogen activated protein kinase (MAPK) pathway. Mechanistically, MCP1 binding to its receptor CCR2 on monocytes results in activation of intracellular signalling cascades which drive the migration of monocytes towards the vascular endothelium thereby driving an inflammatory response[78].

1.7 Vascular Calcification

Vascular calcification (VC) is a phenomenon of soft tissue calcification and is defined as mineral deposition in the vascular wall in the form of hydroxyapatite (calcium-phosphate)[79, 80]. VC was previously presumed to be a passive process caused by shifting of calcium from the bone to the arterial wall; but is now increasingly recognized to be driven by complex cellular mechanisms. The prevalence of VC is age and sex-dependent, affecting approximately 90% of males and aproximately 67% of women aged >60[80, 81]. VC is part of the aging process and is a major complication of chronic kidney disease (CKD) and hypertension, that is accelerated in atherosclerosis and type 2 diabetes[15, 79]. The incidence of VC is highly correlated with increased cardiovascular mortality and morbidity rates, due to reduced vessel compliance, vascular stiffening and reduced coronary perfusion[82]. This leads to ischemia, and other complications such as MI, stroke and leg amputations in PAD, and the later death of these patients[82].

1.7.1 Calcification in Clinical Settings

There are extensive clinical data available to demonstrate the presence of calcification in the clinical settings of PAD, type 2 diabetes and CKD. Its important to note that arterial calcification in these clinical settings commences insidiously and progresses slowly and may only become apparent over a course of time. Patients with PAD often present with multilevel disease, characterised by fatty plaque build-up and high levels of diffused calcium deposits in the media of their peripheral arteries[83]. In addition, lower extremity arterial calcification predicts poor cardiovascular outcomes and is highly associated with limb amputations[15, 34, 84-87], and was reported in peripheral arteries of diabetic and chronic kidney disease (CKD) patients, suggesting an association between arterial calcification and PAD[34, 84, 85]. Because

calcification affects limb vascularization, it is therefore considered a limiting factor for treatment and a potential driver of PAD[15].

The presence of lower extremity arterial calcification as seen on X-rays is highly associated with an increased risk of limb amputations and increased mortality rates in diabetic patients compared to healthy individuals[35]. Additionally, medial calcification is known to result in decreased vessel compliance and cause vascular stiffening, and is thought to affect local blood flow as seen in PAD[15]. In one study, tibial artery calcification (TAC) scores was used to assess the associations of calcification with the severity of symptoms in PAD patients following computed tomography (CT). This study found that patients with elevated TAC scores had a much higher incidence of PAD symptoms and increased risk of limb amputations compared to those with lower scores[34]. In a different study, assesment of human femoralpopliteal arteries showed that calcified arteries had larger diameters, thicker walls, thinner tunica media; with more discontinuous elastic fibres compared to healthy arteries[36]. Based on this evidence, there is an undoubtebly pressing need for a better understanding of the associations linking VC to PAD.

1.7.2 Types of Vascular Calcification

Traditionally, cardiovascular calcification is classified into four different types depending on the location and type of arteries affected. Clinically, the 4 types include atherosclerotic (intimal) calcification, medial arterial calcification (MAC) also known as Monckeberg's sclerosis, cardiac valve calcification and vascular calciphylaxis[61]. All types have distinct yet overlapping pathological mechanisms. In particular, because intimal and medial calcification occur more frequently and associated with cardiovascualr diseases such as PAD, they will be described in more detailed below.

1.7.2.1 Intimal Calcification

Intimal calcification is associated with atherosclerotic plaques and occurs in alongside lipid deposition, cellular necrosis and inflammation, macrophage invasion, vascular smooth muscle cell proliferation and dysfunction of matrix proteins as a result of chronic arterial inflammation[79, 88]. Overtime, as the plaque lesion progresses, osteogenesic markers are released and promote calcium-phosphate mineral deposition in the intimal layer of the artery wall in the form of hydroxyapatite **(Figure 1.8)**. Calcium and phosphate mineral deposition elicits an inflammatory response by releasing tumour necrosis factor (TNF) production by macrophages. Based on this, the role of inflammation in the pathogenesis of VC remains questionable, and it has been proposed that vascular calcification may be an inflammatory-driven process[66, 89]. Long-term effects of intimal calcification result in erosion and rupture of these unstable plaques, thus causing blood flow obstruction and reduced perfusion as seen in obstructive vascular diseases such as PAD[15, 66, 89]. Furthemore, the expression of bone-related regulating proteins such as bone morphogentic proteins (BMPs) are known to be expressed in atherosclerotic plaques by endothelial cells, foam cells and smooth muscle cells[61, 90].

Macrophages, mast cells and VSMCs are the primary cells involved in atheroslerotic intimal calcification. Macrophages are known to release TNF-α in repsonse to oxidised LDL. Macrophages are also known to express a vaerity of ostegenic proteins including alkaline phosphatase, matrix gla protein, osteopontin and bone sialoprotein. Furthermore, TNF-α treatment of VSMCs is known to enhance osteoblastic differentiation and increase ALP expresison thus causing minerlisation[91, 92].

1.7.2.2 Medial Calcification

Medial calcification, or as it is traditionally known, Monckeberg's sclerosis is more commonly associated with chronic kidney disease (CKD)[93]. Medial calcification is associated with aging and occurs independent of atheroslerosis within the medial layer of the vessel wall. The medial layer of the vessel wall is comprised of thick layer of VSMCs and elastin-rich extracellular matrix. Elastin is a protein that is abundantly expressed in the vascular wall of arteries that has crucial role in the maintainance of vascular wall intergrity and function. Therefore, the loss and degradation of elastin exarcebates medial calcification, which may often result in increased arterial stiffness, increased pulse pressue and left ventricular hypertrophy, all independent predictors of cardiovascular mortality[80, 94-97].

VSMCs are the key cell type involved in medial calcification. Under physiologucal conditions, these cells have contractile and proliferative properties and express a range of contractile proteins including smooth muscle α-actin (SMαA), SM-22α, SM myosin heavy chains SM-1 and SM-2, calponin, and smoothelin[94]. However, under pathological conditions, these cells can undergo phenotypic changes in response to local cues which downregulates their contractile proteins thus increasing their proliferative activity[94, 98]. The differentiation of VSMCs towards an osteblast-like phenotype or bone-like cells is the main theory proposed for medial calcification. This change from contractile to osteogenic phenotype is brought about by the development of calcifying matrix vesicles by VSMCs, the loss of SMC markers (SM22α and SM α-actin); and gain of calcification markers (Runx2, Osteopontin, alkaline phosphatase (ALP), type II and type X collagen and osteocalcin[94]. All these factors in turn promote calcium-phosphate deposition within the vessel wall **(Figure 1.8)**.

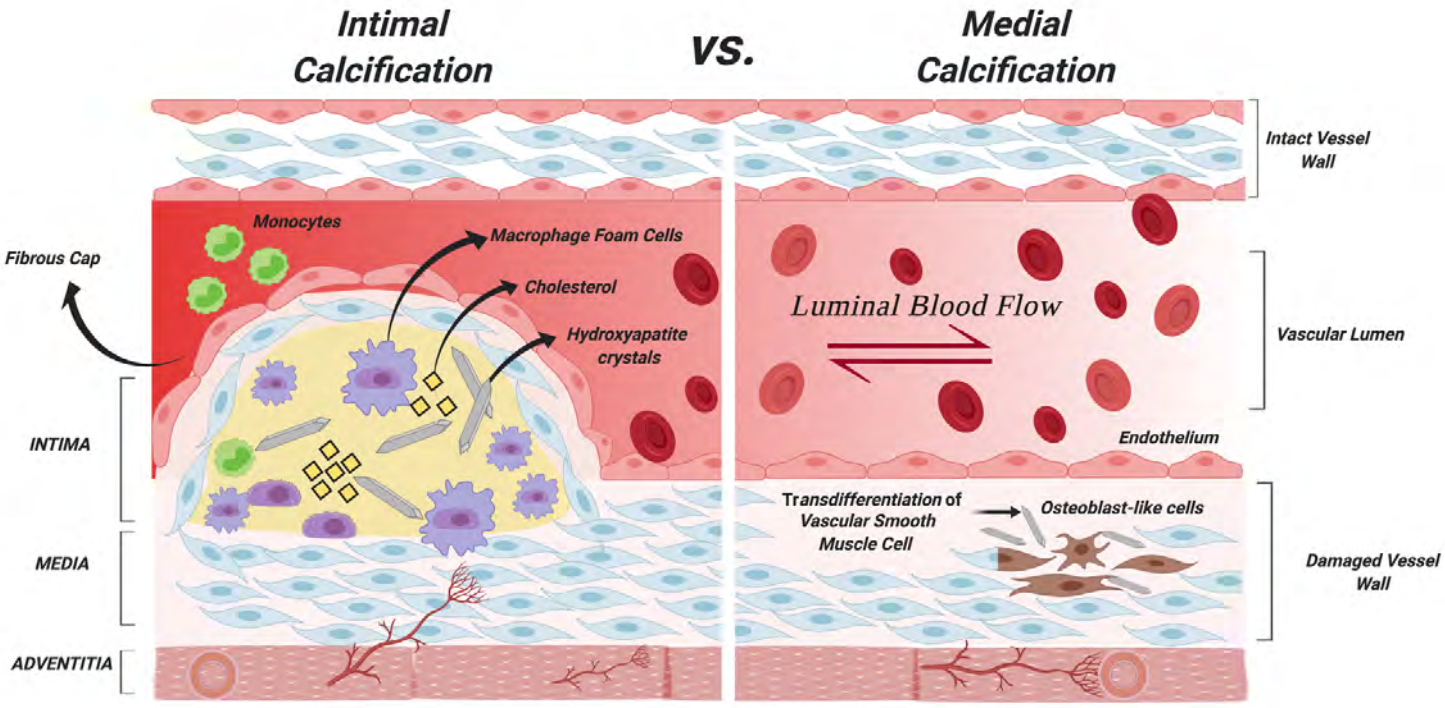

Figure 1.8: Schematic illustrating intimal vs medial calcification in the vessel wall.

Intimal calcification occurs in association with athersclerosis plaque progression within the intimal layer due to lipid deposition, macrophage infiltration, inflammation and calcium-phosphate deposition. Medial calcification occurs within the medial layers of the vessel wall, and is driven by vascular smooth muscle cell (VSMCs) differentiaiton into osteoblst-like cells, which promotes mineral deposition.

1.7.3 Proposed Theories for Vascular Calcification

Long considered a passive process of aging, VC is now considered to be an actively regulated process that occurs in a similar fashion to bone formation[61]. Nummerous theories have been proposed in the pathogenesis of vascular calcification, though the precise molecular and cellular mechanisms remain unclear.

Some of the major hypotheses of VC include failed anticalcific processes due to loss of mineralisation inhibitors, induction of osteochondrogenesis, apoptosis, imbalance of calcium-phosphate homeostasis, bone remodelling and matrix degradation and modifications (reviewed in[79]). Currently there are no treatments available for vascular calcification, thus identification of novel mediators and molecular pathways responsible for the pathological mineralization process are key in providing insight into novel drug targets to treat VC. For the purpose of this thesis, the focus was on 2 theories – loss of mineral homeostasis and loss of calcification inhibitors.

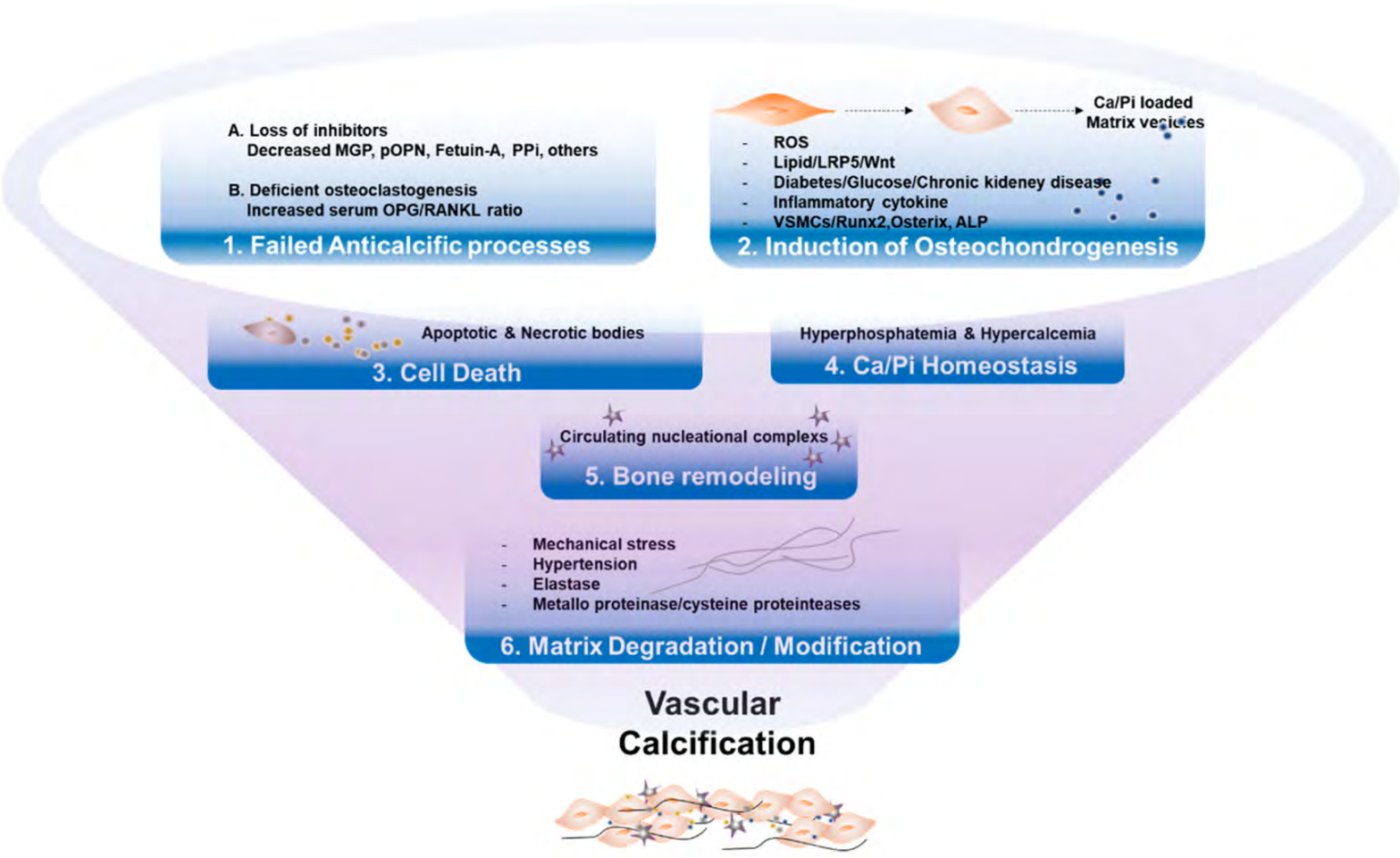

Figure 1.9: Schematic illustrating key mechanisms of vascular calcification[79].

VC is proposed to occur due to many different mechanisms including (1) Failure of anti-calcification processes, caused by loss of mineralisation inhibitors which leads to VC. (2) Numerous factors are able to induce osteogenic transdifferentiation of VSMCs, including products of matrix vesicles, which act as a nidus of calcium phosphate deposition within the vessel wall. (3) Cell death by apoptosis or necrosis can promote the release of apoptotic bodies or necrotic debris, which may act as sites for hydroxyapatite deposition. (4) Dysregulated mineral homeostasis can result in calcium phosphate hydroxyapatite deposition. (5) Nucleational complexes formed during bone remodelling can further promote VC. (6) Environmental stressors can promote matrix degradation/modifications, and thus result in mineral deposition. Image adapted from[79].

1.7.3.1 Disruption of Calcium-Phosphate Homeostasis.

The physiological role of both calcium (Ca) and phosphate are well established in the regulation of numerous cellular signalling processes throughout the body and within the vasculature[99]. Phosphorus (P) has numerous roles in the body and is essential for ATP production, intracellular signalling, pH buffering and is a main constituent of bone, phospholipids and nucleic acids[100]. Normal serum phosphate concentrations range between 1.12-1.45 mmol/L, and elevations greater than 1.8 mmol/L are correlated with increased CVD risk and all-cause mortality in CKD patients[101]. Calcium is crucial for many physiological processes in the body including muscle contraction, neuronal signalling and is a major constituent of bone; with 99% of calcium being stored in bone and the rest in blood and cells. Normal serum concentrations of Ca range within 2-2.5 mmol/L, and elevation of calcium concentration greater than 2.5 mmol results in hypercalcemia. Furthermore, disturbance in mineral homeostasis in hyperphosphatemia (elevated phosphate above 2.0 mM) and hypercalcemia (elevated calcium above 2.4 mM) play a crucial role in the progression of vascular calcification and are highly associated with cardiovascular mortality in CKD patients[79, 93, 99, 100 98].

The intracellular mechanisms by which phosphate is regulated in VC occurs via VSMCs. Increased extracellular calcium promotes mineralization of VSMCs via induction of Pit1 receptor, to raise intracellular levels of inorganic phosphate. This stimulates the release of osteogenic transcription factors such as alkaline phosphatase (ALP) and Runx2, a potent transcription factor for VC, which enhance VSMCs osteogenic differentiation[79]**.** Furthermore, under elevated phosphate concentrations, VSMCs undergo apoptosis and necrosis, which results in the release of apoptotic bodies, serving as a site for calcium-phosphate precipitation[79, 102]. Furthermore, mineral imbalance is known to induce VSMC-derived matrix

vesicles (MVs), precursors of microcalcification[103]**.** It is believed that elevated extracellular concentrations of Ca and P induce the release of these pro-inflammatory macrophage derived MVs, thus contributing to VC[103]. However, the cellular mechanisms underlying vascular calcification in the context of endothelial cells remains very poorly understood.

1.7.3.2 Loss of Mineralization Inhibiting Factors

There are 6 potent inhibitors of mineralization including Matrix Gla Protein (MGP), osteoprotegerin (OPG), Osteopontin (OPN), fetuin-A, Klotho, and inorganic pyrophosphate (PPi); which protect the vessel wall from undergoing calcification[104]. In atherosclerotic calcification and diabetic medial calcification, the expression of these endogenous inhibitors are severely reduced, which results in calcium overload leading to VC[105]. During this process, VSMCs begin to express markers of both osteoblast and chondrocyte differentiation, which thereby further promote VC[93]. When calcium and phosphate exceed their solubility due to significantly elevated concentrations, this inhibits the production of calcification inhibitors, and thus promotes VC. Given the crucial role OPG plays in bone mineralisation and its implication in cardiovascular disease this inhibitor was chosen for the main focus of these studies.

1.7.3.3 Osteopontin (OPN)

OPN (Osteopontin) is a secreted multifunctional glycophosphoprotein that is synthesised by cells involved in osteogenesis and serves important roles for both physiological and pathophysiological processes. OPN's main function is regulating biomineralization and serving as a physiological inhibitor of vascular calcification and

activating osteoclast function[93]. Under normal physiological conditions, OPN is lowly expressed in the circulation and in tissues of the vasculature, however under pathological conditions in response to injury, OPN is acutely upregulates and induces a range of cellular responses and promotes cell adhesion, proliferation, migration, and survival of endothelial cells, vascular smooth muscle cells and macrophages[61, 106]. OPN expression is not only elevated in disease pathologies of CVD but in other inflammatory diseases such as multiple sclerosis, Crohn disease, wound healing and a number of cancer pathologies[106]. Furthermore, in addition its role in regulating vascular calcification, OPN has other multifunctional roles in the vasculature and has been shown to enhance vascular in addition, remodelling and angiogenesis through the activation of matrix metalloproteinases (MMPs)[107]. OPN isoforms have been shown to differentially promote arteriogenesis in response to ischemia via macrophage accumulation and survival in OPN deficient mice[108], thus highlighting its role in regulating angiogenesis.

1.7.3.4 Matrix Gla Protein (MGP)

Matrix Gla Protein also known γ-carboxyglutamate protein (MGP) is a vitamin K-dependent protein and is a strong calcification inhibitor. MPG is primarily produced by chondrocytes and VSMCs in the arterial tunica media. However MGP functionality requires vitamin-K dependent γ -carboxylation and activation within the endoplasmic reticulum[61]. MPG carries out its function to inhibit VC by binding directly to BMP2, thus inhibiting BMP/BMPR2 interactions which results to further inhibition of VSMC osteoblastic differentiation[61]. Calcified vessels show increased expression of calcification markers such as type II collagen and osteocalcin while exhibiting reduced expression of MGP[61]. In addition, MGP null mice have been used to study calcification, and these mice demonstrate extensive arterial calcification in the first weeks of life even in the absence of atherosclerosis[109].

Furthermore, the role of MGP in regulating capillary function and angiogenesis has been previously explored[110-112].

1.7.3.5 Fetuin-A

In contrast to other inhibitors that are found within the vessel wall, Fetuin-A is a circulating inhibitor of calcification found in serum and is predominately synthesized by the liver[61, 93]. In vitro, Fetuin-A binds to Ca^{2+} to inhibit de novo hydroxyapatite crystal formation but does not affect the crystals once formed[93]. Fetuin-A is also expressed in secreted matrix vesicles during vascular calcification; as VSMCs are able to take up circulating Fetuin-A and store it in their ECM-bound matrix vesicles that are known to form a nidus for mineral deposition (site of mineralisation)[93]. In vivo, Fetuin-A null mice demonstrate extensive calcification in different organs including the liver, kidneys, myocardium, tongue, and skin. In chronic kidney patients, reduced Fetuin-A levels are highly associated with increased mortality rates[113].

1.7.3.6 Klotho

The Klotho gene is an aging suppressor that plays important role in regulating mineral metabolism. Klotho protein is responsible for regulating calcium and phosphorus levels in blood, bones and cerebrospinal fluid of all vertebrates[114]. Furthermore, circulating blood levels of Klotho protein are reduced in blood and urine of CKD patients, a population who suffer from vascular calcification. Klotho null mice are widely used to study calcification in CKD, and have been shown to have ectopic calcification in the medial layer of the arteries, arterioles and in the parenchyma of other organs, and develop osteoporosis, and also suffer from premature aging[92, 115]. Furthermore, a defect in this gene in mice results in a syndrome

that resembles human ageing with significantly decreased lifespan, arteriosclerosis, skin atrophy and infertility[92].

1.7.3.7 Inorganic Pyrophosphate

Inorganic pyrophosphate (PP_i) is a potent endogenous inhibitor of vascular calcification that regulates its function via paracrine signalling[61, 93]. Pyrophosphate carries out its function by direct inhibition of hydroxyapatite formation and has also been shown to inhibit VSMC transdifferentiation into osteoblast-like cells, one possible theory for the pathogenesis of VC. PP_i is synthesized by ectonucleotide pyrophosphatase/phosphodiesterase (eNPP), which drives the hydrolyses of extracellular adenosine-5′-triphosphate (ATP) to generate PP_i and AMP. The lack of PP_i and mutations in eNPP1 results in extensive medial calcification in humans[116].

1.7.3.8 Molecular Drivers of Vascular Calcification

A number of potent transcription factors that regulate many osteoblast and chondrocyte functions in bone have been identified in the regulation of VC. These include alkaline phosphatase (ALP), runt-related transcription factor (Runx2) or core binding factor α-1 (Cbfa-1), bone morphogenetic proein-2 (BMP2) and members of the tumour necrosis factor superfamily, receptor activator of nuclear factor-κB ligand (RANKL) and it receptor RANK; and its decoy ligand osteoprotegerin (OPG).

1.7.3.9 Alkaline Phosphatase (ALP)

Alkaline phosphatase (ALP) is a key transcription factor that is released early on during calcium deposition. It is often used as a clinical diagnostic marker of VC, as an early indicator of extracellular matrix (ECM) deposition [61, 80]. Changes in ALP levels are a prominent feature in bone diseases, CKD and cardiovascular diseases, specifically atherosclerotic lesions with vascular calcification[100]. ALP activity is crucial for the process of endochondral ossification as it helps with hydroxyapatite deposition. Furthermore, SMCs express high levels of ALP during medial calcification. The molecular mechanisms by which ALP regulates VC is via decreasing levels of inorganic pyrophosphate, a known potent inhibitor of calcification[61]. The role of ALP in angiogenesis has been well explored in bone cells; with VEGFA reported to stimulate ALP activity[117], and hypoxia shown to increase ALP activity[118].

1.7.3.10 Runt Related Transcription Factor (Runx2)

Runx2 is a master regulator of bone differentiation that is expressed throughout skeletal development and is crucial for vascular invasion[119]. This protein serves as a very important transcription factor that triggers the expression of other major osteoblast-specific lineage genes including Osteopontin (OPN), osteocalcin and type 1 collagen[90]. Runx2 is also co-localized within calcified atherosclerotic plaques and can be found in calcified arterial tissues[79]. Runx2 activation can occur via several routes including the mitogen activated protein kinase (MAPK) and through the extracellular-signal regulated kinase 1/2 (ERK1/2). Runx2 binds to the osteoblast-specific cis-acting element 2 which is found in the promoter regions of all other major osteoblast-specific genes including ALP and Osteopontin.

Inorganic phosphate known to induce VSMC transdifferentiation into bone-like cells induces Runx2 expression[79].

The relationship of Runx2 with angiogenesis has not been fully described however, a deficiency in Runx2 is reported to result in vascularization defects, mainly due to reduced VEGF expression[120, 121]. Runx2 has also been shown to increase HIF-1α protein expression, mainly because it stabilises and protects HIF-1α from degradation, in both normoxic and hypoxic conditions[121]. Overexpression of Runx2 is also associated with significant increases in *Vegfa* mRNA expression, and vice versa. This is thought to occur due to physical interactions of Runx2 and HIF-1α on the Runx2/RUNT domain[122] and possibly through binding of Runx2 on the VEGF promotor region[120]. Since Runx2 is expressed in ECs of developing blood vessels[123], this may explain its role in regulating angiogenesis, and highlights the need for further studies to expand our understanding of this relationship.

1.7.3.11 Bone Morphogenetic Protein (BMP2)

Bone morphogenetic proteins (BMPs) are potent osteogenic differentiation mediators of bone formation; and their role as inducers of vascular calcification has been well established[124, 125]. They are expressed in several cell types of atherosclerotic lesions by endothelial cells, smooth muscle cells and foam cells[61, 125]. BMP2 is a member of the transforming growth factor β-superfamily that is expressed in small amounts in healthy arterial walls[63]. BMP2 has been demonstrated to cause ectopic mineralization in muscle tissue and SMC mineralization both in vitro and in vivo[126]. BMP2 has been linked with endothelial dysfunction, due to its high expression during pathological stimuli such as oxidative stress and inflammation, which induce vascular calcification[61, 125]. In these pathological states, BMP2 induces differentiation of smooth muscle cells towards an

osteoblastic phenotype, thereby promoting calcification. In one study, it was reported that decreasing BMP signalling resulted in a reduction in both atherosclerotic lesion and diabetic medial calcification[125]. BMP2 is expressed in the vascular media where it exerts its osteoinductive effect, whereas BMP4, an isoform of BMP is more expressed in the endothelial cells[61, 125].

1.7.3.12 RANK-RANKL-OPG Cytokine Pathway

Recent molecular and biological studies have suggested that bone-associated genes expressed in vascular tissue may play an important role in the pathophysiology of medial arterial calcification[127, 128]. These pro-calcifying and anti-calcifying regulatory cell biomarkers include osteoprotegerin (OPG), receptor activator of nuclear factor-κB ligand (RANKL) and it receptor RANK; which are all members of the TNF-related family, involved in the homeostasis of bone metabolism[129].

1.7.3.13 Receptor Activator of Nuclear Factor-κB (and Ligand)

RANKL is expressed in tissues such as the heart, lung, kidney, thyroid and in cell types of osteoblasts, stromal cells, T cells and endothelial cells and has been found in calcified valves[128, 130, 131]. RANKL interacts with its cognate receptor RANK, a transmembrane protein located on osteoclast precursors, known to induce osteoclastogenesis through NFκB[131, 132]. Regulatory factor OPG functions as an inhibitor for the process of vascular calcification in the normal vasculature[128]. OPG is expressed at high levels in a variety of tissue including arterial smooth muscle cells and endothelial cells; unlike RANKL and RANK, which are not expressed in cardiovascular tissue under normal physiological conditions[128].

1.7.3.14 Osteoprotegerin (OPG)

OPG is a member of the tumour necrosis factor (TNF) receptor superfamily, also known as tumour necrosis factor receptor superfamily member 11B (TNFRSF11B). It is a cytokine receptor that serves as a soluble decoy receptor for RANKL and TNF-related apoptosis-inducing ligand (TRAIL)[133]. It binds to RANKL and therefore negatively regulates the interaction between RANKL and RANK, thus preventing osteoclast differentiation **(Figure 1.10)**[128, 130, 131]. On the other hand, OPG is also able to bind to TRAIL to inhibit apoptosis of transformed cells and tumour cells, by enhancing endothelial cell survival and acting as a "survival factor[134 133]. Because of this, OPG is considered to be a promising therapeutic candidate as it prevents bone lesions and can inhibit tumour growth. Although OPG is predominantly released in bone, it is also expressed in other tissues such as the lung, heart and blood vessels. OPG is secreted by ECs and their progenitors as well as by VSMCs, megakaryocytes and platelets[135]. OPG expression is also evident in the endothelium of early human atherosclerotic lesions, with another in vitro study showing OPG and RANKL expression in VSMCs and endothelial cells.

There however lies much controversy regarding the role of OPG in disease, with emerging evidence that suggests that OPG does not merely serve a protective factor for bone, but may also be a novel biomarker for cardiovascular disease and arteriosclerosis[136]. OPG has been identified as a pro-angiogenic factor for angiogenesis[137] and is known to enhance the pro-angiogenic properties of endothelial colony-forming cells in

vitro and promote vasculogenesis in vivo[135]. However, despite this, there is growing clinical, epidemiological and experimental evidence for the role of OPG in disease. Elevated OPG serum levels have been associated with the severity of CVD such as atherosclerosis and myocardial ischemia[134, 138, 139]. OPG levels are predictive of coronary artery disease (CAD) as reported in the Framingham Heart Study where participants demonstrated a positive association with circulating OPG levels and CVD incidence and mortality[140]. Furthermore, OPG is known to be associated with severity of osteosclerosis and increased number of disease vessels in type 2 diabetes mellitus[141], atherosclerotic plaque calcification[142], worse long-term cardiac outcomes in patients with acute coronary syndrome (ACS)[143], increased severity and progression of carotid artery disease in cerebrovascular diseases[134] and has been shown to decrease osteoclastic differentiation in stenosis and aortic valves during valvular heart disease[144].

Published murine models for calcification using OPG knockout mice have demonstrated that these mice develop severe hypercalcemia and early calcium deposits within the media and subintima of the aorta, which is accompanied by the formation of typical bone matrix[145, 146]. Furthermore, OPG deficient mice experience significant calcification in their aortas and renal arteries, with increased osteoporosis and advanced plaque progression; confirming both its crucial role in bone metabolism and protective role in VC[128, 145.]. Other studies using this murine knockout model of calcification demonstrated that when OPG deficient mice were treated with WP9QY (W9) peptide, that binds to RANKL to block RANKL-induced osteoclastogenesis; (W9) restored alveolar bone loss in $OPG^{-/-}$ mice by suppressing osteoclastogenesis and enhancing osteoclastogenesis[147]. OPG deficient mice have also been used to study bone marrow adipogenesis, with one study reporting greater number of adipocyte accumulation in the bone marrow of 12-week-old $OPG^{-/-}$ mice compared

to those occurring in bone marrow of wildtype mice[148]. In addition, OPG inactivation in apolipoprotein-E (ApoE)-knockout mice has shown to accelerate advanced atherosclerotic lesion progression and vascular calcification, therefore highlighting its protective role in disease[149]. However, to date, no studies have used this murine model to understand the role of a calcification milieu on ischemia and inflammatory-driven angiogenesis.

Vascular inflammation is also known to regulate OPG expression. Pro-inflammatory mediators such as interleukins- α and growth factors such as platelet-derived growth factors (PDGFs) are able to induce OPG expression in ECs and VSMCs[134, 136]. Despite the evidence available to suggest the role of OPG in vascular pathophysiology, it still remains unclear whether OPG serves a favourable or detrimental effect on the vasculature. In most instances where OPG expression is upregulated, it has been proposed to be a compensatory vascular defence mechanism, to try and stop the activation of other inflammation pathways, a response that is seen in atherosclerosis where OPG expression is highly elevated[134, 139].

OPG-RANK-RANKL Cytokine Pathway In Vascular calcification

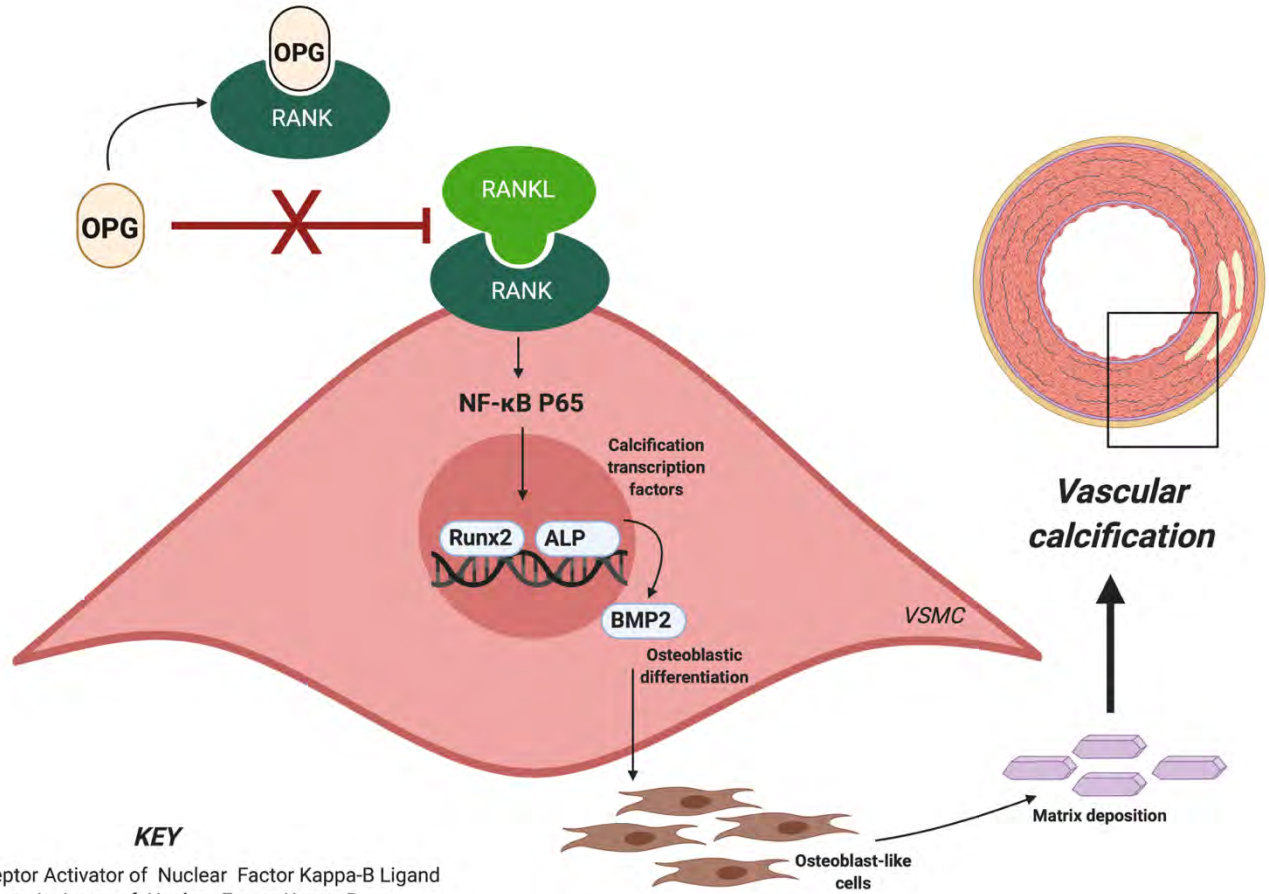

KEY

RANKL: Receptor Activator of Nuclear Factor Kappa-B Ligand
RANK: Receptor Activator of Nuclear Factor Kappa-B
NF-κB P65: Nuclear Factor Kappa-light-chain-enhancer of Activated B Cells
OPG: Osteoprotegerin
BMP2: Bone Morphogenetic Protien 2
Runx2: Runt-related Transcription Factor
ALP: Alkaline Phosphatase
VSMC: Vascular Smooth Muscle Cell

Figure 1.10: Mechanistic pathway illustrating the RANK-RANKL-OPG axis in vascular calcification. Under pro-calcific conditions, RANKL binds to its physiologic receptor, RANK, which in turn promotes osteoclast differentiation and mineral deposition. However, osteoprotegerin (OPG), a decoy ligand interferes with the interaction between RANK and RANKL and inhibits this process.

1.8 Evidence for Calcification and Angiogenesis

Previous studies have demonstrated that angiogenesis may be associated with vascular calcification in blood vessels and heart valves[62]. The first evidence to suggest that soft tissue calcification may be associated with angiogenesis came from imaging studies from the 1980's, whereby silicone polymers were injected into cleared fixed human hearts, and the pattern of vascular filling was recorded by cinematography[62]. Analysis of these cinematographic images showed that abundant neovascularization was associated with sites of lesional calcification in the media and neointima of these lesions[62]. They further identified that around calcified deposits, there was increased proliferation of newly formed vessels [62]. This data however only provides evidence for the role of angiogenesis in the initiation of ectopic calcification in atheromatous lesions and not in blood vessels.

There is growing evidence that ectopic calcification of blood vessels and cardiac valves are associated with angiogenesis[51, 62,150]. The OPG/RANK/RANKL pathway has been suggested to regulate angiogenesis in numerous studies[51, 62,150]. RANKL treatment stimulated angiogenesis in vivo and in vitro by acting as a chemostatic factor for ECs and inducing their migration and proliferation[150,129, 151]; increased vascular permeability and promoted neoangiogenesis via induction of EC migration and proliferation[51, 150, 152]. However, conflicting studies have reported RANKL to cause a reduction in EC proliferation, while inducing endothelial cell apoptosis, therefore suggesting RANKL to be an inhibitor of angiogenesis[153]. Furthermore, the pro-angiogenic role of OPG has been well described to have effects on mature ECs by enhancing EC chemotaxis and cell survival[137, 154]; while promoting cell proliferation and vascular cord formation in Matrigel both in vitro and in vivo[135 153, 155], therefore proposing its potential role in maintaining EC integrity[154]. In addition, VEGFA has been shown to increase the mRNA

expression of *Rank* in human ECs, which upregulated their angiogenic response to RANKL[51,150,45]. It was also shown that in co-cultures of endothelial cells with osteoblasts, proliferation of ECs was enhanced by the production of osteoblast-derived angiogenic factors such as VEGFA[156]. Based on this evidence, the OPG/RANK/RANKL triad may have a potential role in regulating angiogenesis.

During angiogenesis, BMP2 and BMP4 along with other angiogenic factors such as VEGF have shown to induce endothelial cell migration and proliferation[61, 62]. As discussed earlier, endothelial cell migration and proliferation are critical processes needed for angiogenesis. Collett and Canfield[24,] reported that differentiation of VSMCs is brought about by an inflammatory stimuli, which triggers activation of specific osteogenic signals such as BMP2, which thereby stimulate differentiation of VSMCs into osteoblast-like cells, a well proposed mechanisms of vascular calcification [61, 62, 157]. There lies extensive data showing that BMP2 is capable of driving angiogenesis via the induction of VEGFA expression, particularly in cancer pathologies[158, 159]. However, the mechanisms by which BMP2 stimulates angiogenesis in endothelial cells have not been established.

Inflammatory mediators derived from monocyte-macrophages such as TNFα, have been reported to contribute to the progression of VC by promoting osteoblastic differentiation of VSMCs, leading to mineralisation. Furthermore, calcium phosphate mineral deposition is known to elicit an inflammatory response, by stimulating TNF production by macrophages[160, 161]. Though the mechanisms of vascular calcification have been intensely studied for many years, the understanding of its effects on inflammatory-driven angiogenesis in endothelial cells is still incomplete.

1.9 Hypotheses and Aims

The regulation of angiogenesis is important for the treatment of cancer and ischemic diseases. Therapeutic strategies are aimed to deliver single growth factors as treatment options and have been shown to lack efficacy. Despite the abundance of evidence regarding the presence of VC in PAD, the underlying mechanisms remain unknown. Moreover, the presence of calcification and a highly calcific environment has not been studied as a deterrent of this angiogenic process. Therefore, given the above rationale, the studies described in this thesis aimed to:

a) Characterise the effect of high calcium on endothelial cell hypoxia-driven angiogenesis in vitro.

b) Investigate role of a calcification milieu on ischemia-driven angiogenesis in vivo, using the hind-limb model of angiogenesis in OPG knockout mice.

c) Elucidate the role of inflammatory stimuli in driving calcification-induced angiogenesis in endothelial cells in vitro

d) Determine the role of calcification on inflammatory-driven angiogenesis using a peri-arterial cuff in OPG knockout mice.

The hypothesis of this body of work was that high calcium will negatively affect endothelial cell angiogenesis in vitro and that the presence of a calcific milieu will impact ischemia-driven and inflammatory-driven angiogenesis in vivo.

CHAPTER 2:

GENERAL METHODS

2. IN VITRO METHODOLOGY

Table 1: General Solutions & Reagents

Reagent/Material (Product Code)	**Manufacturer**
1-Bromo-3-chloropropane (B9673)	Sigma-Aldrich, MO, USA
1Kb Plus DNA Ladder (10787018)	ThermoFisher Scientific, MA, USA
1-Palmitoyl-2-linoleoyl-phosphatidylcholine (850458P)	Avanti Polar Lipids, AL, USA
Agarose (A9539)	Sigma-Aldrich, MO, USA
Ammonium bicarbonate (A6141)	Sigma-Aldrich, MO, USA
Biotium-GelRedTM 10,000X in Water (GTS41003)	Adelab Scientific, SA, Australia
BoltTM 4-12% Bis-Tris Plus Gels, 10-wells (NW04120BOX)	Life Technologies, CA, USA
BoltTM 4-12% Bis-Tris Plus Gels, 12-wells (NW04122BOX)	Life Technologies, CA, USA
BoltTM 4-12% Bis-Tris Plus Gels, 17-wells (NW04127BOX)	Life Technologies, CA, USA
BoltTM LDS Sample Buffer 4X (B0007)	Life Technologies, CA, USA
BoltTM MES SDS Running Buffer 20X (B0002)	Life Technologies, CA, USA
BoltTM Reducing Agent 10X (B0004)	Life Technologies, CA, USA
Bovine serum albumin (A7906)	Sigma-Aldrich, MO, USA
Calcium Assay Kit (701220)	Cayman Chemical
Calcium Chloride	Sigma-Aldrich, MO, USA
Chloroform (AJA152-2.5L GL)	Ajax Finechem, NSW, Australia
Clarity Western ECL Substrate (1705061)	Bio-Rad Laboratories, CA, USA
Ethanol (E7023)	Sigma-Aldrich, MO, USA
Ethanol (100%) for histopathology (FNNJJ008)	Fronine, NSW, Australia
Fluorescence Mounting Media (S302380-2)	Dako, CA, USA
Foetal bovine serum (AU-FBS/PG)	CellSera, NSW, Australia
Formalin (HT501128)	Sigma-Aldrich, MO, USA
Glacial acetic acid (AJA1-2.5L PL)	Ajax Finechem, NSW, Australia
Glycine (G7126)	Sigma-Aldrich, MO, USA

Goat serum (G9023)	Sigma-Aldrich, MO, USA
Guanidine hydrochloride (G4505)	Sigma-Aldrich, MO, USA
Hexadimethrine bromide (H9268)	Sigma-Aldrich, MO, USA
Hydrogen peroxide solution (216763)	Sigma-Aldrich, MO, USA
iBlotTM 2 Transfer Stacks, regular size (IB23001)	Life Technologies, CA, USA
iBlotTM 2 Transfer Stacks, mini size (IB23002)	Life Technologies, CA, USA
ImmPACT® DAB Peroxidase Substrate (SK-4015)	Vector Laboratories, CA, USA
SsoAdvancedTM Universal SYBR® Green Supermix (1725275)	Bio-Rad Laboratories, CA, USA
iScript cDNA Synthesis Kit (1708841)	Bio-Rad Laboratories, CA, USA
Isopropanol (I9516)	Sigma-Aldrich, MO, USA
LabAssay ALP kit (29158601)	Wako Diagnostics, VA, USA
Lillie Mayer's haematoxylin (AHLM)	Australian Biostain, VIC, Australia
Matrigel® Growth Factor Reduced Basement Membrane Matrix (356231)	Corning Life Sciences, NY, USA
MesoEndo Cell Growth Medium (212-500)	Cell Applications Inc., CA, USA
Methanol (MA004)	Chem-Supply, SA, Australia
NE-PER® Nuclear and Cytoplasmic Extraction Reagents (78833)	ThermoFisher Scientific, MA, USA
Normal horse serum (S-2000)	Vector Laboratories, CA, USA
Nuclease-free water (P1193)	Promega, WI, USA
Opti-MEMTM I Reduced Serum Media (31985070)	Life Technologies, CA, USA
Paraformaldehyde (C004)	ProSciTech, QLD, Australia
Phosphatase Inhibitor Cocktail 2 (P5726)	Sigma-Aldrich, MO, USA
Phosphate-buffered saline (D1408-500ML)	Sigma-Aldrich, MO, USA
Phenylmethylsulfonyl fluoride solution (93482)	Sigma-Aldrich, MO, USA
Phospholipid C Assay Kit (997-01801)	Wako Diagnostics, VA, USA
Pierce BCA Protein Assay Kit (23227)	ThermoFisher Scientific, MA, USA
Polyethylene glycol (P2139)	Sigma-Aldrich, MO, USA
Ponceau S solution (P7170-1L)	Sigma-Aldrich, MO, USA
Potassium bromide (PA006)	Chem-Supply, SA, Australia
Precision Plus Protein Dual Color Standards (1610374S)	Bio-Rad Laboratories, CA, USA

Protease Inhibitor Cocktail (P8340)	Sigma-Aldrich, MO, USA
Proteinase K (17916)	ThermoFisher Scientific, MA, USA
Recombinant human VEGF 165 (293-VE-010)	R&D Systems, MN, USA
RestoreTM Western Blot Stripping Buffer (21059)	ThermoFisher Scientific, MA, USA
Sodium azide (SA189)	Chem-Supply, SA, Australia
Sodium chloride (71380)	Sigma-Aldrich, MO, USA
Sodium Phosphate (S3264-500G)	Sigma-Aldrich, MO, USA
Sodium cholate (C6445)	Sigma-Aldrich, MO, USA
Sodium citrate tribasic dihydrate (C8532)	Sigma-Aldrich, MO, USA
Sodium dodecyl sulfate (L3771)	Sigma-Aldrich, MO, USA
Sodium orthovanadate (S6508)	Sigma-Aldrich, MO, USA
Tissue-Tek® O.C.T. compound (IA018)	ProSciTech, QLD, Australia
TRI® Reagent (T9424)	Sigma-Aldrich, MO, USA
Trichrome Stain Kit (ab150686)	Abcam, Cambridge, UK
Tris hydrochloride (T3253)	Sigma-Aldrich, MO, USA
Tris(hydroxymethyl)aminomethane (AJA2311)	Ajax Finechem, NSW, Australia
Triton X-100 (X100)	Sigma-Aldrich, MO, USA
Trypsin-EDTA (15400054)	ThermoFisher Scientific, MA, USA
Tumour Necrosis Factor-α _Human, (T0157) _ _	Sigma-Aldrich, MO, USA
Trypan Blue solution (T8154)	Sigma-Aldrich, MO, USA
Tween®-20 (P9416)	Sigma-Aldrich, MO, USA
Vectashield® Antifade Mounting Medium with DAPI (H-1200)	Vector Laboratories, CA, USA
Vector® Red Alkaline Phosphatase Substrate kit (SK-5100)	Vector Laboratories, CA, USA
WST-1 Reagent	Roche Applied Science, Mannheim, Germany
Xylene (FNNJJ028)	Fronine, NSW, Australia

2.1 Cell Culture

Human Coronary Artery Endothelial Cells (HCAECs) (Cell Applications) were cultured in MesoEndo Cell Growth Media (Sigma-Aldrich), supplemented with 5% fetal bovine serum (FBS), 10 µg/ml streptomycin, 10 U/ml penicillin and 1 mM L-glutamine, in a T-75cm^2. Cells were grown to 80% confluency and washed with Dulbecco's Phosphate Buffered Saline (PBS) (Sigma-Aldrich) before seeding in 6 well plates. Cells were serum starved for 24 h in Medium-199 (Sigma-Aldrich) containing 10% FBS, supplemented with Earle's salts, L-glutamine and $NaHCO_3$, also containing 1.36mM calcium, a no treatment (NT) control. To induce phosphate mediated calcification, CM was supplemented with calcium and phosphate (2.7mM $CaCl_2$ and 2.0mM NaH_2PO4) referred to as calcification medium (CM).

Cell culture experiments were conducted under 2 different conditions: (1) inflammation or (2) hypoxia. Cells were incubated and maintained in a 37° C humidified atmosphere of 5% CO_2 for 24 h for Normoxic conditions. A hypoxic environment was achieved by incubation in a hypoxic incubator with conditions of 1.2% O_2/5% CO_2 balanced with N_2. For inflammation, cells were pre-treated for 4 h with tumour necrosis factor alpha (TNF-α) at a concentration of 10 ng/mL. Tissue culture media was changed every 2-3 days. All experiments were carried out in triplicates. All cells were used between passages 2 and 5 only in vitro.

2.2 Functional Studies

2.2.1 Tubulogenesis Matrigel Assay

To assess tubulogenesis, growth factor reduced Matrigel (company) was thawed and carefully plated at 40 µL/well into a 96 well plate, ensuring no bubbles were present. This

was left to polymerise at 37°C for 30 minutes. HCAECs were plated at 1 x 10^5 cells/mL in 100 µL MesoEndo Endothelial Cell Media (212-500, Cell Applications Inc., California, USA) and under hypoxia was stimulated with (1.2% O2/ 5% CO2) conditions at 37°C for 4 – 6 hours. HCAEC tubule formation performed for a total of 4 hours and images were imaged at 10X magnification and counted in a minimum of 3 fields of view per well using Image J (National Institutes of Health, Maryland, USA).

2.2.2 Boyden Chamber Cell Migration Assay

HCAECs were cultured and treated as previously described. Cells were harvested using Trypsin EDTA (Sigma-Aldrich) and resuspend in 500 µl of 3% FBS Opti-MEM medium (Gibco) to make up cell suspension. 600 µl of migration media (3% FBS Opti-MEM medium containing VEGF 10 ng/mL) was carefully added to the bottom chamber of 24 well Transwell, ensuring no bubbles were present. 100 µL cell suspension at a density of 1 x 10^5 cells/mL was added into each transwell insert, ensuring that there are no air bubbles on or below the membrane. Plates were incubated overnight at 37°C. The following day, media was carefully aspirated from the upper chamber. Transwell inserts was removed and cells on the upper surface of the transwell membrane were carefully scraped away using a cotton tip. Transwells were then submerged in 1mL of 1x PBS for approximately 1 min to rinse, and then transferred into 4% paraformaldehyde in PBS for 10 min to fix. Excess medium was aspirated from the transwell inserts, and membranes cut out using a scalpel blade, and membranes were placed cell side up onto labelled slides. DAPI staining for nuclei was used to stain membranes. Slides were imaged at 20x magnification in the dark at five separate fields at same magnification with a fluorescent microscope. Analysis for cell counts were performed using ImageJ (National Institutes of Health, Maryland, USA).

2.2.3 Cell Viability Assay

A functional WST-1 cell viability assay was used to assess the effect of calcification stimuli on cell viability in vitro. WST-1 is a colorimetric assay by which the reduction of tetrazolium compound to its formazan products by mitochondrial dehydrogenase activity is measured in viable cells. The greater the number of viable cells and metabolically active cells present, the greater the amount of formazen product formed following the addition of WST-1.

HCAECs were cultured as previously described. Cells were stained for viability with Trypan Blue solution (Sigma-Aldrich) and counted using a haemocytometer. Cells were seeded in a 96 well plate at a density of 10 X 10^3 cells/mL for 24 h, and seeded overnight in low serum media M199, containing 10% FBS. Following treatment for 24 h, cell proliferation reagent WST-1 (Roche, Life sciences) was prepared in a 1:10 final dilution (10 µl/well WST-1 reagent), with a total volume of 100 µL/well, and was added to cells. Cells were incubated in a humidified atmosphere 37°C, 5% CO_2, protected from light, and following a 4 hour incubation period, the formazan products was quantified at 450 nm using the BIO-RAD iMark™ Microplate Reader. Unless otherwise stated, all experiments were carried out in triplicates, with data from 3 independent experiments averaged and used for analysis.

2.2.4 Mechanistic Studies

Mechanistic studies were conducted to assess the effect of calcification on both ischemia-driven and inflammatory driven angiogenesis in vitro. Cells were plated in 6 well plates at a cell density of $1x10^5$ cells/mL. For inflammatory studies, cells were incubated with TNF-α at

10 ng/mL for 4 hours in 10% M199 medium as described earlier and were harvested accordingly for western blotting analysis.

2.2.5 Protein Extraction

Treated cells were harvested from 6 well plates after 24 h. Media was removed, and cells were washed once in cold PBS. Radioimmunoprecipitation assay (RIPA) lysis buffer (20 mM Tris-HCl, 1 mM EDTA, 1 mM EGTA, 1 mM dithiothreitol, 0.5 mM phenylmethylsulphonyl fluoride, 1.5 µg/mL aprotinin, 1 µg/mL leupeptin, 1 µg/mL pepstatin, 1 mM sodium orthovanadate, and 0.2% Triton X-100; pH 7.4), protease inhibitor cocktail (1:100, P8340, Sigma-Aldrich) was added to cells in 100µL (1:100), along with protease inhibitor cocktail (1:100, P8340, Sigma-Aldrich), and phenylmethanesulfonyl fluoride solution (93482, Sigma-Aldrich), and was transferred to Eppendorf tubes. Each sample was sonicated for 2 seconds to further lyse the sample and were centrifuged for 10 minutes at 14,000 rpm at 4^{o}C and stored at -80^{o}C.

2.2.6 Nuclear Extraction

To extract the nuclear fraction of incubated cells, the NE-PER Nuclear and Cytoplasmic Extraction kit (PIE78833, Thermo Fisher Scientific) was used. Following 24 h treatment in 6 well plates, cells were harvested as previously described to achieve a pellet in an Eppendorf tube. Nuclear and Cytoplasmic tubes were labelled and pre-chilled on ice before beginning the assay. To begin extraction, 50 µL ice cold CER I reagent was added to each tube. Tubes were vortexed for 15 seconds before incubation on ice for 10 minutes. Following this, 5 µL CER II reagent was added, tubes were vortexed for 5 seconds and allowed to incubate on ice for 1 minute. Tubes were vortexed once more prior to centrifugation at 16,000 g for 5 minutes at 4^{o}C. The supernatant containing the cytoplasmic fraction was transferred to a new

tube and stored at -80°C. The pellet containing the nuclear fraction was resuspended in 25 µL ice cold NER reagent by vortexing for 15 seconds at 10-minute intervals for a total of 40 minutes. Samples were kept on ice between vortexing. Samples were then centrifuged at 16,000 g for 10 minutes and the supernatant containing the nuclear fraction was transferred to new Eppendorf tubes and stored at -80°C.

2.2.7 Protein Estimation

The protein concentration for each sample was determined using the Bicinchoninic (BCA) Protein Assay (Thermo Fisher Scientific). A standard curve using bovine serum albumin (BSA, A7906-100G, Sigma-Aldrich) concentrations of 0, 0.25, 0.5, 0.75, 1.0, 1.25, 1.5, 2.0 mg/mL was constructed from 2 mg/mL BSA stock as prepared in Table 2.1.

Table 2.2: Standard BSA Solutions Used in BCA Assay.

Standard Protein concentrations		
BSA (mg/mL)	**BSA stock (µL)**	**MilliQ water (µL)**
0	0	600
0.25	75	525
0.5	150	450
0.75	225	375
1	300	300
1.25	375	225
1.5	450	150
2	600	0

This assay was performed in a 96 well plate. 5 µL of standard and sample was added to each well in duplicate, and 195 µL of reagent mix consisting of 50 parts reagent A (23223, Thermo Fisher Scientific) and 1-part reagent B (copper (II) sulphate) (23224, Thermo Fisher Scientific). The plate was then incubated at 37°C for 30 minutes and absorbance of each well measured at 595 nm using microplate reader (Flex Station 3, Molecular Devices, San Jose, CA, USA) using the SoftMax Pro program (v5.3, Molecular Devices) for data acquisition and analysis. The protein concentration of unknown samples was interpolated from the standard curve using GraphPad Prism, Version 8.

2.2.8 Western Blotting

Whole cell protein lysate was used to determine changes in angiogenic and calcification markers. To prepare samples, protein was added to 8 µL Boltᵀᴹ LDS Sample Buffer (4X) and 3 µL Boltᵀᴹ Reducing Agent (10X) that had been diluted 1:10 in distilled water from the stock provided. Samples were then denatured by heating at 95ºC for 5 minutes before placing on ice for 2 minutes. 8 µL of (ladder name) Pre-stained Protein Standard (Life Technologies) and 40 µL sample were loaded into 10, 12 and 17 well Bolt® 4% Bis-tris plus gel (Life Technologies). Equal protein of 10-20 µg was loaded on each gel. Gels were run at 120 V for 1 hour and 15 minutes in Bolt® MES SDS Running Buffer Life Technologies) diluted in distilled H2O. Following this, proteins from the gel were then transferred onto nitrocellulose membranes (Life Technologies) using the iBlot Gel Transfer system (Life Technologies) run at 20 V for 7 minutes. Membranes were then blocked in 10% (w/v) skim milk or 5% BSA (Sigma Aldrich) in 1xTBST (20 mM Tris, 136 mM NaCl, and 0.1% [w/v] tween 20, pH 7.4) for 1 hour at room temperature on a rocking platform. Following this, membranes were washed 3 times in TBST for 5 minutes at room temperature. Membranes were probed with

antibodies as for total HIF-1α (Novus, NB100-449, 1:500), VEGFA (Abcam, ab461154, 1:2000), Runx2 (D130-3; MBL, 1:1000), RANKL (Santa Cruz, Sc3770779, 1:500), BMP2 (Novus, NOVNBP119751, 1:1000), total eNOS (BD, 610297, 1:1000), phosphorylated (S^{1177}) eNOS (BD, 61293, 1:1000), total Erk1/2 (Cell Signalling Technology; 9102, 1:1000), phosphorylated (Tyr^{202}/Tyr^{204}) Erk1/2 (Cell Signalling Technology; 4370, 1:1000), total p38 MAPK (Cell Signalling Technology; 86901, 1:1000), phosphorylated p38 MAPK (T^{180}/Y^{182}), (Cell Signalling, 4511, 1:1000), total VEGFR2 (2479; Cell Signalling Technology, 1:1000), phosphorylated (y^{1175}) VEGFR2 (Cell Signalling 2478, 1:1000), PHD2 (Novus, NB100-2219, 1:1000), PHD3 (Novus, NB100-303, 1:1000). Even loading was confirmed by alpha-tubulin (Abcam, ab729, 1:5000) for total lysate; and Lamin B 1 Nuclear Envelope Marker (Abcam, ab160-048, 1:1000) for nuclear extracts. Membranes were developed by chemiluminescence on the Chemidoc MP Imaging System (machine details) with ECL reagents in a 1:1 ratio of Clarity Western Peroxide Reagent and Clarity Western Luminol/Enhancer Reagent (170-5061, Biorad). Images were recorded using Image Lab Software (v.5.0, 170-9692, BioRad).

Treated cells were harvested from 6 well plates 24h later. Media was removed, and cells washed once in cold PBS. Radioimmunoprecipitation assay (RIPA) lysis buffer (20 mM Tris-HCl, 1 mM EDTA, 1 mM EGTA, 1 mM dithiothreitol, 0.5 mM phenylmethylsulphonyl fluoride, 1.5 μg/mL aprotinin, 1 μg/mL leupeptin, 1 μg/mL pepstatin, 1 mM sodium orthovanadate, and 0.2% Triton X-100; pH 7.4), protease inhibitor cocktail (1:100, P8340, Sigma-Aldrich) was added to cells in 100 μL (1:100), along with protease inhibitor cocktail (1:100, P8340, Sigma-Aldrich), and phenylmethanesulfonyl fluoride solution (93482, Sigma-Aldrich), and was transferred to Eppendorf tubes. Each sample was sonicated for 2 seconds to further lyse the sample and were centrifuged for 10 minutes at 14,000 rpm at 4°C and stored at -80°C. Protein concentrations were determined using the bicinchoninic assay (BCA), and total protein concentration between 10-15 μg of the protein were loaded for

Western blot analysis and probed with antibodies as for total HIF-1α (Novus, NB100-449, 1:5000), VEGF (Abcam, ab461154, 1:2000), and nuclear NF-κB (P65) (Abcam, ab86299). Even loading was confirmed by alpha-tubulin (Abcam, ab729, 1:5000) for total lysate; and Lamin B 1 Nuclear Envelope Marker (Abcam, ab160-048, 1:1000) for nuclear extracts. Protein levels were quantified and analysed using Bio-Rad ImageLab software (Bio-Rad Laboratories).

2.2.9 RNA Extraction

Extraction of pure RNA was performed by adding 500µL Trizol reagent (Ambion, Life Technologies) to cells in 6 well plates following 1 x quick wash with old 1 x PBS. Cells were scraped using cell scrapers and 1/10 volume of Bromo-chloropropane (BCP) (Sigma-Aldrich) (50 µl) was then added, and supernatant was transferred to labelled Eppendorf tubes. Sample tubes were vortexed for 15 seconds then rested at room temperature for 5 minutes prior centrifugation at 14,000 rpm for 15 mins at 4°C on the Eppendorf Centrifuge 5424R (details). Colourless upper aqueous phase was transferred to a new tube and 0.5 volume of 2-propanol (250 µl) was added and tubes incubated overnight at -20°Celsius. The following day, samples were centrifuged at 14,000 rpm for 15 minutes at 4°C and supernatant was decanted. The remaining pellet was washed with 0.5 volume of ice-cold 75% ethanol (250 µl) and centrifuged at 14,000 rpm for 10 minutes at 4°C. The pellet was dried, and RNA was dissolved in pre-warmed RNA-nuclease free water (20 µL). Nanodrop 2000 spectrophotometer (Thermo Scientific, CA, USA) was used to quantify all RNA concentrations. To assess RNA quality and purity, samples with A_{260}/A_{280} ratio values between 1.8-2.0 were deemed acceptable.

2.2.10 Reverse Transcriptase- Polymerase Chain Reaction (RT-PCR)

Complementary DNA (cDNA) synthesis was performed using iSCRIPT buffer (Bio-RAD, Hercules, CA, USA) for all RNA samples at 100 ng/µL. The final volume of reaction was 10 µL. RNA samples were prepared in duplicates and were incubated in the BIO-RAD T100™ Thermal Cycler at varying temperatures at different time points of; 25°C for 5 minutes, 42°C for 30 minutes. 85°C for 5 minutes and 15°C for infinity (∞). The cDNA was then diluted 1:3 via the addition of 20 µL nuclease-free water and stored at -20°C until use in real-time PCR.

Table 2.2. Reverse Transcription Reaction Mix.

Component	Volume (µL)
iScript Reverse Transcriptase	0.5
5X iScript Reaction Buffer	2.0
Nuclease-Free Water	5.5
Normalised RNA Sample	2.0
Total	10.0

2.2.11 Quick Reverse Transcriptase- Polymerase Chain Reaction (qRT-PCR)

Real-time PCR were performed for the analysis of gene expression on endothelial cells. Universal SYBR© Green Supermix (SsoAdvanced™) was used for preparation of mastermix for cDNA samples, and all PCR reactions were performed in triplicate and ran on the Bio-Rad CFX96 thermocycler. Steps included initial denaturation and enzyme activation 95°C for 3 minutes; 40 cycles of denaturation 95°C for 30 seconds, annealing 60°C for 30 seconds, followed by extension 72°C for 30 seconds. A non-template control (NTC) was included to

monitor contamination and primer-dimer formation that could produce false positive results. 18s was used as a housekeeping gene. The relative changes in gene expression between treatments was determined using the $2^{-\Delta\Delta cT}$ method. Primers sequences for each cDNA are depicted in table 2.4.

Table 2.3: Quantitative Real-time PCR Reaction Mix

Components	Volume (µL)
iQ SYBR Green Supermix	7.5
Primer F'	0.6
Primer R'	0.6
Nuclease-fee water	4.8
CDNA sample	1.5
Total	15

Table 2.4: Primer Sequences for qRT-PCR

Human Primers			
	Gene	**Forward Primer 5'-3'**	**Reverse Primer 5'-3'**
1	***18S***	GAAGGCTGGGGCTCATTT	CAGGAGGCATTGCTGATGAT
2	***RANK***	ATGCGGTTTGCAGTTCTTGTC	ACTCCTTATCTCCACTTAGG
3	***OPG***	GCTTGAAACATAGGAGCTG	GTTTACTTTGGTGCCAGG
4	***RANKL***	ACTACCAGAAACGAGTGGGAA	GCATCTGTTCTCGGAAAACCT
5	***RUNX2***	TGGTTACTGTCATGGCGGGTA	TCTCAGATCGTTGAACCTTGCTA
6	***BMP2***	ACTACCAGAAACGAGTGGGAA	GCATCTGTTCTCGGAAAACCT
7	***VEGFA***	TGTGAATGCAGACCAAAGAAAGA	TGCTTTCTCCGCTCTGAGC
8	***HIF-1A***	AACGTCGAAAAGAAAAGTCTCG	CCTTATCAAGATGCGAACTCACA
9	***SIAH1***	CACCAGCAGTTCTTCACCATTTAGC	CAATCGTCGCCTATGACCATTTAGC
10	***SIAH2***	CCCTTCCTGCCTGCCCAGCCATCG	TCAGTGTCTATTAGCGCAATCG
11	***VEGFR2***	TTTGGTTCTGTCTTCCAAAGT	ATGCTCAGCAGGATGGCAA

2.3 IN VIVO METHODOLOGY

2.3.1 Animal Studies and Ethics.

All animal experimental procedures were conducted with approval from the South Australian Health and Medical Research Institute (SAHMRI) Animal Ethics Committee (SAM265) and were conducted in accordance to the Australian Code for the Care and Use of Animals for Scientific Purposes (8th edition, 2013). OPG-/- mice (C57BL/6J background) were obtained from Jax Laboratories (Maine, United States). Matching wildtype littermates (C57BL/6J background) were utilised as controls in all the experiments. Male mice were divided into two groups: 8-12 weeks of age for young adults, and 12-24 weeks of aged for ageing cohort. All animals were housed in the animal care facility at SAHMRI and maintained on a standard mouse chow diet (Speciality Feeds, Glen Forrest, WA, Australia).

2.3.2 Hind-Limb Ischemic Surgery (HLI)

All animal experimental procedures were conducted with approval from the South Australian Health and Medical Research Institute (SAHMRI) Animal Ethics Committee (SAM265) and were conducted in accordance with the Australian Code for the Care and Use of Animals for Scientific Purposes (8th edition, 2013). OPG-/- mice (C57BL/6J background) were obtained from Jax Laboratories (USA). Matching wildtype littermates (C57BL/6J background) were utilised as controls in all the experiments. Male and female mice were divided into two groups: 8-10 weeks of age for young adults, and 24 weeks for ageing cohort. All animals were housed in the animal care facility at SAHMRI and maintained on a standard mouse chow diet (Speciality Feeds, Glen Forrest, WA, Australia).

Mice were anaesthetized by inhalation of isoflurane and euthanized by cardiac exsanguination post-surgery. At euthanasia, blood was collected by right ventricular puncture with a heparinised 1 cc/mL syringe. Blood was kept on ice until centrifugation at 3,000 rpm for 10 minutes. Plasma was stored in 50 μL aliquots at -80°C. The hindlimb ischemia model was conducted as previously described[162] to ensure ischemia of the distal regions of the hindlimb. Following inhalation of isoflurane (2%), the proximal end of the femoral artery and distal end of the saphenous vein were ligated with 8-0 silk suture, and the artery and all side branches were dissected free and excised to induce ischemia in the foot and the gastrocnemius muscle; and the overlying skin sutured with 6-0 silk sutures (n = 12 per group). A sham operation was performed on the right hind-limb as a control. Post-surgical pain was managed by buprenorphine (0.1mg/kg) administration 2 days post-surgery and animals were monitored daily. Mice were anesthetized using isoflurane and euthanized by cardiac exsanguination at 1 and 14 days after ischemic surgery. Angiogenesis predominates in the ischemic distal bed, so the gastrocnemius muscles were isolated at euthanasia.

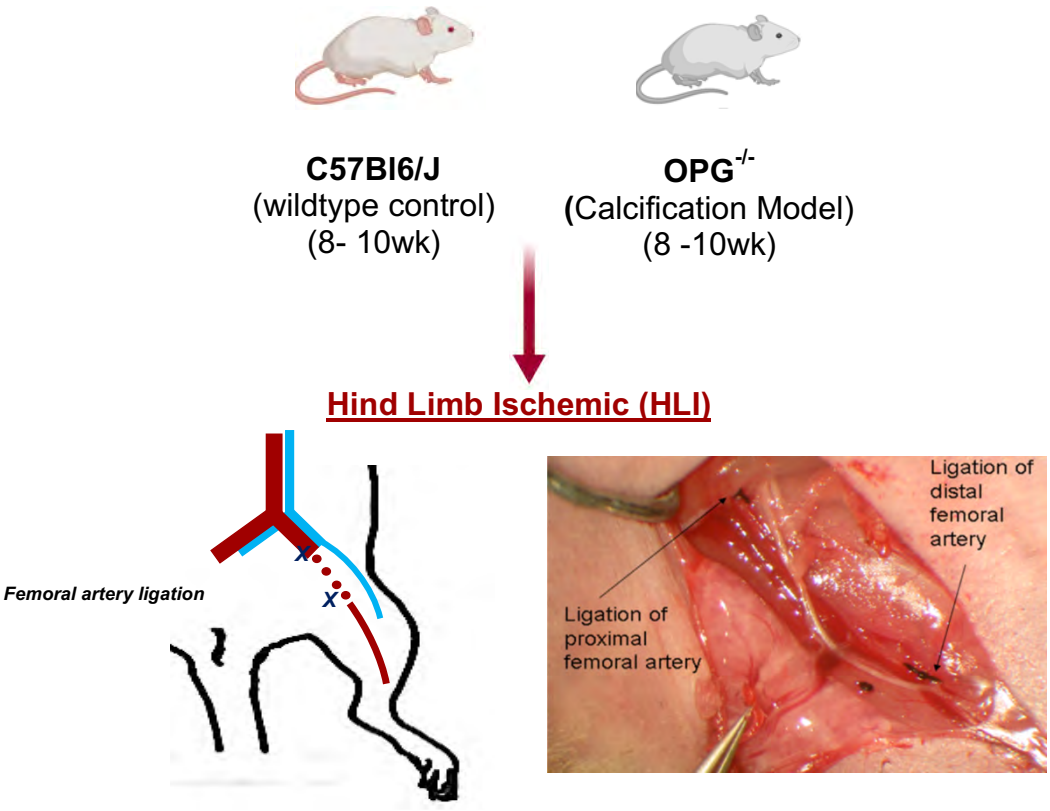

Figure 2.1: Schematic Demonstration of The Hind Limb Ischemia Model Study Design.

The proximal end of the femoral artery and distal end of the saphenous vein were ligated with 8-0 silk suture. The artery and all side branches were dissected free and excised to induce ischemia in the foot and the gastrocnemius muscle.

2.3.3 Laser Doppler Perfusion Imaging

Blood reperfusion of the hindlimb was determined by Laser Doppler Perfusion imaging (moorLDI2-IR, Moor Instruments, Devon, UK) at baseline, immediately post-surgery and on days 1, 3, 7, 10 and 14 following surgeries, with three scans taken per mouse at each time point.

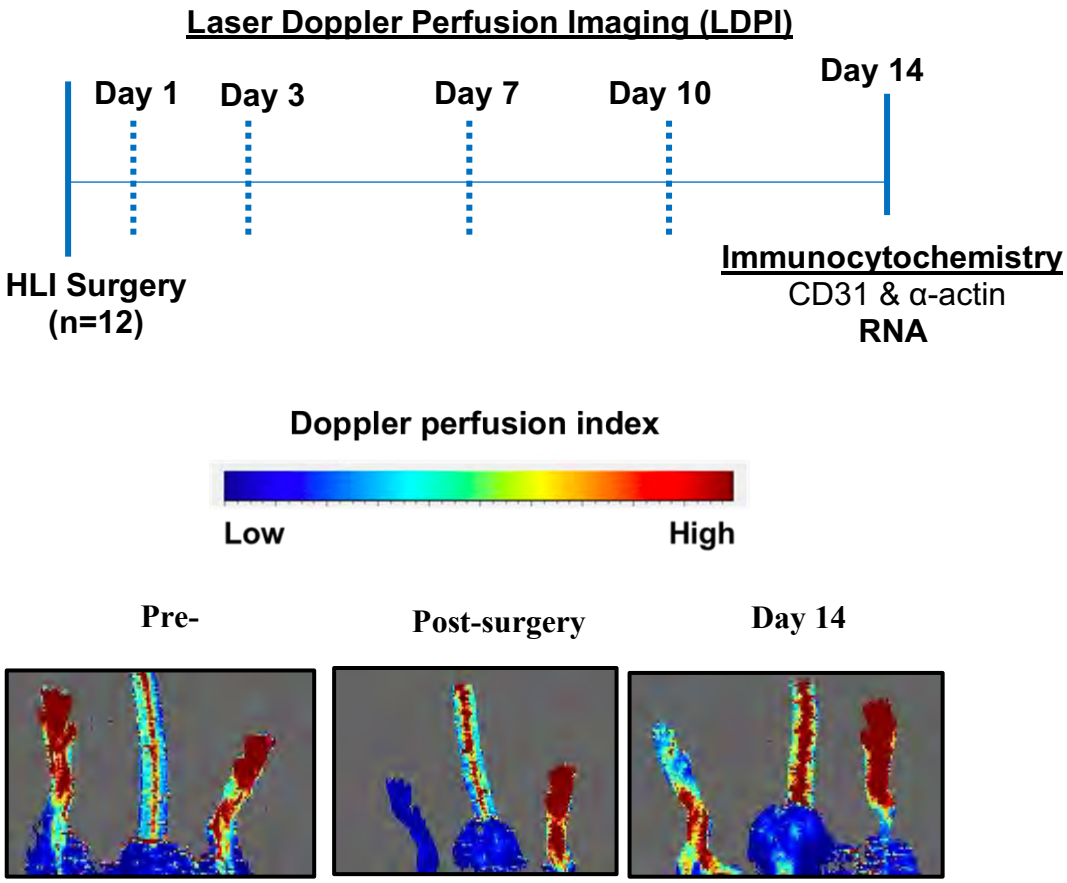

Figure 2.2: Laser Doppler Perfusion Imaging. Blue indicates low blood flow; red indicates high blood flow. Blood flow return was assessed in the hindlimbs of these mice on days 1, 3, 7, 10 and day 14 endpoint, with three scans taken per mouse at each time point. Data was analysed using the laser Doppler imaging system (moorLDI2-IR, Moor instruments, Devon, UK).

2.3.4 Tissue Processing

Mice were anesthetised using isoflurane and euthanised by cardiac exsanguination 14 days following surgery. The gastrocnemius muscles of both the ischaemic and non-ischaemic hindlimbs, were halved and snap frozen at -80^{o} C in Eppendorf tubes for RNA/protein analysis. The other half was placed in Tissue-Tek® optimal cutting temperature (OCT) compound (IA018, ProSciTech, Kirwan, QLD, Australia) within Tissue-Tek® cryomolds

then immediately placed on dry ice. The muscle and all other tissues were snap frozen in liquid nitrogen and stored at -80^{o} C until ready to be processed for histology.

2.3.5 Plasma Isolation from Whole Bloods

Whole blood was collected in heparin sulphate tubes (Interpath 22/12/45) by right ventricular puncture and was kept on ice until centrifugation at 3000 rpm for 10 minutes at 4^{o}C. The plasma layer was collected in three 50 µl aliquots and was stored at -80^{o}C. Plasma was isolated for detection of calcium levels (Calcium Assay, Cayman Chemical, 701220) and alkaline phosphatase activity (LabAssay ALP, WAKO, 291-58601).

2.3.6 RNA Extraction, cDNA Synthesis and Quantitative Real-Time PCR

Quantitative real-time PCR (qRT-PCR) was performed on cDNA in triplicates using SSoAdvanced Universal SYBR Green Supermix in a CFX Connect Real Time System (Bio-Rad). Relative changes in mRNA expression were normalised using the ΔΔCt method to housekeeping gene 36B4. Genes of interest included angiogenic markers: HIF-1α, VEGFA, VEGFR2, RANKL, Runx2, BMP2, Siah 1, Siah 2, PHD2 and PHD3 (For full extraction protocol, see chapter 2, section 2.3.7. For primer sequences see Table 2.5.

2.3.7 Immunohistochemistry

OCT embedded gastrocnemius muscle tissues were sectioned to 5 µm thickness on the Shandon Cryotome E Cryostat (ThermoFisher Scientific); and mounted on superfrost plusTM Adhesion Microscope Slides (J1800AMNT, ThermoFisher Scientific). Prior to staining, slides were dried overnight at room temperature, fixed in 2% paraformaldehyde for

10 minutes, then washed with 0.1 M glycine in PBS for 3 x 2 minute to quench unreacted aldehydes. Tissues were washed in PBST containing 0.1% (v/v) Twenn-20 for 3x5 minutes, followed by blocking in 5% goat serum (G9023, Sigma-Aldrich) in PBST for 1 hour at room temperature.

Tissues sections were then incubated overnight with primary antibodies in antibody diluent to detect Smooth muscle α-actin positive arterioles (1:1000, F3777, Sigma-Aldrich, St Louis, MO, USA) and laminin B (1:200) MAB1905, Merck Millipore, Burlington, MA, USA) to assess myocytes. The next day following primary antibody incubation, tissues were washed with PBST for 4 x 2 minutes and were incubated with secondary antibodies Alexa Fluor^{Ò} 555 (1:1000; A-21434; Invitrogen, Carlsbad, CA, USA) in antibody diluent for 1 hour at 37 degrees, which was followed by 6 x 2-minute washes in PBST. Sections were again blocked with 5% goat serum for 1 hour at room temperature, and stained for CD31 positive neovessels (1:50, ab28364, abcam, Cambridge, UK). Slides were washed for 4 x 2 minutes in PBST then incubated with Alexa Fluor^{Ò} 647 (1:500; A-32733; Life technologies, Carlsbad, CA, USA) secondary antibody in antibody diluent respectively, for 1 hour. Slides were finally washed in PBST for 6 x 2 minute each and mounted with Fluorescence Mounting Media (S302380-2, Dako), and a cover slip was applied to each slide. Control sections probed with only secondary antibodies were also run to assess and adjust for the degree of background staining during the imaging process. These were mounted with Prolong Antifade Mounting Media with DAPI (P36935, Life Technologies) so that cell nuclei could be detected.

All slides were allowed to dry in the dark for 24 hours and were imaged on the Nikon Eclipse Ni-U microscope using NIS-Elements software (Melville, NY, USA) with five high-magnification fields (20X) of view taken for each section using the Cy5 (CD31), FITC (α-

SMA) and Cy5 (laminin) filters. For analysis, CD31+ neovessels SMA+ arterioles and myocytes were manually quantified using ImageJ software.

2.3.8 Clinical Scoring

To assess tissue ischemia and limb function, mice were observed after surgery using a slightly modified version of the well-established Tarlov Clinical Scoring System as previously described[163] at each perfusion assessment. For limb function clinical scoring was scaled as (0=normal gait movement, 1= plantar but no toe flexion, 2=no flexion, 3= dragging foot). For tissue ischemia, scoring was based on (0=no damage, 1=discoloration 1 nail, 2= discoloration of 2 nails, 3= discoloration of 1 toe, 4=discoloration of 2 toes, 5=foot necrosis, 6=leg necrosis and 7=auto-amputation of leg).

Tarlov Score	
0	No movement
1	Barely perceptible movement, non-weight bearing
2	Frequent movement, non-weight bearing
3	Supports weight, partial weight bearing
4	Walks with mild deficit
5	Normal but slow walking
6	Full and fast walking
Ischemia Score	
0	Auto-amputation > half lower limb
1	Gangrenous tissue > half foot
2	Gangrenous tissue < half foot, with lower limb muscle necrosis
3	Gangrenous tissue < half foot, without lower limb muscle necrosis
4	Pale foot or gait abnormalities
5	Normal
Modified Ischemia Score	
0	Auto-amputation of leg
1	Leg necrosis
2	Foot necrosis
3	Discoloration of > two toes
4	Discoloration of one toe
5	Discoloration of > two nails
6	Discoloration of one nail
7	No necrosis

Modified Tarlov Scale	
Score	**Descriptions**
Limb Function	
0	**Normal**
1	**Plantar but no toe flexion**
2	**No flexion**
3	**Dragging of foot**
Tissue Ischemia	
0	**No damage**
1	**Discoloration ->1 nail**
2	**Discoloration -> 2 nails**
3	**Discoloration of 1 toe**
4	**Discoloration of 2 toes**
5	**Foot Necrosis**
6	**Leg necrosis**
7	**Auto-amputation of leg**

Table 4.1: Tarlov Functional scoring system. ***(A)*** *Original Tarlov scores used to assess animal locomotor recovery from spinal cord injury, and limb-function of mice post-hindlimb surgery as previously described*[163]. ***(B)*** *Modified Tarlov Scoring System Used to score mice post-HLI surgery in aged mice. Mice were scored for limb function (LF) or tissue ischemia (TI) based on the above scores. All data was recorded into an excel spreadsheet and scores were tallied per mouse.*

2.3.9 Murine Peri-Arterial Femoral Cuff Surgery

The murine femoral periarterial cuff model is a validated model of inflammatory-driven neointima formation and adventitial angiogenesis[164]. This model is used to induce an inflammatory response to vascular injury by placing a non-occlusive polyethylene cuff around the femoral artery. Peri-arterial cuff placement induces adventitial inflammation, that triggers an influx of proinflammatory cytokines (neutrophils, macrophages) which secrete growth factors to the injury site, thereby causing mild endothelial cell damage, SMC proliferation and migration & inflammation in the adventitia.

In this study, wildtype C57BL/6J and OPG deficient mice were anaesthetised prior to surgery by inhalation of 2% isoflurane. Briefly, an incision of approximately 1 cm in length was made at the midpoint of the left hindlimb to expose the left femoral artery, and the femoral artery was then carefully dissected away from the neurovascular bundle (left femoral vein and nerve). Next, a 2.0 mm non-occlusive polyethylene cuff made of PE-50 tubing (427410, BD Bioscience, MA, USA) was slit along its length and with the use of forceps was opened and placed around the left femoral artery of each mouse. Carefully the cuff was secured and tied closed using non-absorbable 6-0 silk sutures, while ensuring blood flow was not obstructed (Figure 6.1). The skin was apposed over the cuff with 6-0 sutures and iodine-based antiseptic solution applied to the wound post-operatively. For post-surgical analgesia, buprenorphine (0.1 mg/kg) was administered subcutaneously immediately following surgery and day 1 post-surgery for recovery. A sham operation was performed without the polyethylene tube placement on the right femoral artery as a control. 21 days post-surgery, mice were anaesthetized by inhalation of isoflurane and euthanized by cardiac exsanguination 21 days post-surgery. The heart was perfused with saline (10 ml) via the left ventricle and both the cuffed femoral artery, and the sham were excised for immunohistochemical analysis (IHC). An additional cohort (n = 6 per group) was used to assess changes in mRNA

expression of key angiogenesis and inflammation genes in cuffed and non-cuffed arteries after 24 hours.

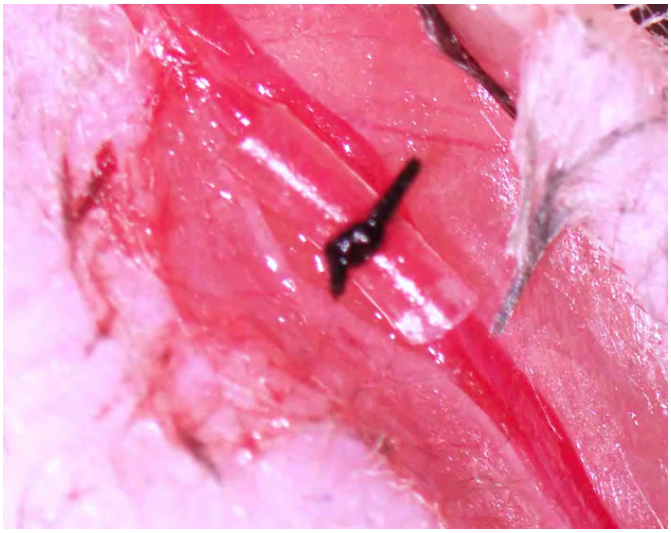

Figure 2.3: Polyethylene Cuff Placed Around Mouse Femoral Artery.

2.3.10 Histology

2.3.10.1 Sample Preparation

Femoral arteries were excised following cuff implantation and were placed into 10% (v/v) formalin for 24 hours and then into 70% (v/v) ethanol until they could be processed further. All collected arteries were embedded in 3% (w/v) agarose to prevent loss of these samples from the tissue cassettes (CASLID-01, Techno Plas, SA, Australia) during tissue processing. The arteries were then paraffin-embedded in blocks using a HistoStarTM Embedding Workstation (ThermoFisher Scientific) and stored at room temperature prior to microtome sectioning. Tissues were sectioned at 5 µm on the M325 Microtome (Thermo Fischer Scientific) and were dried for 4 nights at 60°C.

2.3.10.2 Immunohistochemistry

IHC was used to detect the angiogenic response from cuff placement. Samples were probed for CD31 adventitial neovessels, α-SMA to detect adventitial arterioles, and CD68 to assess macrophage infiltration. Prior to staining, slides were first deparaffinised by incubating with xylene (FNNJJ028, Fronine, Riverstone, NSW, Australia) for 5 minutes, then 1 minute, followed by decreasing ethanol concentrations of 100% for 2 x 1 minute, 95% (v/v) ethanol for 2 x 1 minute, 70% (v/v) ethanol for 1 minute followed by distilled water for 1 minute. All sections were then microwaved at a high-power setting (P70) in sodium citrate buffer for antigen retrieval for 20 minutes. Endogenous peroxidase was blocked by incubating in hydrogen peroxide solution (0.3% H_2O_2 in methanol) for 20 minutes at room temperature (RT), followed by a 1x 5-minute wash in phosphate buffer saline with Tween 20 (PBST; PBS with 0.1% (v/v) Tween- 20). Non-specific binding was prevented by blocking in goat serum (10% (v/v) goat serum in PBS) for 4 hours at RT for α-SMA and CD1, and 3% Horse serum for CD68.

CD31: Sections were incubated overnight at 4°C with rabbit polyclonal primary antibody against CD31 (1:25, ab28364, Abcam) in PBST. Excess antibody was removed by washing for 2 × 5 min in PBST before incubating with goat anti-rabbit IgG horseradish peroxide (HRP)-conjugated secondary antibody (1:50, NBP2-30348H, Novus Biologicals) for 2 hours at room temperature. The slides were washed for 3 × 5 min in PBST, then HRP was detected by incubating the sections in the dark for 10 min at room temperature with ImmPACT® 3,3'-diaminobenzidine (DAB) Peroxidase Substrate (SK-4105, Vector Laboratories), made by adding 1 drop DAB reagent per 1 mL of ImmPACT® DAB diluent. The reaction was stopped by immersing the slides in distilled water for 5 min. The sections were counterstained with Lillie Mayer's haematoxylin (AHLM, Australian Biostain, VIC, Australia) for 45 seconds, rinsed in distilled water for 1 min, dipped twice in acid-alcohol (0.3% [v/v] HCl in 70% [v/v] ethanol) then Scott's Solution (2% [w/v] MgSO4, 0.35% [w/v]

NaHCO3) for 45 seconds, before a final rinse with distilled water for 1 min. The sections were dehydrated in increasing concentrations of ethanol by reversing the previous steps for hydration, before being cleared in xylene for 5 min and mounted in DPX (06522, Sigma-Aldrich).

α-SMA: Sections were incubated overnight with monoclonal primary antibody against α-SMA conjugated to alkaline phosphatase (1:100, A5691, Sigma-Aldrich). Tissues were washed in 2 x 5 minute in PBST then incubated for 12 minutes with Vector Red Alkaline Phosphatase substrate (SK-5100, Vector Laboratories). Colour change was halted by rinsing tissues in distilled water. Sections were counterstained and cover slips were applied as stated above.

CD68: Following antigen retrieval, tissue sections were incubated in 0.3% (w/v) hydrogen peroxide in methanol for 30 min, washed in PBST for 5 min, then blocked with 3% (v/v) normal horse serum (NHS, S-2000, Vector Laboratories) in PBS for 4 hours at room temperature. The sections were incubated overnight at 4°C with rat monoclonal primary antibody against CD68 (1:200, MCA1957GA, Bio-Rad) diluted in NHS. Excess antibody was removed with 2 × 5 min washes with PBST, followed by incubation with biotinylated goat anti-rat IgG secondary antibody (1:250, BA-9401, Vector Laboratories) in NHS for 30 min at room temperature. The sections were again washed with PBST for 2 × 5 min then incubated with PierceTM streptavidin poly-HRP (1:500, 21140, ThermoFisher Scientific) diluted in NHS for 15 min at room temperature. Following 2 × 5 min washes in PBST, peroxidase activity was detected by incubating with ImmPACT® DAB Peroxidase Substrate as above for 10 min, after which the reaction was stopped by immersing in distilled water for 5 min. The tissue sections were finally counterstained, dehydrated with increasing concentrations of alcohol, cleared in xylene and mounted with DPX as for CD31 staining.

Masson's Trichrome Staining was performed using the Trichrome Stain Kit (ab150686, Abcam) according to the manufacturer's instructions. Briefly, the sections were deparaffinised first as previously described, then stained with Weigert's Iron Haematoxylin solution for 5 min. The slides were rinsed in running water for 2 min, then immersed in Biebrich Scarlet/Acid Fuschsin solution for 15 min, and were rinsed again in distilled water for 2 min prior to differentiating in phosphomolybdic/phosphotungstic acid solution for 15 min. The slides were then immersed in Aniline Blue solution for 10 min, rinsed in distilled water for 2 min, then immersed in 1% (v/v) acetic acid solution for 5 min. After this, the sections were dehydrated quickly in two changes of 95% (v/v) ethanol then two changes of absolute ethanol, before finally clearing in xylene for 5 min and mounting with DPX as described previously.

All samples were imaged using a Carl Zeiss Axio microscope and AxioCamER camera using the ZEN lite software (Oberkochen, Germany). One high-magnification field of view was taken per section for analysis. All analysis was completed using Image J software and Image-Pro Premier software (v9.0.4, Media Cybernetics, Rockville, MD, USA).

2.3.11 RNA Extraction, cDNA Synthesis and Quantitative Real-Time PCR

Quantitative real-time PCR (qRT-PCR) was performed on cDNA in triplicates using SSoAdvanced Universal SYBR Green Supermix in a CFX Connect Real Time System (Bio-Rad). Relative changes in mRNA expression were normalised using the ΔΔCt method to housekeeping gene 36B4. Genes of interest included angiogenic markers: HIF-1α, VEGFA, VEGFR2, RANKL, Runx2, and inflammatory markers: NF-κB (p65) and CD68 and MCP1.

For full extraction protocol and primer sequences, see chapter 2, section 2.3.7-2.3.8, Table 2.4.

2.3.12 Plasma Analyses

Plasma analysis were perfumed using OPG mice plasma for ALP, calcium and OPG. To assess alkaline phosphatase activity, an ALP assay (LabAssay ALP, WAKO, 29158601) was used according to the manufacturer's instructions. Calcium concentration was quantified in plasma samples using a calcium assay (Calcium Assay, Cayman Chemical, 701220) according to the manufacturer's instructions. To confirm OPG knockdown in the calcification mouse model, an OPG ELISA (Quantikine ELISA Mouse Osteoprotegerin/TNFRSF11B Immunoassay) was used to measure serum OPG levels in mice that had undergone peri-arterial cuff surgery. The assay was performed as per manufacturer's instructions.

2.3.13 Euthanasia

Mice were anaesthetized by inhalation of isoflurane (SAHMRI SOP1/027) and euthanized by cardiac exsanguination post-surgery. The heart was perfused with saline (10 ml) via the left ventricle for collection of the aorta and for the peri-arterial femoral cuff surgery.

2.3.14 Blood Collection

At euthanasia, blood was collected in heparin sulphate tubes (Interpath) by right ventricular puncture using the 27-gauge needle syringe. Blood was kept on ice until centrifugation at 5,000 rpm for 5 minutes. Plasma was stored in 100 μL aliquots at -80°C.

2.3.15 Histology

2.3.15.1 Immunohistochemistry

2.3.15.1.1 Sample Preparation

Femoral arteries excised following cuff implantation were fixed in 10% formalin (v/v) and paraffin embedded. Tissues were sectioned at 5 μm on the M325 Microtome (Thermo Fischer Scientific) and were baked for 2 nights at 60°C. Samples were either probed for neovessels (CD31+), arterioles (smooth muscle α-actin) and macrophages (CD68). Slides were first deparaffinised in incubations of xylene and rehydrated in decreasing ethanol concentrations of 100%, 95% and 70%.

2.3.15.2 CD31, CD68 and Smooth Muscle α-actin Staining

To determine capillaries, CD31 immunohistochemical staining was performed on paraffin embedded tissue sections from the peri-arterial cuff. Tissue sections were submerged in sodium citrate buffer for antigen retrieval and were microwaved at 80 high-power setting. Endogenous peroxidase was blocked by incubation in hydrogen peroxide solution (0.3% H_2O_2 in methanol) for 20 minutes at room temperature (RT), followed by a phosphate buffer saline with Tween 20 (PBST) wash (PBS with 0.1% (v/v) Tween- 20). To prevent non-specific binding, goat serum (10% (v/v in PBS) was used for blocking for 4 hours at RT. Slides were then incubated overnight with primary antibodies for CD31 (1:25; ab28364;

Abcam), smooth muscle a-actin conjugated to alkaline phosphatase (1:100, A5691, Sigma-Aldrich); and CD68 (ab31630, 1:100) respectively at 4°C. Subsequently, CD31 slides were incubated with horseradish peroxidase (HRP) secondary antibody (1:100, goat anti-rabbit NBP2-30348H, Novus) for 2 hours at RT. For CD68, this was coupled with biotinylatedanti0mouse HRP antibody (DETAILS), followed by incubation with streptavidin peroxidase (DETAILS) for 15 minutes. For both, HRP enzyme was detected using 3,3′-Diaminobenzidine (DAB) substrate (Vector Laboratories, Burlingame, CA, USA) for 12 minutes. Smooth muscle a-actin slides were incubated with Vector Red alkaline phosphatase substrate (SK-5100, Vector Laboratories) for 12 minutes. Slides were counterstained with haematoxylin, dehydrated and mounted with DPX.

2.3.15.3 Imaging and Analysis

Samples were imaged using a Carl Zeiss Axio microscope and AxioCamER camera using the ZEN lite software (Oberkochen, Germany). One high-magnification field of view was taken per section for analysis.

2.3.15.4 Immunofluorescence Triple Staining

The gastrocnemius muscles from ischemic and non-ischemic hindlimbs were harvested and embedded in OCT (Sakura Finetek, Torrance, CA, USA). OCT-embedded tissues were then sectioned at 5 μm on the Shandon Cryotome E Cryostat (Thermo Fisher Scientific, MA, USA) and allowed to dry overnight at room temperature prior to staining. The following day, tissue samples were fixed in 2% paraformaldehyde and washed in PBST (PBS with 0.1% (v/v) Tween-20). To target non-specific binding, goat serum (10% (v/v) goat serum in PBS)

was used for blocking tissues for 1 hour at RT. Tissues were then incubated with primary antibodies for 1 hour, probing for CD31 (1:50; ab28364; Abcam, Cambridge, UK) to assess $CD31^+$ neovessels, smooth muscle a-actin (1:1000; F3777; Sigma-Aldrich, St. Louis, MO, USA) to assess arterioles and laminin (1:200; MAB1905; Merck Millipore, Burlington, MA, USA) to assess myocytes. Tissues were then incubated with secondary antibodies for 1 hour at room temperature respectively using Alexa Fluor® 555 (1:1000; A-21434; Invitrogen, Carlsbad, CA, USA) and Alexa Fluor® 647 (1:500; A-32733; Life Technologies, Carlsbad, CA, USA). Samples were imaged on the Nikon Eclipse Ni-U microscope using NIS-Element's software (Melville, NY, USA) with five high-magnification fields of view taken for each section for analysis.

2.3.16 Calcium Assay

Calcium concentration was quantified in plasma samples using a calcium assay (Calcium Assay, Cayman Chemical, 701220) according to the manufacturer's instructions. In this colorimetric assay, in an alkaline environment, calcium reacts with o-Cresolphthalein Complexone to form a complex with a purple colour that absorbs between 560 and 590 nm. The intensity of the colour is directly proportional to the concentration of calcium in the sample. To begin the assay, calcium standards with final concentration of 0, 0.5, 1, 2, 4, 6, 8 10 mg/dl were performed. Subsequently, to set up the 96 well plate, 10 µl of calcium standard were added to standard wells. 10 µl samples were added in duplicates to the 96 well plate. Finally, 200 µl of Working Detector Reagent was added to all wells, and plate was gently shaken for 20-30 seconds. The 96 well plate was incubated at room temperature for five minutes, and absorbance was measured at 570-590 nm using the BIO-RAD iMark™ Microplate Reader. Data was normalised to protein via a BCA Protein Assay. Averages of

duplicates were recorded using Microsoft Excel (2016), and R^2 value was used to calculate the concentration of ALP in each sample.

2.3.17 ALP Assay

Alkaline Phosphatase (ALP) is an important hallmark for physiological phenomena as osteogenesis. To assess alkaline phosphatase activity, an ALP assay (LabAssay ALP, WAKO, 29158601) was used according to the manufacturer's instructions. HCAECs were cultured and harvested as previously described and were plated in a 96 well plate at a density of $1x10^5$. Following treatment for 24 h, cell culture medium from each sample were collected and stored at 20 °C. For plasma samples, a 1:10 dilution was performed prior to conducting the assay. To prepare the buffer solution, 1 ALP substrate tablet was dissolved into 5 mL of buffer solution. Standard solutions of 0.5, 0.25, 0.125, 0.0625 mmol/L. were prepared by diluting with distilled water. The assay was performed in a 96 well plate, whereby 100 µL of working assay solution was added to 100 µL of standard and 20 µL sample. The 96 well plate was then agitated on a plate mixer for 1 minute then incubated at 37°C for 15 minutes. Subsequently, 80 µL of stop solution was added to all wells and plate was placed on the plate mixer for 1 minute, and absorbance was measured at 405 nm wavelength using the BIO-RAD iMark™ Microplate Reader. Data was normalised to protein via a BCA Protein Assay. Averages of duplicates were recorded using Microsoft Excel (2016), and R^2 value was used to calculate the concentration of ALP in each sample.

2.3.18 Tissue RNA Extraction

RNA was isolated from gastrocnemius muscle and femoral arteries of mice post- hindlimb and peri-arterial cuff surgery, respectively. Tissues were homogenised, and total RNA was extracted using TRI reagent (Sigma-Aldrich) and quantified spectrophotometrically as previously described. Following quantification, RNA samples were normalised to 100 ng/mL and were reverse transcribed to generate complimentary cDNA using iSCRIPT cDNA synthesis kit (Bio-Rad, Hercules, CA, USA).

2.3.19 Quantitative Real-Time PCR

Quantitative real-time PCR (qRT-PCR) was performed on cDNA in triplicates using SSoAdvanced Universal SYBR Green Supermix in a CFX Connect Real Time System (Bio-Rad). Relative changes in mRNA expression were normalised using the ΔΔCt method to housekeeping gene 36b4. Genes of interest included angiogenic markers: *Hif-1α, Vegfa, Vegfr2, Rankl, Runx2,* and inflammatory markers: *NF-Kb (P65) and Cd68, Icam, Vcam* and *Mcp1* (See table 2.5).

Table 2.5: Murine Mouse Primers used for qRT-PCR

Murine Primers			
	Gene	Forward Primer 5'-3'	Reverse Primer 5'-3'
12	***36b4***	CAACGGCAGCATTTATAACCC	CCCATTGATGATGGAGTGTGG
13	***Vegfa***	GGCTGCTGTAACGATGAAG	CTCTCTATGTGCTGGCTTTG
14	***Vegfr2***	GCCCAGACTGTGTCCCGCAG	AGCGCAAGACCGGGGAGAGC
15	***HIF1-α***	TCCCTTGCTCTTTGTGGTTGGGT	AACGTAAGCGCTGACCCAGG
16	***Rankl***	CCAGCTATGATGGAAGGCTCA	ACCGAAGATAATGGACATGC
17	***Runx2***	AACGATCTGATTTGTGGCC	CCTGCGTGGGATTTCTTGGTT
18	***Bmp2***	GGGACCCGCTGTCTTCTAGT	TCAACTCAAATTCGCTGAGGAC
19	***Siah1***	GACTGCTACAGCATTACCCACT	GTTGGATGCAGTTGTGCCG
20	***Siah2***	CTAACGCCCAGCATCAGGAA	GAACAGCCCGTGGTAGCATA
21	***Phd1***	TAAGGTGCATGGCGGCCTGC	TGGCTGCTGCCCGTTCCTTG
22	***Phd2***	ATCACCTGGATCGAGGGCAA	CGTTCGGCCGTTTATCCTGT
23	***Mcp1***	GCTGGAGCATCCACGTGTT	ATCTTGCTGGTGAATGAGTAGCA
24	***Cd68***	GGACAGCTTACCTTTGGATTCAA	CTGTGGGAAGGACACATTGTATTC
25	***Nf-Kb (p65)***	AGTATCCATAGCTTCCAGAACC	ACTGCATTCAAGTCATAGTCC-

2.3.20 Statistical Analysis

Analyses were performed using PRISM software (GraphPad Prism). All data were quantified using imageJ and ImagePro Premier and analysed for statistical significance by an unpaired t-test amongst the independent groups of data. A value of $p<0.05$ was deemed significant. One-way ANOVA test was also conducted, and using Bonferroni's multiple comparison test, all treatment groups were compared to control groups. All data was represented as mean ± SEM of triplicate replicates from 3 independent experiments.

CHAPTER 3:

HIGH CALCIUM IMPAIRS ISCHEMIA-DRIVEN ANGIOGENESIS IN VITRO

3. Introduction

Angiogenesis is a fundamental process that describes the formation of new blood vessels from pre-existing capillary beds, and is severely impaired in pathological diseases such as peripheral arterial disease[7]. VC is a phenomenon of soft tissue calcification that occurs due to the deposition of hydroxyapatite in the form of calcium phosphate within the arterial wall [15, 100, 105, 165]. The pathogenesis of lower extremity PAD remains poorly described but is regarded secondary to atherosclerosis due to fatty plaque build-up within the arterial wall[15]. Therapies for PAD are centred around alleviating stenosis and promoting tissue revascularization following ischemia[15], and while atherosclerosis is recognised as the main cause of PAD, acute or chronic limb ischemia may be the result of various other cardiovascular risk factors [15].

Recent literature has implicated vascular calcification as a potential driver of angiogenesis in PAD [15]. There are several lines of evidence that bone-related osteogenic markers are involved in regulating vascular calcification in VSMCs, although lacking in the context of ECs[126, 129, 131, 145, 166-171]. These regulators include members of the TNF superfamily of cytokines, receptor activator of nuclear factor κappa-B (RANK) and its ligand (RANKL); and its soluble decoy receptor osteoprotegerin (OPG); and other bone regulatory factors such as runt related transcription factor 2 (runx2); the main transcriptional regulator of osteogenesis; bone morphogenetic protein 2 (BMP2); a strong inducer of bone formation, and alkaline phosphatase (ALP), an key early diagnostic marker of VC[126, 131, 169, 170]. The mechanism underlying VC pathology suggests the differentiation of VSMCs towards an osteoblastic phenotype, as demonstrated in numerous in vitro studies showing VSMC mineralization when cultured in a pro-calcific enviroment[86, 172-174].

Additionally, the OPG/RANK/RANKL pathway known to drive bone formation has been suggested to regulate angiogenesis[51, 62,150]. RANKL treatment has been reported to stimulate angiogenesis both in vivo and in vitro by acting as a chemostatic factor for ECs

and inducing their migration and proliferation[150,129, 151]; increased vascular permeability and promoted neoangiogenesis via induction of EC migration and proliferation[51, 150, 152]. However, conflicting studies have reported RANKL to cause a reduction in EC proliferation, while inducing EC apoptosis, therefore suggesting RANKL to be an inhibitor of angiogenesis, and OPG a promotor.[153] In addition, VEGFA has been shown to increase the mRNA expression of *Rank* in human ECs, which upregulated their angiogenic response to RANKL[51,150,45]. Furthermore, OPG was also shown to facilitate an increase in EC proliferation and tubule formation in vitro, whilst stimulating neovascularization in vivo[153, 155]. Based on this evidence, the OPG/RANK/RANKL triad may have a potential role in regulating angiogenesis.

While the involvement of bone regulatory genes in angiogenesis has been explored, there remains a poor correlation between angiogenic marker expression in the presence of elevated calcium levels. Since the endothelium regulates many of the processes involved in atherogenesis and other pathological diseases of the vasculature including PAD; the present study examined the effects of elevated calcium levels on EC-driven angiogenesis and hypothesised that high calcium will attenuate this process.

To test these hypotheses, the response of HCAECs to calcium/phosphate was assessed with measures of proliferation, migration, and tubule formation in vitro. In combination with this the expression of both calcification and angiogenic markers were analysed to understand their roles in regulating disease processes.

3.1 Results

3.1.1 Calcification Medium Increases Calcium Levels and ALP Activity in ECs.

An increase in calcium (Ca^{2+}) has been a key player in the pro-angiogenic pathway in ECs[175]. Increased calcium signaling is induced by growth factor and chemokine activation involved in angiogenesis which then stimulates a cascade of events for angiogenesis including EC proliferation, migration, and tube formation[176]. Furthermore, the process of vascular calcification occurs due to hydroxyapatite mineral deposition in the form of calcium and phosphate. To ensure our calcification medium was indeed eliciting a calcification response, calcium levels were measured. Calcium levels in cell culture supernatants of ECs treated with CM and were found to be elevated in normoxia compared to controls, (414.20±11.52 vs 299.20±15.09, P<0.027, Figure 3.1A). This response was also maintained in hypoxia (423.80±30.71 vs 305.80±37.17, P<0.024, Figure 3.1A), suggesting that elevated calcium may influence EC activation of calcification-driving markers to help drive vascular calcification.

In the early events of calcification, specific osteogenic factors are released to initiate the process of mineralisation; including ALP[105]. Changes in ALP levels are a prominent feature bone diseases, CKD and cardiovascular diseases, specifically atherosclerotic lesions with vascular calcification[100]. The role of ALP in angiogenesis has been well explored in bone cells; with VEGFA reported to stimulate ALP activity[117], and hypoxia shown to increase ALP activity[118]. ALP activity was measured in cell culture supernatants of ECs treated with CM. ALP activity was upregulated by CM compared to untreated ECs in both normoxia (6.90±0.72 vs 4.09±0.45, P<0.023 Figure 3.1B) and hypoxia (6.12±0.45 vs 4.06±0.26, P<0.114, Figure 3.1B), though not reaching statistical significance. This data may therefore suggest the role of CM in the upregulation of ALP activity.

A

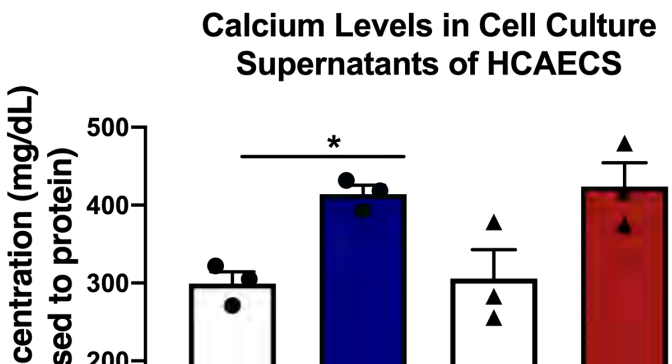
Calcium Levels in Cell Culture Supernatants of HCAECS
centration (mg/dL)
sed to protein)
500
400
300
200
*

Figure 3.1: Calcification Medium Upregulates Calcium Levels and ALP Activity in ECs.

*HCAECs cultured and treated with calcification medium containing 2.0mM HNa_2PO_4 and 2.7mM $CaCl_2$ for 24h, in normoxia (37° C humidified atmosphere with 5% CO_2) and hypoxia (37° C humidified atmosphere with 1.2% O_2/5% CO_2) conditions. Calcium Assay (Cayman, Calcium Assay) and ALP Assay (Wako, Lab Assay) were used to quantify ALP and calcium concentrations in cell culture supernatants following treatment. A) ALP Activity, (B) Calcium Levels All data is represented as mean ± SEM; One-Way ANOVA with Bonferroni's multiple comparisons test, (n=3), *P<0.05). HCAEC, human coronary artery endothelial cells, M199, medium 199 (Sigma-Aldrich), ALP, alkaline phosphatase, EC, endothelial cell.*

3.1.2 Calcification Medium Increases EC Viability in Normoxia.

Ischemia occurs when oxygenated blood supply is impaired and is present in disease states such as post-MI, PAD and diabetes[64]. As a result of reduced oxygen supply to tissues, cellular and tissue modifications occur often leading to cell death. However, the influence of elevated calcium on EC functions or viability during ischemia remain unknown. To understand the effects of elevated calcium on EC viability, a WST-1 cell viability assay was performed on cells treated for 24 h with CM and conditioned to both normoxic and hypoxic stimuli. Treatment with CM for 24 h significantly upregulated EC viability in normoxia compared to untreated cells (1.49±0.04 vs 1.04±0.03 P<0.0001) with no change observed in hypoxia, (Figure 3.2). However, there was significant decrease in cell viability when comparing CM normoxia (1.49±0.04) to CM hypoxia (1.00±.02, P<0.0005); which suggests negative effect of CM-induced cell viability in hypoxic conditions.

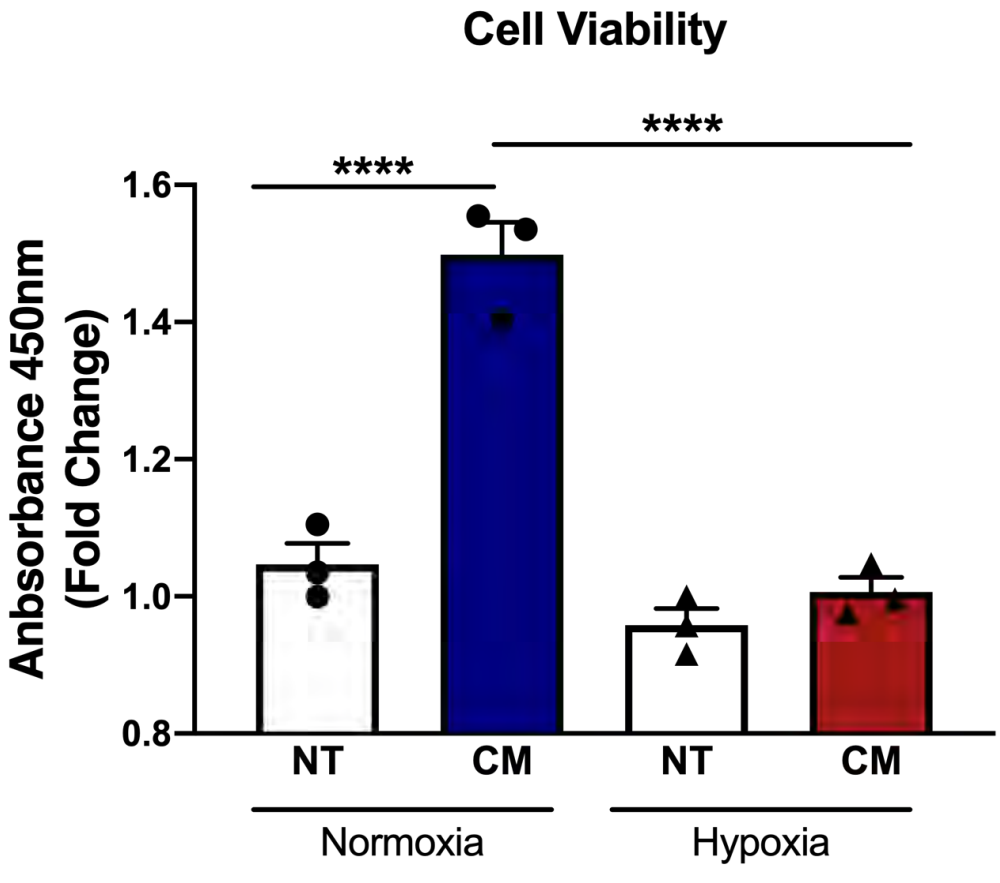

Figure 3.2: Calcification Medium Increases EC Viability in Normoxia.

*HCAECs cultured and treated with calcification medium containing 2.0mM HNa2PO4 and 2.7mM CaCl2 for 24h, in normoxia (37° C humidified atmosphere with 5% CO2) and hypoxia (37° C humidified atmosphere with 1.2% O2/5% CO2) conditions. A WST-1 cell viability assay performed. All data is represented as percentage of controls, mean ± SEM; One-Way ANOVA with Bonferroni's multiple comparisons test t-test, (n=4/5), ****P<0.0001. HCAEC, human coronary artery endothelial cells, M199, medium 199 (Sigma-Aldrich).*

3.1.3 Calcification Medium Impairs EC Migration In Vitro.

EC migration is a crucial step during physiological angiogenesis for the formation of new blood vessels, and also during pathological angiogenesis[177]. In this study, incubation of ECs with CM suppressed EC migration in normoxia alone compared to untreated cells (202.30±13.37 vs 257.60±10.84, $P<0.0085$, Figure 3.3). In addition, CM significantly reduced migration in cells conditioned to hypoxia relative to normoxia-treated cells (110±8.25 vs 202.30±13.37, $P<0.0001$). Interestingly, hypoxic conditions caused a significant reduction in EC migration in untreated cells compared to those in normoxic conditions. This is the first study that has looked at the effect of high calcium on EC, and further studies are required to fully understand these interactions.

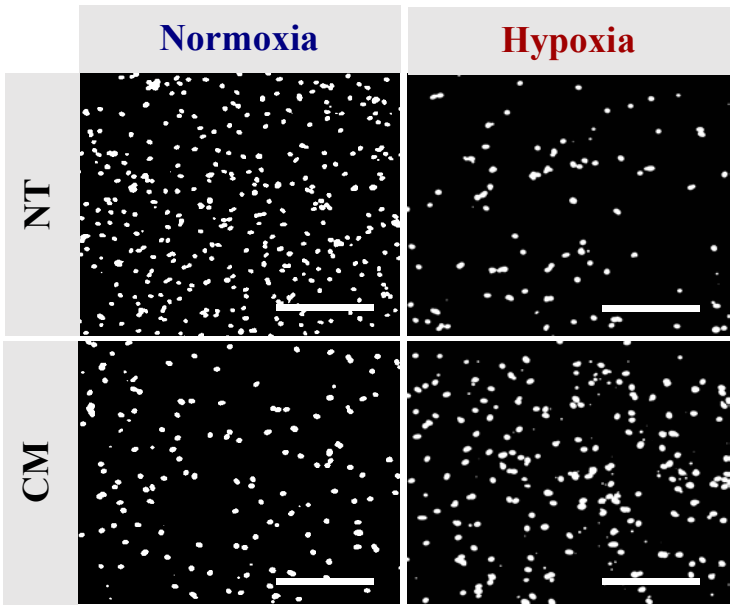

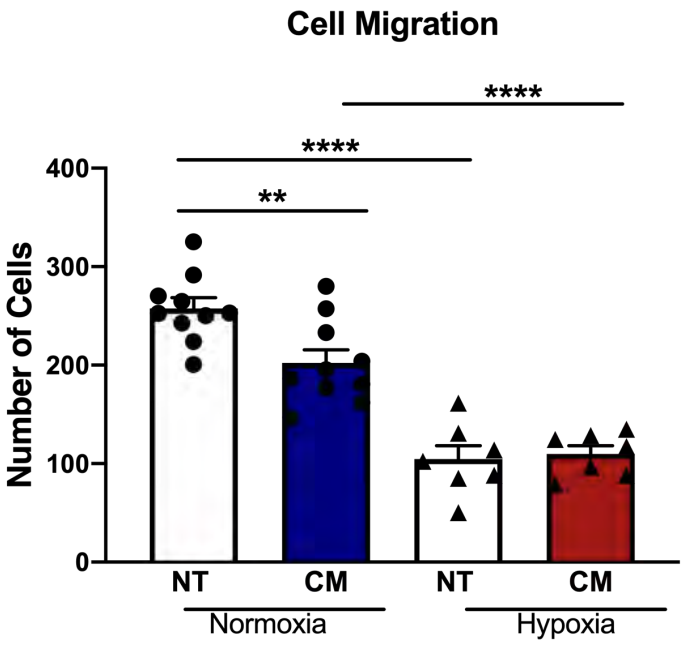

Figure 3.3: Figure 3.3.4: Calcification Medium Impairs EC Cell Migration In Vitro

(A-B) EC migration. HCAECs cultured and treated with calcification medium containing 2.0mM HNa_2PO_4 and 2.7mM $CaCl_2$ for 24h, in normoxia (37° C humidified atmosphere with 5% CO_2) and hypoxia (37° C humidified atmosphere with 1.2% O_2/5% CO_2) conditions. Boyden chamber assay was performed to assess cell migration. All data is represented as percentage of controls, mean ± SEM; One-Way ANOVA with Bonferroni's multiple comparisons test t-test, (n=4/5), **P<0.01, ****P<0.0001. HCAEC, human coronary artery ECs, M199, medium 199 (Sigma-Aldrich).

3.1.4 Calcification Medium Impairs EC Tubule Formation In Vitro.

Tubule formation is the final process of angiogenesis that results in the formation of tubular networks and is strictly controlled by different extracellular signals [50, 70, 178]. To elucidate further mechanisms of CM on angiogenesis and its effects on ECs, functional assays of tubulogenesis were carried out in vitro. In this study, incubation of ECs with CM further supressed EC tubule formation in normoxia compared to untreated cells (0.98±0.05 vs 1.26±0.06, $P<0.0001$, Figure 3.4). There was however no difference observed for number of tubules formed in hypoxia with CM and untreated cells. Together, this result highlights the unfavorable effects of high calcium on EC functionality.

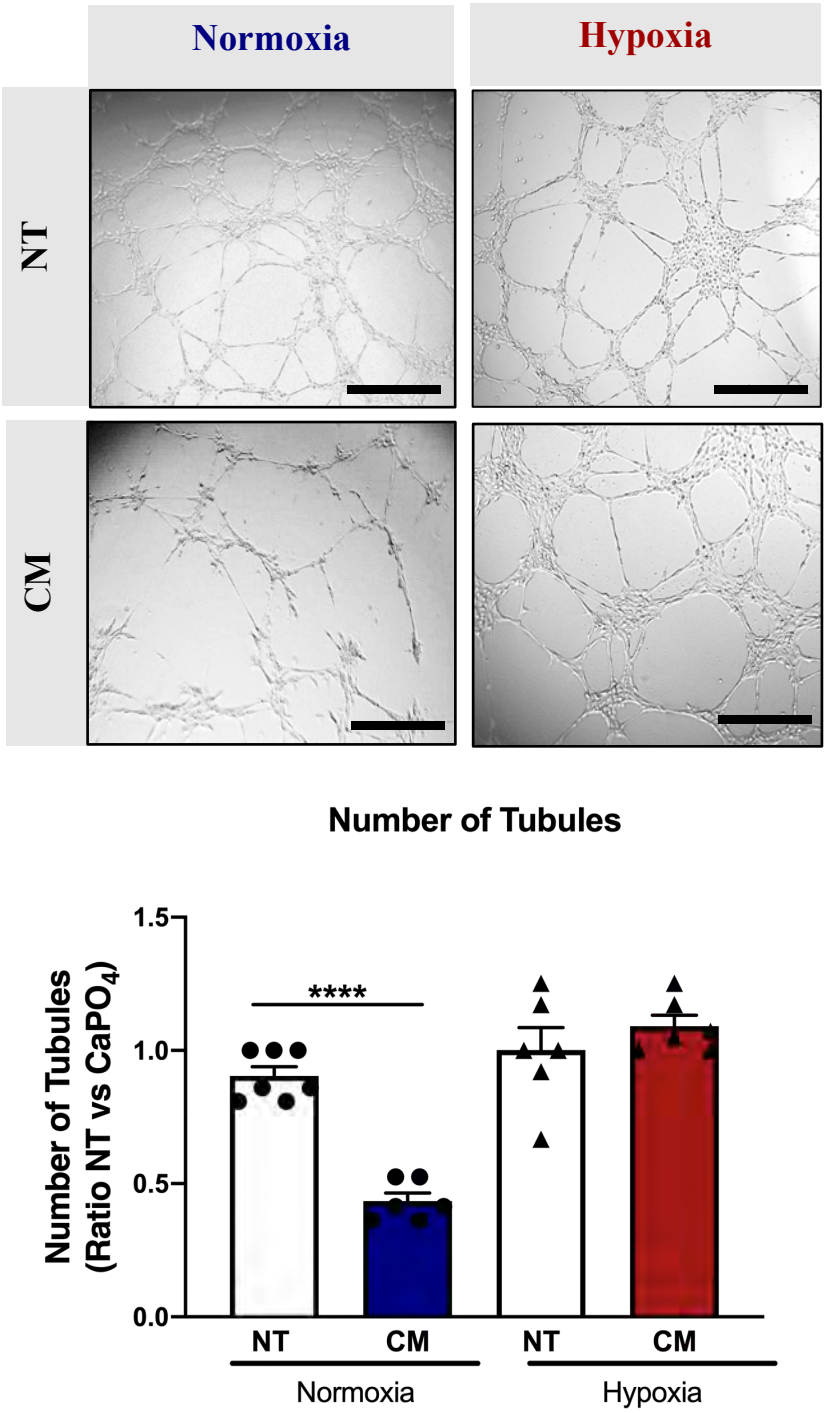

Figure 3.4: Calcification Medium Impairs EC Tubule Formation in Normoxia.

*(**A-B**) EC Tubule formation. HCAECs cultured and treated with calcification medium containing 2.0mM HNa_2PO_4 and 2.7mM $CaCl_2$ for 24h, in normoxia (37° C humidified atmosphere with 5% CO_2) and hypoxia (37° C humidified atmosphere with 1.2% O_2/5% CO_2) conditions. Matrigel tubulogenesis assay was conducted to assess tubule formation at 4h. All data is represented as percentage of controls, mean ± SEM; One-Way ANOVA with Bonferroni's multiple comparisons test t-test, (n=4/5), *P<0.05, **P<0.01, ***P<0.001. HCAEC, human coronary artery endothelial cells, M199, medium 199 (Sigma-Aldrich).*

3.1.5 Calcification Medium Differentially Regulates the Expression of Calcification Markers.

Runx2 is the main transcription factor of vascular calcification and its role in both osteogenesis and vascular calcification have been well established[93, 120, 123]. A previous study has shown that angiogenic cytokines upregulated Runx1 and Runx2 expression in murine EC model[179]. However, little is known about the regulation of Runx2 expression in EC following calcification stimulus. In this study, gene expression and protein levels of Runx2 were analysed. CM had no effect in regulating *Runx2* mRNA expression in normoxia or hypoxia conditions (Figure 3.5 A). Interestingly, RUNX2 protein expression was significantly downregulated in normoxia with CM treatment compared to untreated cells (64.59±6.82 vs 93.80±2.97, $P<0.0079$, Figure 3.5 B); with further downregulation observed in hypoxia (71.49±6.77 vs 105.50±5.32, $P<0.0039$, Figure 3.5 B).

Bone morphogenetic proteins (BMPs) are a group of secreted growth factors from the TGF-β superfamily of cytokines that possess significant osteogenic capacity and play an essential roles in vascular disease180, osteoblastic differentiation and bone formation181. CM significantly upregulated the mRNA expression of *Bmp2* in normoxia compared to untreated cells (240.40±32.43 vs 100.70±3.66, $P<0.0108$ Figure 3.5C). Conversely, stimulation of ECs with hypoxia decreased *Bmp2* gene expression when treated with CM (96.10±13.13.93 vs 281.20±75.83, $P<0.0073$, Figure 3.5C). In addition, CM treatment increased BMP2 protein expression in normoxia conditions (121.90±12.52 vs 100.70±0.65, Figure 3.5D) though not statistically significant. Hypoxia stimulation also decreased *Bmp2* expression with CM treatment (56.22±11.84 vs 99.31±1.22, $P<0.05$, Figure 3.5 D). though not statistically significant. Since BMP2 is expressed in ECs, and is known to drive the

activation of Runx2, together this data suggests a potential mechanistic pathway by ECs to upregulate calcification markers.

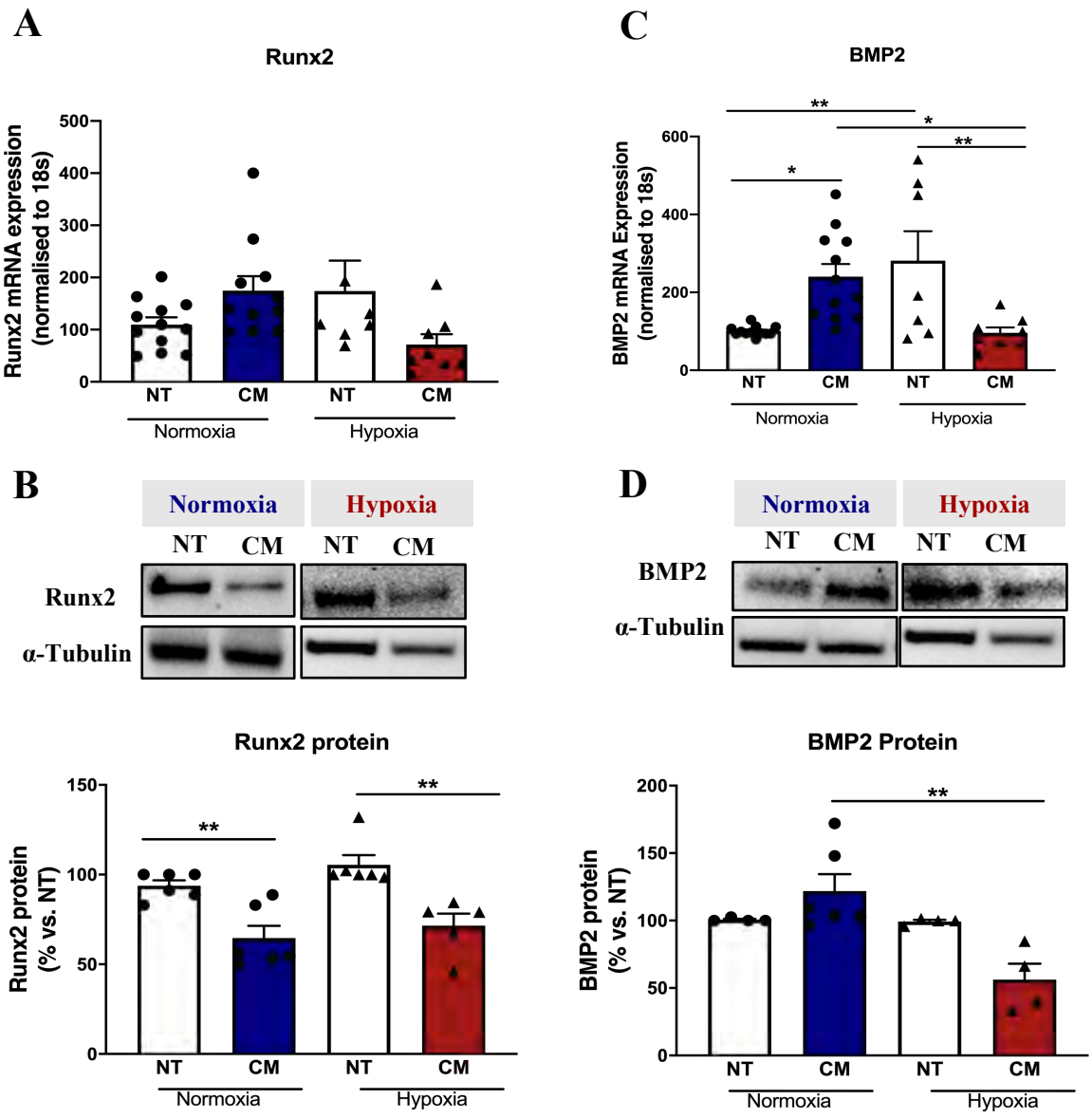

Figure 3.5: Calcification medium differentially regulates the mRNA expression of osteoblastic differentiation factor Runx2 and BMP2. **(A)** *Runx2* mRNA expression, **(B)** RUNX2 protein expression, **(C)** *Bmp2* mRNA expression, **(D)** BMP2 protein expression. HCAECs cultured and treated with calcification medium containing 2.0mM HNa_2PO_4 and 2.7mM $CaCl_2$ for 24h, in normoxia (37° C humidified atmosphere with 5% CO_2) and hypoxia (37° C humidified atmosphere with 1.2% O_2/5% CO_2) conditions. RNA extracted using Trizol, and. RNA was reverse transcribed into cDNA using iSCRIPT buffer. Real-time PCR was performed using universal SYBR© Green Supermix. Relative changes in mRNA expression were calculated using the ΔΔCt method**.** Whole cell lysates extracted for to measure immunoblotting. All data is represented as mean ± SEM; One-Way ANOVA with Bonferroni's multiple comparisons test, (n=3/4), *P<0.05, **P<0.01. HCAEC, human coronary artery endothelial cells, M199, medium 199 (Sigma-Aldrich), Runx2: runx2 related transcription factor, BMP2, bone morphogenetic protein 2.

3.1.6 Calcification Medium Differentially Regulates the OPG-RANK-RANKL axis in ECs.

The RANK-RANKL-OPG cytokine pathway comprises of members of the TNF superfamily of ligands and are highly associated with vascular calcification and stimulate mineral deposition in VSMCs[138, 153]. Previous studies investigating this pathway have consistently been evaluated in VMSCs[182], however, the role of calcium-phosphate on EC is still yet to be established. In this study, CM treatment had no significant effect in regulating *Rankl* mRNA expression in normoxia. However, hypoxia stimulation downregulated *Rankl* mRNA expression with CM treatment compared to untreated cells (52.69±8.00 vs 107.50±14.82, P<0.0158 Figure 3.6B). When RANKL protein was assessed, CM had no effect on RANKL protein expression in normoxia whilst decreasing its expression with hypoxia stimulation (80.22±12.95 vs 163.80±40.09, P<0.0357, Figure 3.6B).

CM increased *Rank* receptor mRNA expression in normoxia relative to untreated cells (CM: 152.80±9.34 vs 100.60±3.41, P<0.0001); which was further decreased with hypoxia stimulation following CM treatment (40.86±6.01 vs 104±13.53, P<0.0001, Figure 3.6C).

OPG is a soluble decoy receptor for RANKL, expressed in the heart, arteries and veins, and is secreted by ECs[183]. OPG is a physiological and pharmacological inhibitor of bone resorption and is highly elevated in cardiovascular disease, obesity and diabetes[184, 185, 30]. Gene expression for *Opg* was significantly upregulated with CM treatment in normoxia (181.10±32.96 vs 104.60±8.94, P<0.0371, Figure 3.6D), and was significantly downregulated with hypoxia stimulation (62.80±12.79 vs 158.80±34.60, P<0.0455, Figure 3.6D). Though the protective role of OPG against calcification is well known**,** such increased

expression in ECs in normoxia presumably reflects a vascular defense that helps to prevent excessive RANKL signaling via a negative feedback regulation. Together, this data demonstrates the negative effect of CM on hypoxia in regulating key calcification drivers.

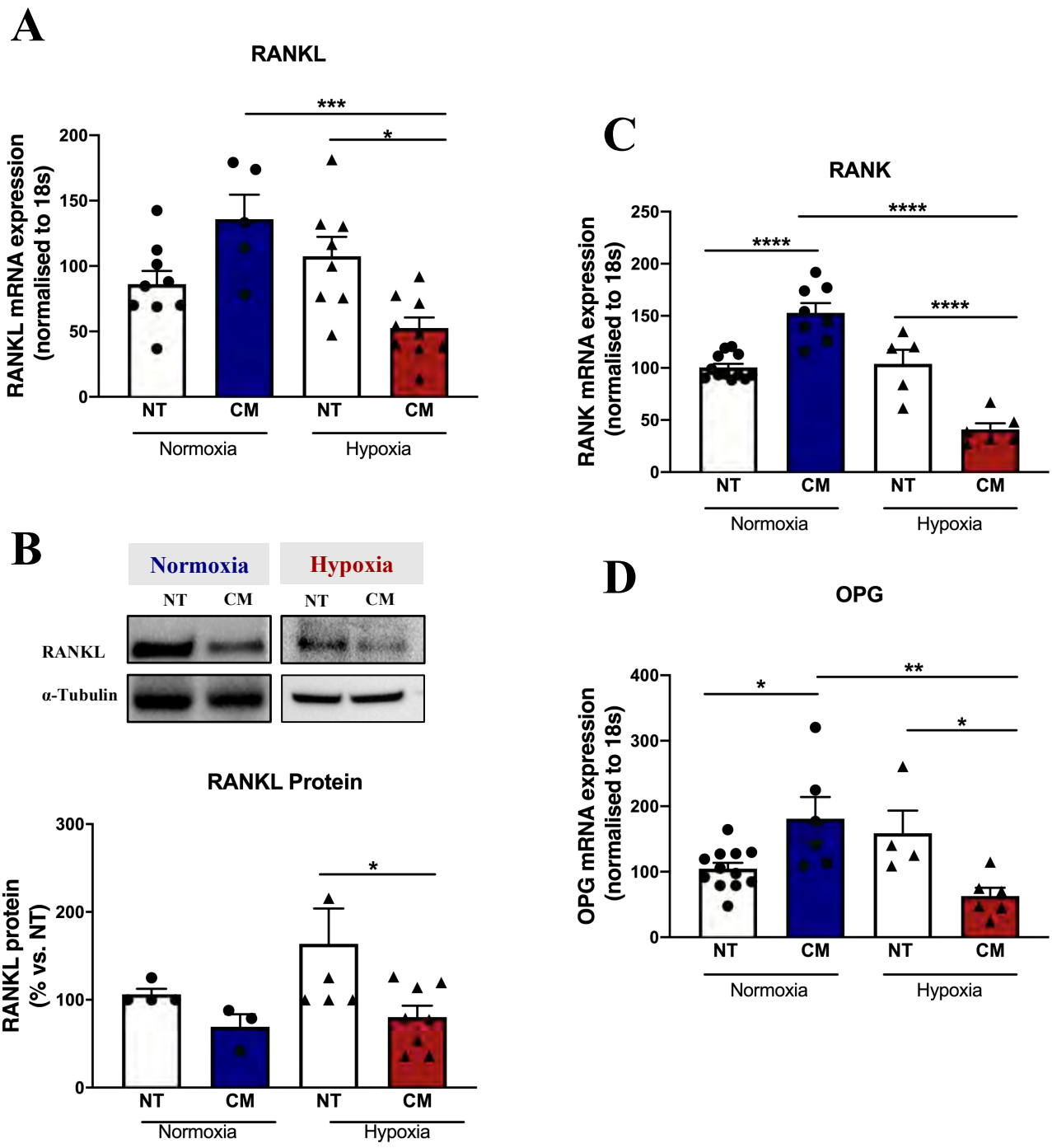

Figure 3.6: Calcification Medium Differentially Regulates RANK-RANKL axis in ECs.

Rank mRNA expression (B) RANKL protein expression, (C) Rankl mRNA expression. HCAECs cultured in MesoEndo medium, serum starved in 10% FBS M199 medium, then treated with calcification medium containing 2.0mM HNa_2PO_4 and 2.7mM $CaCl_2$ for 24h. RNA extracted using Trizol, and. RNA was reverse transcribed into cDNA using iSCRIPT buffer. Real-time PCR was performed using universal SYBR© Green Supermix. Relative changes in mRNA expression were calculated using the ΔΔCt method. Whole cell lysates extracted for to measure immunoblotting. All data is represented as mean ± SEM; One-Way ANOVA with Bonferroni's multiple comparisons test, (n=3/4). HCAECs, human coronary artery endothelial cell, RANKL, receptor activator of nuclear factor κB ligand, and receptor RANK.

3.1.7 CM-Induced Upregulation of HIF-1α Gene Expression.

HIF-α is a pivotal driver of angiogenesis both under physiological and pathological conditions, particularly in response to ischemia. During hypoxia, HIF-1α translocates to the nucleus where it complexes with the HIF-1β subunit and binds to the hypoxia response element (HRE)[67]. This drives the expression of pro-angiogenic mediators such as VEGFA that drive angiogenesis. Previously, hypoxia stimulation was shown to enhance phosphate-induced VSMC calcification and transdifferentiation[186], however there is a paucity of data investigating high calcium effects on EC expression of HIF-1α in angiogenesis. In this study, EC incubation with CM had no effect in regulating *Hif-1α* gene expression in normoxia (Figure 3.7 A). Because HIF-1α is post-translationally regulated, protein expression was measured and significant upregulation was observed in normoxia with CM treatment (507.10±59.70 vs 113.80±13.80, P<0.0001, Figure 3.7 B). HIF-1α protein expression was however significantly downregulated when comparing normoxia CM (507.10±59.70) vs hypoxia CM (118.30±14.74, P<0.0001, Figure 3.7 B), demonstrating a negative effect of CM on hypoxia-driven HIF-α expression.

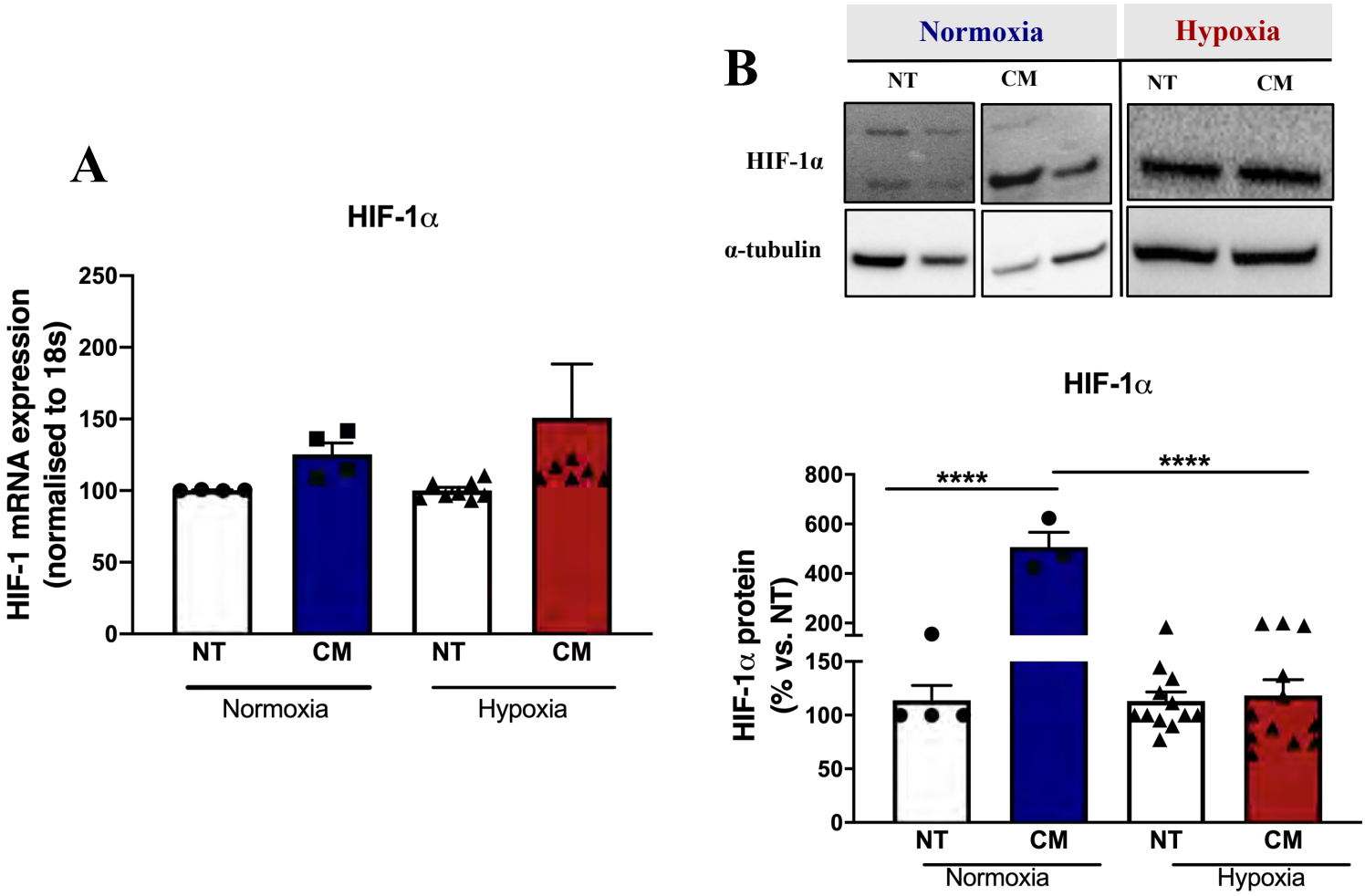

Figure 3.7: Hypoxia Upregulates CM-Induced Gene Expression of HIF-1α in Normoxia Only.

*HCAECs cultured in MesoEndo medium then treated with calcification medium containing 2.0mM HNa2PO4 and 2.7mM CaCl2 in 10% FBS M199 medium for 24h. RNA extracted using Trizol, and. RNA was reverse transcribed into cDNA using iSCRIPT buffer. Real-time PCR was performed using universal SYBR© Green Supermix. Relative changes in mRNA expression were calculated using the ΔΔCt method. Whole cell lysates were extracted to measure protein expr3ession via immunoblotting technique. Even protein loading was confirmed by α-Tubulin. All data is represented as mean ± SEM; One-Way ANOVA with Bonferroni's multiple comparisons test, (n=3/4), *P<0.05, ***P<0.001. HCAEC, human coronary artery endothelial cells, M199, medium 199 (Sigma-Aldrich), HIF-1α, hypoxia-inducible factor-1 alpha.*

3.1.8 Calcification Medium Regulation of Upstream Signalling Pathways for HIF-1α to Drive Angiogenesis.

HIF-1α is post-translationally modulated, and under normoxic conditions, propyl hydroxylase domain proteins (PHD1/2) hydroxylate the proline residues of HIF-1α allowing the Von-Hippel Lindau ubiquitin ligase complex to target HIF-1α for proteasomal degradation[46, 67], as depicted in Figure 1.4 (chapter 1). Currently, very little is known of the effects of elevated calcium on PHD regulation in calcification. To understand the regulation of HIF-1α, PHD2 and PHD3 protein expression were measured. CM had no effect in regulating PHD2 protein expression in normoxia or hypoxia conditions relative to untreated cells Figure 8 A). however as expected, PHD2 protein expression was significantly downregulated when comparing normoxia CM (308.60±46.92) versus hypoxia CM (139.20±29.71, $P<0.0337$, Figure 3.8 A). Similarly, no change was observed with PHD3 protein expression in both normoxia of hypoxia conditions (Figure 3.8 B). This data may therefore suggest that regulation of these angiogenic markers by CM is not via the PHD signalling.

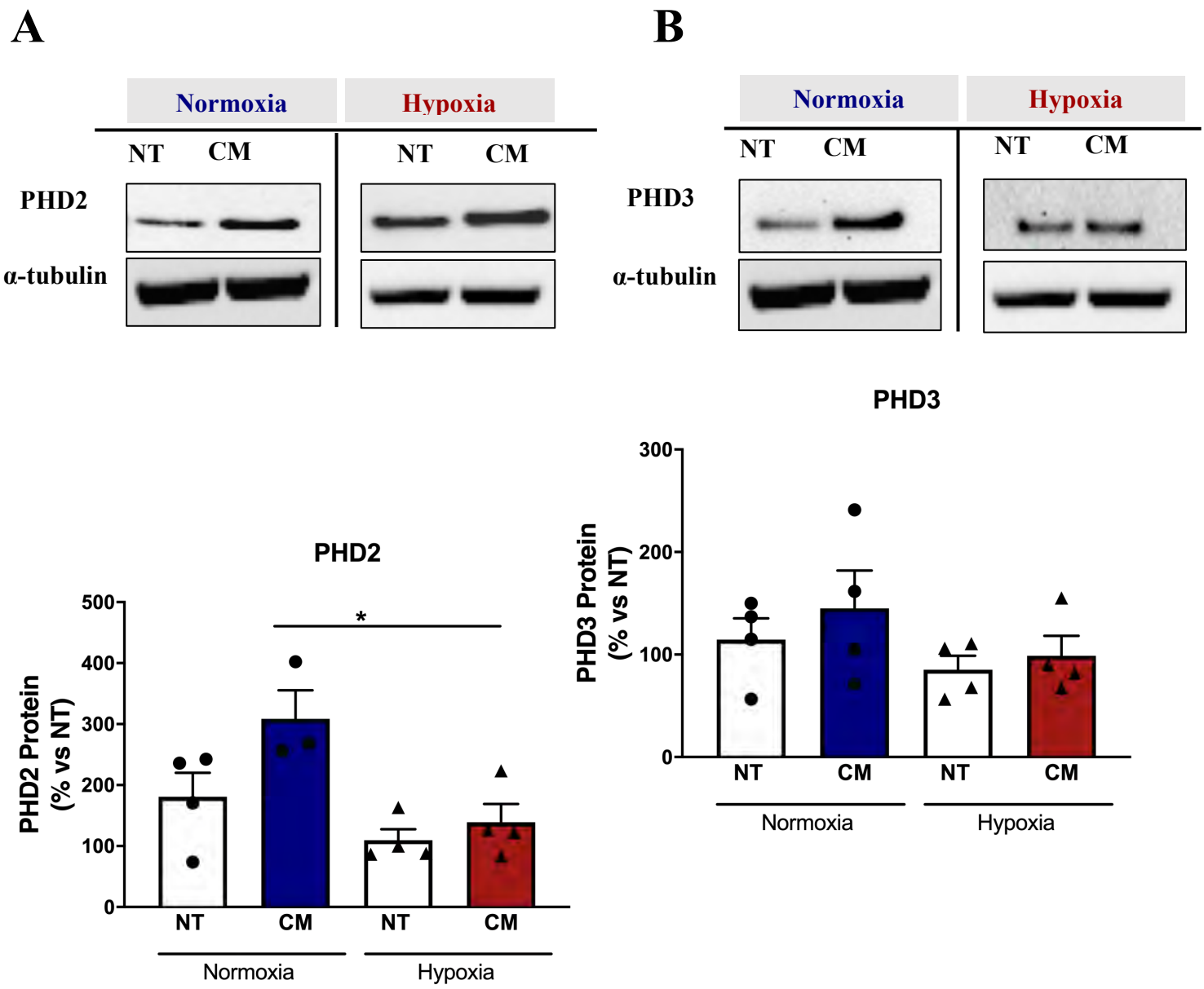

Figure 3.8: Normoxia Upregulates PHD2 and PHD3 Protein expression in ECS.

HCAECs cultured in MesoEndo medium then treated with calcification medium containing 2.0mM HNa2PO4 and 2.7mM CaCl2 in 10% FBS M199 medium for 24h. Whole cell lysates were extracted to measure protein expression via immunoblotting technique. Even protein loading was confirmed by α-Tubulin. All data is represented as mean ± SEM; One-Way ANOVA with Bonferroni's multiple comparisons test, (n=3/4). HCAEC, human coronary artery endothelial cells, M199, medium 199 (Sigma-Aldrich), PHD2-3, propyl hydroxylase 2 &3.

Furthermore, in hypoxic conditions, the PI3/Akt signalling pathway is activated resulting in the induction of E3 ubiquitin ligases Siah 1 & Siah 2. These target and promote degradation of PHDs, which leads to HIF-1α stabilisation, allowing HIF-1α translocation to the nucleus where it complexes with the HIF-1β subunit and binds to the hypoxia response element (HRE)[67] as depicted in Figure 1.4 (chapter 1). In this study, normoxic conditions had no effect in regulating *Siah1 and Siah2* mRNA expression with CM treatment. However, when ECs were stimulated with hypoxia, CM caused significant downregulation in *Siah1* mRNA expression compared to control cells (46.10±10.62 vs 107.40±2.24, P<0.0207, Figure 3.9 A); and *Siah 2* mRNA expression (59.99±11.31 vs 101.0±0.30, P<0.1737 Figure 3.9 B).

Collectively, this data illustrates CM-induced downregulation of PHD and Siah activity in ECs following hypoxia stimulation. It however remains unclear as to how CM regulates PHD and Siah expression in ECs and thus further studies are warranted to fully understand these molecular interactions.

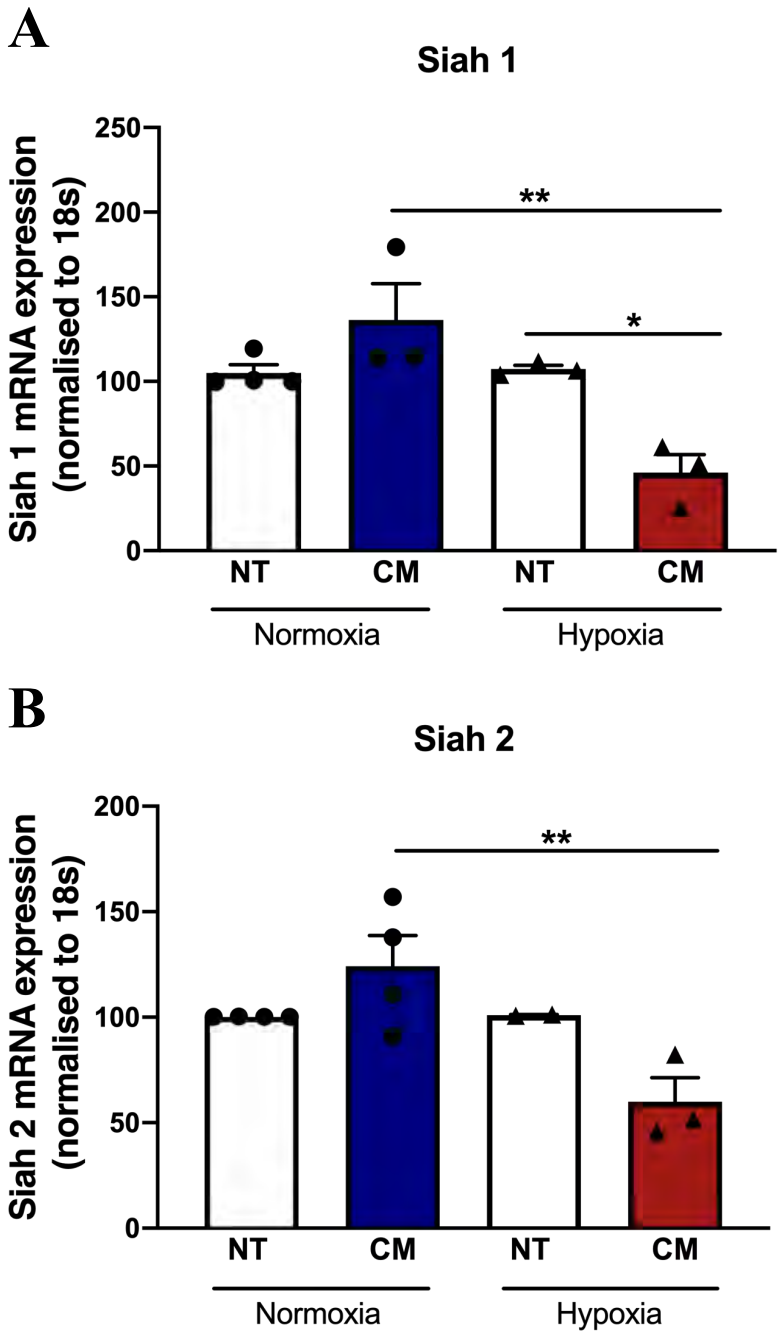

Figure 3.9: Hypoxia Decreases Siah 1 and Siah 2 Expression in ECS.

*HCAECs cultured in MesoEndo medium, serum starved in 10% FBS M199 medium, then treated with calcification medium containing 2.0mM HNa_2PO_4 and 2.7mM $CaCl_2$ for 24h. RNA extracted using Trizol, and. RNA was reverse transcribed into cDNA using iSCRIPT buffer. Real-time PCR was performed using universal SYBR© Green Supermix. Relative changes in mRNA expression were calculated using the ΔΔCt method. All data is represented as mean ± SEM; One-Way ANOVA with Bonferroni's multiple comparisons test, (n=3/4), **P<0.01. HCAEC, human coronary artery endothelial cells, M199, medium 199 (Sigma-Aldrich).*

3.1.9 CM Upregulates Angiogenesis via the VEGFA-VEGFR2 axis.

During angiogenesis, HIF-1α modulates the expression of downstream targets by regulating the transcription of VEGF, the principle regulator of angiogenesis [50, 70]. VEGFA protein expression was significantly upregulated in normoxia with CM treatment relative to untreated cells (849.40±197.60 vs 116.50±16.55, P<0.0001); with no effect seen in hypoxia conditions (Figure 3.10 B). However, when comparing normoxia CM vs hypoxia CM, VEGFA protein expression was decreased (74.47±7.66 vs 849.40±197.60, P<0.0001, Figure 3.10 B). *Vegfr2* mRNA expression remained unchanged in both normoxia and hypoxia (Figure 3.10 C). Furthermore, CM had no effect on phosphorylated VEGFR2 protein expression compared to untreated cells in normoxia or hypoxia (Figure 10 D). Collectively, based on this data, upregulation of VEGFA in normoxia proposes a compensatory mechanism for CM-induced VEGFA expression with CM treatment.

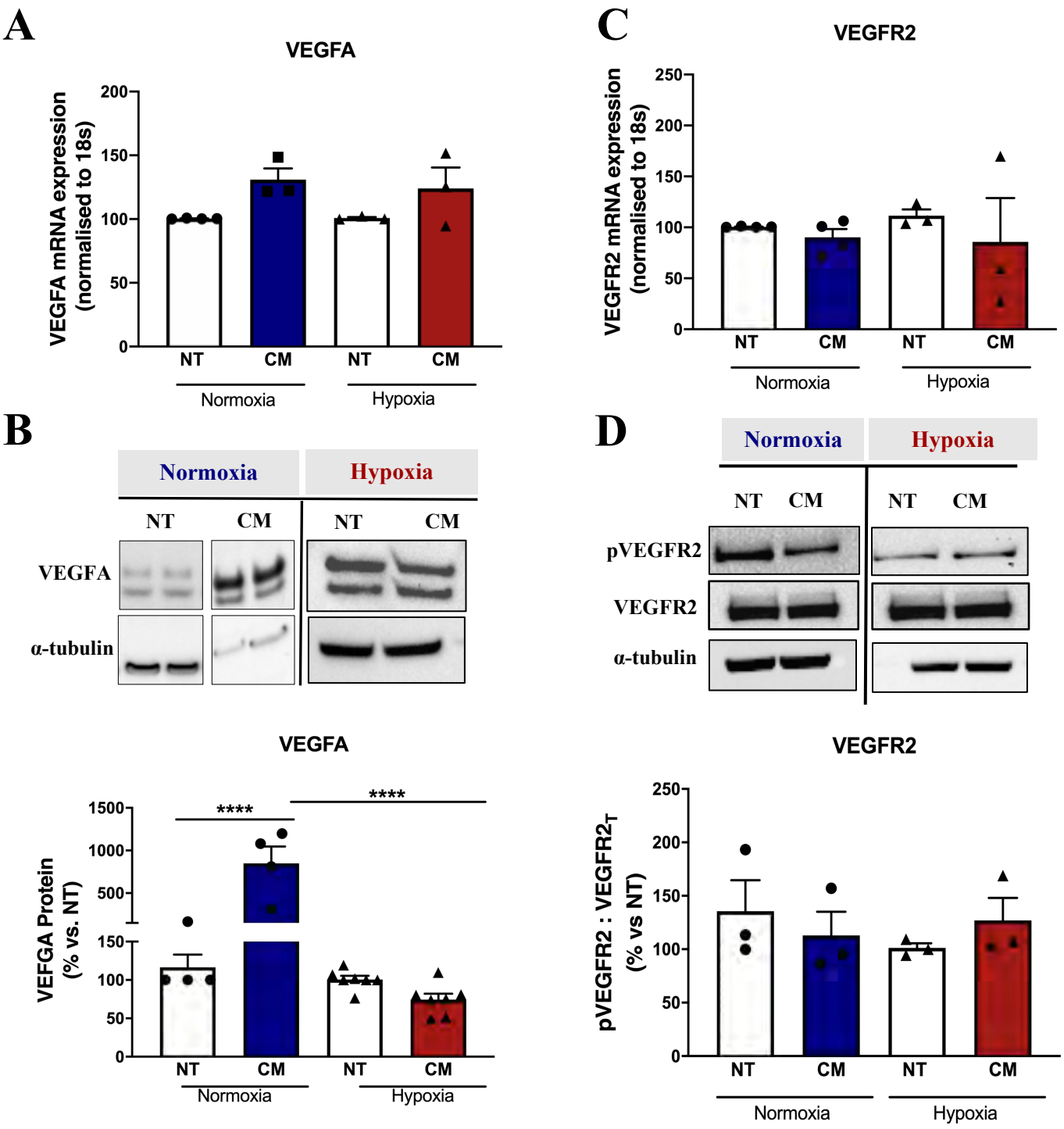

Figure 3.10: CM Upregulates Angiogenesis via the VEGFA-VEGFR2 Axis

*HCAECs cultured and treated with calcification medium containing 2.0mM HNa_2PO_4 and 2.7mM $CaCl_2$ for 24h, in normoxia (37° C humidified atmosphere with 5% CO_2) and hypoxia (37° C humidified atmosphere with 1.2% O_2/5% CO_2) conditions. RNA extracted using Trizol, and. RNA was reverse transcribed into cDNA using iSCRIPT buffer. Real-time PCR was performed using universal SYBR© Green Supermix. Relative changes in mRNA expression were calculated using the ΔΔCt method. Whole cell lysates were extracted to measure total and phosphorylated protein expression via immunoblotting technique. Even protein loading was confirmed by α-Tubulin. (A) vegfa mRNA expression, (B) VEGFA protein expression, (C) vegfr2 mRNA expression, (D) phosphorylated VEGFR2 (pVEGFR2) and total VEGFR2 ($VEGFR2_T$). All data is represented as mean ± SEM; One-Way ANOVA with multiple comparisons, Bonferroni test, (n=4/5), *P<0.05, **P<0.001. HCAEC, human coronary artery endothelial cells, VEGFA, vascular endothelial growth factor and receptor, VEGFR2, vascular endothelial growth factor receptor 2.*

3.1.10 Calcification Medium Negatively Affects Angiogenesis via Suppression of eNOS.

To further determine the mechanism of calcification medium in driving angiogenesis, downstream signalling pathways were assessed. Endothelial nitric oxide (eNOS) is located downstream of the HIF-1α-VEGFA pathway[71]. During hypoxia, eNOS produces nitric oxide (NO) to help enhance EC proliferation, migration and to increase VEGFA expression; which ultimately increases angiogenesis[72]. In this study, EC incubation with CM significantly mitigated eNOS phosphorylation in both normoxia (66.75±7.86 vs 112.9±6.78, $P<0.0151$); and hypoxia (49.44±9.78 vs 92.75±11.62, $P<0.0208$, Figure 3.11). In line with previous data from Figure 3.4 where significant reduction in EC tubule formation and cell migration were observed with CM; this reduction in eNOS expression may suggest a downstream signalling effect of high calcium in supressing angiogenesis, despite increased angiogenic marker expression.

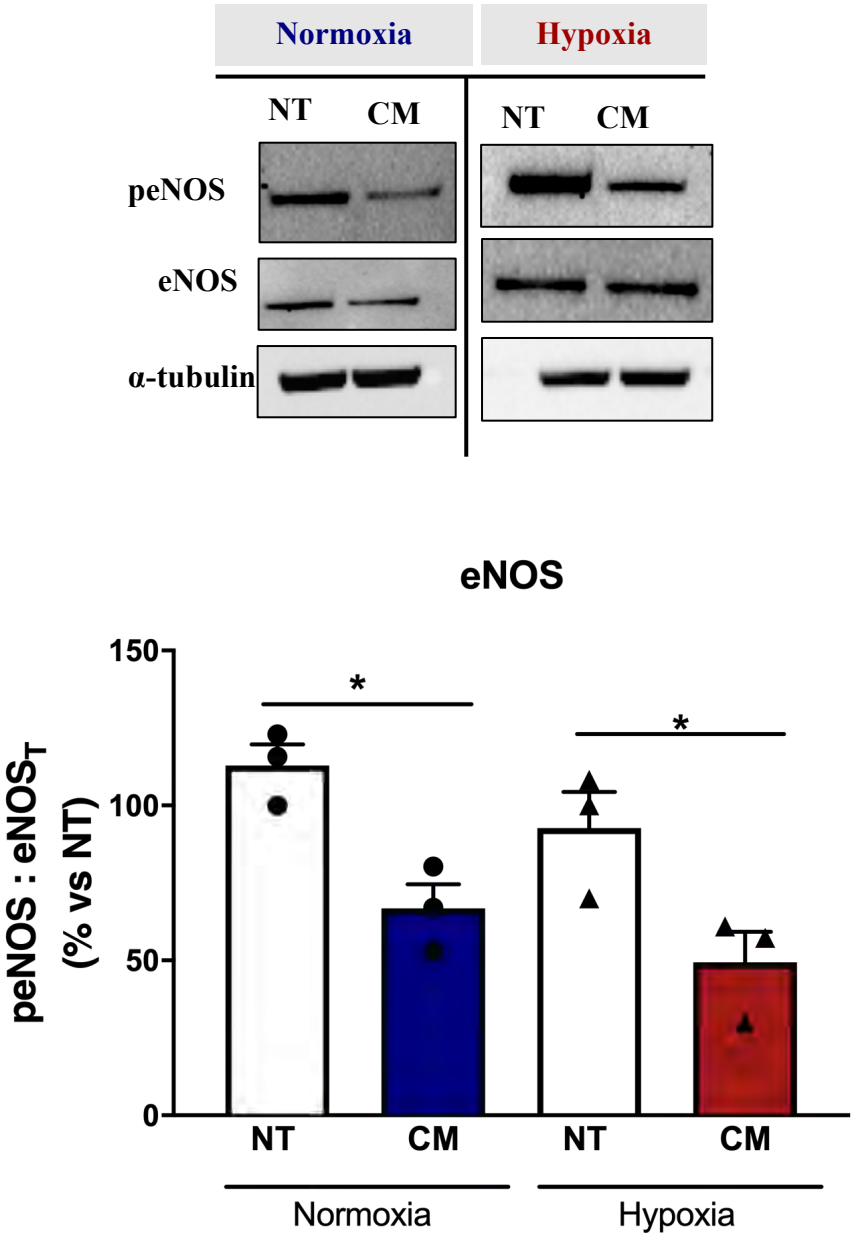

Figure 3.11: Calcification Medium Negatively Affects Angiogenesis via Suppression of eNOS.

*HCAECs cultured and treated with calcification medium containing 2.0mM HNa_2PO_4 and 2.7mM $CaCl_2$ for 24h, in normoxia (37° C humidified atmosphere with 5% CO_2) and hypoxia (37° C humidified atmosphere with 1.2% O_2/5% CO_2) conditions. Whole cell lysates were extracted to measure total and phosphorylated protein expression via immunoblotting technique. Even protein loading was confirmed by α-Tubulin. All data is represented as mean ± SEM; One-Way ANOVA with multiple comparisons, Bonferroni test, (n=4), *P<0.05, **P<0.001. HCAEC, human coronary artery endothelial cells, eNOS, endothelial nitric oxide synthase.*

3.1.11 Discussion

Vascular calcification (VC) is associated with atherosclerotic lesions and is thought to be a potential driver of PAD by affecting limb revascularization following ischemia[100]. In this case, angiogenesis or blood vessel formation is affected by the presence of calcific lesions within the peripheral arteries. These studies report for the first time that high levels of calcium impair endothelial cell angiogenesis in vitro. CM treatment attenuated the ability of ECs to form tubes and migrate, suggesting potential inhibition of angiogenesis, despite the increased cell viability that was observed in normoxia.

Previous studies have reported that incubation of human umbilical vein EC (HUVECs) with hypoxia showed resistance to hypoxia-induced cell death, with 98% cell viability after 24 h and 55% viability after 48 h of continuous exposure[187], thus suggesting that chronic hypoxia is necessary for EC viability. However, despite this result, there remains limited studies showing the effect of elevated calcium-phosphate on EC viability in hypoxia conditions. Furthermore, another study reported significant proliferative activity of mesenchymal stem cells and bone marrow mesenchymal stem cells treated with calcium concentrations above 1.8mM[188]. This is however the first study to explore the effect of high calcium on EC proliferation, placing a great need for future studies to fully understand its interactions.

There exist several lines of evidence that bone-related osteogenic markers are involved in regulating vascular calcification in VSMCs, although lacking in the context of ECs. These regulators include members of the TNF superfamily of cytokines, RANK and its ligand (RANKL); and its soluble decoy receptor OPG; and other bone regulatory factors such runx2, BMP2 and ALP[189]. In this study, these calcification markers were evaluated and were found to be elevated with CM treatment in normoxia conditions, thus highlighting the

presence or initiation of a calcification process. However, when cells were stimulated with hypoxia, this response was negated. A previous study conducted in human periodontal cells demonstrated that hypoxia stimulated the expression of Rankl mRNA and protein expression at 12 h, 24 h and 48 h while downregulating Opg mRNA and protein expression[190]. In a different study, hypoxia enhanced the expression of both RANKL and RANK in breast cancer cells, via activation of the HIF-1α known to drive angiogenesis[191]. Collectively, these studies suggest chronic hypoxia regulates these calcification markers, and because of the lack of studies conducted in ECs, further research is required to fully understand this.

Additionally, there lies extensive work to address the potential role of BMP2 in angiogenesis. In previous published work, BMP2 enhanced and stimulated blood vessel formation in developing tumours, to increase neovascularization[192]. Furthermore, in this same study, recombinant BMP2 induced tubule formation in human aortic EC (HAEC) and HUVECs, whilst also stimulating proliferation of HAECs. BMP2 regulation of endothelial cell processes is proposed to be modulated mechanistically via phosphorylation of ERK 1/2 and SMAD pathways[192]. In line with this, data from this study demonstrated that treatment of ECs with CM increased mRNA expression of *Bmp2* in normoxia, which coincides with increased cell viability (Figure 3.13). Previous studies however have reported conflicting results whereby hypoxia up-regulated *Bmp2* mRNA and protein expression in bovine capillary EC and human microvascular ECs, a result that was also enhanced with VEGF treatment after 24h and 48h of treatment[193]. In other cell types such as osteoblasts, hypoxia also stimulated upregulation of *Bmp2* mRNA and protein expression[181]. There lie arguments suggesting that different ECs will respond differently.

OPG is highly elevated in cardiovascular disease, obesity and diabetes[184, 185, 30], and while this clinical finding is not well understood it is possible the increased levels act as a compensatory mechanism for protection against disease[154, 194]. Our findings demonstrate that a calcification milieu is capable of upregulating both the drivers (RANKL, Runx2, BMP2) and the inhibitor (OPG) of calcification with detrimental effects on proliferation, cell migration and tubule formation, all hallmark measures of angiogenesis (Figure 3.13).

Ischemia is a potent stimulus for hypoxia-driven angiogenesis in pathological conditions of MI, stroke and peripheral arterial disease. In clinical settings, hypoxia increases HIF-1α which further promotes VEGFA and VEGFR2 signalling to promote angiogenesis[46]. Interestingly, this study demonstrated that this calcification milieu also promotes the release of key angiogenic markers HIF-1α and VEGFA; which may, at least in part be a compensatory mechanism by the cells to counteract this mineral imbalance, thus favouring angiogenic protein synthesis; suggesting that this is not occurring via the HIF-1α pathway, and may be occurring via alternative mechanisms. Furthermore, based on data from section 3.3.10, where CM treatment to ECs increased *Siah 1 & Siah 2* mRNA expression in hypoxia; this study confirms the role of Siah 1 and Siah 2 in suppressing PHDs activity in hypoxia, to therefore increase HIF-1α stability. These results thereby suggest a plausible role of calcium phosphate in driving angiogenesis via upregulation of HIF-1α in normoxia conditions, though further analysis is required to fully understand these interactions.

Both HIF-1α and Runx2 are transiently expressed in vascular endothelial cells, which may elude to their potential role in the regulation of angiogenesis[123]. HIF-1α is expressed early in embryonic development and is necessary for bone development[195], while Runx2 is

also expressed throughout skeletal development and is crucial for vascular invasion[119]. Deficiency in Runx2 is reported to result in vascularization defects, mainly due to reduced VEGF expression, a key growth factor essential for angiogenesis [120, 121]. Runx2 has also been shown to increase HIF-1α protein expression, mainly because it stabilises and protects HIF-1α from degradation, in both normoxic and hypoxic conditions[121]. Overexpression of Runx2 is also associated with significant increases in *Vegfa* mRNA expression, and vice versa. This is thought to occur due to physical interactions of Runx2 and HIF-1α on the Runx2/RUNT domain[122] and possibly through binding of Runx2 on the VEGF promotor region[120].

From these results, suppression of angiogenesis was also associated with upregulation of angiogenic markers HIF-1α and VEGFA and its receptor VEGFR2 in normoxia. Since Runx2 is expressed in ECs of developing blood vessels[123], this may explain its role in regulating angiogenesis, and highlights the need for further studies to expand our understanding of this relationship. Additionally, the time of exposure of cells to hypoxia may influence the angiogenic response. Previous studies have reported that ECs exposed to 24 h of hypoxia attenuated VEGF-induced EC migration, proliferation and tubule formation; demonstrating the negative effect of chronic hypoxia on angiogenesis[71]. In this study, cells were conditioned to hypoxia for only 4 hours, reflecting acute hypoxia, and may therefore help explain the increase in angiogenic marker expression (HIF-1α and VEGF). Based on these results, I propose a potential mechanistic link in our study, where treatment of ECs with $CaPO_4$ increased the expression of both Runx2, and HIF-1α. Therefore, it is clear that both factors can interact to regulate VEGFA angiogenic signalling, which also showed increased expression with $CaPO_4$ treatment.

There are a myriad of approaches for calcifying cells in cell culture with calcification medium. The commonly used form of calcification medium is supplemented with inorganic (sodium phosphate 1-5mM) or organic (β-glycerophosphate e.g., 10 mM) phosphate[196]. Dexamethasone is a steroid that is often used to stimulate calcification in vitro. However, these readily available methods do not recapitulate hyperphosphatemia, hypercalcemia, inflammation or a calcification environment as seen in the human body[196]. This thesis utilised the method of supplementing calcium and phosphate to cells as means to induce a physiological high calcific environment in these cells. A limitation that exists across all studies in calcification is the lack of consensus on which calcification stimulus is the most effective and for what purpose. The use of calcium phosphate in these studies does not preclude the results observed elsewhere, it only highlights the need for a standardised approach

3.1.12 Conclusion

Overall, observations from this study found that CM impaired EC angiogenesis in normoxia, as demonstrated in the functional assays for tubule formation and cell migration. When evaluated mechanistically, I observed decreased expression of downstream signalling pathways of eNOS, a known to drive EC angiogenesis. Furthermore, I observed upregulation of key calcification markers in both normoxia and hypoxia conditions, which coincided with upregulation of key pro-angiogenic factors HIF-1α and VEGFA, suggesting a compensatory mechanism or other alternative pathways.

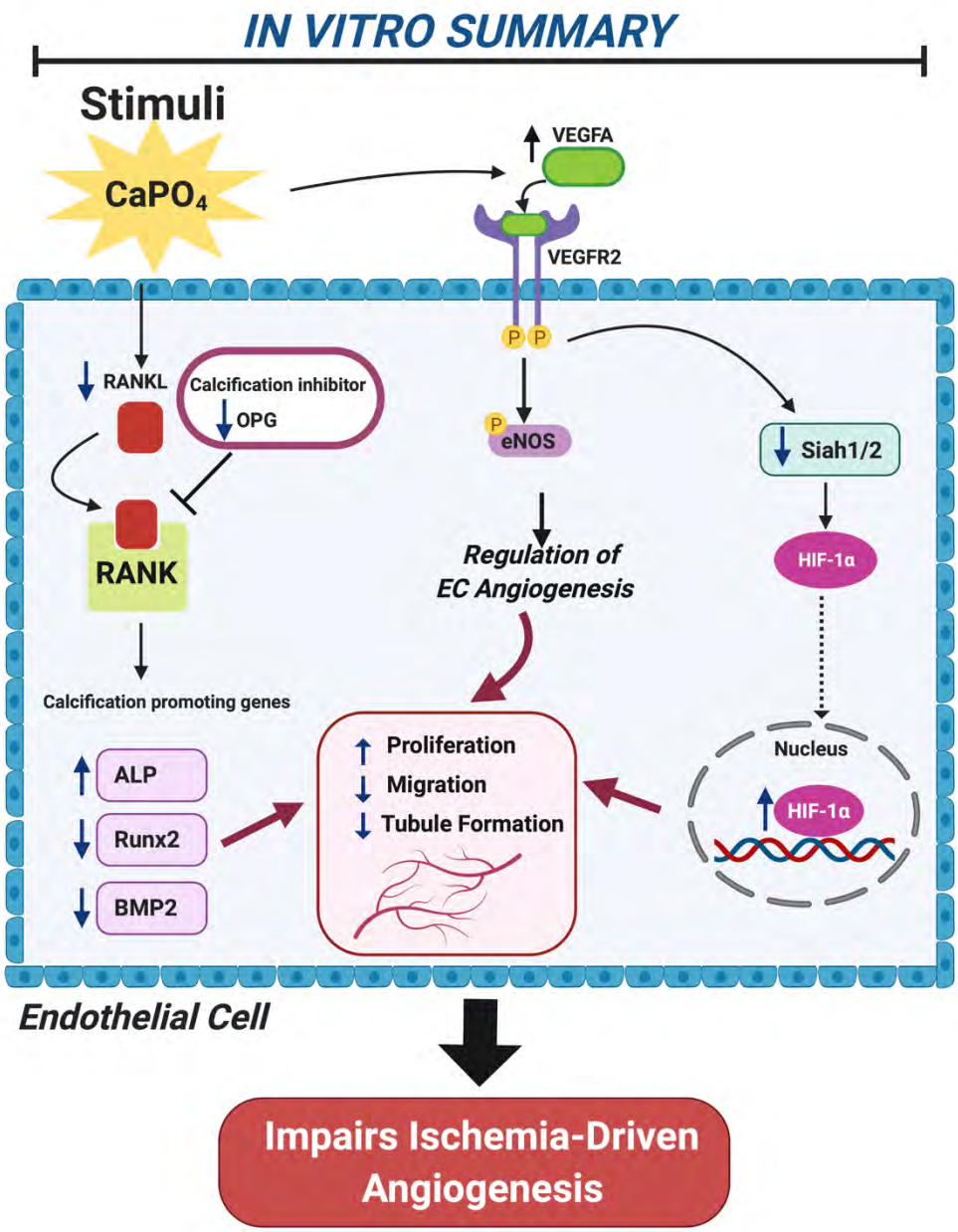

Figure 3.13 : In Vitro Ischemia Summary diagram.
EC: Endothelial Cell, HIF-1α: Hypoxia-inducible factor-1 alpha, VEGFA: Vascular endothelial growth factor, VEGFR2: Vascular endothelial growth factor receptor 2, BMP2: Bone morphogenetic protein 2, Runx2: Runx2 related transcription factor, RANK/RANKL: Receptor activator of nuclear factor κ-B & ligand, OPG: Osteoprotegerin, ALP: Alkaline Phosphatase, eNOS: Endothelial Nitric Synthase

CHAPTER 4:

CALCIFICATION MILLIEU IMPAIRS ISCHEMIA-DRIVEN ANGIOGENESIS IN VIVO

2.1 Introduction

Ischemia reperfusion occurs in various pathologies post-MI, due to occlusion and obstruction of major arteries that block the flow of oxygenated blood from reaching the tissue[175]. A major consequence of chronic ischemia is irreversible injuries to affected cells, resulting in cell death. One other risk factor known to result to chronic ischemia is the presence of calcified lower extremity vessels as observed in diabetic and PAD patients[33, 34, 37, 197]. Arterial calcification is highly associated with increased risk of limb amputations, however the causal link between calcification in lower extremity arteries and the severity of ischemia remains unclear.

Findings from chapter 3 showed differential regulation of ischemia-driven angiogenesis with calcification medium (CM) in vitro. There was upregulation of transcription markers for calcification with CM, and functionally, CM decreased angiogenic processes of tubule formation and cell migration, which was accompanied by increased expression of pro-angiogenic markers as a compensatory mechanism for angiogenesis.

To further understand the relationship between high calcium in regulating angiogenesis, in vivo mouse studies were employed. In disease, ischemic tissue stimulates the growth of new blood vessels as an important strategy to revascularize the damaged area. The presence of calcification and a highly calcific environment has not been studied as a deterrent of this angiogenic process. The aim of this study was to assess the effects of vascular calcification on ischemia-driven angiogenesis using murine models of both angiogenesis and vascular calcification. The osteoprotegerin (OPG) knockout mouse is a well validated model used to study vascular calcification and has been shown to exhibit calcification in their aortas and renal arteries[145]. In this study, $OPG^{-/-}$ mice were compared against their WT counterparts (C57BL6/J) using a well-validated model of physiological angiogenesis, namely the hindlimb ischemia model (HLI), which is primarily driven by hypoxia. Since both peripheral arterial

disease and vascular calcification are age-associated diseases, two different aged cohorts were utilised: 8-10wk (young)- and 24wk (aged).

2.2 Results

2.2.1 Confirmed Absence of OPG using an assay OPG ELISA assay to measure plasma OPG levels in mice following peri-arterial cuff and HLI surgeries.

OPG deficient mice showed reduced plasma OPG levels compared to C57BL6/J wildtype controls as expected.

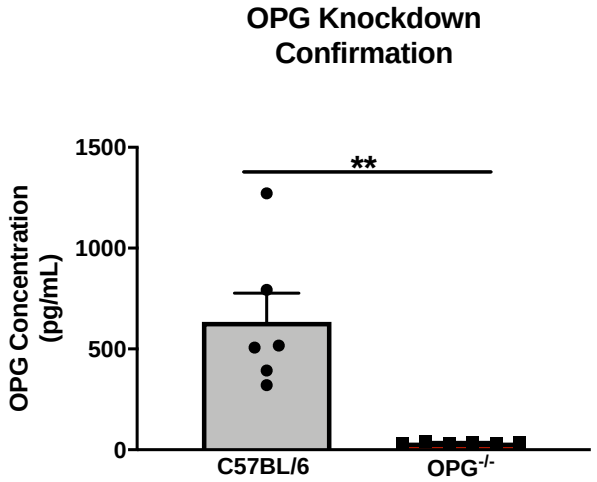

Figure 4.1: The loss of OPG was confirmed using an assay OPG ELISA assay to measure plasma OPG levels in mice following peri-arterial cuff and HLI surgeries. *Results are represented as mean ± SEM, n=8 per group, **P<0.01, statistical analyses done using a Mann Whitney t-test.*

2.2.2 OPG$^{-/-}$ Mice Have Significantly Elevated Serum Calcium and ALP Activity Post-HLI.

Alkaline phosphatase (ALP) is a well-used diagnostic marker for vascular calcification. To establish the presence of a calcification milieu, both calcium and ALP levels

were measured in blood plasma collected from both C57BL6/J and OPG knockout mice. Calcium levels were elevated in the OPG deficient mice compared to C57BL6/J controls (12.90 ±1.30 vs 6.60 ±1.60, P<0.0108 **Figure 4.2 A**). Plasma analysis also demonstrated significantly elevated ALP activity in the OPG deficient mice compared to C57BL6/J controls (2.80 ± 0.18 vs 1.14 ± 0.15, P<0.001, **Figure 4.2 B**). These results are consistent with previous studies where serum ALP levels have been shown to be elevated in $OPG^{-/-}$ mice than in WT mice[145, 198, 199], showing significant differences in serum concentrations of calcium and phosphate between $OPG^{-/-}$ and WT mice[199].

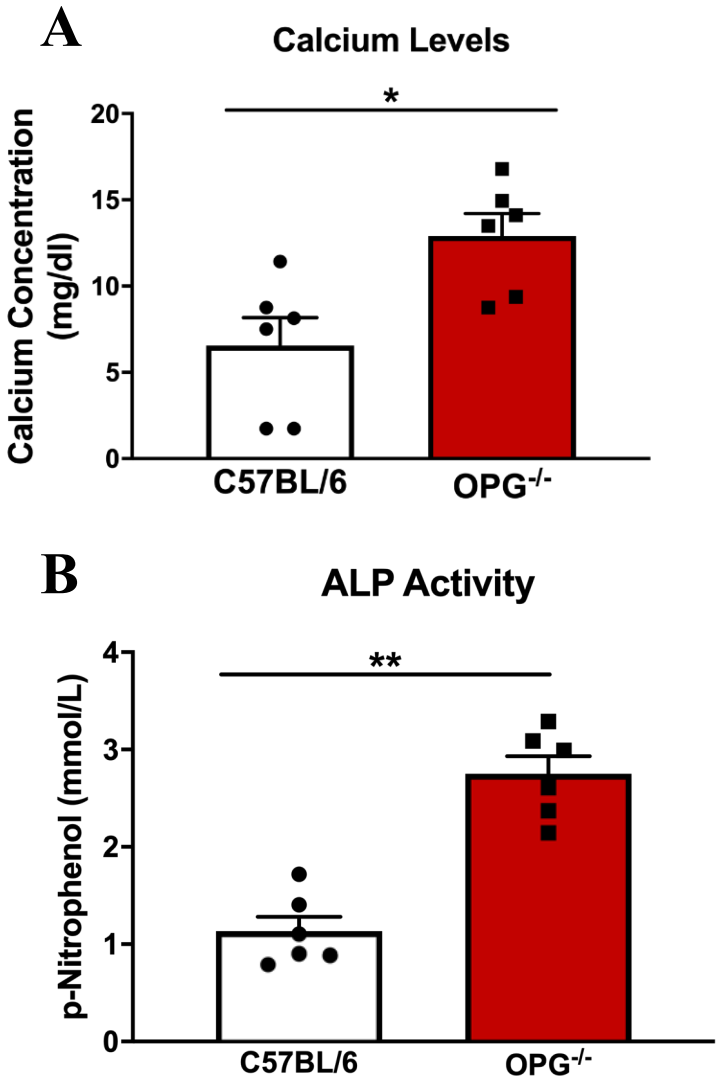

Figure 4.2: Calcification Milieu In OPG$^{-/-}$ Mice Upregulates Calcium and ALP Activity In 8wk Old Mice. *Femoral artery ligation was performed on 8wk old C57Bl6/J mice (controls) and OPG$^{-/-}$ mice.* ***(A)*** *Circulating calcium* ***(B)*** *ALP activity. Blood plasma was isolated 14 days post-HLI surgery, and calcium concentration was measured using a calcium assay (Cayman Chemical) and ALP activity using ALP assay (Wako, ALP Lab assay). Data is represented as mean ± SEM, *P<0.05, ***P<0.001, (n=9/group). Statistical analysis was performed using a Mann-Whitney t-test, OPG$^{-/-}$: osteoprotegerin deficient mice, ALP, alkaline phosphatase.*

2.2.3 High Calcium Impairs Blood Flow Reperfusion In OPG$^{-/-}$ Mice Post-HLI.

Laser Doppler Perfusion Imaging (LDPI) was used to assess blood perfusion as a marker of angiogenesis in control C57BL/6 mice compared to the OPG knockout mice. The LDPI ratio was determined as a ratio of the ischemic leg compared to the non-ischemic leg for each mouse. In this study, LDPI following unilateral femoral artery ligation showed striking reductions in blood flow reperfusion of 8wk old OPG$^{-/-}$ mice compared to C57BL/6 at day 6 (013±0.04 vs 0.37±0.06, P<0.0024); day 10 (0.18±0.03 vs 0.40±0.04, P<0.0088) and day 14 (0.21±0.02 vs 0.45±0.08, P<0.0083) post HLI **(Figure 4.3 A).** Furthermore, OPG deficient mice played necrotic toes at day 14 post-HLI surgery, an observation that wasn't seen in wildtype C57BL6/J (**Figure 4.3 B)**. Collectively, this data demonstrates that elevated calcification milieu present in the OPG deficient mice is associated with decreased limb perfusion and worse functional recovery.

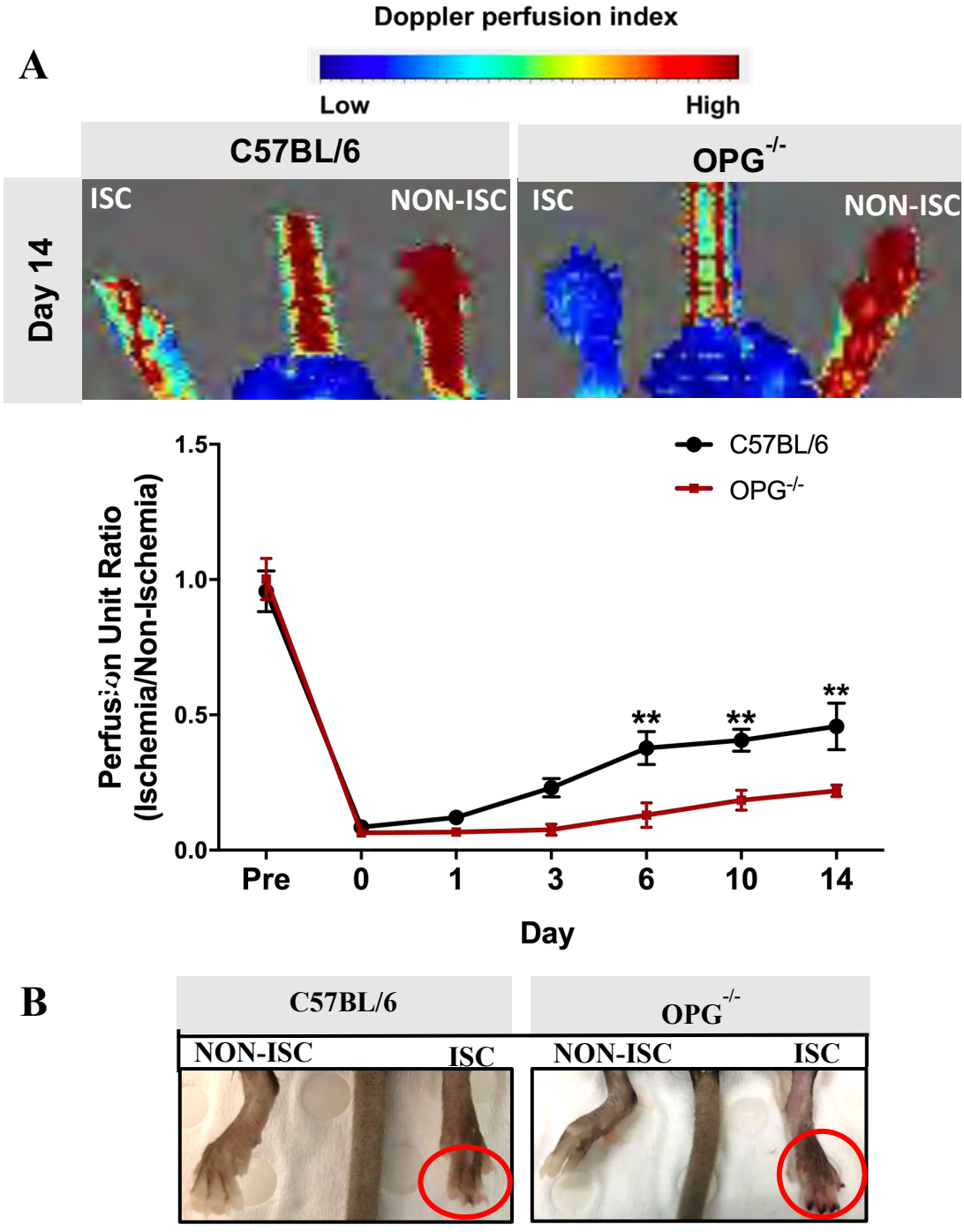

Figure 4.3: High Calcium Impairs Blood Flow Reperfusion In 8-Wk Old OPG$^{-/-}$ Mice Post-HLI At Days 6, 10 And 14. *Ischemia-driven neovascularization: femoral artery ligation was performed on 8wk old male C57Bl6/J mice (controls) and OPG$^{-/-}$ mice (n=9/group). Blood flow perfusion was measured non-invasively using Laser Doppler Perfusion Imaging (LDPI). Representative laser doppler perfusion images, images show high (red) to low (blue) blood flow at day 14. Perfusion unit*

*ratio was determined based in the ratio of ischemic (ISC) to non-ischemic (NON-ISC) hindlimb. (C) OPG deficient mice displayed necrotic toes at day 14 post-HLI surgery. Data is represented as mean ± SEM, *P<0.05, **P<0.01. Statistical analysis was performed using an unpaired student t-test and a two-way ANOVA with Bonferroni's multiple comparison test. OPG$^{-/-}$, osteoprotegerin deficient mice.*

2.2.4 High Calcium Reduces Neovessel and Arteriole in Gastrocnemius Muscle Tissues of OPG$^{-/-}$ Mice Following HLI.

The effect of high calcium on neovascularisation was assessed in the gastrocnemius muscle sections by measuring capillary density (CD31^{+} neovessels) and arteriole density (smooth muscle α-actin positive arterioles); which were quantified as number of vessels (CD31^{+} per myocyte) using laminin staining **(Figure 4.4 A)**. Consistent with the blood flow perfusion data, OPG$^{-/-}$ mice showed significantly decreased capillary density as shown by CD31^{+} neovessels relative to C57BL6/J wild-type (0.80±0.08 vs 1.37±0.15, P<0.0052, **Figure 4.4 B).** Conversely, OPG$^{-/-}$ mice showed increased arteriolar density compared to wildtype controls (1.12±0.11 vs 0.76±0.09, P<0.0449, **Figure 4.4 C).**

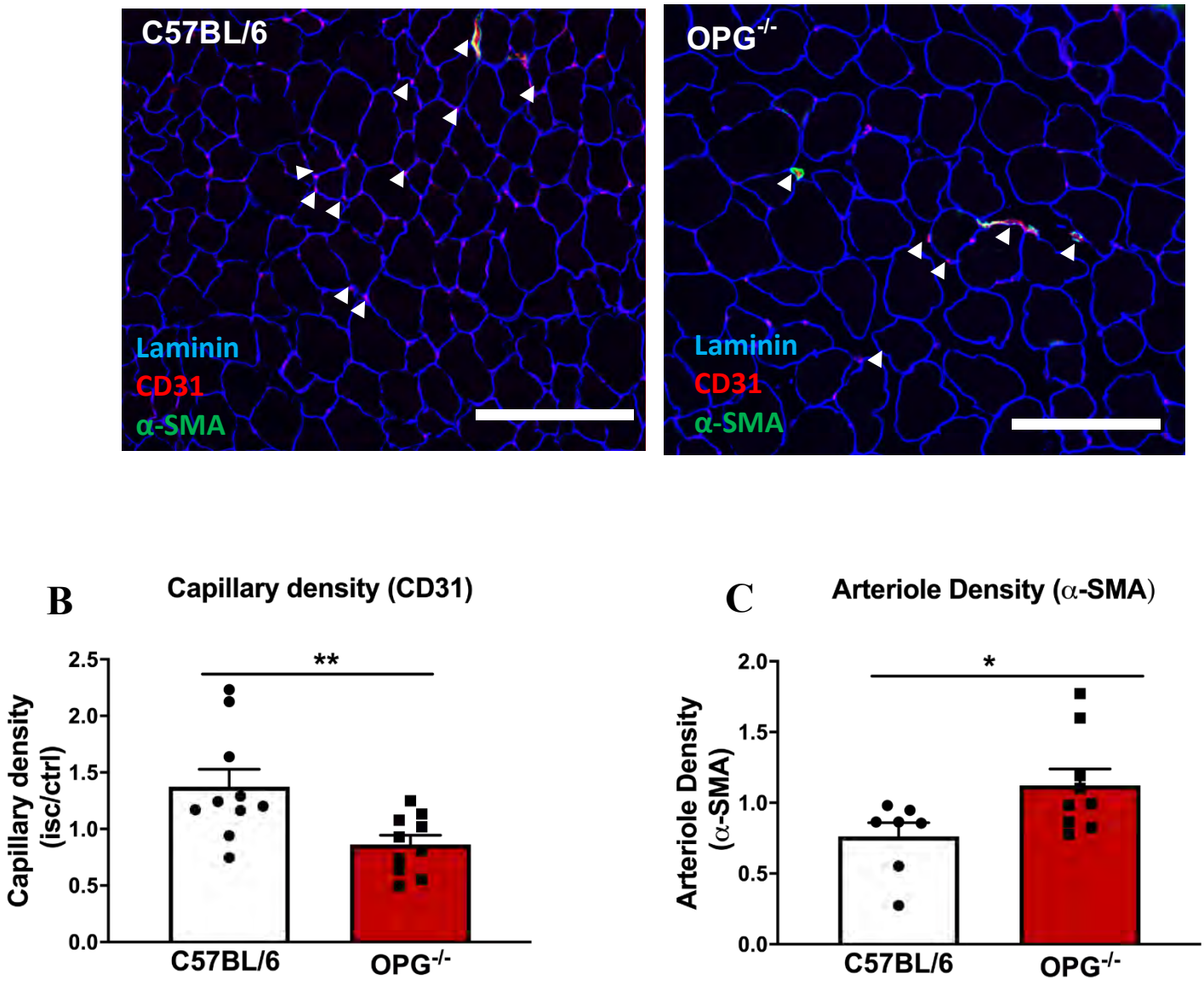

Figure 4.4: High calcium Reduces Neovessel and Arteriole Formation in Gastrocnemius Tissues of OPG$^{-/-}$ Mice Following HLI

Ischemia-driven neovascularization: femoral artery ligation was performed on 8wk old male C57Bl6/J mice (controls) and OPG$^{-/-}$ mice. Blood flow perfusion was measured invasively using Laser Doppler Perfusion Imaging (LDPI). ***(A)*** *Photomicrographs representing Immunocytochemistry staining performed on OCT frozen gastrocnemius muscle sections to detect* ***(B)*** *CD31^{+} neovessels (red staining), and* ***(C)*** *smooth muscle α-actin positive arterioles (green staining), which was quantified as number of vessels (CD31^{+} per myocyte) using laminin staining (blue staining) (n=10-12/group). Data is represented as mean ± SEM, *P<0.05, **P<0.01. Statistical analysis was performed using a Mann-Whitney t-test, Scale bars represent 50 µm. OPG$^{-/-}$: osteoprotegerin deficient mice.*

2.2.5 Calcification Milieu Regulates Gene Expression of Angiogenic Genes in Ischemic Limbs Of OPG$^{-/-}$ Mice Following HLI.

Ischemia-driven angiogenesis is regulated by the key transcription factor HIF-1α, which is post-translationally regulated by the E3 ubiquitin ligases, Siah1 and Siah2 and the propyl hydroxylase family (PHD 1-3). During hypoxia, Siahs 1 and 2 supress PHDs (PHD 1-3) which render HIF-1α for ubiquitination and degradation[72]. The effect of OPG deficiency on mRNA expression of these pro-angiogenic regulators was assessed. Elevated calcium levels as observed in OPG deficient mice had no effects on *Siah1* and *Siah 2* mRNA expression in both the ischemic and non-ischemic limbs of OPG$^{-/-}$ mice compared to C57BL6/J controls **(Figure 4.5 A-B)**. However, PHD levels were decreased in ischemic limbs of OPG deficient mice compared to C57BL6/J controls; for both PHD1 (55.82±14.95 vs 139.60±19.52, P<0.0279, **Figure 4.5 C**), and PHD2 (48.38±13.73 vs 146.10±14.14, P<0.0329, **Figure 4.5 D**). Together, these findings demonstrate how a calcific environment can upregulate pro-angiogenic markers to regulate angiogenesis.

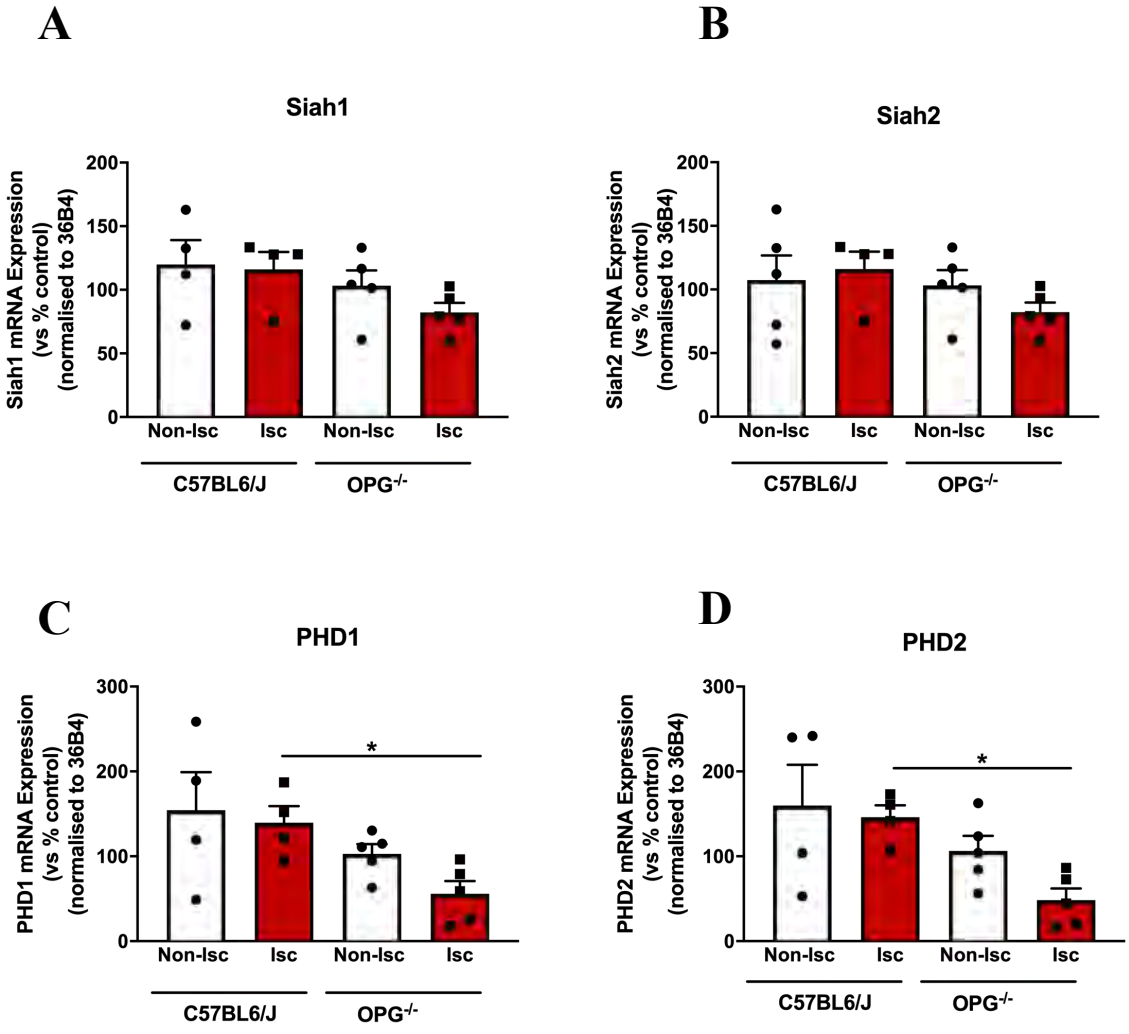

Figure 4.5: Calcification Milieu Regulates Gene Expression of Angiogenic Genes in Ischemic Limbs OPG$^{-/-}$ mice following HLI. *Real-time PCR was performed to assess mRNA expression of* ***(A)*** *Siah1,* ***(B)*** *Siah2,* ***(C)*** *Phd1,* ***(D)*** *Phd2 in gastrocnemius muscle of both C57Bl6/J and OPG$^{-/-}$ mice (n = 5 per group). Data is represented as non- ischemic (Non-Isc) for control hindlimb, and ischemic (Isc) and surgical hindlimb. Data is represented as percentage of controls, mean ± SEM; One-way ANOVA with Bonferroni's Multiple comparisons test, *P<0.05, **P<0.01. OPG$^{-/-}$: osteoprotegerin deficient mice, PHD1-2: propyl hydroxylase domains.*

2.2.6 High Calcium Differentially Upregulates mRNA Expression of Pro-Angiogenic HIF-1α, VEGFA and VEGFR2 In Ischemic Limbs OPG$^{-/-}$Mice.

HIF-1α is the pivotal driver of ischemia-driven angiogenesis following occlusion of vessels during diseases of PAD and post-MI. To understand its regulation in OPG deficient mice following hind-limb ischemic insult, I measured its gene expression. As expected, ischemic limbs of OPG deficient mice had significant upregulation of *Hif-1α* mRNA expression compared to wildtype controls (332.50±72.05 vs 94.75±12.69, P<0.0056, **Figure 4.6 A**). Furthermore, OPG deficient mice had higher expression of total Hif-1α relative to wildtype controls when expressed as a ratio of the non-ischemic to ischemic hindlimb (3.57±0.69 vs 0.99±.27, P<0.0286, **Figure 4.6 B**).

The downstream effects of HIF-1α involve upregulation of VEGFA to drive angiogenesis during ischemia. In this study, there was no significant change in *Vegfa* gene expression in ischemic limbs of OPG deficient mice compared to wildtype controls (**Figure 4.6 C**); with no change also observed for its receptor *Vegfr2* (**Figure 4.6 E**); and when expressed as a ratio, *Vegfa* or *Vegfr2* gene expression remained unchanged (**Figure 4.6 D-F**). In this study, increased expression of angiogenic markers suggests a compensatory mechanism to stimulate angiogenesis via induction of the HIF-1α pathway.

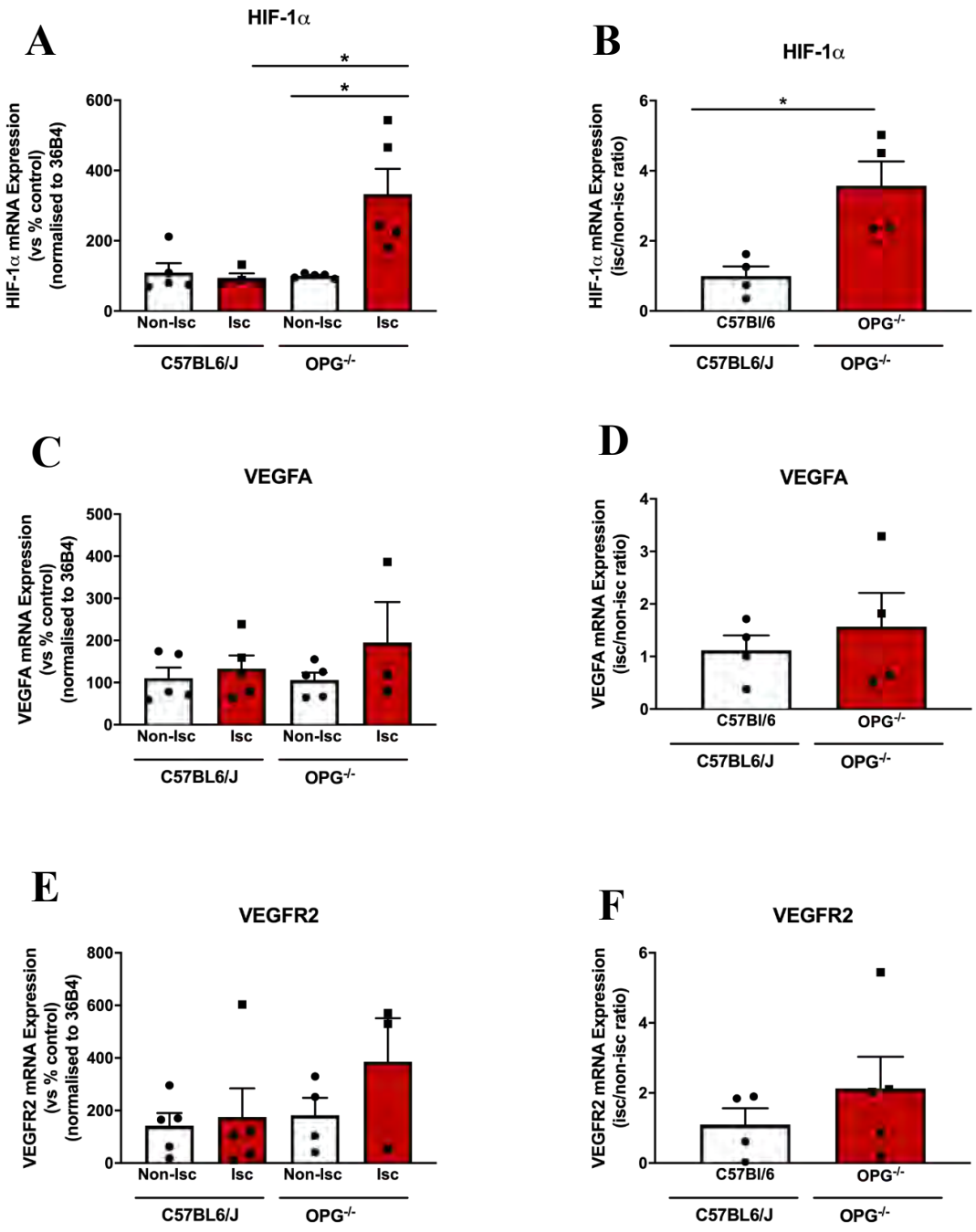

Figure 4.6: Calcification Milieu Upregulates Gene Expression of Pro-Angiogenic Markers HIF-1α, VEGFA and VEGFR2 In Ischemic Limbs OPG$^{-/-}$ Mice. *Real-time PCR was performed to assess gene expression of* ***(A-B)*** *Hif-1a and* ***(C-D)*** *Vegfa,* ***(E-F)*** *Vegfr2 in gastrocnemius muscle of both C57Bl6/J and OPG$^{-/-}$ mice (n = 6 per group). Data is presented as non- ischemic (Non-Isc) for control hindlimb, and ischemic (Isc) and surgical hindlimb. Data is represented as percentage of controls, mean ± SEM; One-way ANOVA with Bonferroni's Multiple comparisons test, Mann-Whitney t-test, *P<0.05. OPG$^{-/-}$: osteoprotegerin deficient mice. HIF-1α: hypoxia-inducible factor-1 alpha, VEGF: vascular endothelial growth factor, VEGFR: vascular endothelial growth factor receptor 2.*

2.2.7 OPG$^{-/-}$show increased mRNA expression of calcification-regulating genes in ischemic limbs following HLI.

There is growing evidence highlighting the role of the Runx2, RANKL and BMP2 as regulators of vascular calcification and in cardiovascular and metabolic disease states[138, 198]. To further evaluate calcification in these mice, I assessed *Runx2* gene expression, a key transcription factor involved in the initiation of vascular calcification; and RANKL, a known driver of calcification. There were no significant differences in *Rankl* mRNA expression in the ischemic limbs of OPG deficient mice compared to C57BL6/J controls (**Figure 4.7 A**). Furthermore, *Rankl* expression appeared to be more elevated in OPG deficient mice compared to wildtype controls when expressed as a ratio of the non-ischemic to ischemic hindlimb (2.28±0.92 vs 0.74±0.21, P<0.2222 **Figure 4.7 B**) though not statistically significant.

There were no significant differences in *Runx2* gene expression in the non-ischemic limbs versus ischemic limbs of C57BL6/J. Furthermore, when comparing the ischemic and non-ischemic limbs of the OPG$^{-/-}$ mice alone, there was significant upregulation in *Runx2* gene (525.80 ±91.40 vs 62.04 ±10.37, P<0.0002, **Figure 4.7 C**). In addition, when comparing ischemic limbs of C57BL6/J versus ischemic limbs of OPG deficient mice, *Runx2* gene expression was significantly upregulated (525.80 ±91.40 vs 120.00±32.32, P<0.0003, **Figure 4.7 C**). This increase in *Runx2* expression was further reflected when the data was expressed as a ratio of the non-ischemic to ischemic hindlimb (5.12±0.92 vs 1.79±0.62, P<0.0159, **Figure 4.7 D**).

Bmp2 gene expression was significantly upregulated in OPG deficient mice, when comparing the ischemic limbs versus the non-ischemic limbs (1722±470.80 vs 271.40±103.40, P<0.0068, **Figure 4.7 E**). Furthermore, *Bmp2* gene expression was upregulated when

comparing ischemic limbs of OPG deficient mice versus those of wildtype C57BL6/J mice, (1722±470.80 vs 34.46±11.72, P<0.01, **Figure 4.7 E**). When the data was expressed as a ratio of ischemic/non-ischemic, *Bmp2* mRNA expression was increased (P<0.0635, **Figure 4.7 F)** though not statistically significant.

In combination with our blood flow reperfusion data and neovessel/arteriole data, these findings highlight the presence of a calcific milieu in the OPG deficient mice, which clearly has negative effects in regulating angiogenesis. However, while there is upregulation of calcification makers, data from figure 4.5 demonstrated increased expression of angiogenic markers which may likely serve as a compensatory mechanism.

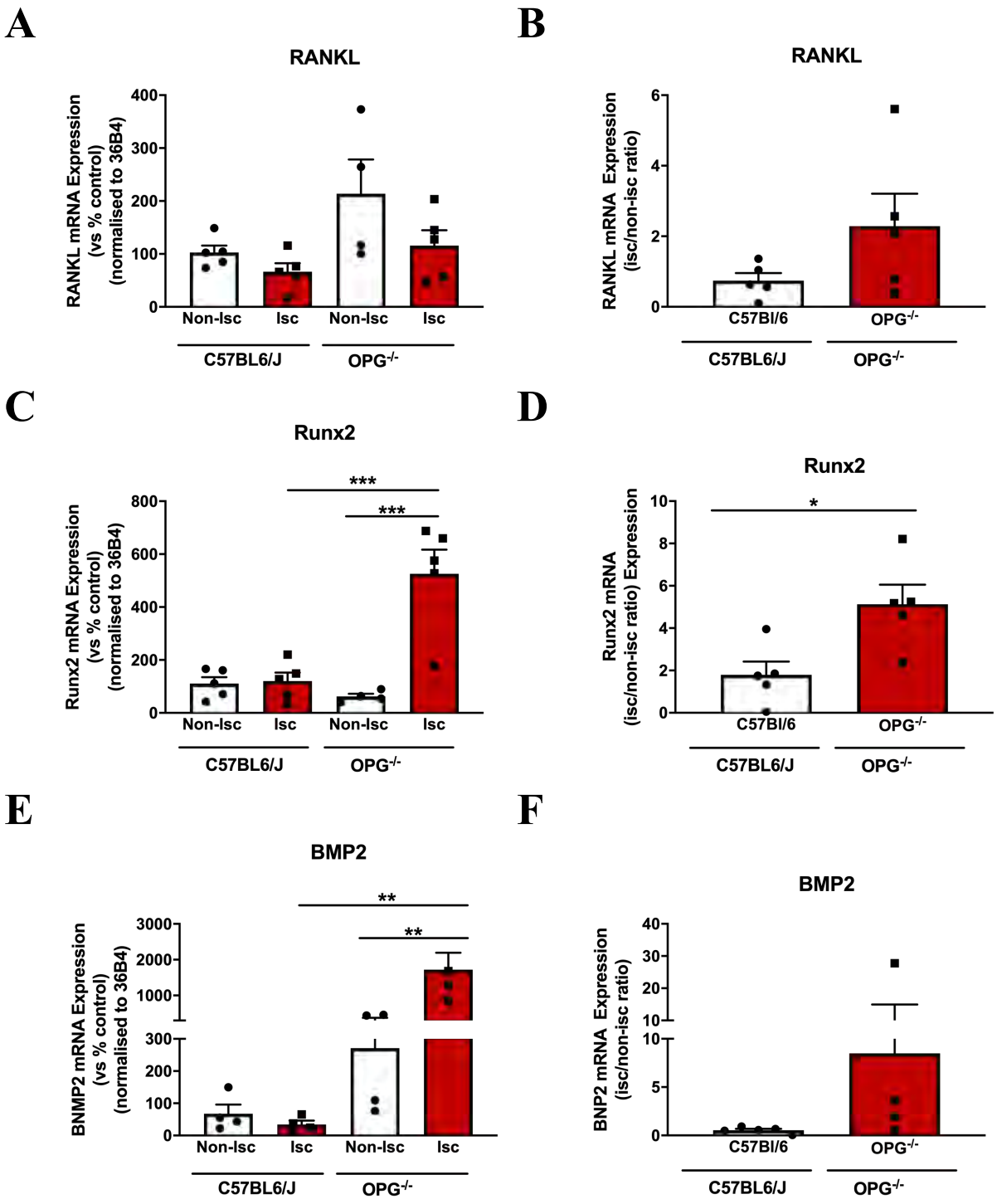

Figure 4.7: OPG$^{-/-}$Show Increased mRNA Expression of Calcification-Regulating Genes in Ischemic Limbs Following HLI. *Real-time PCR was performed to assess gene expression of* ***(A-B)*** *Rankl,* ***(B-C)*** *Runx2,* ***(E-F)*** *Bmp2 in gastrocnemius muscle of both C57Bl6/J and OPG$^{-/-}$ mice (n=5 per group). Data is represented as non- ischemic (Non-Isc) for control hindlimb, and ischemic (Isc) and surgical hindlimb. Data is represented as percentage of controls, mean ± SEM; One-way ANOVA with Bonferroni's Multiple comparisons test, Mann-Whitney t-test, *P<0.05, **P<0.01. OPG$^{-/-}$: osteoprotegerin deficient mice, Runx2: runx2 related transcription factor, RANKL, receptor activator of nuclear factor κ-B ligand.*

2.2.8 Aged OPG$^{-/-}$ Mice Exhibit Elevated Serum ALP Activity Following HLI.

Both VC and PAD are age-associated diseases and therefore I studied the effects of elevated calcium in an aged cohort of mice. Interestingly, there was no difference in calcium levels in the aged OPG deficient mice compared to the C57BL6/J mice (**Figure 4.8 A**), which could indicate a saturation or plateau effect as a result of calcium uptake by tissues. In line with the previous data from the 8wk-old study, OPG deficient mice had significantly elevated ALP activity compared to C57Bl6/J controls (2.55±0.07 vs 1.12±0.9, P<0.0001, **Figure 4.8 B**).

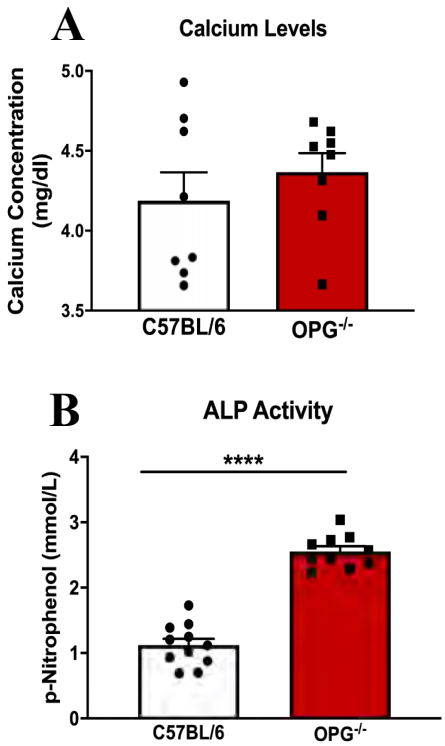

Figure 4.8: Aged OPG$^{-/-}$ Mice Exhibit Elevated Serum ALP Activity Following HLI

Ischemia-driven neovascularization: femoral artery ligation was performed on 8wk old C57Bl6/J mice (controls) and OPG$^{-/-}$ mice (n=9/group). ***(A)*** *Circulating calcium* ***(B)*** *ALP activity. Blood plasma was isolated 14 days post-HLI surgery, and calcium concentration was measured using a calcium assay (Cayman Chemical) and ALP activity using ALP assay (Wako, ALP Lab assay). Data is represented as mean ± SEM, Mann-Whitney t-test, ****P<0.0001. Statistical analysis was performed using a Mann-Whitney t-test. OPG$^{-/-}$: osteoprotegerin deficient mice, ALP, alkaline phosphatase.*

2.2.9 Calcification Milieu Impairs Blood Flow Recovery in Aged OPG$^{-/-}$ Mice Post-HLI.

The effects of high calcium on neovascularization were also assessed in an aged cohort of mice following hind-limb ischemia surgery. As expected, the aged model of calcification showed exacerbated effects on angiogenesis. Consistent with the younger cohort, aged OPG$^{-/-}$ mice showed striking reductions in blood flow as measured by LDPI compared to C57BL6/J wildtype controls, particularly at day 10 (0.14±0.03 vs 0.31±0.03, P<0.0034) and day 14 (0.19±0.05 vs 0.39±0.02, P<0.0001, **Figure 4.9 A-B**).

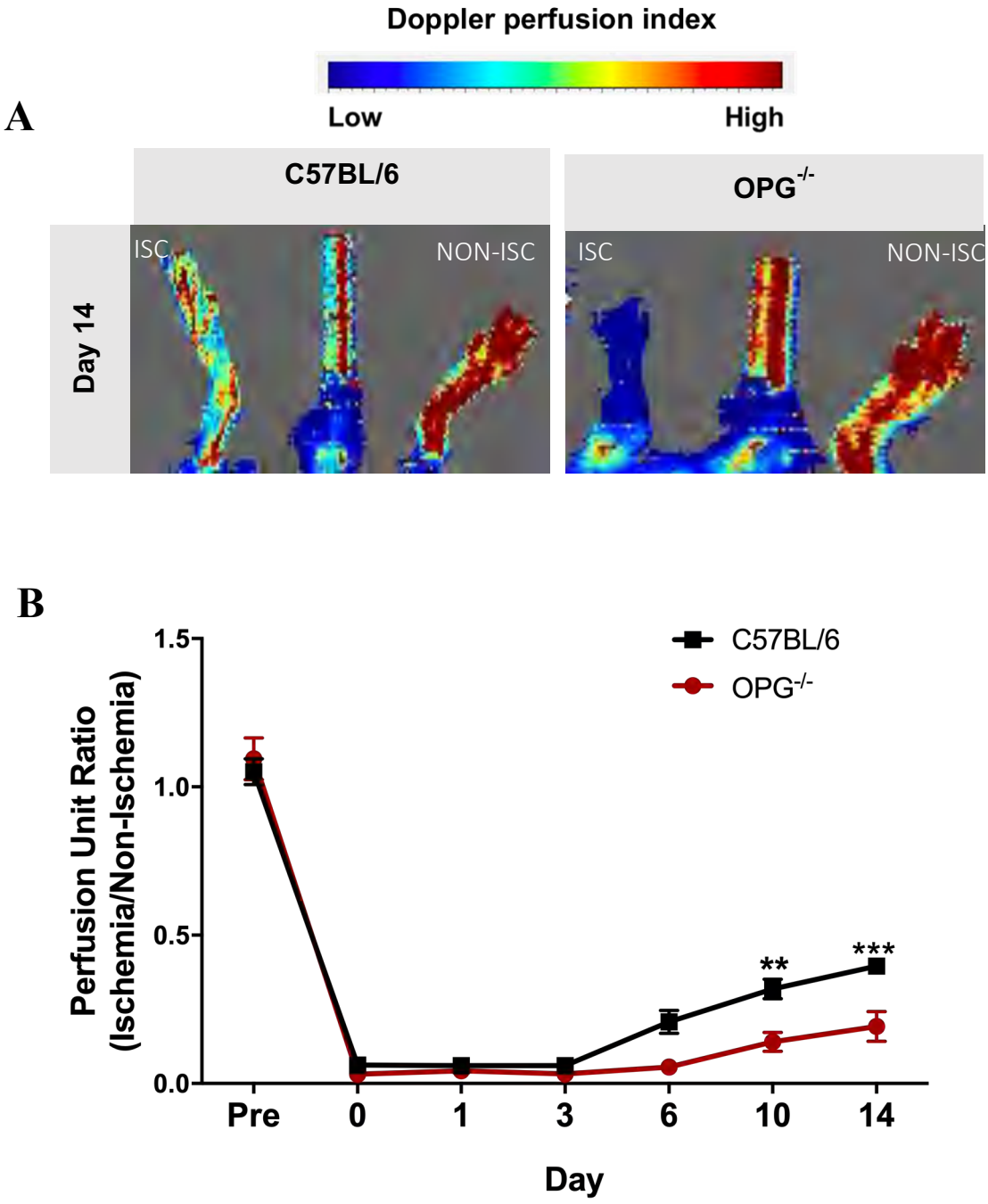

Figure 4.9: High Calcium Impairs Blood Flow Reperfusion In 24-Wk Old OPG$^{-/-}$ Mice Post-HLI. *Ischemia-driven neovascularization: femoral artery ligation was performed on 24wk old C57Bl6/J mice (controls) and OPG$^{-/-}$ mice (n=9/group). Blood flow perfusion was measured invasively using Laser Doppler Perfusion Imaging (LDPI), (A-B) Representative laser doppler perfusion images, images show high (red) to low (blue) blood flow at day 14. Perfusion unit ratio was determined based in the ratio of ischemic (ISC) to non-ischemic (NON-ISC) hindlimb. Data is represented as mean ± SEM, **P<0.01, ***P<0.001. Statistical analysis was performed using a two-way ANOVA with Bonferroni's multiple comparison test. OPG$^{-/-}$: osteoprotegerin deficient mice.*

2.2.10 High Calcium Impairs Reduces Neovessel Formation in Gastrocnemius Muscle Tissues Of OPG$^{-/-}$ Mice Following HLI.

The effects of high calcium on neovascularisation were further evaluated in an aged murine model of angiogenesis. Consistent with data from the 8wk-old study, aged OPG deficient mice also had decreased capillary density ($CD31^{+}$ neovessels) (0.47±0.10 vs 0.80±0.09, P<0.0186, **Figure 4.10 A**); which were quantified as number of vessels ($CD31^{+}$ per myocyte) using laminin staining. Furthermore, OPG deficient mice showed decreased arteriole density (smooth muscle α-actin positive arterioles) (0.48±0.31 vs 1.77±0.41, P<0.0255, **Figure 4.10 B**). This data coincided with the blood flow perfusion data in section 4.3.10.

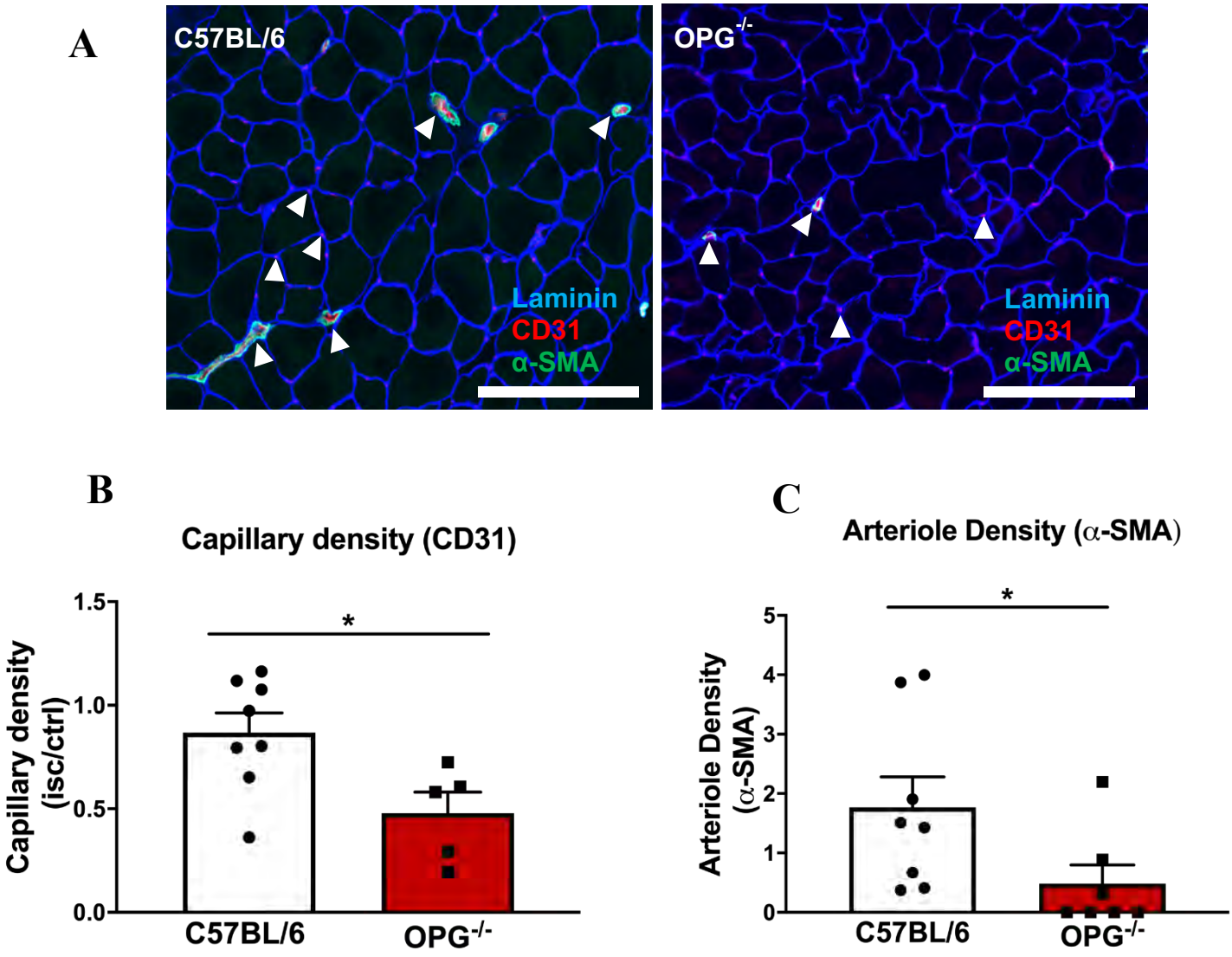

Figure 4.10: High Calcium Impairs Reduces Neovessel Formation in Gastrocnemius Muscle Tissues Of OPG$^{-/-}$ Mice Following HLI. Ischemia-driven neovascularization: femoral artery ligation was performed on 8wk old C57Bl6/J mice (controls) and OPG$^{-/-}$ mice (n=9/group). Blood flow perfusion was measure invasively using Laser Doppler Perfusion Imaging (LDPI), (A) Photomicrographs representing Immunocytochemistry staining performed on OCT frozen gastrocnemius muscle sections to detect (B) CD31^{+} neovessels (red staining), and (C) smooth muscle α-actin positive arterioles (green staining); which was quantified as number of vessels (CD31^{+} per myocyte) using laminin staining (blue staining) (n=6/group). Data is represented as mean ± SEM, *P<0.05, ***P<0.001, ****P<0.0001. Statistical analysis was performed using a Mann-Whitney t-test, (n=10/group), Scale bars represent 50 µm. OPG$^{-/-}$: osteoprotegerin deficient mice.

2.2.11 Aged OPG$^{-/-}$ Mice Show Impaired Tissue Ischemia and Limb Function, And Severe Foot Necrosis in Ischemic Limbs Following HLI Compared to Controls.

To functionally evaluate decreased angiogenesis in OPG deficient mice compared to wildtype C57BL/6J mice, tissue ischemia and limb function were assessed in these mice using a modified version of the well-established Tarlov Scoring System as previously described[163]. Tarlov scoring revealed significantly worse outcomes for both tissue ischemia (177 vs 95, P<0.0001, **Figure 4.11 B**) and limb functions (126 vs 72, P<0.0004, **Figure 4.11 C**) (with higher scoring indicating a worse prognosis) in the OPG$^{-/-}$ mice compared to controls **(Table 4.1)**. This was associated with severe amputations and higher level of foot necrosis as demonstrated in **Figure 4.11. A.** So far, the doppler perfusion data from both the 8wk and aged study have shown that OPG deficiency leads to significant impairment in blood flow reperfusion, decreased capillary and arteriole density in the ischemic tissues of these mice, which has clear physical manifestations on the limbs of these mice.

Table 4.1: Tarlov Scores for Limb Function and Tissue Ischemia

TARLOV SCORES			
Score	**Descriptions**	**C57Bl6/J**	**OPG$^{-/-}$**
Limb Function			
0	Normal	**72**	**123**
1	Plantar but no toe flexion		
2	No flexion		
3	Dragging of foot		
Tissue Ischemia			
0	No damage	**95**	**173**
1	Discoloration ->1 nail		
2	Discoloration -> 2 nails		
3	Discoloration of 1 toe		
4	Discoloration of 2 toes		
5	Foot Necrosis		
6	Leg necrosis		
7	Auto-amputation of leg		

Table 4.1: Tarlov Scores for Limb Function and Tissue Ischemia In 24 Wk-Old OPG-/- Mice Following HLI. *Ischemia-driven neovascularization: femoral artery ligation was performed on 24wk old C57Bl6/J mice (controls) and OPG$^{-/-}$ mice (n=12/group). Tarlov Scoring System[163] was used to assess limb function (scores 0-3) and Tissue ischemia (scores 0-8), with a higher value indicating poor prognosis for both. Mice were monitored and photos were taken at each doppler time point for identification of toe necrosis and amputations. Excel was used to tally all scores. OPG$^{-/-}$: osteoprotegerin deficient mice.*

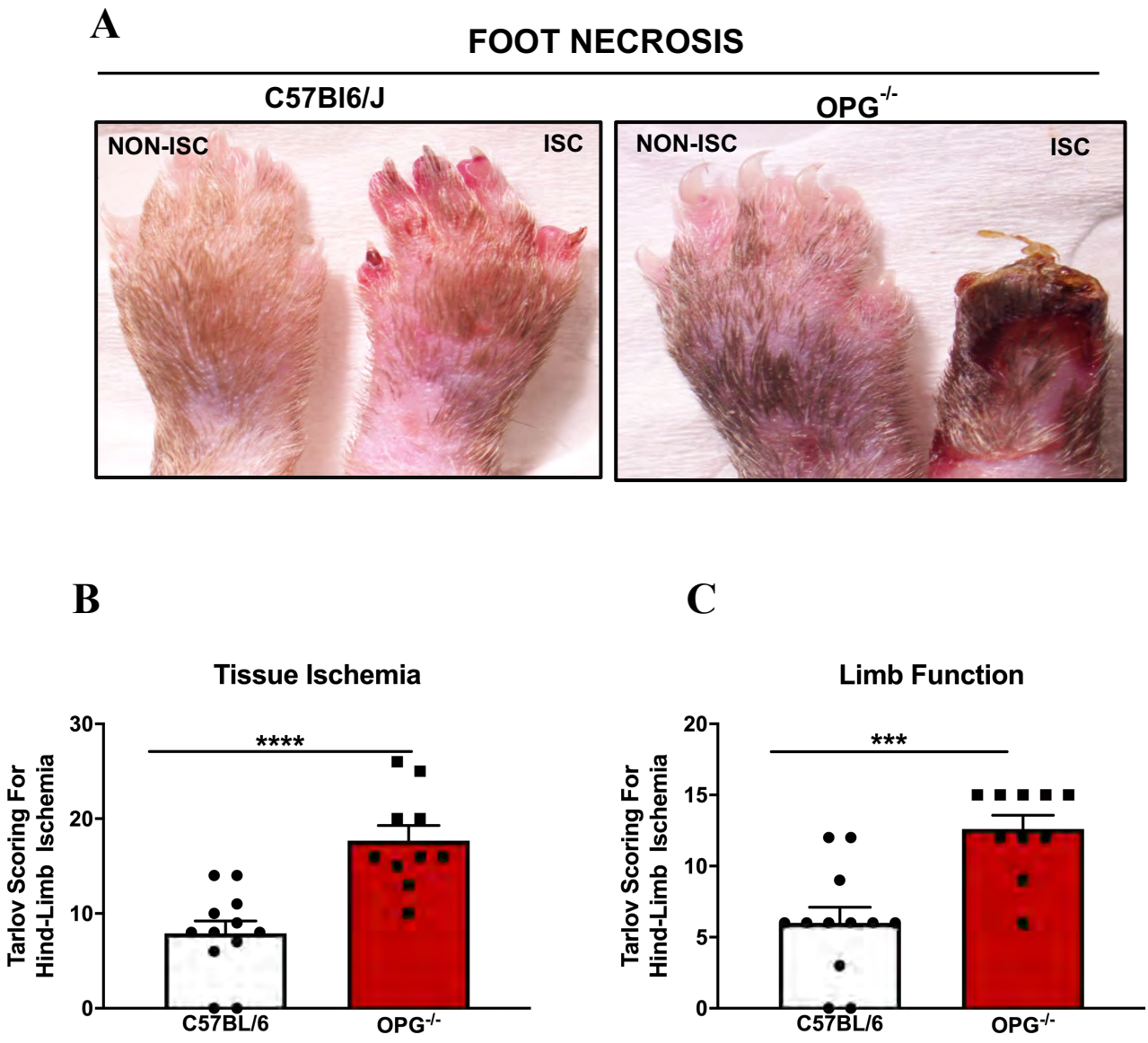

Figure 4.11: Aged OPG$^{-/-}$ Mice Show Impaired Tissue Ischemia and Limb Function, And Severe Foot Necrosis in Ischemic Limbs Following HLI Compared to Controls.

Ischemia-driven neovascularization: femoral artery ligation was performed on 24wk old C57Bl6/J mice (controls) and OPG$^{-/-}$ mice (n=12/group). Tarlov Scoring System[163] was used to assess ***(A)*** *tissue ischemia (scores 0-3) and* ***(B)*** *tissue ischemia (scores 0-8); with a higher value indicating poor prognosis for both. Mice were monitored and photos were taken at each doppler time point for identification of toe necrosis and amputations. Excel was used to tally all scores. Data is represented as mean ± SEM, *P<0.05, ***P<0.001. Statistical analysis was performed using a Mann-Whitney t-test, (n=10/group), OPG$^{-/-}$: osteoprotegerin deficient mice.*

2.3 Discussion

This data demonstrated that a highly calcific environment in the OPG deficient mouse model resulted in severe loss of revascularisation with observed differences in neovessel formation in OPG deficient mice compared to controls. Furthermore, calcific milieu resulted in significant impairment in tissue ischemia and limb function, with OPG mice demonstrating toe necrosis and amputations.

Patients with PAD often present with multilevel disease, characterised by fatty plaque build-up and high levels of diffused calcium deposits in the media of their peripheral arteries[83]. In addition, lower extremity arterial calcification predicts poor cardiovascular outcomes and is highly associated with limb amputations[15, 34, 84-87], and is reported in peripheral arteries of diabetic and chronic kidney disease (CKD) patients, suggesting an association between arterial calcification and PAD[34, 84, 85]. Because calcification affects limb vascularization, it is therefore considered a limiting factor for the treatment of PAD and a potential driver of PAD[15].

The most prominent type of calcification that occurs in the lower extremity is medial calcification, very distinct from intimal calcification occuring in the coronary arteries, although both may co-exist in diseases such as atherosclerosis[37]. Calcification in PAD is proposed to affect limb vascularization due to reduced vessel compliance, increased arterial stiffening and reduced coronary perfusion [37, 82]. In a previous study, tibial artery calcification (TAC) score was used to assess the associations of calcification with the severity of symptoms in PAD patients following computed tomography (CT). This study found that patients with elevated TAC scores had a much higher incidence of PAD symptoms and increased risk of limb amputations compared to those with lower scores[34]. In a different study, assesment of human femoralpopliteal arteries showed that calcified arteries had larger diameters, thicker

walls, thinner tunica media; with more discontinuous elastic fibres compared to healthy arteries[36]. This therefore suggests that the extent of calcification in lower exremity arteries may influence the severity of symptoms in PAD patients.

Indeed, OPG is known to be essential for angiogenesis in vitro[184], however, to date no studies have reported this critical observation in vivo. The calcific milieu present in this model was a unique opportunity to assess the effects of elevated calcium and the resulting detrimental consequences. Furthermore, the presence of calcification and a highly calcific environment has not been studied as a deterrent of this angiogenic process. Here I used an OPG-deficient mouse model, as these mice develop extensive vascular calcification in their aorta and renal arteries[145]. Utilising this model, ischemia-induced angiogenesis was assessed in vivo and demonstrated a profound detrimental suppression of vascularisation, with significant elevation of calcification markers (Runx2 and RANKL). The association of calcification on angiogenesis and ischemia however remains unclear, though it's been proposed that new blood vessels may arise within atherosclerotic plaques as a result of cross-talk and coordinated interplay by ECs, SMCs, pericytes, osteoblasts and other osteoprogenitor cells residing within the vessel wall, which may therefore drive the differentiation of ECs into bone-like cells to induce vascular calcification[61].

In this study, I utilised the OPG knockout mice as a calcification model to mimic high calcific environment. OPG has been shown to have numerous functions in both physiological and pathological processes. Clinical studies have reported that higher levels of serum OPG is associated with poor cardiovascular outcomes in coronary artery disease, chronic kidney disease and rheumatoid arthritis[137, 139, 141, 149]. Additionally, the pro-angiogenic role of OPG was reported in a study whereby OPG stimulated the recruitment of endothelial colony

forming cells from the bone marrow to sites of neovascularization during vasculogenesis[153]. Furthermore, while OPG deficient mice result in greater calcium level, and have been validated as a vascular calcification model, it cannot be discounted that the dramatic ischemia-related effects could be due to the loss of OPG itself. This serves as a limitation in this study as there are other available models used to study vascular calcification. Therefore further investigation is required to fully understand the role of OPG in angiogenesis, however some in vitro studies have reported the "protective effects" of OPG, where OPG enhanced the pro-angiogenic properties of endothelial colony forming cells which are recruited from the bone marrow to sites of revascularisation during vasculogenesis[153]. Therefore, it still remains unclear that the presence of calcification is detrimental to the progression of angiogenesis and PAD.

Ageing plays a crucial role in endothelial dysfunction and the progression of calcification[200]. Our aged cohort of OPG-deficient mice displayed significant loss of angiogenic ability in concert with extensive tissue ischemia and impaired limb function with decreases in capillary and arteriole density compared to control mice (Figure 4.12). The combination of increased age and severe calcification in these mice created a largely unfavourable environment for revascularisation, similar to the consequences observed in patients with PAD. PAD patients presenting with femoral calcification often have reduced coronary perfusion and are at a higher risk for amputations[37, 82]. In a different published study using mice deficient in osteopontin, another known inhibitor of vascular calcification, $OPN^{-/-}$ demonstrated decreased running abilities compared to control wildtype mice 7 days post hind-limb ischemia[108].

The angiogenic process or development of collateral vessels originates from co-existing blood vessels in the vicinity of an ischemic insult to bypass sistes of obstruction, and

to restore blood flow and preserve tissue fucntion[47]. During an ischemic environment, the initial step is activation of endothelial cells to stimualte proliferation and migration by growth factors. An ischemic environment induces HIF-1α which further stimulates VEGF synthesis to drive neovascularization to rescue blood flow in the affected area. Data from this study demonstrated that following the induction of ischemia by femoral artery ligation, there was an attempt to increase pro-angiogenic marker expression for HIF-1 alpha, VEGFA and its receptor VEGFR2 in ischemic limbs of OPG deficient mice compared to wildtype controls (Figure 4.12). This may explain the increased arteriole formation observed with the 8wk-old mice where there is increase in arteriolar density in OPG deficient mice compared to wildtype mice. Furthermore, while OPG deficient mice result in greater calcium level, and have been validated as a vascular calcification model, futher investigation is required to fully understand the role of OPG in angiogenesis.

2.4 Conclusion

This study provides important insights into the mechanisms of high calcium in regulating angiogenesis. I found that high calcium environment impairs ischemia-driven angiogenesis and upregulates ALP and calcification markers. While the mechanisms underlying the effects of calcification on angiogenesis are still not clear, this study has provided some evidence to identify how elevated calcium levels may have devastating effects on revascularisation. The degree of calcification in patients with PAD can often be a limiting factor when providing standard therapies and these findings may have implications for the development of new targets in calcification for those with PAD.

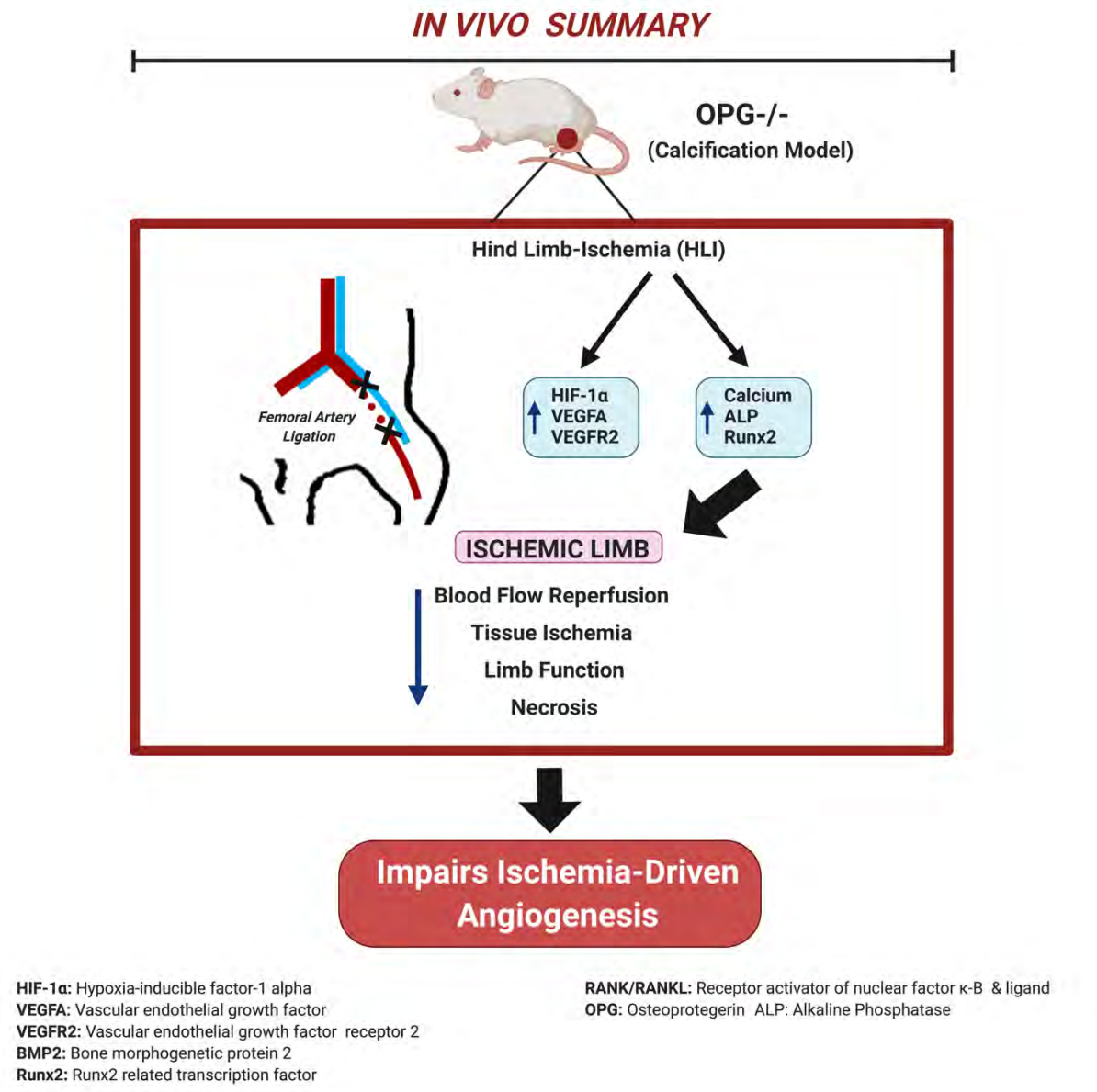

Figure 4.12: Summary Schematic for the Effects of Calcification Milieu on Ischemia-Driven Angiogenesis In Vivo.

CHAPTER 5:

THE INTERACTION BETWEEN INFLAMMATION AND CALCIFICATION IN DRIVING ANGIOGENESIS

5.1 INTRODUCTION

VC is now considered to be surrogate marker for the burden of atherosclerotic disease and a potential contributor to disease progression. Angiogenesis is a multi-step process that occurs in several well-defined stages of atherosclerosis and involves a complex orchestration of growth factors, cytokines, signalling cascades and cellular events[46]. Depending on the pathophysiological context, angiogenesis is driven by two distinctly different, yet partially overlapping, pathways[64, 67]. In contrast to ischemia-driven angiogenesis which is primarily modulated by the main hypoxic transcription factor, HIF-1α; NF-κB, a pivotal transcription factor for inflammatory-driven angiogenesis[66]. Inflammatory-driven pathological angiogenesis is implicated in several inflammatory disease processes such as atherosclerosis, cancer and peripheral vascular diseases[46].

Inflammatory-driven angiogenesis can be triggered by direct or indirect stimulation. Direct stimulation involves increased expression of inflammatory cytokines on endothelial cells (EC) to regulate EC proliferation and migration, leading to angiogenesis[67]. In contrast, indirect stimulation involves the release and recruitment of macrophages to the inflamed site in response to an inflammatory stimulus, which then triggers the secretion of a host of pro-angiogenic factors including vascular endothelial growth factor (VEGFA), tumour necrosis factor-α (TNF-α), basic fibroblast growth factor (bFGF) and interferon gamma (IFNγ) to promote angiogenesis[67]. This effect is however not beneficial as it enhances plaque growth making them more prone to rupture. Other key promoters of inflammatory-driven angiogenesis include TNF-α, NF-κB, cell adhesion molecules (CAMs) including vascular cell adhesion molecule (VCAM), intracellular adhesion molecule (VCAM) and monocyte chemoattractant protein-1 (MCP1)[66, 67]. Notably, VEGF is an important stimulator of angiogenesis in both ischemia and inflammatory conditions; modulated by HIF-1α and NF-

κB, respectively. VEGF is known to possess a response element for both NF-κB and HIF-1α in its promoter region; thus, allowing for conditional regulation via activation of both signalling pathways independently.

TNF-α is a well-studied pleiotropic cytokine, that has been shown to play a role in vascular pathologies relating to angiogenesis, and also in bone pathophysiology[91]. Inflammatory mediators derived from monocyte-macrophages such as TNF-α, have been reported to contribute in the progression of VC by promoting osteoblastic differentiation of VSMCs, leading to mineralisation[91, 201]. Furthermore, calcium phosphate mineral deposition is known to elicit an inflammatory response, by stimulating TNF production by macrophages[160, 161]. In other studies, exposure of macrophages to calcium or phosphate nanocrystals resulted in a change from M0 to M1 polarization, which was followed by TNF-α release[202]. Macrophages may contribute to the vicious cycle of inflammation and calcification in the vessel wall through paracrine activation of VSMCs, and by ingesting calcium-phosphate deposits (hydroxyapatite) whilst also secreting TNF-α[160]. In addition, it has been shown that basic calcium-phosphate crystals stimulated the release of TNF-α and other pro-inflammatory cytokines from differentiated human macrophages[161].

Though the mechanisms of TNF-α in regulating VC have been intensely studied, the understanding of its effects on inflammatory-driven angiogenesis in ECs is incomplete. In this study, I aimed to investigate the effect of calcification medium on TNF-α-induced responses on ECs, and its effect on angiogenesis. I hypothesised that calcification stimuli will exacerbate inflammatory-driven angiogenesis in vitro.

5.2 Results

5.2.1 Calcification Medium Upregulates Calcium Levels and ALP Activity Following TNF-α Stimulation.

The physiological importance of both calcium and phosphate are well established for their roles in muscle contractions, mineralisation of skeletal bones and nerve transmissions[203]. Calcium phosphate homeostasis is well regulated in the vasculature, however disrupted balance in both can lead to vascular calcification commonly seen in CKD[101, 105, 204]. To understand the effect of inflammation on ECs, cells were stimulated with and without inflammatory mediator TNF-α. Consistent with the previous data in chapter 3, cells treated with calcification media alone demonstrated elevated levels of calcium secretion compared to control cells (341.4±48.65 vs 288.20±28.61, **Figure 5.1 A**). When cells were stimulated with TNF-α , this had no effect on calcium levels; however, when cells were co-treated with both TNF-α and CM, there was a significant elevation in calcium secretion by endothelial cells (454.60±47.06 vs (305.30±26.23, P<0.0197, **Figure 5.1 A**).

Alkaline Phosphatase (ALP) is an early marker of osteogenic activity that plays an important role in the initiation of mineralisation in bone osteogenesis and also during VC[105]. Previously, ALP secretion was upregulated via hypoxia signalling in endothelial cells following incubation with CM. To further delineate its role in inflammatory-driven angiogenesis, ALP activity was measured in ECs following CM treatment and co-incubation with TNF-α. In this study, CM upregulated ALP secretion in ECs relative to un-treated cells (6.53±0.56 vs 4.96±0.27, P<0.0337, Figure **5.1 B**). Subsequent exposure of ECs with both TNF-α and CM also stimulated increase in ALP secretion and activity (6.79±.37 vs 5.29±0.31, P<0.0138, **Figure 5.1 B**). This data supports previous findings in ECs where

TNF-α promoted calcifying vascular cell mineralization; via increasing the expression of ALP, an important driver for matrix mineralization[91].

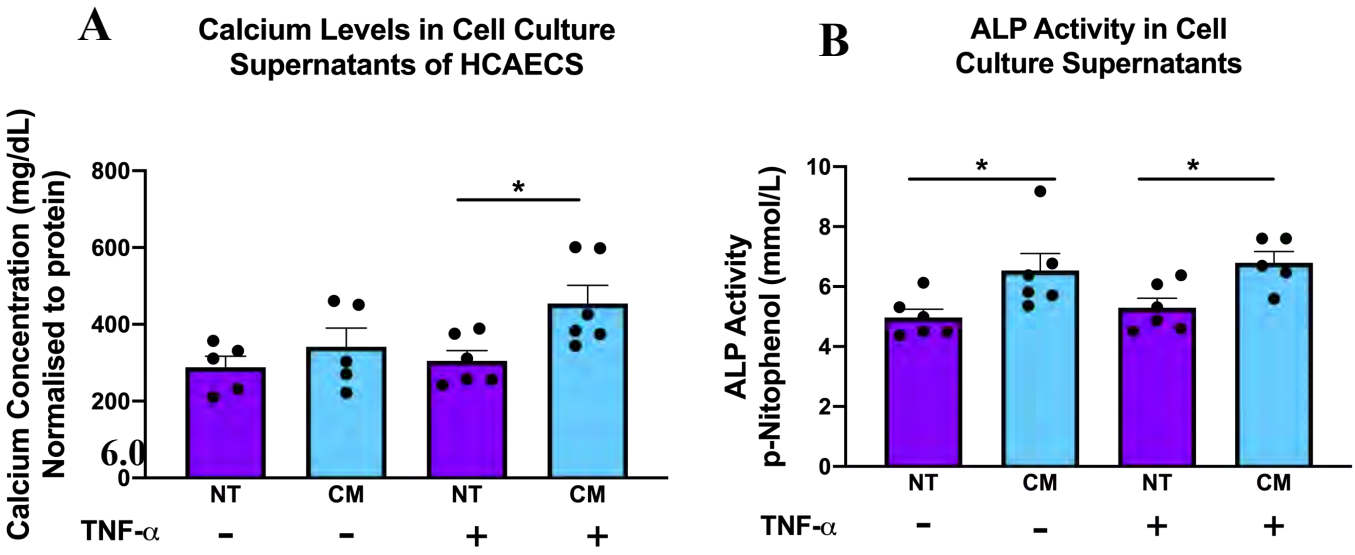

Figure 5.1: CM Raises Calcium Levels and ALP Activity Despite the Presence of TNF-α.

HCAECs cultured in MesoEndo medium then treated with calcification medium containing 2.0mM HNa_2PO_4 and 2.7mM $CaCl_2$ in 10% FBS M199 medium for 24h. Cells were then treated with a concentration of 1 ng/mL of TNF-α for 4h. ***(A)*** *Circulating calcium (Cayman, Calcium Assay) and* ***(B)*** *ALP activity (WAKO, ALP LabAssay) were used to quantify calcium concentrations in cell culture supernatants following treatment. All data is represented as mean ± SEM; One-way ANOVA with Bonferroni's Multiple comparisons test, (n=6), *P<0.05), ALP, alkaline phosphatase.*

5.2.2 Calcification Medium Effects on Angiogenic Assays With TNF-α Stimulus.

The effect of calcification medium in driving endothelial cell viability, migration and tubule formation was assessed under the influence of inflammation. Incubation of ECs with CM stimulated an increase in cell viability compared to untreated cells (2.13±0.09 vs 1.16±0.11, P<0.0065, Figure 5.2). In addition, co-incubation of ECs with TNF-α and CM demonstrated a significant increase in cell viability when compared to cells unstimulated with TNF-α (2.32±0.14 vs 1.83±0.15, P<0.0427, **Figure 5.2**).

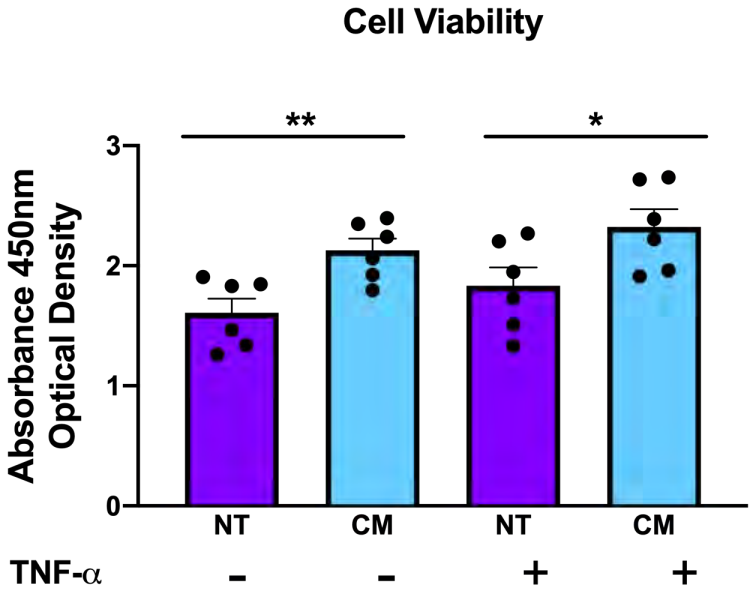

Figure 5.2: CM Induces Change in Cell Viability Despite TNF-α Presence

HCAECs cultured in MesoEndo medium then treated with calcification medium containing 2.0mM HNa_2PO_4 and 2.7mM $CaCl_2$ in 10% FBS M199 medium for 24h. Cells were then treated with a concentration of 1 ng/mL of TNF-α for 4h. WST-1 cell viability reagent was added to cells and incubated for 4h to assess total cell viability. All data is represented as percentage of controls, mean ± SEM; One-way ANOVA with Bonferroni's Multiple comparisons test, (n=6), HCAEC, human coronary artery endothelial cells, M199, medium 199 (Sigma-Aldrich).

When assessed for migratory effect, CM significantly reduced endothelial cell migration relative to non-treated cells (44.85±3.74 vs 75.87±9.60, P<0.0062, **Figure 5.3**). Stimulation with TNF-α also significantly decreased cell migration compared to untreated cells. Interestingly however, when cells were co-incubated with both TNF-α and CM, cell migration was significantly increased compared to cells treated with TNF-α alone (58.47±6.73 vs 39.52±3.14, P<0.0289 **Figure 5.3**). Taken together this data demonstrates differential regulation of cell migration by both CM and TNF-α and may therefore suggest other molecular interactions requiring further investigation.

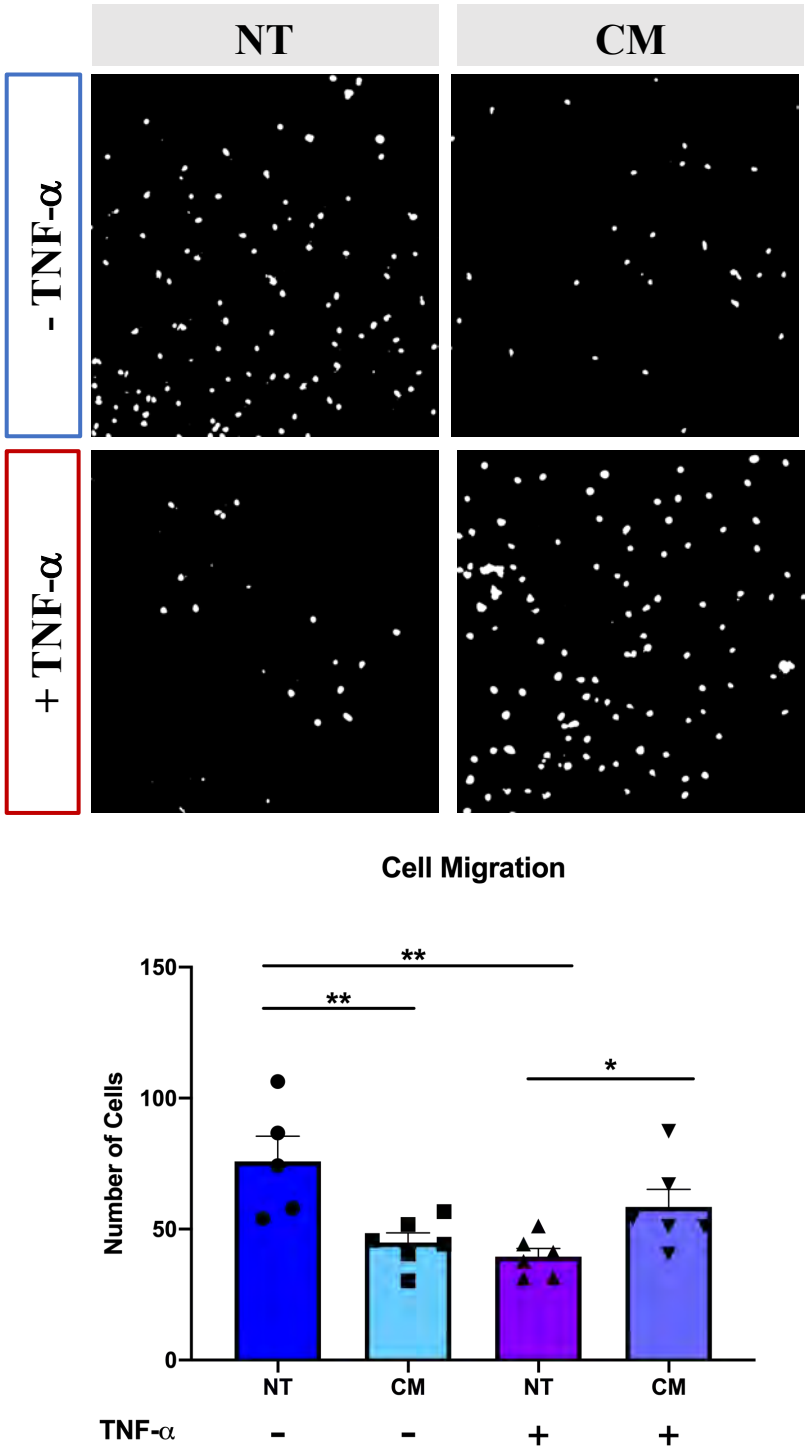

Figure 5.3: TNF-α Drives CM-Induced Increase in Endothelial Cell Migration.

*HCAECs cultured in MesoEndo medium then treated with calcification medium containing 2.0mM HNa_2PO_4 and 2.7mM $CaCl_2$ in 10% FBS M199 medium for 24h. Cells were then treated with a concentration of 1 ng/mL of TNF-α for 4h. Boyden cell migration assay was conducted. All data is represented as percentage of controls, mean ± SEM; One-way ANOVA with Bonferroni's Multiple comparisons test, (n=6), *P<0.05, **P<0.01, HCAEC, human coronary artery endothelial cells, M199, medium 199 (Sigma-Aldrich).*

Tubule formation is the final stage of angiogenesis, regulated by numerous pro-angiogenic factors. Consistent with data from previous chapters, CM supressed endothelial tubule formation when compared to control cells (15.50±3.59 vs 48.61±5.38, P<0.0001, **Figure 5.4**). Stimulation with TNF-α had no effect on ECs tubule formation capacity when compared to untreated cells (53.89±4.30 vs 48.61±5.38). However, when cells were co-incubated with both CM and TNF-α, there was a significant increase in the number of tubules formed when compared to cells treated with CM alone (45.61±4.35 vs 15.50±3.59, P<0.0001, **Figure 5.4**). This indicates that stimulation with TNF-α in this instance overrode the ability of CM to reduce tubule formation.

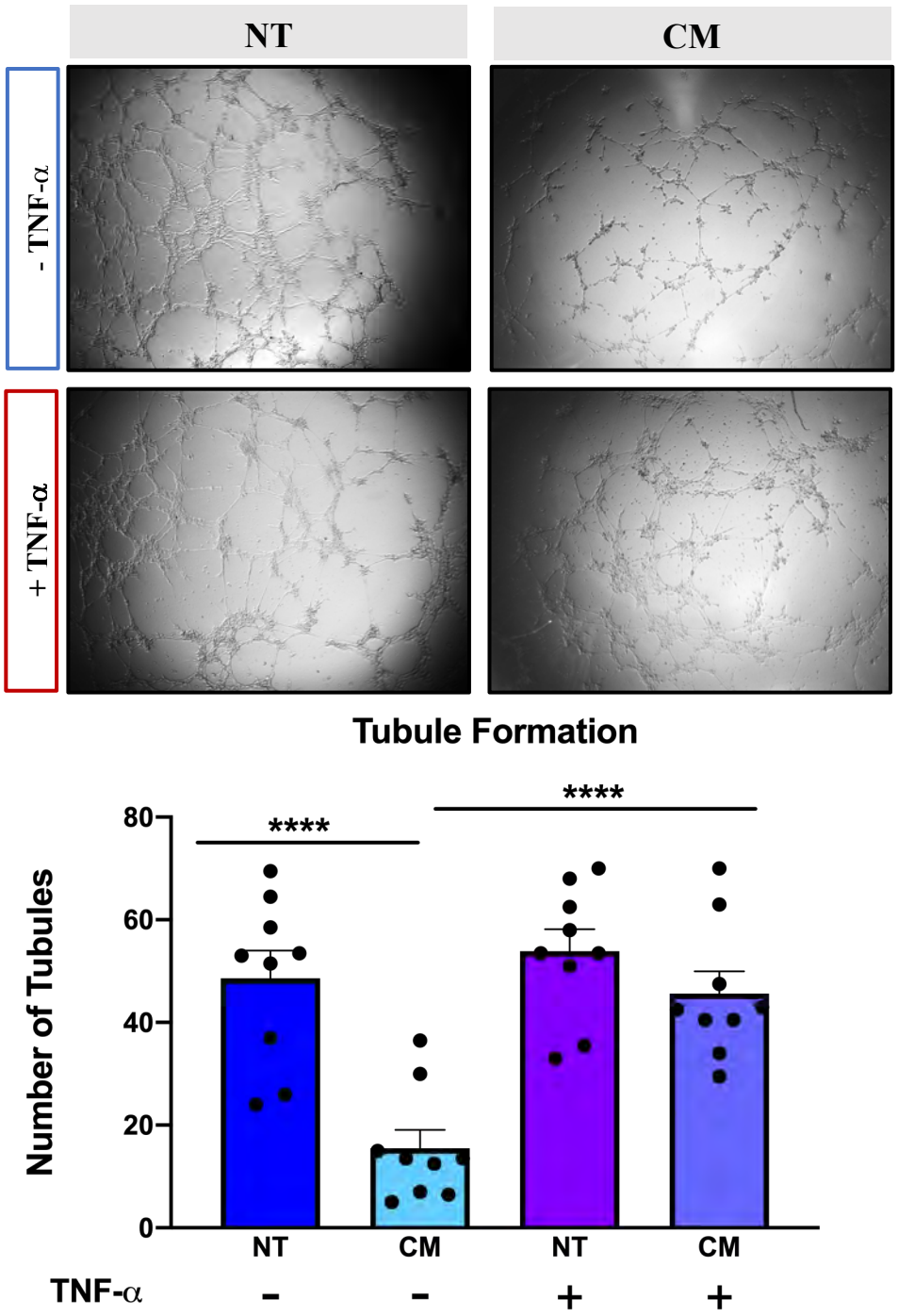

Figure 5.4: Inflammation Has No Effect on EC Tubule Formation. HCAECs cultured in MesoEndo medium then treated with calcification medium containing 2.0mM HNa_2PO_4 and 2.7mM $CaCl_2$ in 10% FBS M199 medium for 24h. Cells were then treated with a concentration of 1 ng/mL of TNF-α for 4h. Matrigel Tubulogenesis assay was performed to assess number of tubes formed over 4 h. All data is represented as percentage ratio of controls, mean ± SEM; One-way ANOVA with Bonferroni's Multiple comparisons test, (n=9), ****P<0.0001, n=9. HCAEC, human coronary artery endothelial cells, M199, medium 199 (Sigma-Aldrich, TNF-α, tumour necrosis factor alpha.

5.2.3 Inflammation Had No Effect on Pro-Angiogenic Marker HIF-1α Expression

The HIF-1α pathway is known to be a key regulator of angiogenesis and is conditionally regulated by both ischemia and inflammatory stimulus[46]. However, the role of calcification in driving HIF-1α-upregulation in inflammatory-driven angiogenesis has not been explored. In this study, treatment of ECs with CM alone upregulated *Hif-1α* mRNA expression compared to non-treated cells (152.80±26.10 vs 96.71±6.80, P<0.0355 (**Figure 5.5**). When cells were treated with TNF-α, there was no change in HIF-1α expression when compared to non-TNF-α treated cells **(Figure 5.5**), with no effect also seen with co-incubation with both CM and TNF-α. These findings collectively imply that CM may have more striking effects on HIF-1α expression in basal conditions compared to an inflammatory condition.

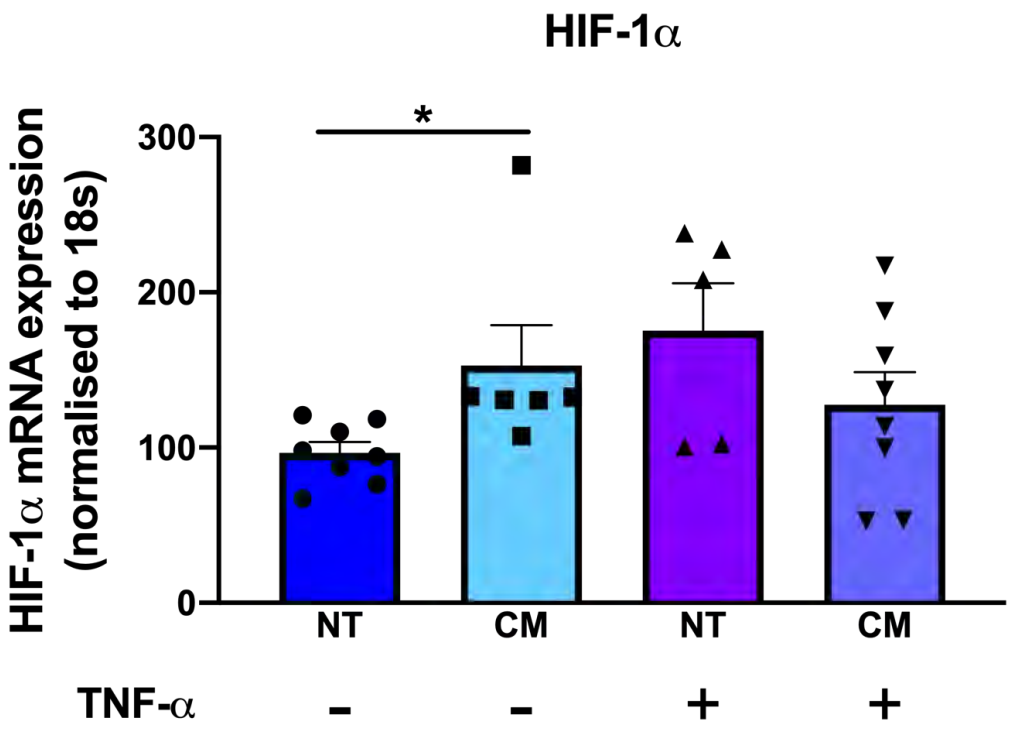

Figure 5.5: CM Alone Drives TNF-α-Induced Hif-1α expression.

*HCAECs cultured in MesoEndo medium then treated with calcification medium containing 2.0mM HNa_2PO_4 and 2.7mM $CaCl_2$ in 10% FBS M199 medium for 24h. Cells were then treated with a concentration of 1 ng/mL of TNF-α for 4h. RNA extracted after 24 h, reverse transcribed into cDNA, then real-time PCR performed. mRNA was normalised to human 18s. All data is represented as percentage of controls, mean ± SEM; One-way ANOVA with Bonferroni's Multiple comparisons test, (n=4-8), *P<0.05. HCAEC, human coronary artery endothelial cells, M199, medium 199 (Sigma-Aldrich), HIF-1α, hypoxia-inducible factor-1 alpha, TNF-α, tumour necrosis factor alpha.*

5.2.4 Inflammation Differentially Effects The Vegfa-Vegfr2 Signalling Pathway to Regulate Angiogenesis.

The VEGFA-VEGFR2 axis is well regulated in angiogenesis. Very little is known about the regulation of this pathway by calcification, particularly in its ability to influence angiogenesis. In this study, treatment of ECs with CM upregulated *Vegfa* mRNA expression in the absence of an inflammatory stimulus (134.40±19.67 vs 90.72±5.97, P<0.0438, **Figure 5.6 A**). However, when cells were treated with TNF-α, there was significant upregulation in *Vegfa* mRNA expression compared to non-treated cells (176.90±15.04 vs 90.72±15.04, P<0.035, **Figure 5.6 A**). However, there was no change in VEGFA protein expression with CM treatment alone and when cells were co-incubated with both CM and TNF-α when compared to non-treated cells **(Figure 5.6 C)**.

Based on these findings and to understand the mechanisms further, Vegfr2 expression was measured following CM and TNF-α treatment. CM alone had no effect on *Vegfr2* mRNA expression when compared to non-treated cells (**Figure 5.6 C**). When cells were treated with TNF-α, this elicited no change on *Vegfr2* mRNA expression (**Figure 5.6 C**). Furthermore, the addition of TNF-α alone had no effect on *Vegfa* gene expression (**Figure 5.6 C**).

These findings collectively demonstrate differential regulation of the VEGFA-VEGFR2 axis at both the transcriptional and translational level by CM and TNF-α, potentially implicating alternative regulatory mechanisms to be involved. This data also suggests that CM may elicit more striking effects on VEGFA expression at the translational rather than the transcriptional level.

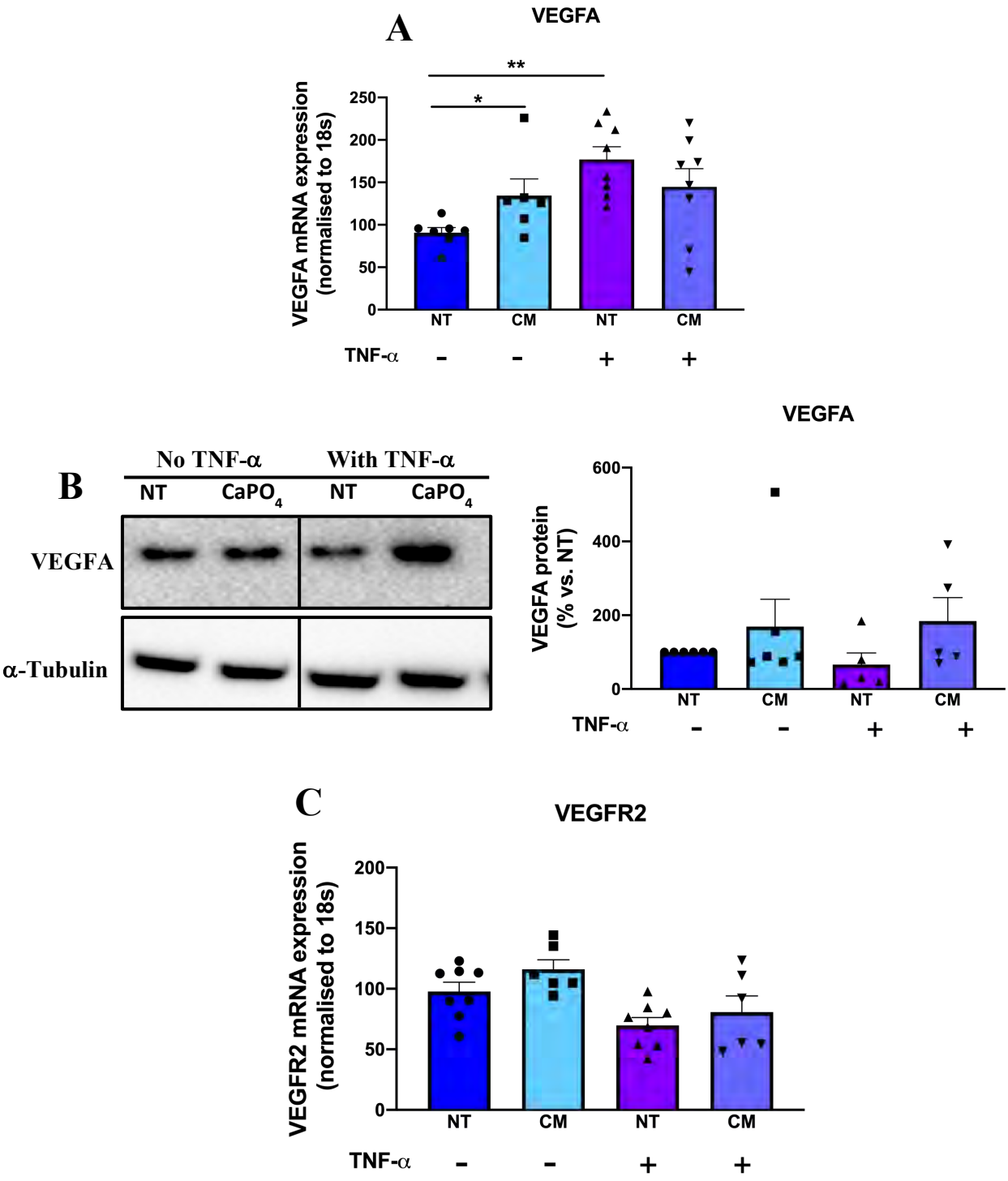

Figure 5.6: CM Differentially Regulates Vegfa-Vegfr2 Axis With TNF-α Stimulation.

*HCAECs cultured in MesoEndo medium then treated with calcification medium containing 2.0mM HNa_2PO_4 and 2.7mM $CaCl_2$ in 10% FBS M199 medium for 24h. Cells were then treated with a concentration of 1 ng/mL of TNF-α for 4h. RNA extracted after 24 h, reverse transcribed into cDNA, then real-time PCR performed. mRNA was normalised to human 18s. All data is represented as percentage of controls, mean ± SEM; One-way ANOVA with Bonferroni's Multiple comparisons test, (n=4-8), *P<0.05, **P<0.01 HCAEC, human coronary artery endothelial cells, M199, medium 199 (Sigma-Aldrich), VEGFA, vascular endothelial growth factor, VEGFR2, vascular endothelial growth factor receptor 2.*

5.2.5 CM Elicits No Change on Runx2 Expression Following TNF-α Treatment.

Runx2 is an important transcription factor involved in the calcification process, that regulates the expression of a cascade of mineralization regulating proteins such as alkaline phosphatase, osteopontin and osteocalcin[89]. In chapter 3, CM decreased *Runx2* mRNA expression in ECs in hypoxia compared to normoxia. In this chapter, the role of Runx2 in inflammatory-driven angiogenesis was explored. ECs treated with CM showed no change in *Runx2* mRNA expression compared to control cells. Furthermore, co-incubation of ECs with both CM and TNF-α did not appear to have any effect on *Runx2* mRNA expression (**Figure 5.7**). This data suggests Runx2 expression in ECs does not respond to an inflammatory stimulus.

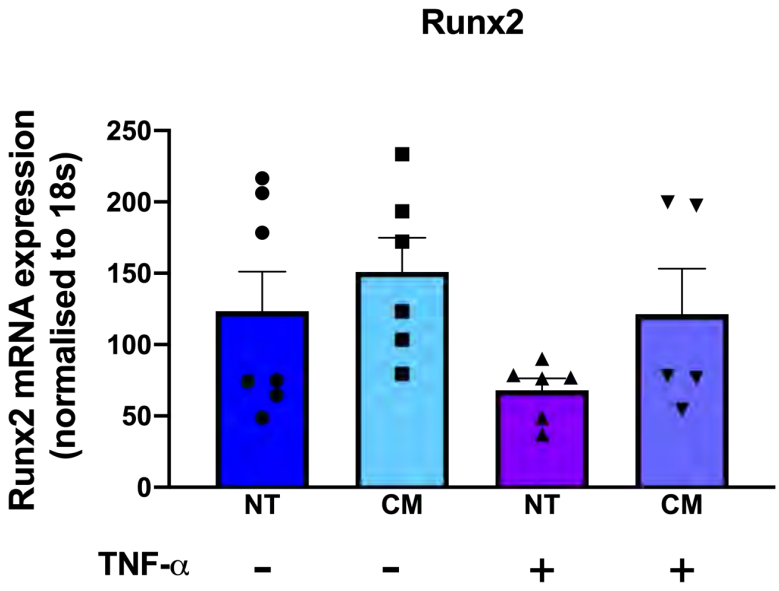

Figure 5.7: CM Has No Effect in Regulating Runx2 Expression Following TNF-α Treatment in ECs
HCAECs cultured in MesoEndo medium then treated with calcification medium containing 2.0mM HNa_2PO_4 and 2.7mM $CaCl_2$ in 10% FBS M199 medium for 24h. Cells were then treated with a concentration of 1 ng/mL of TNF-α for 4h. RNA extracted after 24 h, reverse transcribed into cDNA, then real-time PCR performed. mRNA was normalised to human 18s. All data is represented as percentage of controls, mean ± SEM; One-way ANOVA with Bonferroni's Multiple comparisons test, (n=5-8). HCAEC, human coronary artery endothelial cells, M199, medium 199 (Sigma-Aldrich), Runx2, runt-related transcription factor.

5.2.6 TNF-α and Calcification Medium Upregulated Osteogenic Marker BMP2 Expression.

Bone morphogenetic proteins (BMPs) are potent osteogenic differentiation mediators of bone formation; and their role as inducers of VC has been well established[124, 125]. In this study, treatment of ECs with CM induced upregulation of *Bmp2* mRNA expression compared to non-treated cells (225.30±52.30 vs 104.10±9.67, P<0.0290); a response that was further increased with TNFα treatment (557.20±83.76, P<0.0001**, Figure 5.8**). Likewise, co-incubation of ECs with both CM and TNF-α showed further elevation in *Bmp2* mRNA expression compared to CM treated cells (599.40±126 vs 225.30±52.30, P<0.0131). Although there was no change compared to cells treated with TNF-α alone, elevated *Bmp2* expression suggests a proinflammatory effect of TNF-α in driving calcification marker expression in ECs.

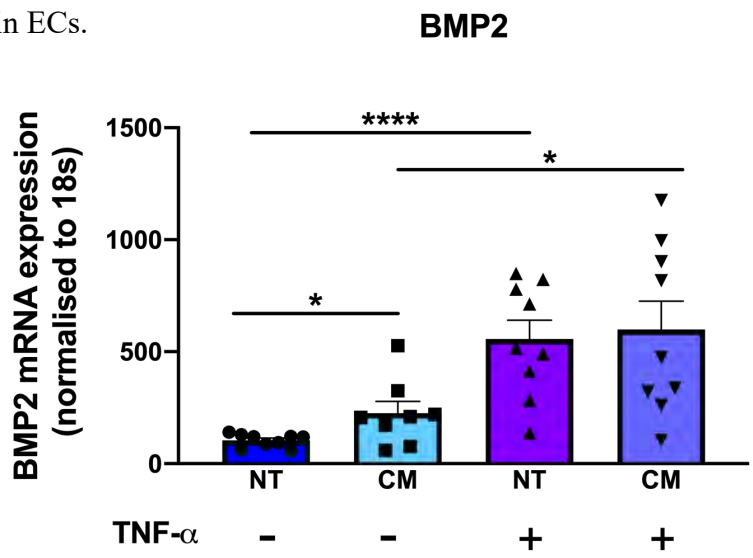

Figure 5.8: CM Upregulates Bmp2 Expression With TNF-α-Treatment in ECs.

*HCAECs cultured in MesoEndo medium then treated with calcification medium containing 2.0mM HNa_2PO_4 and 2.7mM $CaCl_2$ in 10% FBS M199 medium for 24h. Cells were then treated with a concentration of 1 ng/mL of TNF-α for 4h. RNA extracted after 24 h, reverse transcribed into cDNA, then real-time PCR performed. mRNA was normalised to human 18s. All data is represented as percentage of controls, mean ± SEM; One-way ANOVA with Bonferroni's Multiple comparisons test, (n=5-9, *P<0.05, **P<0.01. HCAEC, human coronary artery endothelial cells, M199, medium 199 (Sigma-Aldrich), BMP2, bone morphogenetic protein 2.*

5.2.7 CM Differentially Regulates the RANK-RANKL-OPG Axis Under Inflammatory Conditions.

There is growing evidence that ectopic calcification of blood vessels and cardiac valves are associated with angiogenesis[51, 62,150]. Several processes have been proposed to regulate calcification, including the RANK/RANKL/OPG signalling pathway[129, 166, 169]. Treatment of ECs with CM upregulated *Rankl* mRNA expression compared to non-treated cells (372.80±90.09 vs 113.30±20.99, P<0.0026, **Figure 5.9 A**). When cells were stimulated with TNF-α, there was no effect on *Rankl* expression. Co-incubation with TNF-α and CM also had no effect on *Rankl* mRNA expression (**Figure 5.9 A**). CM also upregulated *Rank* mRNA levels compared to non-treated cells (136.50±14.22 vs 98.02±9.77, P<0.0308, **Figure 5.9 B**). However, all other treatments had no effects in regulating *Rank* gene expression (**Figure 5.9 B**). The only effect on the pro-calcific mediators of this axis came from calcification treatment with no additive effects from inflammation.

OPG is a known decoy receptor and has protective role in preventing vascular calcification. EC stimulation with TNF-α is known to stimulate the release of OPG under basal conditions[205]. Consistent with previous data, treatment of ECs with CM significantly upregulated *Opg* mRNA expression compared to non-treated cells (187.30±44 vs 111.70±11.09, P<0.0360, **Figure 5.9 C**). TNF-α alone had negligible effects on *Opg* expression, however when ECs were co-incubated with both TNF-α and CM, there was a significant reduction in *Opg* mRNA expression compared to cells treated with CM alone (79.43±20.44 vs 187.30±44, P<0.0310, **Figure 5.9 C**).

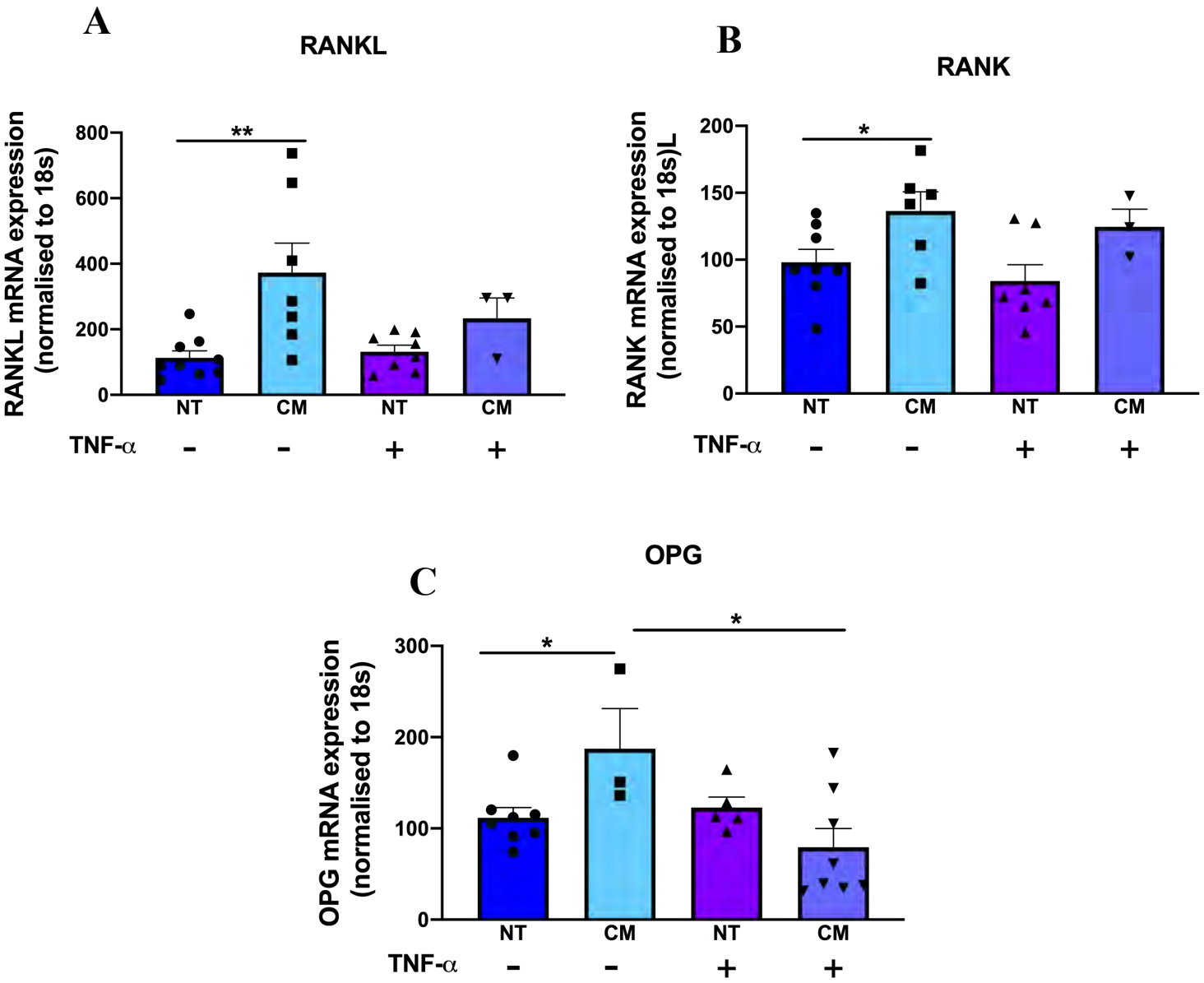

Figure 5.9: CM Differentially Regulates the Rankl/Rank/Opg Axis Under Inflammatory Conditions.

*HCAECs cultured in MesoEndo medium then treated with calcification medium containing 2.0mM HNa_2PO_4 and 2.7mM $CaCl_2$ in 10% FBS M199 medium for 24h. Cells were then treated with a concentration of 1 ng/mL of TNF-α for 4h. RNA extracted after 24 h, reverse transcribed into cDNA, then real-time PCR performed. mRNA was normalised to human 18s. All data is represented as percentage of controls, mean ± SEM; One-way ANOVA with Bonferroni's Multiple comparisons test, (n=5-9), *P<0.05. HCAEC, human coronary artery endothelial cells, M199, medium 199 (Sigma-Aldrich), RANKL, receptor activator of nuclear factor κB ligand, and receptor RANK, OPG, osteoprotegerin.*

5.2.8 Calcification Medium Upregulates NF-κB Activation Under Inflammatory Response.

The transcription factor NF-κB is a key driver of inflammatory-driven angiogenesis[65]. The effects of elevated calcium levels in combination with inflammation and the subsequent effects on NF- κB (p65), however have not been fully characterised. CM treatment had no significant effect on NF-κB (P65) protein expression compared to non-treated cells (**Figure 5.10**); however when ECs were stimulated with TNF-α, there appeared to be an increase in NF-κB (P65) compared to non-treated cells (825±421.2 vs 99.20±3.6) though not statistically significant. Co-incubation of ECs with both CM and TNF-α increased NF-κB (P65) protein expression relative compared to cells treated with CM alone (3028±2939 vs 158±32.29, $P<0.0049$, **Figure 5.10)**. These findings suggest a pro-inflammatory effect of high calcium on ECs which can be further exacerbated by an inflammatory stimulus.

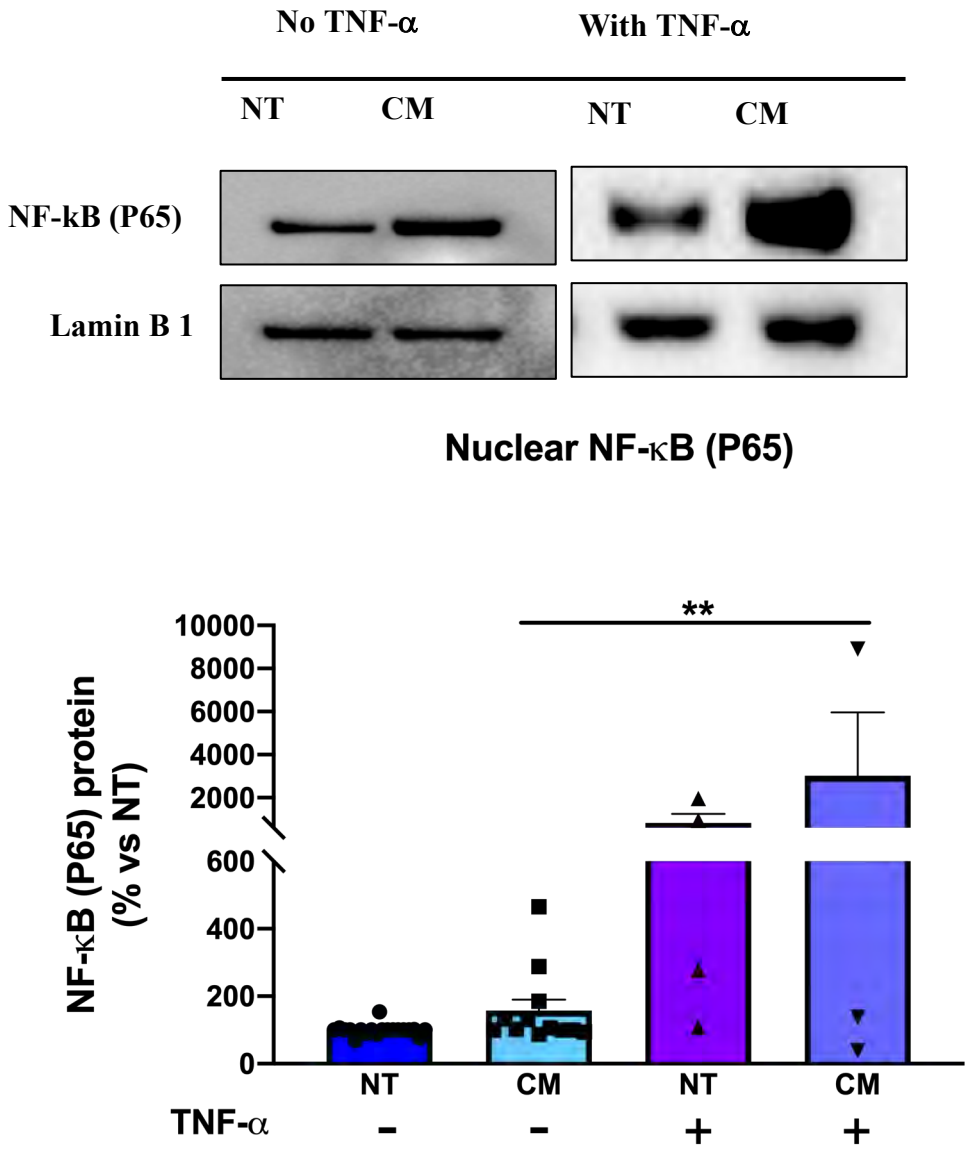

Figure 5.10: CM Drives NF-B (P65) Activation Under Inflammatory Response.

HCAECs cultured in MesoEndo medium then treated with calcification medium containing 2.0mM HNa_2PO_4 and 2.7mM $CaCl_2$ in 10% FBS M199 medium for 24h. Cells were then treated with a concentration of 1 ng/mL of TNF-α for 4h. Nuclear protein was extracted measure protein expression via immunoblotting technique. Even protein loading was confirmed by Lamin B 1 Nuclear Envelope Marker. All data is represented as percentage of controls, mean ± SEM; One-way ANOVA with Bonferroni's Multiple comparisons test, (n=3-9). HCAEC, human coronary artery endothelial cells, M199, medium 199 (Sigma-Aldrich).

5.2.9 CM Drives Upregulation of Inflammatory Markers ICAM, VCAM and . MCP1

ICAM-1 is a well-studied acute inflammatory marker that is highly expressed in endothelial cells. ICAM-1 expression is known to be stimulated by various stimuli including TNF-α, interleukins (IL-1beta, IL-6), lipopolysaccharide (LPS) and oxidised low-density lipoproteins (oxLDL). ICAM-1 activation is also dependent on the transcription factor NF-κB[206, 207]. Currently, little data is currently available to highlight the effect of a calcification stimuli on ICAM-1 expression in ECs, particularly in the regulation of inflammatory-driven angiogenesis. In this study, treatment of ECs with CM significantly upregulated *Icam-1* mRNA expression compared to non-treated cells (234±46.90 vs 106.30±14.16, P<0.0191, **Figure 5.10 A**). Additionally, when cells were stimulated with TNF-α, there was striking increase in *Icam-1* mRNA expression compared to non-treated cells (2364±408.30 vs 106.30±14.16, P<0.0001). Furthermore, while co-incubation with both TNF-α and CM had no additional effects on *Icam-1* expression relative to TNF-α only treated cells, they remained substantially elevated when compared to CM alone (2006±388 vs 106.30±14.16; P<0.0002, **Figure 5.10 A**).

VCAM-1 is also expressed on the luminal surface of endothelial cells[208]. Unlike ICAM-1, VCAM-1 expression is not normally present in basal conditions, only following stimulation with pro-inflammatory cytokines such as TNF-α and IL-1β and IL-6[208]. VCAM-1 expression is also regulated by NF-κB, namely its two subunits p65 and p50. CM significantly upregulated *Vcam-1* mRNA expression compared to non-treated cells (317±58.94 vs 105.30±13.0, P<0.0014, **Figure 5.10 B**). When cells were stimulated with TNF-α, there was a striking elevation in *Vcam-1* expression compared to non-treated cells

(4389±754.4 vs 105.30±13.10, P<0.0001, **Figure 5.10 B**). Once again, co-incubation with both TNF-α and CM showed no additional effects on TNFα stimulated *Vcam-1* expression but significantly increased it compared to CM alone (3389±835.40 vs 105.30±13.10, P<0.0035, **Figure 5.10 B**).

MCP-1 is a chemokine secreted by numerous cell types including endothelial cells, fibroblasts, smooth muscle cells, monocytes and macrophages[209]. Regulation of MCP-1 occurs via NF-κB and the mitogen activated protein kinase (MAPK) signalling pathways.[210] In this study, treatment of ECs with CM significantly upregulated *Mcp-1* mRNA expression compared to non-treated cells (289.90±49.03 vs 125.30±11.67, P<0.0151, **Figure 5.10 C**) and when cells were stimulated with TNF-α, this resulted in a marked increase in *Mcp-1* expression compared to non-treated cells (1450±285.3 vs 125.30±11.67, P<0.0022, **Figure 5.10 C**). Consistent with the data above, co-incubation with both TNF-α and CM had no additional effects on *Mcp-1* expression compared to TNFα alone but elevated the expression seen with CM treatment (1857±389.80 vs 125.30±11.67, P<0.0002, **Figure 5.10 C**). Taken together, these findings demonstrate a pro-inflammatory effect of elevated calcium on endothelial cells.

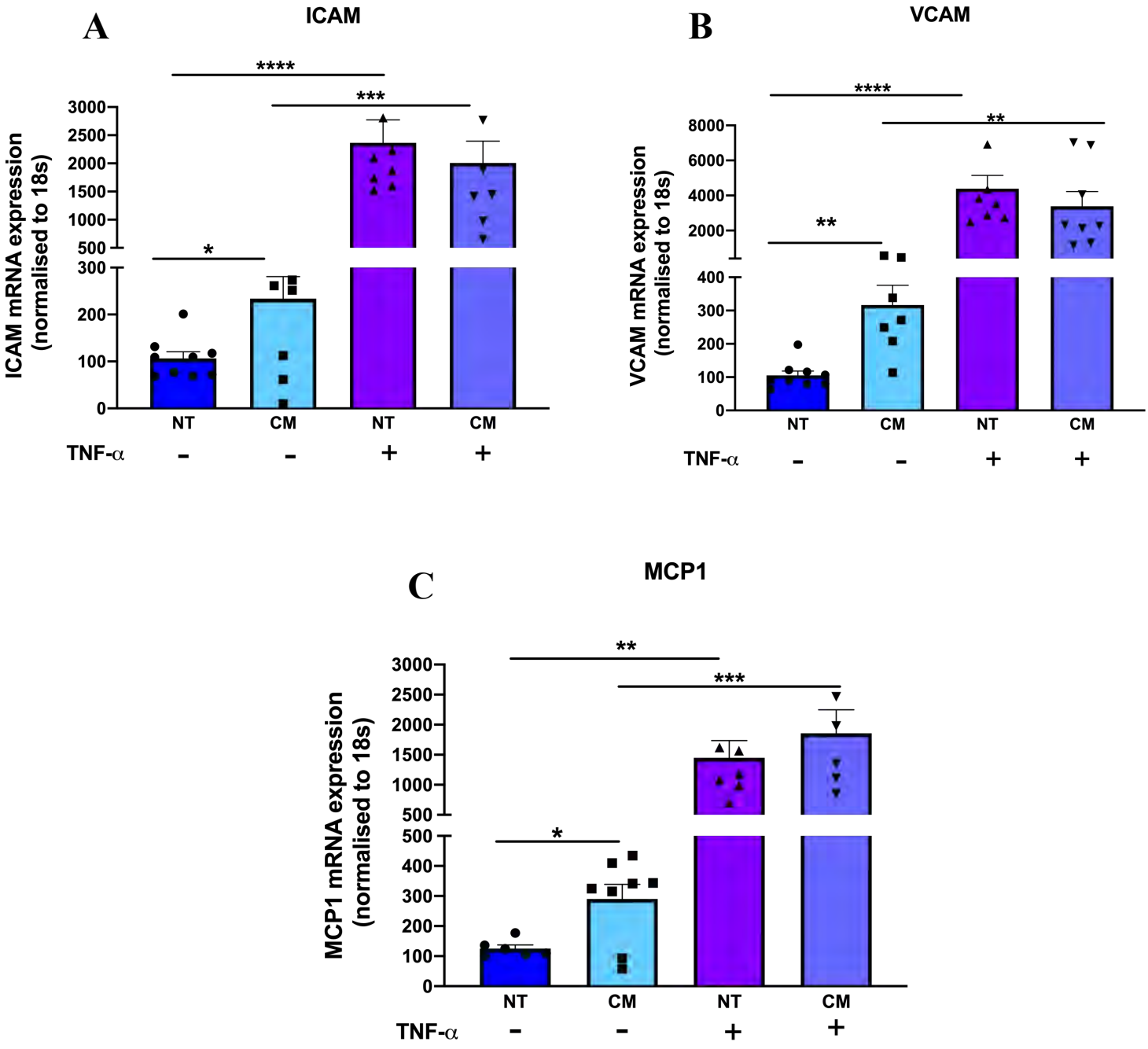

Figure 5.11: CM Upregulates Icam, Vcam and Mcp1 Expression.

*HCAECs cultured in MesoEndo medium then treated with calcification medium containing 2.0mM HNa_2PO_4 and 2.7mM $CaCl_2$ in 10% FBS M199 medium for 24h. Cells were then treated with a concentration of 1 ng/mL of TNF-α for 4h. RNA extracted after 24 h, reverse transcribed into cDNA, then real-time PCR performed. mRNA was normalised to human 18s. All data is represented as percentage of controls, mean ± SEM; One-way ANOVA with Bonferroni's Multiple comparisons test, (n=3-9). *P<0.05, **P<0.01, ***P<0.001, ****P<0.0001. HCAEC, human coronary artery endothelial cells, M199, medium 199 (Sigma-Aldrich), ICAM, intracellular adhesion molecule, VCAM, vascular cell adhesion molecule, MCP1, monocyte chemoattractant protein 1.*

5.1 DISCUSSION

This study demonstrated consistent upregulation of inflammatory markers with calcification treatment, while treatment with TNF-α had little effect on both angiogenic and calcification markers. It was also clear that a combination of calcification with inflammation had additive effects for inflammatory markers. However, as a result of the discrepant effects of the combination treatment on the angiogenic markers the precise mechanism for the role of calcification in inflammatory-induced angiogenesis remains unknown.

Inflammatory macrophages colocalise with basic calcium phosphate crystals/deposits in developing atherosclerosis lesions and can promote VC through the release of TNF-α[161]. Our data appears to oppose this idea because when cells were co-incubated with both TNF-α and CM, this was unable to drive gene expression for osteogenic markers (Figure 5.12). Furthermore, when comparing CM treatment alone with the combination treatment, there was significant downregulation in expression of protective factor OPG and RANKL. It therefore remains unclear whether calcification is purely a pathological response or simply represents an adaptive protective mechanism by the vasculature. Based on data collected from previous studies by Aikawa et al.[211, 212], not all calcification is proinflammatory, as medial calcification occurs in the absence of macrophage infiltration. This is an area that requires further investigation particularly in the regulation of endothelial cell angiogenesis.

This study demonstrated significant upregulation of NF-κB (P65) protein expression with co-incubation with both TNFα and CM; therefore, suggesting a pro-inflammatory role of CM in driving inflammatory driven angiogenesis (Figure 5.12). This was supported by a previous study with human fibroblasts where treatment with hydroxyapatite caused a striking increase in NF-κB activation[213]. The functional studies in this thesis demonstrated increases

in endothelial cell migration following TNF-α treatment and during angiogenesis, BMP2 along with other angiogenic factors such as VEGF have been shown to induce EC migration and proliferation[61, 62]. Furthermore, in other literature, TNF-α has been shown to upregulate EC expression for BMP2 through activation of the NF-κB pathway, which causes nuclear translocation of NF-κB, suggesting that NF-κB activation is required for BMP2 activation and expression[214]**.** In addition, TNF-α and interleukin-1 beta (IL-1β) were shown to induce endothelial-to-mesenchymal transitions in human aortic-endothelial cells and promoted BMP-mediated osteogenic expression and mineralisation[215]. Therefore, in line this with, our data demonstrates a potential mechanistic pathway involving both BMP2 and the NF-κB pathway and provides a potential avenue for future research.

Based on previous results from chapter 3, it was demonstrated that Runx2 may play a role in driving HIF-1α expression in ECs in normoxia. In this study TNF-α stimulation decreased Runx2 expression, findings similar to those of previous studies which have shown TNF-α inhibited Runx2 expression, but increased ALP activity and mineralisation of mesenchymal stem cells[216]. Other results have also demonstrated similar findings of TNF-α inhibition of Runx2 expression[217, 218]. There was however no observed change in HIF-1α expression with TNF-α treatment. Interestingly, co-incubation with both TNF-α and CM upregulated Runx2 expression whilst downregulating HIF-1α expression (Figure 5.12). Data from a previous study showed that TNF-α treatment stimulated an increased in BMP2 expression in a time-dependent manner at 2 h and 8 h, with significant increases seen following TNF-α treatment, though no changes were observed at 24 h[63]. Data from our study corresponds in with this as cells were treated with TNF-α for 4 hours, and I observed increased BMP2 expression with TNF-α treatment; an effect which was further increased

with the combination treatment. This therefore proposes a role of BMP2 in driving inflammatory cytokine TNF-α to potentially drive angiogenesis in disease.

Calcification-induced expression of inflammatory markers was observed in this study, with calcification treatment significantly upregulating key inflammatory markers ICAM-1, VCAM-1 and MCP-1 (Figure 5.12). It is important to note that very little is known regarding the expression of inflammatory markers during vascular calcification. During atherogenesis, lipids, particularly cholesterol delivered by low-density lipoprotein (LDL) particles accumulate and are deposited into the sub-endothelial lumen. Oxidation occurs by reactive oxygen species (ROS) which cause modification of LDL to be oxidised (oxLDL), driving the inflammatory response seen in atherosclerosis. So, while very little is known regarding the role of ICAM-1, VCAM-1 and MCP1 in vascular calcification, due to their well-established role in plaque atherogenesis, it is likely that they may also play a role in regulating calcification-induced inflammatory-driven angiogenesis.

Functional angiogenic assays demonstrated that TNF-α treatment increased endothelial cell viability. A similar trend was reported in a previous study, where HUVECs exposed to TNF-α with different concentrations of 100, 20, 10 and 1 ng/ml showed significantly increased cell proliferation activity at the concentration above 1 ng/ml as compared with the control group[219]. In addition, tubule formation reflects the final stage of endothelial cell angiogenesis and in this study, calcification dampened the ability of ECs to form tubule networks. More interesting, stimulation of cells with TNF-α had no additional effect on EC tubule formation, however with combination treatment there were greater number of tubules formed. These results demonstrated that the combination treatment was not sufficient to drive angiogenesis or the expression of calcification markers, thus highlighting inflammation to be a sole regulator. However, very little is known of the

association between calcium-phosphate crystals and TNF-α-induced inflammation. Nevertheless, the present findings demonstrated that high calcium may be acting via alternative pathways to drive EC tube formation; thus, warranting further studies. As previously stated in chapters 3, the same limitations also apply to this study; including the use of one mode of calcification stimulus, thus warranting future studies to test out other calcification-inducing approaches *in vitro*.

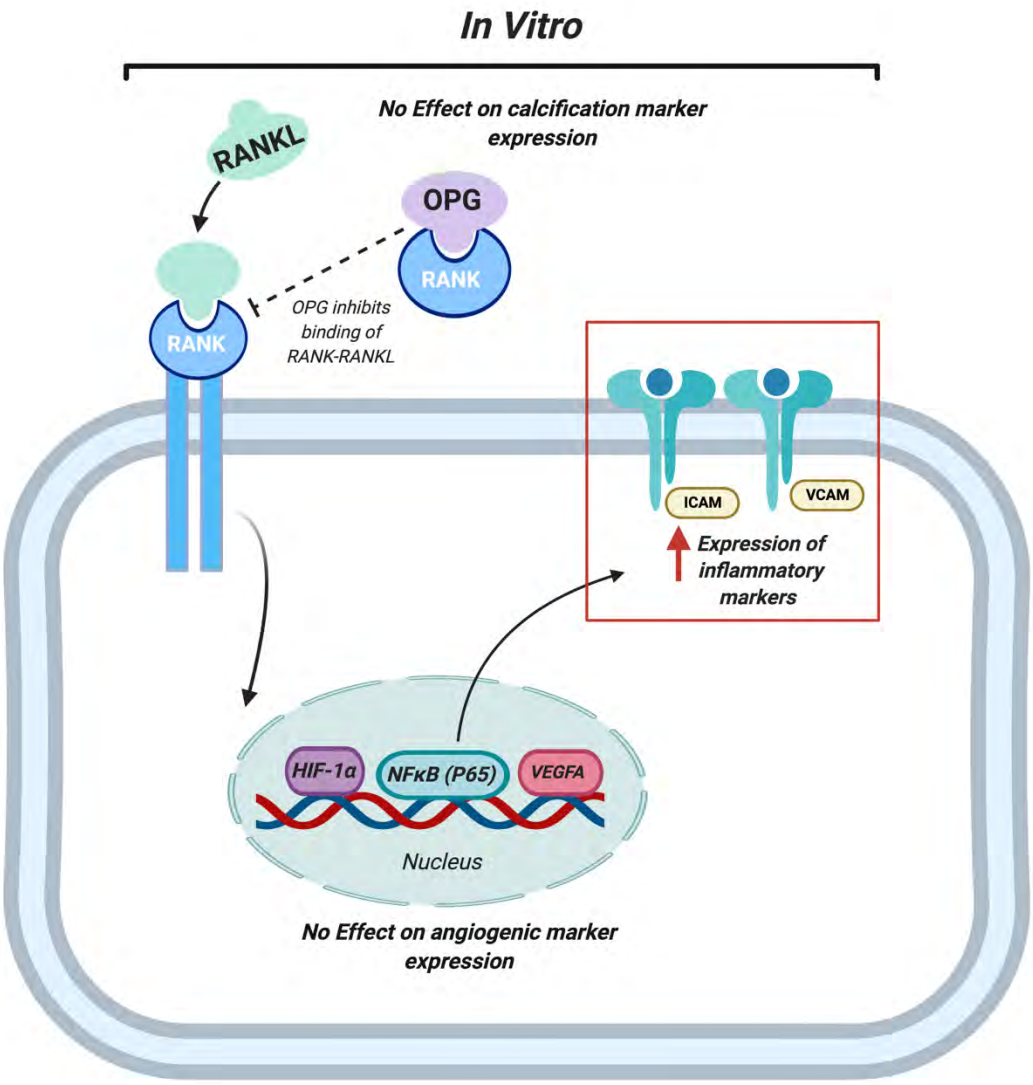

Figure 5.12: Summary Diagram for CM Effects on Inflammatory-Driven Angiogenesis In Vitro

CHAPTER 6:

THE EFFECT OF CALCIFIC ENVIRONMENT ON IN VIVO INFLAMMATORY-DRIVEN ANGIOGENESIS

6. Introduction

As outlined in previous chapters, angiogenesis is defined as the formation of new blood vessels from pre-existing capillary beds[46, 62]. This process is tightly controlled by specific growth and inhibiting factors which create a delicate balance between blood vessel formation and inhibition. Impairment in this balance from either excessive or insufficient blood vessel growth; can exarcabate and lead to the pahotlogical form of angiogenesis as seen in cancer and cardiovascular atherosclerotic diseases[46]. New blood vessel formation is however beneficial for tissue neovascularisation in response to ischemia such as that following a MI, peripheral vascular diseases and wound healing. Neovacularisation however is detrimental in the setting of atheroslerosis or cancer as it may exacerbate inflammatory-driven angiogenesis, therefore accelerating the progression of disease[64].

The studies in chapter 5 demonstrated that stimulation of ECs with TNF-α alone had no effect in driving the expression of calcification and angiogenic markers. However, these in vitro results demonstrated a combination effect of calcification medium and TNF-α in stimulating the expression of calcification markers BMP2 and inflammatory markers VCAM-1, ICAM-1, MCP1 and NF-κB (P65); whilst driving EC viability and migration.

As previously stated in chapter 1, atherosclerosis is a chronic inflammatory disease that occurs in the vessel wall. During this process, there is involvement of different cell types including ECs, VSMCs, fibroblasts, monocytes/macrophages and adipocytes from the tunica intima, media and adventitia which all play a role in driving this inflammatory response via multiple intricate pathways. During atherogenesis, LDL accumulates within the vessel wall and becomes oxidised to ox-LDL. Ox-LDL drives the recruitment of inflammatory mediators ICAM-1, VCAM-1 and MCP1, which further stimulates monocyte recruitment and differentiation into macrophages, a main event during atherogenesis. As a result, these

cascades of inflammatory responses promote atherosclerotic plaque growth. Furthermore, cardiovascular calcification most commonly occurs within inflamed plaques and is characterized by lipid deposition and macrophage accumulation. Monocyte-derived macrophages located in atherosclerotic lesions display osteoclast-like functions and can present with a heterogeneous phenotype, from classical proinflammatory M1 to alternative anti-inflammatory M2 macrophages. In one study, macrophages were observed to surround calcium deposits in atherosclerotic plaques[220]. In the same study, monocytes/macrophages were capable of undergoing osteoclastogenesis when treated with RANKL and colony-stimulating factor in vitro[220]. In addition, numerous studies have demonstrated that macrophage-derived proinflammatory cytokines (IL-1β, IL-6, IL-8, TNF-α) promote atherosclerosis-associated calcification by regulating the differentiation of calcifying VSMCs within the vessel wall[91, 221].

Based on this, the present studies sought to assess whether these striking in vitro findings could be extended to an in vivo model of inflammatory-driven angiogenesis. Based on results from chapter 3 where in vivo studies showed significant impairment in ischemia-driven angiogenesis in OPG deficient mice compared to wildtype controls, this study evaluated the functional role of a calcification milieu on inflammatory-driven angiogenesis in the same model using a pathological femoral periarterial cuff model.

6.1 Results

6.1.1 *OPG Deficient Mice Exhibit Elevated Serum Calcium Level Following Peri-Arterial Femoral Cuff Surgery.*

To establish the presence of a calcification milieu, both calcium and ALP levels were measured in blood plasma collected from both C57BL/6J and OPG deficient mice following peri-arterial femoral cuff surgery. Plasma analysis demonstrated no change in ALP activity in the OPG deficient mice compared to C57BL/6J controls (Figure 6.2 A). Calcium levels were however elevated in the OPG deficient mice compared to C57BL/6J controls (44.80±7.48 vs 24.04±3.09, $P<0.0196$, Figure 6.1 B). These results are consistent with previous studies where serum concentrations of calcium and phosphorus were elevated between $OPG^{-/-}$ and WT mice[199].

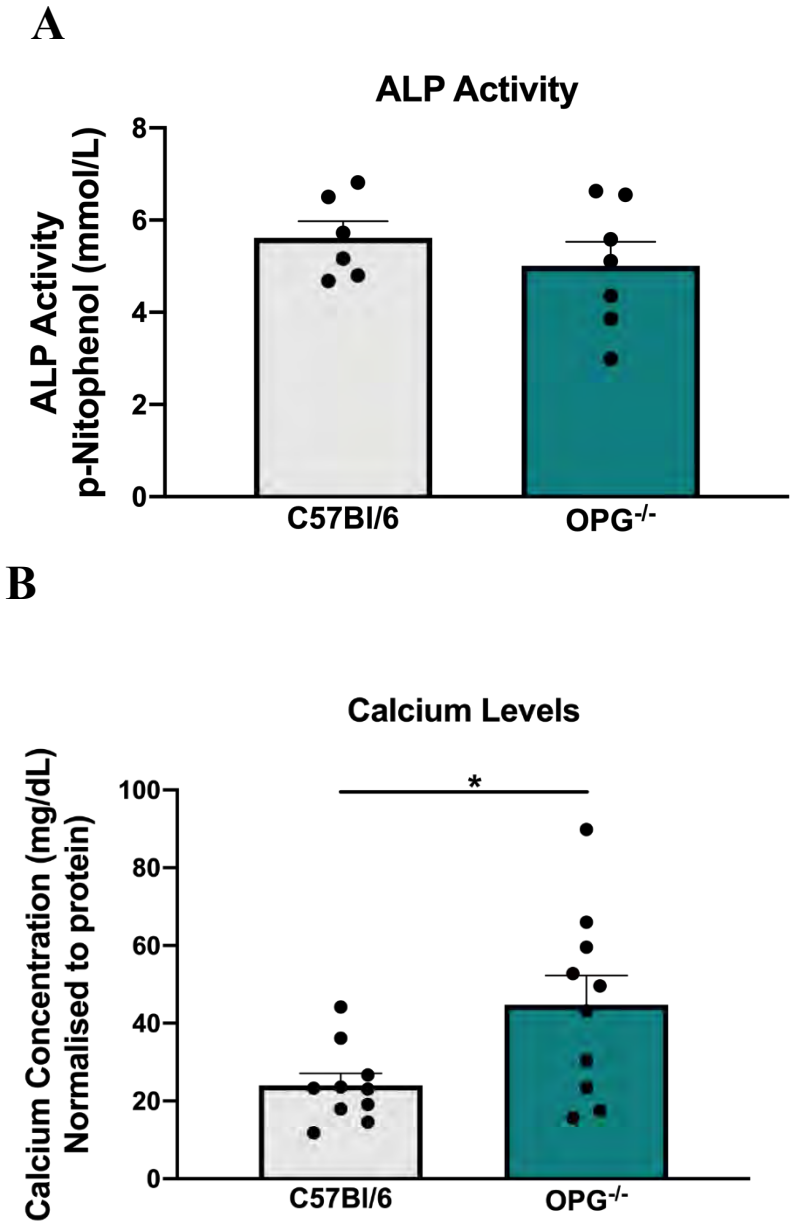

Figure 6.1: OPG Deficient Mice Exhibit Elevated Serum Calcium Levels Following Peri-Arterial Femoral Cuff Surgery. *C57BL/6J and OPG$^{-/-}$ mice underwent peri-arterial femoral cuff surgery, mice were culled 21 days post-surgery and blood plasma collected for analyses. ALP and calcium assays were carried out to measure circulating calcium and ALP activity in these mice.* ***(A)*** *ALP Activity* ***(B)*** *Calcium concentration. Data is represented as mean ± SEM, *P<0.05, (n=8-10/group). Statistical analysis was performed using an unpaired student a Mann Whitney t-test. OPG$^{-/-}$, osteoprotegerin deficient mice, ALP, alkaline phosphatase.*

6.1.2 *OPG Deficiency Affects Adventitial Neovascularisation, Arteriole Formation and Macrophage Infiltration Following Peri-Arterial Cuff Placement.*

Neovessels and arterioles were determined by histological staining for CD31 (endothelial cells in neovessels) and smooth muscle α-actin (smooth muscle in arterioles). Neovessels indicate vessels in the early stage of development whilst arterioles represent the more advanced vessels that contain a smooth muscle cell outerlayer. In this peri-arterial femoral cuff model, $OPG^{-/-}$ mice demonstrated no change in CD31 positive neovessels (Figure 6.2) or arterioles (Figure 6.3) as quantified by α-SMA staining in the cuffed arteries when compared to wildtypes. This may be attributed to sample size and variability as two contributing factors.

Moreover, when macrophage infiltration into the adventitia was assessed following peri-arterial cuff placement using CD68 macrophage staining, there was no change in CD68 expression in cuffed arteries of OPG deficient mice (152%, 329.30±138.90 vs 130.40±25.63) when compared to their WT littermates (Figure 6.4). It's important to note that this result is being driven by a couple of outliers with quite variable results, therefore in future if sample size was increased, this may help improve the statistics.

In addition, intima-to-media thickness was assessed using the massons trichrome staining, which allows visualisation of the 3 layers of the artery wall. In this study, there OPG deficient mice appeared to have a greater intima-to-media thickness compared to wildtype control mice (183±57.07 vs 62.85±24.59, Figure 6.5), although a larger sample size is warranted to confirm the statistics.

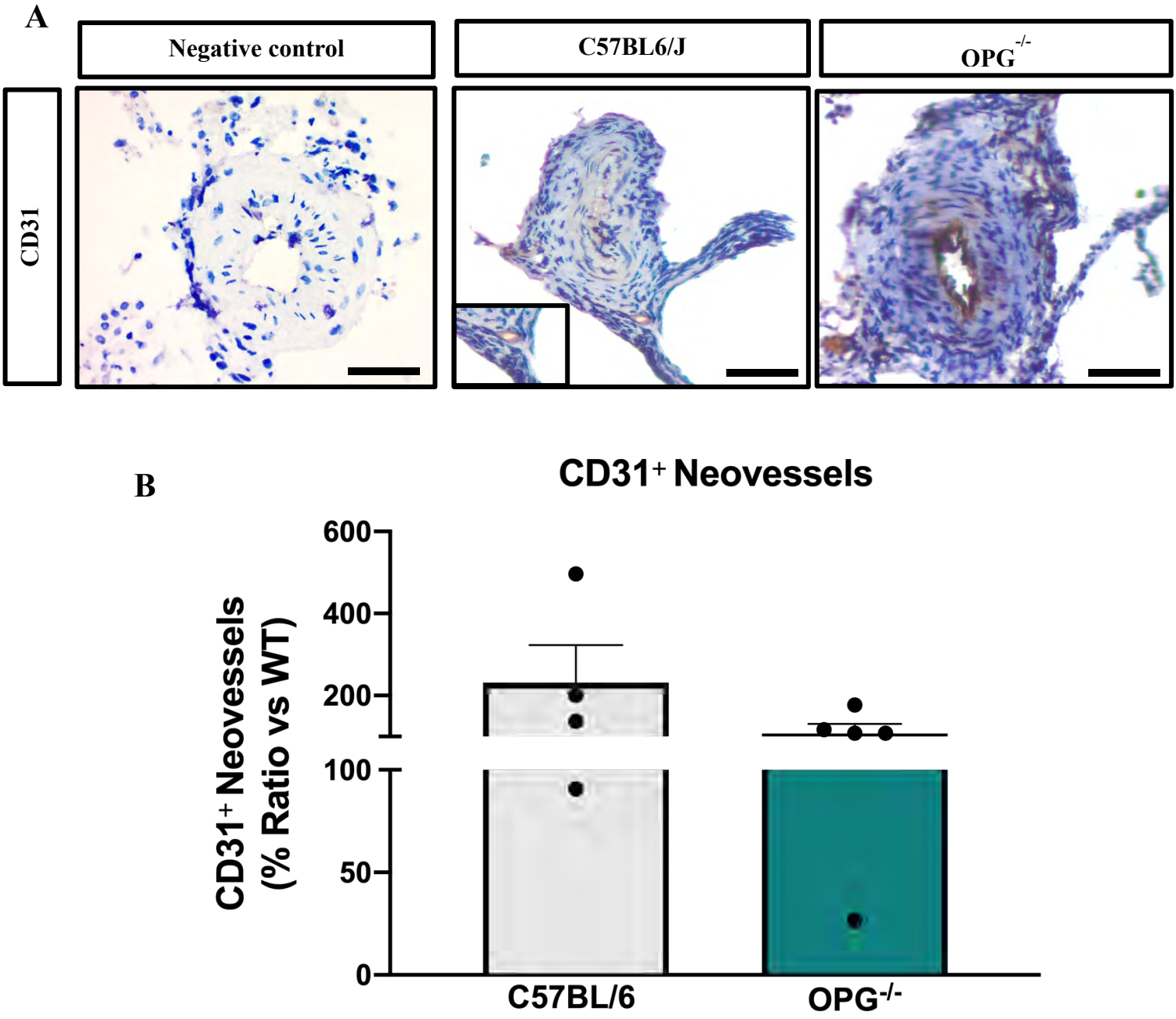

Figure 6.2: OPG Deficiency Affects Adventitial Neovascularisation Following Peri-Arterial Cuff Placement. *C57BL/6J and OPG$^{-/-}$ mice underwent peri-arterial femoral cuff surgery, and mice were culled 21 days post-surgery. (A) Representative images of neovessels as detected by CD31 staining (brown) in the femoral artery adventitia of OPG deficient and C57BL/6J wildtype mice following surgery. Negative control panel were tissues not treated with primary antibody (B) Number of neovessels were determined as CD31^{+} cells in the adventitia. Scale bars represent 50 µm. Data is represented as mean ± SEM, (n=4-5/group). OPG$^{-/-}$, osteoprotegerin deficient mice.*

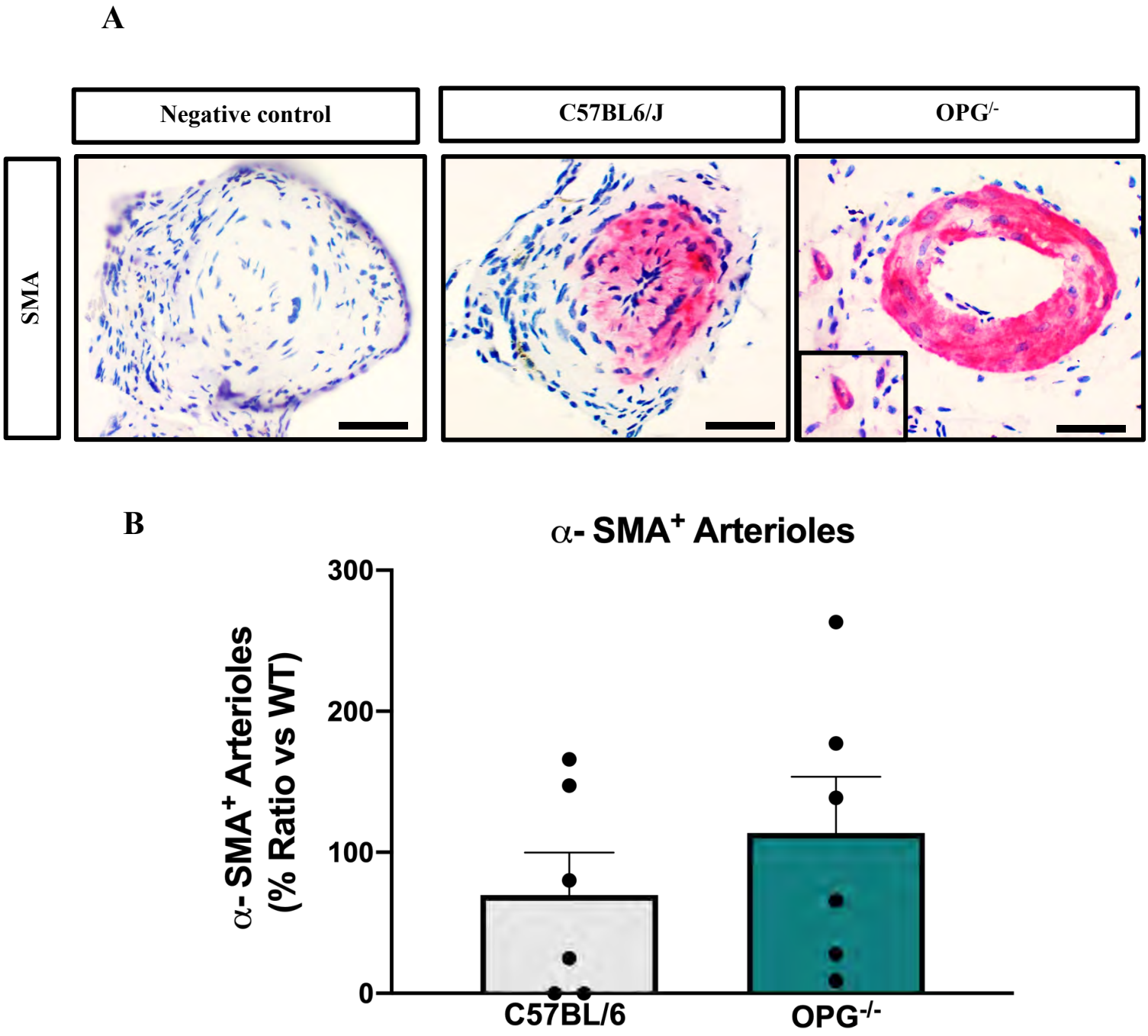

Figure 6.3: OPG Deficient Affects Adventitial Arteriole Formation Following Peri-Arterial Cuff Placement. *C57BL/6J and OPG$^{-/-}$ mice underwent peri-arterial femoral cuff surgery, and mice were culled 21 days post-surgery. (A) Representative images of arterioles identified by α-actin staining (pink) in the femoral artery adventitia of OPG deficient and C57BL/6J wildtype mice following surgery. Negative control panel were tissues not treated with primary antibody (B) Number of arterioles were determined as α-actin^{+} staining in the adventitia. Scale bars represent 50 µm. Data is represented as mean ± SEM, (n=6/group). OPG$^{-/-}$, osteoprotegerin deficient mice.*

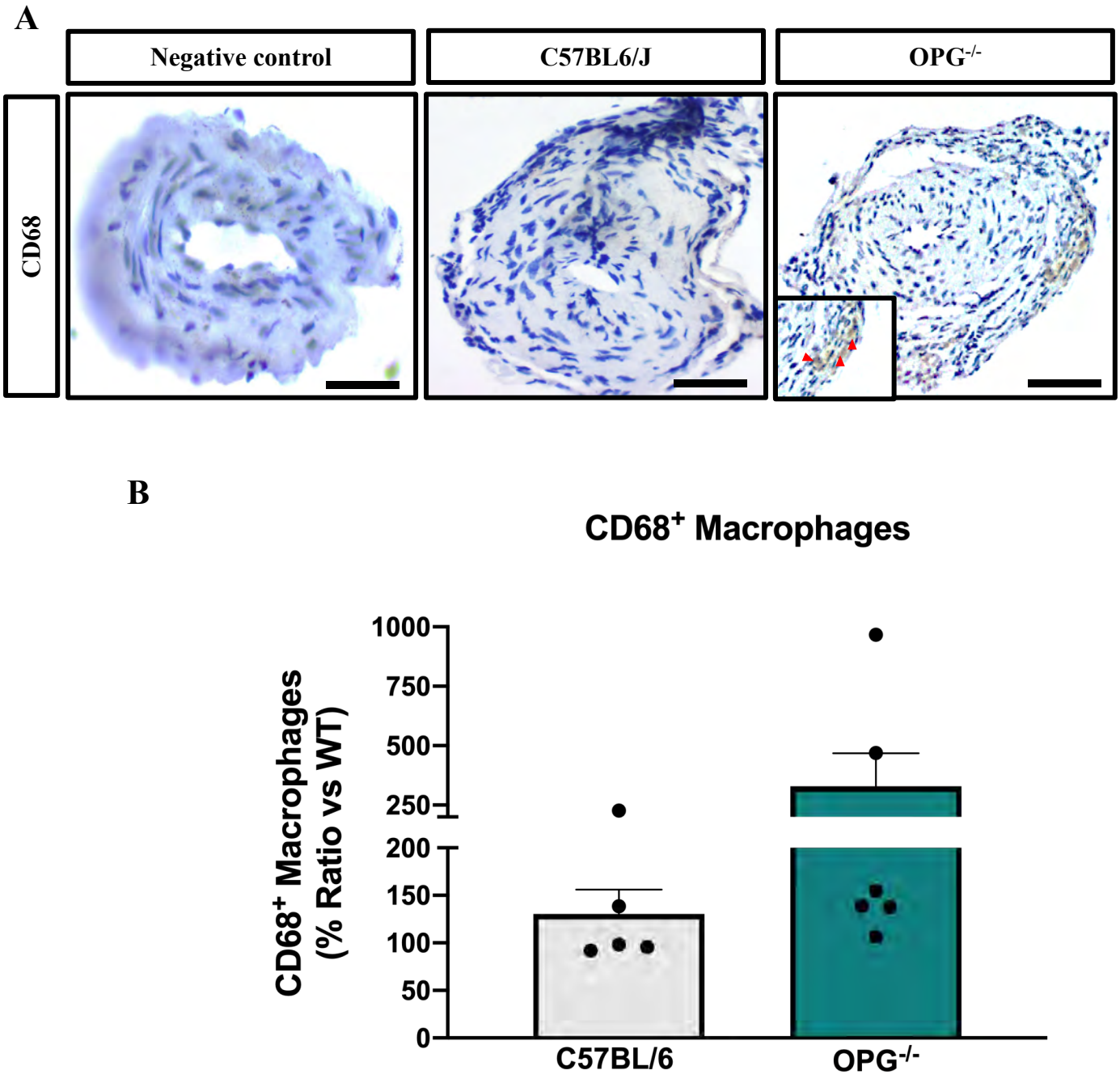

Figure 6.4: Macrophage infiltration is increased in OPG deficient mice following peri-arterial cuff surgery. *C57BL/6J and OPG$^{-/-}$ mice underwent peri-arterial femoral cuff surgery, and mice were culled 21 days post-surgery. (A) Representative images and quantification of CD68+ macrophages in the adventitia of cuffed arteries from WT and OPG deficient mice, normalised to WT C57BL/6J mice. Adventitial macrophages detected by CD68 staining (arrowheads). Negative control panel were tissues not treated with primary antibody. (B) CD68+ macrophages were quantified. Scale bars represent 50 µm. Data is represented as mean ± SEM, (n=5-6/group). OPG$^{-/-}$, osteoprotegerin deficient mice.*

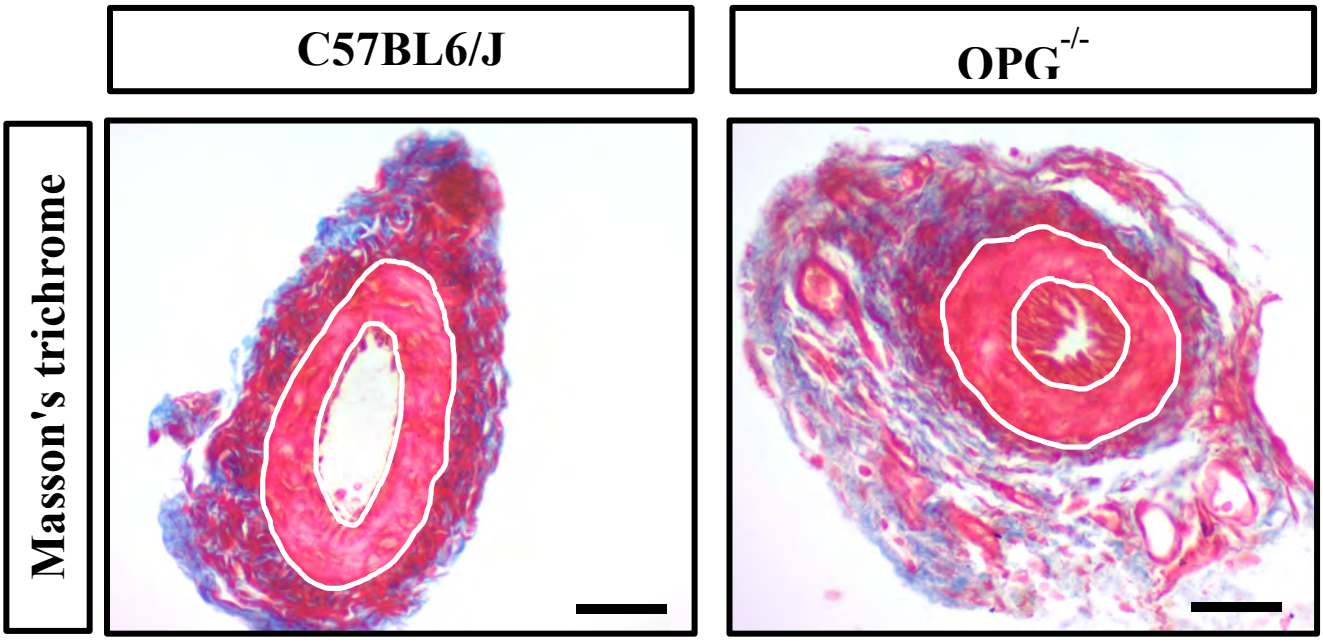

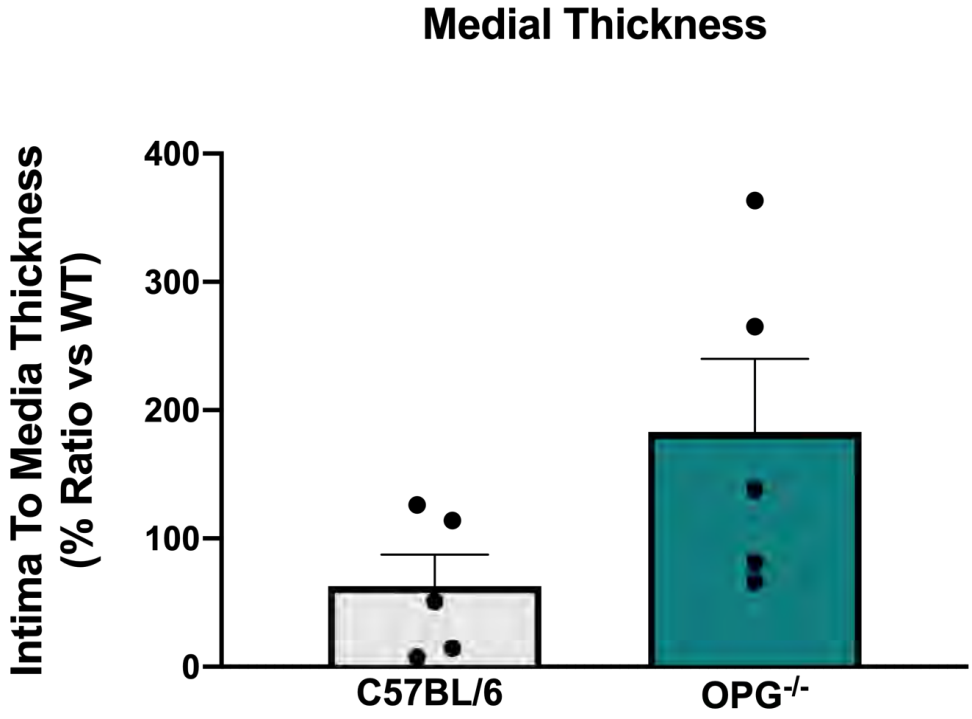

Figure 6.5: OPG Deficient Mice Display Greater Intima-Medial Thickness Compared to WT controls. *C57BL/6J and OPG$^{-/-}$ mice underwent peri-arterial femoral cuff surgery, and mice were culled 21 days post-surgery. Representative images and quantification of CD68+ macrophages in the adventitia of cuffed arteries from WT and OPG deficient mice, normalised to WT C57BL6/J mice. adventitial macrophages detected by CD68 staining (arrowheads). Scale bars represent 50 µm. Data is represented as mean ± SEM, (n=5/group). OPG$^{-/-}$, osteoprotegerin deficient mice.*

6.1.3 *Peri-Arterial Cuff Placement Differentially Regulates mRNA Expression of Key Inflammatory Mediators.*

Previously in chapter 5, in vitro data demonstrated that inflammatory stimulus TNF-α upregulated inflammatory and calcification markers in ECs. To assess this further in in vivo, mRNA was isolated from both non-cuffed and cuffed femoral arteries in wildtype C57BL/6J and OPG deficient mice following peri-arterial cuff placement, and inflammation markers were assessed.

Inflammatory-driven angiogenesis is primarily regulated by activation of the transcription factor NF-κB, which is responsible for the recruitment of monocytes and macrophages to the inflamed site. *Nf-κb (p65)* activity was downregulated in cuffed arteries of C57BL/6J mice compared to non-cuffed arteries following femoral cuff placement (24.82±11.85 vs 94.48±10.71, $P<0.05$, Figure 6.5A). *Nf-κb (p65)* activity was further downregulated in cuffed arteries of OPG deficient mice compared to non-cuffed arteries (71.99±6.34 vs 381.10±187.6, Figure 6.5A), though not statistically significant ($P<0.06$). Interestingly, as expected, cuffed arteries of OPG deficient mice exhibited greater expression of *Nf-κb (p65)* activity compared to cuffed arteries of C57BL/6J mice (71.99±6.34 vs 25.82±11.85, $P<0.01$, Figure 6.5A).

Analysis of *Cd68* mRNA expression showed significant increase in cuffed arteries compared to non-cuffed arteries of wildtype C57BL/6J mice (499.90±64.60 vs 112.80±34.19, $P<0.01$, Figure 6.5C). Consistent with this, OPG deficient mice showed increase in *Cd68* mRNA expression in cuffed arteries compared to non-cuffed arteries (2013±490.90 vs 341.50±122.20, $P<0.05$, Figure 6.5C). Furthermore, *Cd68* mRNA expression was markedly increased in cuffed arteries of OPG deficient mice compared to cuffed arteries of wildtype C57BL/6J mice (2013±490.90 vs 499.90±64.60, $P<0.05$, Figure 6.5B).

Monocyte chemoattractant protein (MCP1) is regarded as an important marker of inflammation as it is responsible for the transmigration of monocytes into the intima at sites of arterial injury. Following periarterial cuff placement on the femoral artery, *Mcp1* mRNA expression was significantly upregulated in cuffed arteries compared to non-cuffed arteries of wildtype C57BL6/J mice (349.30±64.30 vs 132.20±55.69, $P<0.05$, Figure 6.5E), an effect that was further increased in OPG deficient mice (1268±252.60 vs 222.90±91.16, $P<0.01$, Figure 6.5E). *Mcp1* expression was also upregulated in cuffed arteries of OPG deficient mice compared to cuffed arteries of C57BL6/J mice (1268±252.60 vs 349.30±64.30, $P<0.01$, Figure 6.5E).

Taken together, these findings show that periarterial cuff placement on the femoral artery drives inflammation, suggesting exacerbated effect in the presence of a high-calcific milieu.

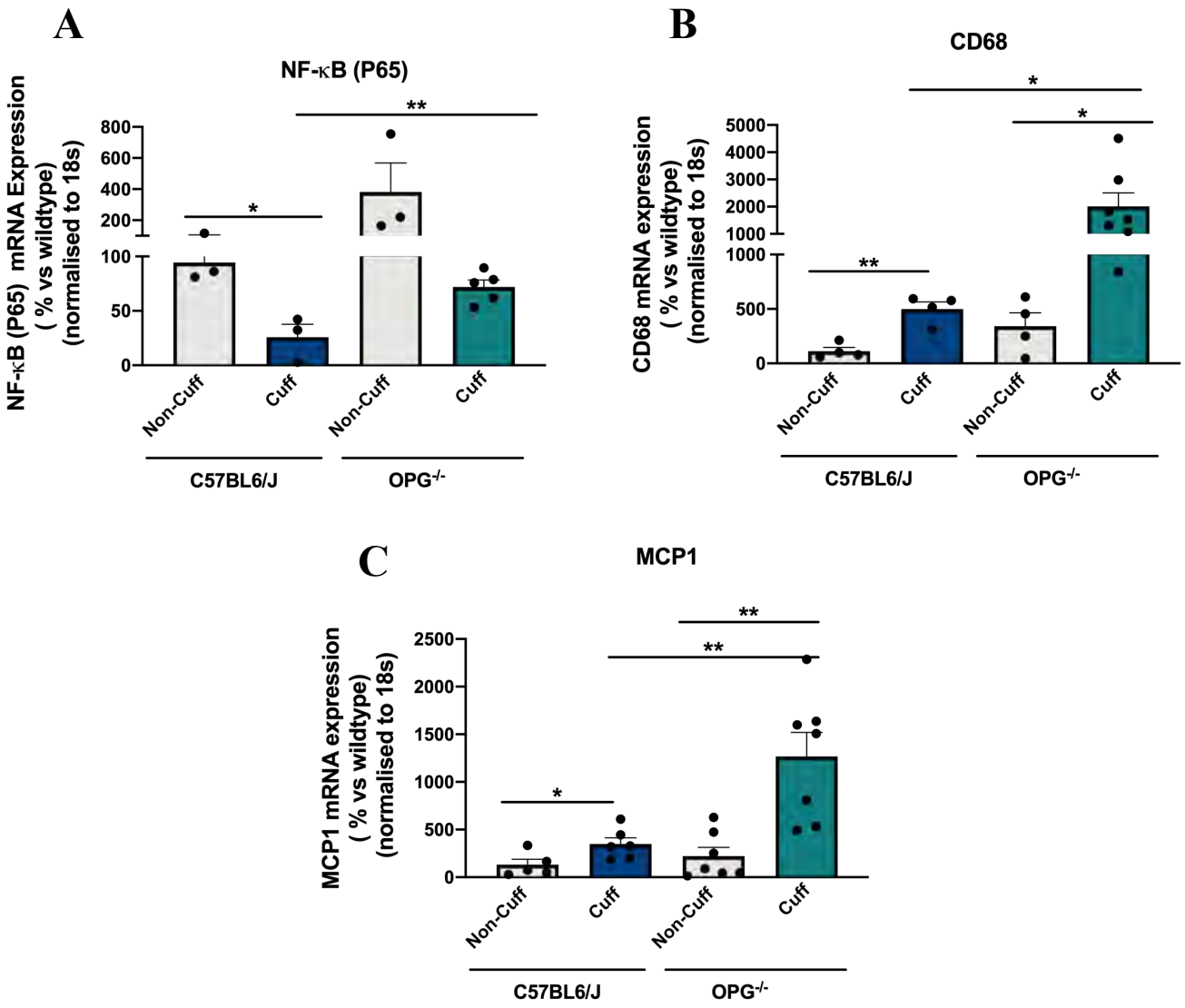

Figure 6.5: Peri-Arterial Cuff Placement Differentially Regulates mRNA Expression of Key Inflammatory Mediators. *C57BL/6J and OPG$^{-/-}$ mice underwent peri-arterial femoral cuff surgery, mice were culled 21 days post-surgery and Real-time PCR was performed to assess gene expression.* ***(A)*** *Nf-κb (P65),* ***(B)*** *Cd68,* ***(C)*** *Mcp1. Data is represented as mean ± SEM, *P<0.05, **P<0.01, (n=5-6/group). Statistical analysis was performed using a One-way ANOVA with Bonferroni's multiple comparison test and an unpaired student a Mann Whitney t-test. OPG$^{--/-}$: osteoprotegerin deficient mice, NF-kB (P65): nuclear factor kappa B P65 subunit, MCP: monocyte chemoattractant protein 1.*

6.2.4 OPG Deficiency Inhibits the Expression of Key Angiogenic Factors Following Peri-Arterial Cuff Placement.

To further understand the role of elevated calcium on inflammatory-driven angiogenesis, angiogenic factors Hif-1α, Vegfa and its receptor Vegfr2 mRNA levels were examined following peri-arterial cuff placement. There was no significant change in *Hif-1α* mRNA expression in cuffed arteries compared to non-cuffed arteries of wildtype C57BL/6J and OPG deficient mice (Figure 6.6A); with no change also observed when expressed as a ratio of cuffed versus non-cuffed (Figure 6.6B)

Similarly, there was no change in *Vefga* mRNA expression in wildtype C57BL/6J mice between non-cuffed and cuffed arteries, even when expressed as a ratio of cuffed: non-cuffed (Figure 6.6D). In addition, Peri-arterial cuff placement had no effects on *Vegfr2* mRNA expression in non-cuffed and cuffed arteries of wildtype C57BL/6J mice (Figure 6.6E); and the same response was also evident when expressed as a ratio of cuffed: non-cuffed (Figure 6.6F).

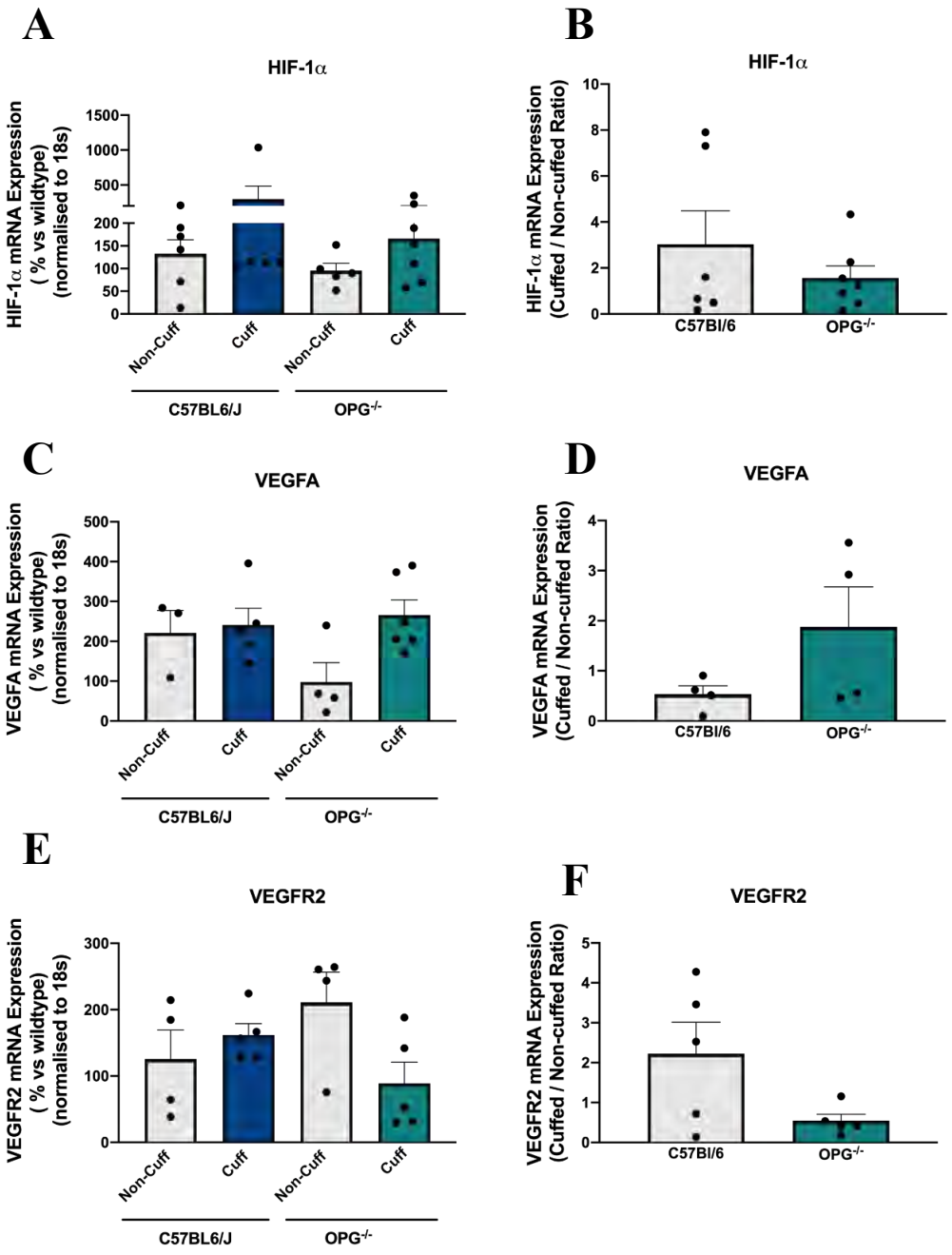

***Figure 6.6: OPG* Deficiency Inhibits the Expression of Key Angiogenic Factors Following Peri-Arterial Cuff Placement.** *C57BL/6J and OPG$^{-/-}$ mice underwent peri-arterial femoral cuff surgery, mice were culled 21 days post-surgery and Real-time PCR was performed to assess gene expression. (A-B) Hif-1α,, (C-D) Vegfa, (E-F) Vegfr2. Data is represented as mean ± SEM, (n=5-6/group). Statistical analysis was performed using a One-way ANOVA with Bonferroni's multiple comparison test and an unpaired student a Mann Whitney t-test. OPG$^{-/-}$: osteoprotegerin deficient mice, HIF-1α, hypoxia-inducible factor-1 alpha, VEGF, vascular endothelial growth factor, VEGFR, vascular endothelial growth factor receptor 2.*

6.2.5 OPG Deficiency Inhibits the Expression of Calcification Transcription Factors.

To better understand the role of calcification on inflammatory-driven angiogenesis, I examined the expression of key transcription factors Runx2 and RANKL following peri-arterial cuff placement. While there was no change in *Runx2* mRNA expression in cuffed vs non-cuffed arteries compared of C57BL/6J mice, cuff placement resulted in significant reductions in *Runx2* mRNA expression compared to non-cuffed arteries in OPG deficient mice (46.11±26.48 vs 186.90±36.22, $P<0.05$, Figure 6.7A). When expressed as a ratio of cuffed versus non-cuffed, this effect was lost (Figure 6.5 B).

Rankl expression was significantly downregulated in cuffed arteries of wildtype C57BL6/J compared to non-cuffed arteries (39.09±12.20 vs 241.50±72.11, $P<0.05$, Figure 6.7C), a response that was also present in OPG deficient mice (22.11±6.88 vs 540.60±195.50, $P<0.05$, Figure 6.7C. Additionally, *Rankl* mRNA expression was also reduced in OPG deficient mice compared to C57BL6/J mice when expressed as a ratio of cuffed: non-cuffed (Figure 6.5 D) though not statistically significant.

Altogether, the gene expression analyses indicate that while the placement of the cuff on the femoral arteries caused an inflammatory response evidenced by an increase in inflammatory markers, this did not cause any downstream activation of angiogenic markers. Interestingly expression of calcification markers was reduced suggesting that high calcium present in the OPG model may act alone to drive inflammation independently via other unknown alternative pathways.

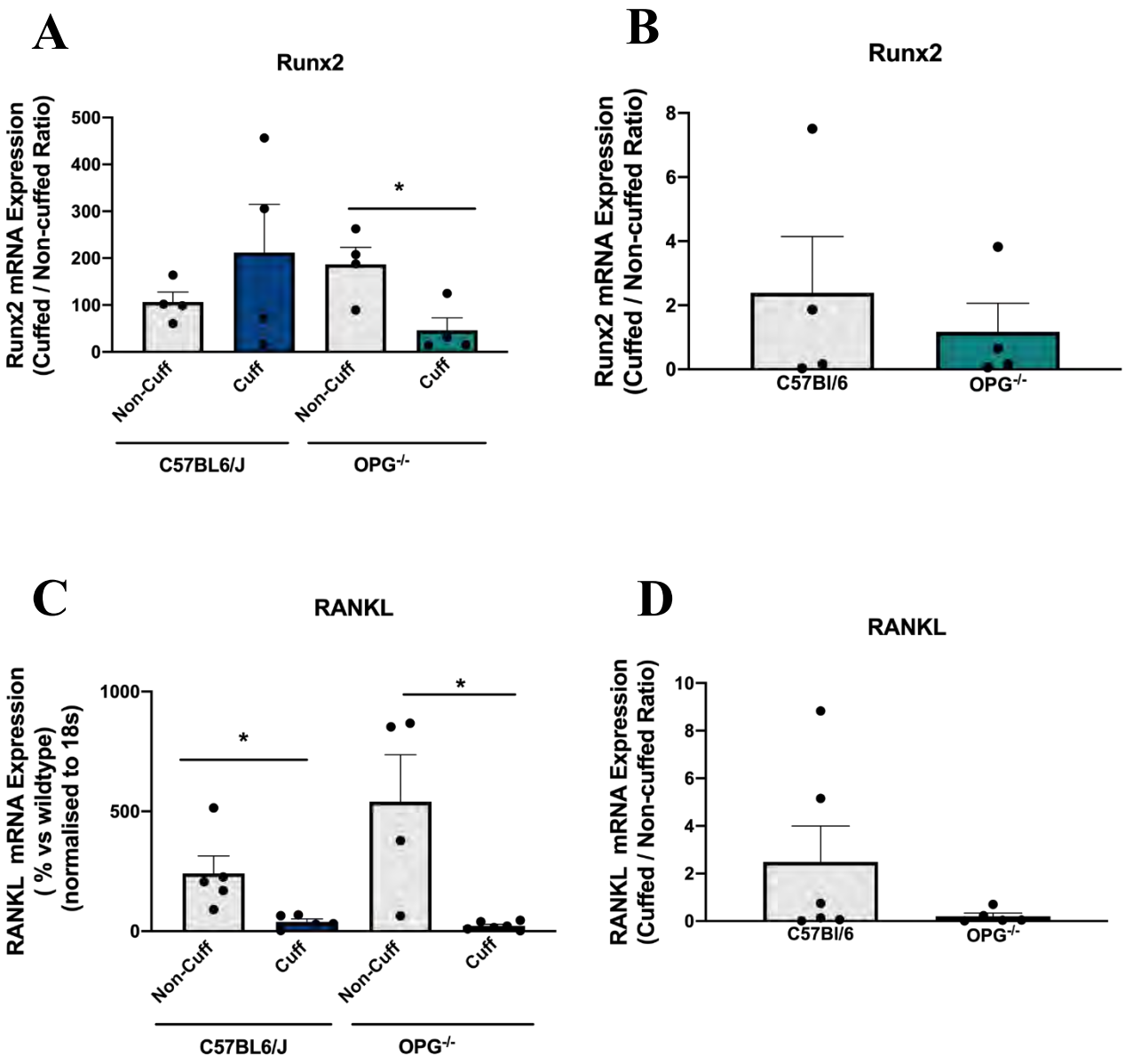

Figure 6.7: OPG Deficiency Inhibits the Expression of Calcification Transcription Factors. *C57BL/6J and OPG$^{-/-}$ mice underwent peri-arterial femoral cuff surgery, mice were culled 21 days post-surgery and Real-time PCR was performed to assess gene expression.* ***(A-B)*** *Runx2,* ***(C-D)*** *Rankl. Data is represented as mean ± SEM, (n=5-6/group). Statistical analysis was performed using a One-way ANOVA with Bonferroni's multiple comparison test and an unpaired student a Mann Whitney t-test, *P<0.05. OPG$^{-/-}$: osteoprotegerin deficient mice, Runx2: runt related transcription factor, RANKL: receptor activator Nuclear Factor Kappa B.*

6.3 Discussion

The present study was designed to further understand the role of calcification on inflammatory-driven angiogenesis in vivo. While calcification is known to be associated with inflammation very little is known regarding its effect in driving the pathological form of angiogenesis. It is important to note that no previous literature has reported any known role for the regulation of calcification genes during inflammation. However, there are evidence for the association of inflammation in vascular calcification. Chronic inflammation is a central factor in soft tissue calcification and is a common site for atherosclerotic calcification in mice[222]. Oxidation of lipids from atherosclerotic plaques can induce RANKL expression to drive calcification[223, 224]. Therefore, based on this evidence, calcification may therefore contribute in regulating inflammatory-driven angiogenesis.

The peri-arterial cuff model was used to stimulate inflammatory-driven angiogenesis in OPG and C57BL/6J mice. This murine model involved placing a cuff around the femoral artery to stimulate a localised inflammatory response which triggers the recruitment of macrophages and the release of pro-inflammatory cytokines and growth factors that drive increased neovessel formation at the site of injury. To assess angiogenesis, histological staining was performed to measure $CD31^+$ endothelial cells (neovessels) and α-actin+ for smooth muscle cells (arterioles), which represent early and late neovessels. Cuff placement caused a reduction in the number of neovessels within the adventitial space, while increasing the number of arterioles in the adventitia in OPG deficient mice compared to wildtype C57BL/6J mice (Figure 6.8). It is important to also note that cuff placement had no effect in regulating pro-angiogenic factor expression for HIF-1α or VEGFA, and may therefore demonstrate differential effects of high calcium on inflammatory-driven angiogenesis

Macrophages play a key role in the regulation of inflammatory-driven angiogenesis and are known to secrete pro-angiogenic cytokines and growth factors to regulate this process. In this study, placement of the peri-arterial cuff around the femoral artery stimulated an increase in inflammation as demonstrated by increased *Cd68* and *Mcp1* mRNA expression, responses that were see in both wildtype C57BL/6J mice and further increased in OPG deficient mice Figure 6.8); highlighting that a calcification milieu may drive a greater inflammatory response. While there was increased pro-inflammatory marker expression, there was also concomitant decrease in the expression of calcification markers Runx2 and Rankl in cuffed arteries of OPG knockout mice. This effect could be attributable to other mechanisms independent of inflammation and is an area that requires further investigation. Therefore, it is likely that the mechanism by which cuff placement exerts its inflammatory effects may be occurring via modulation of the NF-κB signalling pathway and may explain the results observed in this study.

VEGFA is an important regulator of angiogenesis under both ischemic and inflammatory conditions, as it contains both hypoxia (HIF-1α) and inflammatory (NF-κB) response elements in its promoter region. As a result, VEGFA can drive both physiological ischemia-driven angiogenesis and pathological inflammatory-driven angiogenesis, thus allowing conditional regulation of the two processes. In this study, when key pro-angiogenic markers were assessed, cuff placement elicited no significant change in *Hif-1α* and *Vegfa* mRNA expression in OPG knockout mice, a trend that was also observed in wildtype C57BL/6 J mice. This response in pro-angiogenic marker expression may suggest increased regulation of pathological angiogenesis, though a greater sample size is required to fully confirm this response. Interestingly, *Nf-κb (p65*) mRNA expression was decreased in cuffed arteries of both C57BL6/J and OPG deficient mice following cuff placement, a response that

was unexpected. This decrease in *Nf-κb (p65)* expression in cuffed arteries of OPG deficient mice may reflect alternative mechanisms that may be suppressing *Nf-κb* activation during inflammation, thus warranting further studies.

Additionally, RANKL signalling involves activation of NF-κB located downstream of the RANK receptor. This is known to result in the activation and initiation of osteogenic differentiation, and release of transcription factor Runx2 which drives vascular calcification. In this study, decreased *Nf-κb* signalling coincides with decreased *Rankl* and *Runx2* expression in cuffed arteries of OPG deficient mice. Therefore, potentially, the inhibition of *Rankl* may subsequently inhibit the expression of inflammatory marker *Nf-κb (p65)*, which suggests other downstream pathways to be involved.

As previously stated in chapters 4, the same limitations also apply to this study. OPG deficient mice have been validated as a vascular calcification model and therefore it cannot be discounted that the response seen is due to the loss of OPG itself. Furthermore, a small sample size is another limitation, and thus increasing sample size will increase statistical significance in future studies.

In conclusion, data from this study has provided evidence that high calcification milieu may help drive pathological inflammatory-driven angiogenesis, a response that isn't favourable as it exacerbates plaque progression in atherosclerosis settings.

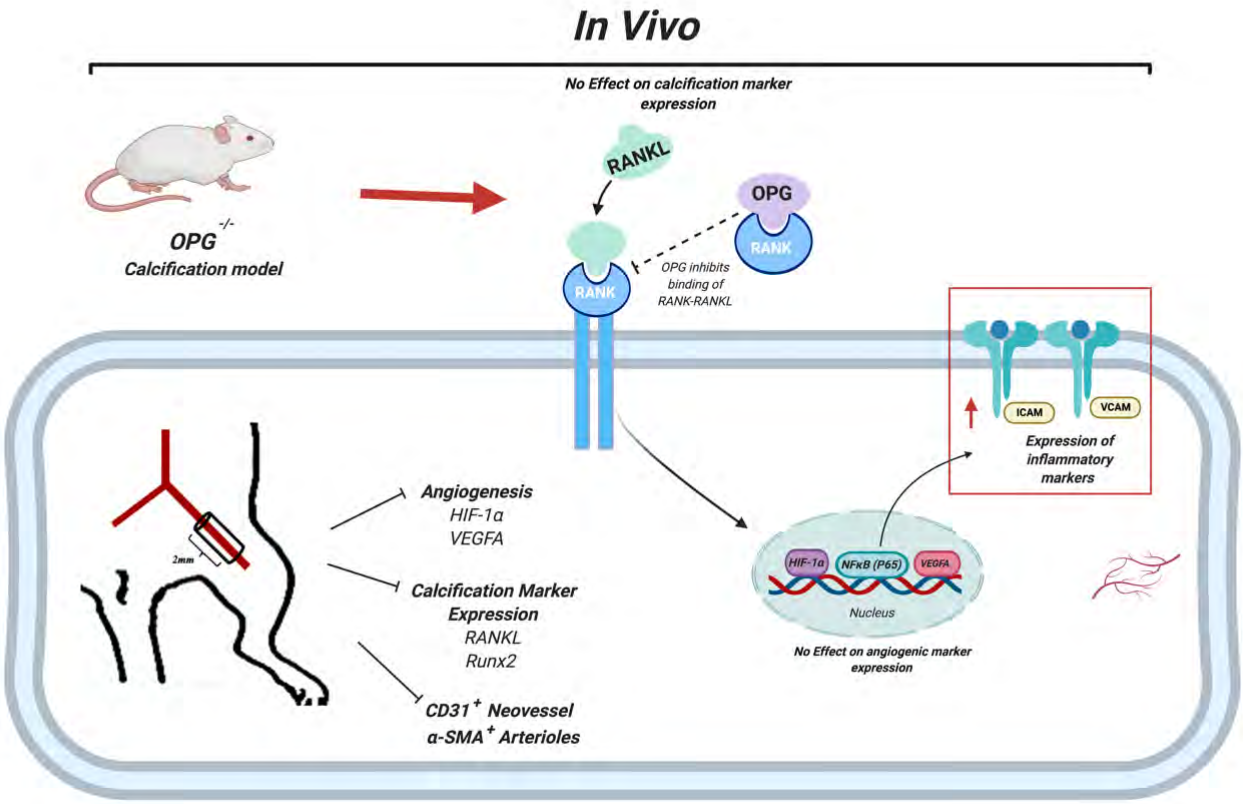

Figure 6.8: Summary Schematic for the Effect of High Calcium on Inflammatory-Driven Angiogenesis Following Peri-Arterial Cuff Placement

CHAPTER 7:

GENERAL DISCUSSION

7.1 Introduction

PAD and CAD are increasingly recognized as two major causes of mortality, affecting approximately 200 million individuals worldwide[33]. During the course of disease progression, reduced tissue perfusion of the limbs results in ischemic ulcerations and gangrene formation; which increases the risk of developing limb amputations, also known as critical limb ischemia (CLI) [9]. In response to ischemia, the body works to compensate this via increasing the development of collateral vessels to bypass and alleviate stenosis, and thus restore blood flow to preserve tissue function, a process that is regulated by both hypoxia and inflammatory processes. However, the formation of collateral vessels is dependent on the environment. In patients with PAD, the ability to form collateral vessels is suboptimal or impaired due to many factors, one of them being the presence of calcification within the vessel wall[15, 33, 34, 225, 226]. As a result, most treatment options for patients suffering from PAD are limited to lifestyle and surgical interventions which are not always effective especially in severe/chronic cases where limb amputations are required. Therefore, it is crucial to understand the mechanisms to promote new collateral vessel formation, as this will lead to potential non-surgical therapeutic approaches to treat patients with PAD.

7.2 Purpose of Thesis and Summary of Results

This study sought to understand how calcification regulates essential processes of neovascularisation. In endothelial cells the effect of calcium/phosphate on angiogenesis[172, 227], has demonstrated conflicting results with one study reported to increase proliferation[66], while inhibiting proliferation in another[65.] Because of the myriad of effects that both calcium and phosphate have in regulating physiological processes and cell signalling within the body, it

remains unclear the exact mechanism by which calcium/phosphate may regulate angiogenesis in ECs. In an attempt to understand the mechanisms driving EC-angiogenesis in response to calcification, in vitro studies were conducted to investigate the effect of high calcium on two mechanisms known to regulate neovascularisation: ischemia-driven angiogenesis and inflammatory-driven angiogenesis. In vivo studies utilised a pre-clinical calcification model using OPG knockout mice to mimic a high calcific environment against wildtype C57BL6/J mice. These mice were subjected to two models of angiogenesis namely the hind-limb ischemia model to induce hypoxia-driven angiogenesis, and the peri-arterial femoral cuff model to induce inflammatory-driven angiogenesis.

Based on data from Chapter 3, treatment with calcification medium (CM) in vitro significantly reduced key functional angiogenic assays when subjected to normoxic conditions but had very little to no effect in hypoxic conditions. Mechanistically, in vitro studies demonstrated that CM downregulated angiogenesis in ECs, via reductions in tubule formation and cell migration; whilst mitigating the phosphorylation of key pathways for eNOS, P38 MAPK, and ERK1/2 signalling that are known to drive angiogenesis **(Figure 7.1)**. Furthermore, in vivo data presented in Chapter 4 demonstrated significant impairment of ischemia-driven angiogenesis following hind-limb ischemia surgery in our calcification model using OPG deficient mice. The negative effects of high calcium were further demonstrated as $OPG^{-/-}$ mice experienced severe impairment in blood flow reperfusion following HLI surgery, with decreased capillary and neovessel formation. $OPG^{-/-}$ mice also developed necrosis and spontaneous foot amputations following HLI, and as a result had impaired tissue and limb function which was exacerbated with age **(Figure 7.1)**.

In vitro data presented in Chapter 5 showed that stimulation of ECs with TNF-α resulted in CM-induced upregulation in key inflammatory markers of MCP1, ICAM-1,

VCAM-1 and NF-κB (P65). These results coincided with significant upregulation of key calcification markers of BMP2, Runx2 and ALP **(Figure 7.2)**. In vivo data from Chapter 6 demonstrated that following peri-arterial femoral cuff placement, there was no effect on inflammatory-induced angiogenesis in OPG deficient mice compared to controls. Cuff placement however induced the expression of inflammatory markers *Nf-κb (p65)* and *Mcp1*; whist decreasing both *Runx2* and *Rankl* gene expression in OPG deficient mice relative to controls **(Figure 7.2)**. Overall, the data presented in these chapters highlights the idea that high calcium may drive inflammation alone independent of effects on angiogenesis.

Physiological angiogenesis is a crucial process that occurs post-ischemia following a myocardial infarct, stroke or in PAD. Impairment in pro-angiogenic pathways can exacerbate and lead to pathological form of angiogenesis, that occurs in atherosclerosis and cancer tumour growth. Following assessment of both forms of angiogenesis, collectively, this data has demonstrated negative regulation of ischemia-driven angiogenesis with a calcification milieu both in vitro and in vivo; while having very little effect in regulating inflammatory-driven angiogenesis.

7.3 Effect of High Calcium on The Endothelium

This study utilised endothelial cells as the primary model to study angiogenesis in vitro. These cells were chosen because as they are the primary cells that line the vessel wall, they are responsible for regulating key angiogenic processes of proliferation, migration and tubule formation; whilst also mediating a range of reparative responses including inflammation in response to injury[56]. ECs are the first cell targets to be involved following ischemia-induced responses in different organs, and their functions are immediately impaired by ischemia[175]. It is important to note that this is the first study that has assessed the direct role

of calcium-phosphate on EC angiogenesis. Majority of studies relating to calcification have been conducted on VSMCs as these cells are capable of osteoblast-differentiation[98]. Furthermore, to date, only one study has evaluated the role of endothelium in VC, which involved the knockdown of calcification inhibitor matrix-gla protein. This study reported that the vascular endothelium may act as a source of multipotent cells that contribute to VC in states of high BMP activity[228]. Furthermore, based on the in vivo data, it would be interesting to assess OPG knockdown in endothelial cells to fully to confirm the results obtained from this study and to see whether the absence of OPG a compounding for the regulation of angiogenesis, as OPG has been shown to drive EC angiogenesis in published in vitro studies[153].

7.4 The Effect Calcification on Hypoxia-Driven Angiogenesis

Results from the in vitro studies demonstrated that hypoxia had no effect in driving angiogenic processes of cell viability, migration, or tubule formation. CM however induced upregulation of pro-angiogenic markers HIF-1α and VEGFA in both normoxia and hypoxia conditions, despite reduced angiogenesis. It is plausible that this effect is dependent on the incubation time and exposure to hypoxia, as in this study, cells were incubated in hypoxia for only 4 hours. In previous studies, human umbilical vein endothelial cells (HUVECs) exposed to hypoxia showed resistance to cell death with only a 2% reduction in viability at 24 h and 45% reduction in viability at 48 h[187]. Studies in chapter 3 showed that hypoxia had no effects on EC viability, and based on this evidence, future studies should be conducted at longer time points such as 48 h.

The interplay between calcium (Ca^{2+}) and reactive oxygen species (ROS) signalling pathways is an important determinant in normal physiology and in several pathophysiologies.

Ca^{2+} modulates reactive oxygen species (ROS) homeostasis by regulating ROS generation in both the mitochondria and cytosol[229]. In addition, calcium phosphate is known to regulate cell signalling in the body and are coupled with oxygen availability. During hypoxia, the reduction of oxygen molecule results in the formation of reactive oxygen species (ROS). So it is likely that decreased O_2 via hypoxia may affect the cells ability to function and thus affect their ability to regulate calcium signalling in order to drive cellular processes. Furthermore, ROS have been reported to be important in processes of physiological ischemia-induced angiogenesis and wound healing in vivo. In one study, mice lacking Superoxide dismutase displayed significant inhibition in ischemia-induced increase in blood flow recovery, collateral vessel formation, and capillary density[230]. This data support findings from our study where eNOS phosphorylation is significantly decreased in vitro following incubation with calcification medium. However, in futures, eNOS activity could be further investigated in our in vivo model of calcification to fully understand these interactions.

In angiogenesis, ROS production stimulates VEGFA expression to augment angiogenesis in endothelial cells[231]. There are various sources involved in producing ROS in ECs, including xanthine oxidase, NADPH oxidase, mitochondrial electron transport chain, eNOS uncoupling and cytochrome P450. During angiogenesis, eNOS is important and is located downstream of the HIF-1α signalling pathway and helps to enhance angiogenesis following an ischemic insult. In this study, CM treatment significantly mitigated eNOS phosphorylation in ECs compared to untreated cells in both normoxia and hypoxia conditions, despite an increase in HIF-1α in normoxic conditions. This reduction in eNOS expression suggests a downstream signalling effect of high calcium in supressing angiogenesis. Since calcification is highly associated with aging, as is the role of oxidative stress - the correlation between VC and vascular aging has been well established. Aging induces mitochondrial dysfunction and augments ROS production, which plays an important

role in regulating cell signalling pathways during senescence and contributes to extracellular vesicle formation during calcification[232]. ROS production has opposing effects in calcification, as oxidative stress stimulates calcification by activating specific signalling cascades to increase Runx2 transcription factor expression. Interestingly, Runx2 expression is maintained by ROS production, particularly by hydrogen peroxide[233]. Furthermore, BMP2 activates NADPH oxidases to increase VC. Therefore, based on results obtained from this study where CM reduces eNOS phosphorylation, this suggests the involvement of ROS and potentially alternate sources of ROS including NADPH oxidase, xanthine oxidase and mitochondria should be investigated to fully understand their role in calcification-induced angiogenesis[232].

The hindlimb ischaemia model employed in Chapter 4 is a well-established model of ischaemia-driven neovascularisation that is commonly used to study PAD in vivo; and allows both angiogenesis and arteriogenesis to be investigated. Data from Chapter 4 demonstrated that a calcification milieu caused striking reductions in revascularisation in OPG deficient mice compared to controls in an 8wk old cohort, as illustrated by reductions in CD31 positive neovessels in the gastrocnemius muscle of these mice. Surprisingly, there was significantly increased smooth muscle alpha actin-positive arterioles in the gastrocnemius muscle of OPG deficient mice following HLI. This increase may demonstrate late stage remodelling or arteriogenesis, as arterioles demonstrate more mature vessels compared to those seen in angiogenesis. Furthermore, OPG deficient mice demonstrated significant increases in circulating calcium and ALP levels relative to wildtype C57BL6/J mice. Moreover, because both PAD and calcification are age-associated diseases, $OPG^{-/-}$ mice were aged and angiogenesis was assessed. Aged $OPG^{-/-}$ mice demonstrated significantly exacerbated effects as demonstrated by the doppler perfusion data, where there was impairment in angiogenesis and revascularisation following HLI. $OPG^{-/-}$ mice surprisingly self-amputated following HLI,

which was associated with decreased limb function and tissue ischemia. However due to the clinically reported effects of OPG[139, 143, 146, 234] , it remains unclear whether the response observed in this study is due to the absence of OPG or the increased calcium in this OPG model; an observation that needs to be investigated further.

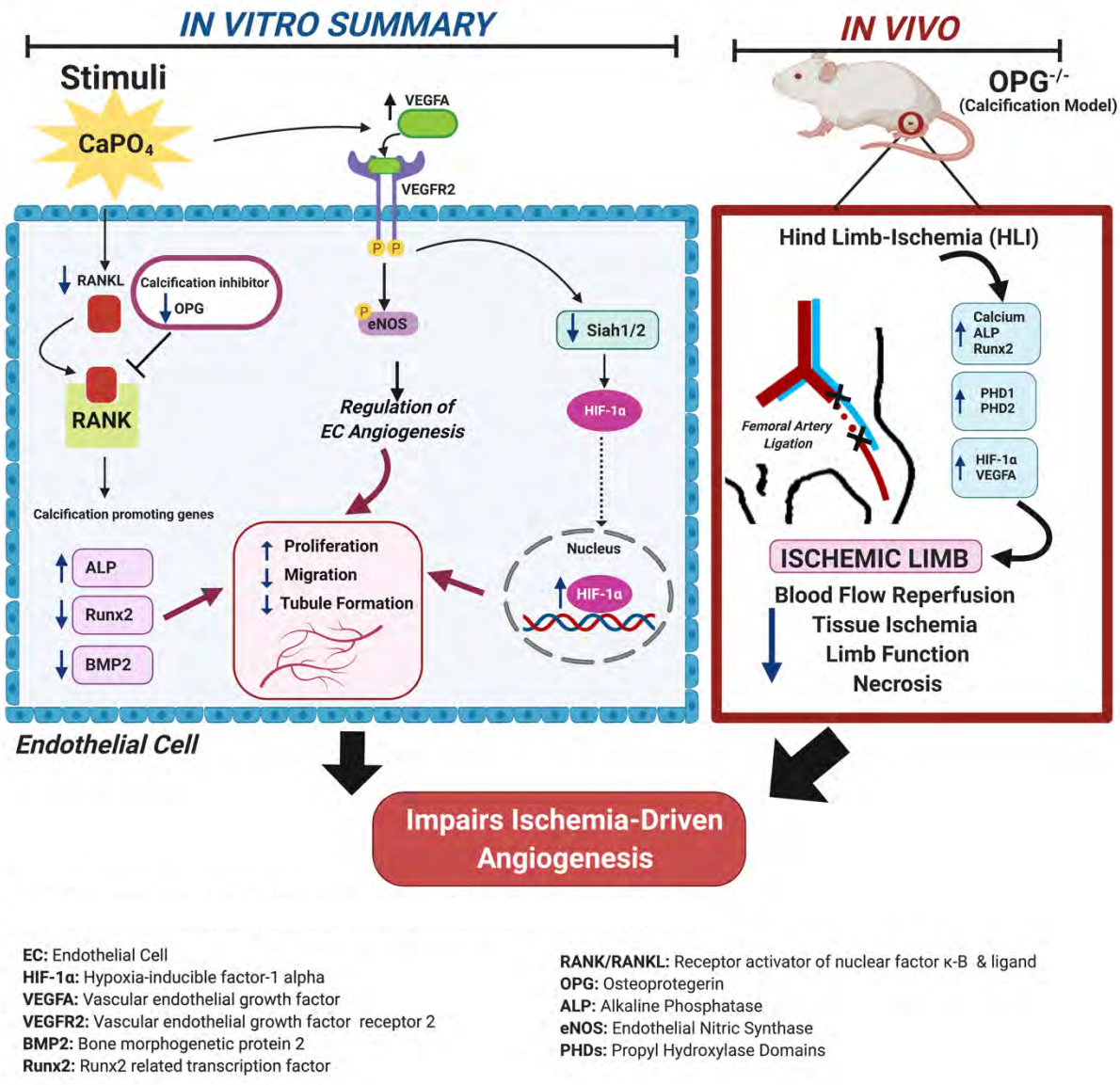

Figure 7.1: Summary schematic illustrating the effects of calcification stimuli on ischemia-driven angiogenesis.

7.5 The Effect Calcification on Inflammatory-Driven Angiogenesis

The pathophysiology of PAD is often considered secondary to atherosclerosis and is characterised by fatty plaque build-up within the peripheral arteries of the vessel wall. In the vessel wall there are two types of calcifications; intimal calcification which is associated with atherosclerosis alongside lipid deposition and inflammation; and medial calcification that occurs independently of atherosclerosis in the medial layer due to differentiation of VSMCs towards osteoblast-like cells. Numerous risk factors such as smoking, high cholesterol, oxidative stress, aging and high blood pressure drive the process of calcification and inflammation in atherosclerosis.

In Chapter 5, ECs treated with CM and TNF-α exhibited increased ALP activity and calcium secretion in cells; as well as increased expression of inflammatory markers of ICAM-1, VCAM-1, MCP1 and transcription factor NF-κB (P65); a response that coincided with increased cell migration, cell viability and tubule formation following treatment with both CM and TNF-α **(Figure 7.2)**. This was also associated with increased expression of calcification markers BMP2 and Runx2. While very little is known regarding the effect of calcification on ICAM-1, VCAM-1 and MCP1, because of their well-established role in plaque atherogenesis it is likely that calcification may regulate their expression in inflammatory-driven angiogenesis.

During early atherogenesis, a network of microvessels within the adventitial and outer medial layer stimulate neovascularisation to deliver oxygen and nutrients to support plaque growth, resulting in expansion of the vaso vasorum. In this study, CD31 neovessels were non-significantly decreased following cuff placement in OPG mice compared to C57BL6/J mice.

Previously, data by Collett and Canfield[24,] reported that differentiation of VSMCs is brought about by an inflammatory stimulus, which triggers activation of specific osteogenic signals such as BMP2. This subsequently stimulates differentiation of VSMCs into osteoblast-like cells, a well proposed mechanism of vascular calcification [61, 62, 157]. In addition, studies have proposed OPG as a marker of endothelial dysfunction during inflammatory disease processes**.** Previous findings reported that OPG induced the expression of intercellular adhesion molecules, such as VCAM-1 and E-selectin in ECs, and promoted leukocyte adhesion, an early step in EC dysfunction, thus supporting a pro-inflammatory role for OPG[184, 205]. In a different study, treatment of HUVECs with 5 ng/ml of TNF-α over 24 h increased OPG expression[235]. In this study, data from Chapter 5 demonstrated that OPG expression remained unchanged when cells were stimulated with TNF-α alone compared to untreated cells; however, when cells were co-incubated with both TNF-α and calcification medium, OPG expression was significantly downregulated. There currently lies much controversy regarding the role of OPG, particularly since elevated OPG is considered a predictive biomarker of cardiovascular disease mortality and morbidity[137, 149, 153, 235].

Inflammatory-driven angiogenesis is primarily regulated by the NF-κB signalling pathway. Moreover, VEGFA is also a regulator of inflammatory-driven angiogenesis as it contains a NF-κB response element in its promotor region. Data from Chapter 5 demonstrated no change in expression of VEGFA, with TNF-α and calcification medium co-incubation, while NF-κB (P65) protein expression was increased **(Figure 7.2)**. Since VEGFA can promote both ischemia and inflammatory-driven angiogenesis, HIF-1α expression was also assessed with calcification medium treatment, and no change was observed. In other studies, with smooth muscle cells, TNF-α enhanced *HIF-1α* mRNA expression levels in both normoxic and hypoxic conditions[236]. Additionally, using human adenocarcinoma cells, TNF-α treatment

increased HIF-1α expression, whilst also inhibiting cell viability[191]. Furthermore, it was previously shown that TNF-α induced accumulation of HIF-1α in normoxic cells requires activation of NF-κB pathway[237]. To date, there are no studies demonstrating the expression of HIF-1α in response to calcification stimulus with or without inflammatory stimuli, thus further studies are needed to fully understand the molecular mechanisms driving this response.

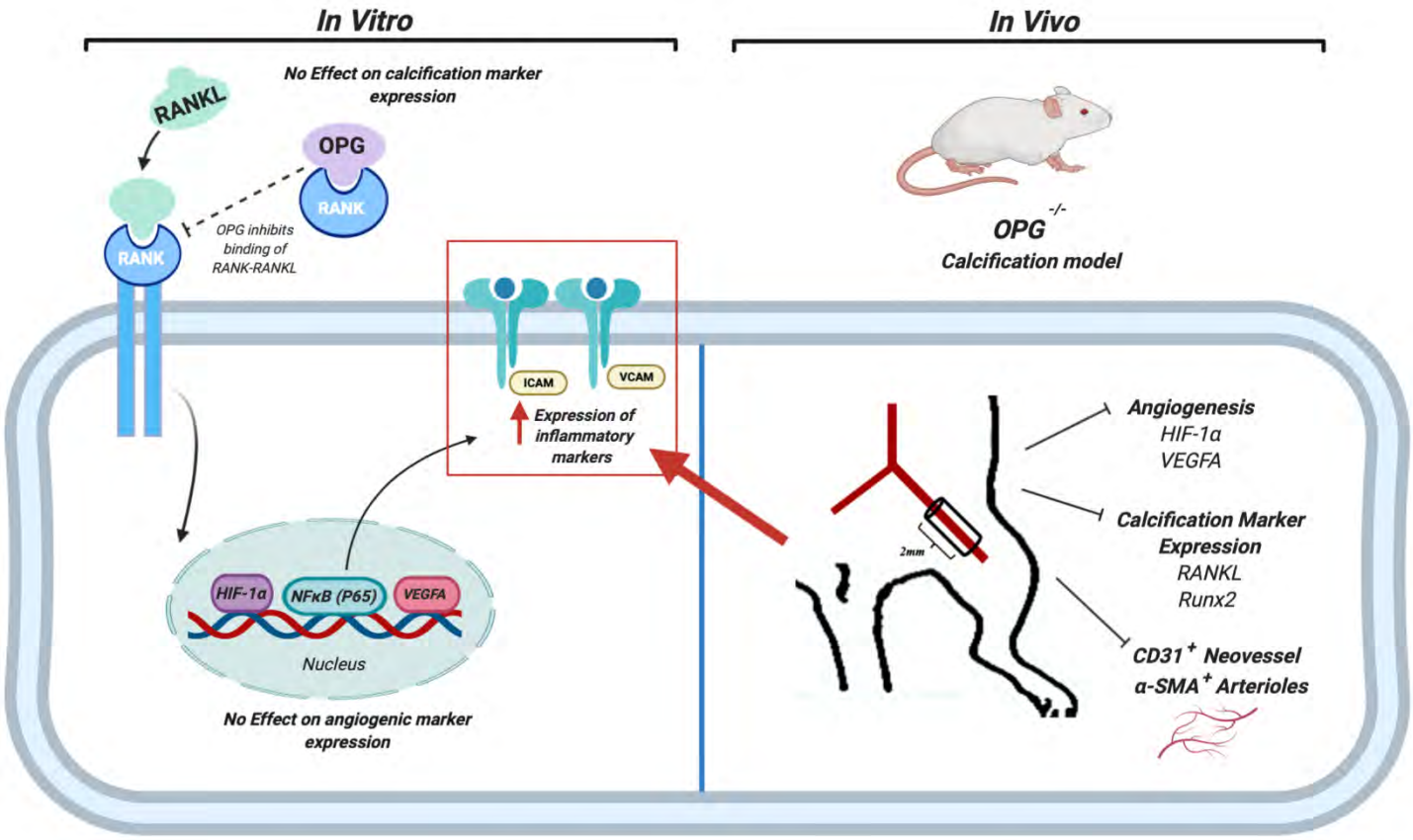

Figure 7.2: Summary schematic illustrating the effects of calcification stimuli on inflammatory-driven angiogenesis.

7.6 Future directions

Damage to the endothelium is one of the earliest responses in the development of CVD, and occurs due to changes in vasoactive mediators which promote vasosonstricion[189]. Given the organisation of the vessel wall with the endothelium being in close proximity to the medial layer containing smooth muscle cells, crosstalk between ECs and VSMCs contributes to the progression of disease. The mechanisms accounting for the link between angiogenesis and calcification are multifactorial as these processes involve the coordinated interplay of many different cell types expressed within the vessel wall including ECs, VSMCs, pericytes, circulating and resident osteoprogenitors, as well as osteoblastic cells. The three known primary cell drivers of angiogenesis are ECs, VSMCs and pericytes [23, 24, 238]. While these studies utilised ECs, the other cells involved could also be utilised for future studies in vascular calcification. As discussed earlier, endothelial cell migration and proliferation are critical processes required for angiogenesis. A subpopulation of SMCs have been identified within the vessel wall and termed calcifying vascular cells (CVCs), accounting for approximately 20-30% of the total VSMC population[61, 80 239]. These cells have high expression of ALP and are able to calcify and form large nodules when maintained in culture for extended periods of time. CVCs also have the potential for undergoing multiple mesenchymal lineages for osteoblasts[61]. Furthermore, it has been suggested that osteogenic signals or osteogenic precursor cells may be delivered into the arterial wall by collateral vessels that develop in response to inflammatory signals; a theory that is based on the known relationship between angiogenesis and the progression of atherosclerotic plaques. Therefore, it has been proposed that the development of collaterals within the adventitia during atherosclerosis allows migration of multipotent adventitial myofibroblasts and other cells types including pericytes into the intima and medial layer of the vessel wall, where they are able to differentiate into osteoblast-like cells through signalling mechanisms regulated by BMP2, Runx2 and OPG[33].

Pericytes are resident cells that are expressed in the vessel wall that are involved in regulating angiogenesis. Pericyte migration and activation is an important step in the later stages of angiogenesis as demonstrated in Figure 1.3. Pericytes are often proposed to be mesenchymal progenitor cells that are capable of undergoing cell differentiation towards other several lineages including osteogenic (osteoblasts) and chondrogenic (chondrocytes); and are therefore proposed to be involved in regulating vascular calcification processes[239]. Furthermore, pericytes also produce nodules of cells and ECM in long-term culture, which contain calcification markers of type I collagen, OPN, MGP and osteocalcin. Therefore based on this , pericyte activation within the vessel wall may provide a source of osteoprogenitors and thus help drive VC[61]. Based on results obtained from this study, I suspect that calcium phosphate may regulate angiogenesis by mechanisms other than directly stimulating endothelial cells. Co-culture experiments with other cell types such as pericytes, VSMCs and/or endothelial progenitor cells would be beneficial to fully understand any potential autocrine/paracrine effects of calcium-phosphate-induced angiogenesis.

The involvement of Tie-2 and angiopoietin have been suggested to play potential roles in driving calcification. This is because elevated expression of growth factors such as VEGFA and angiopoietins are associated with increased cholesterol and OPG, which are two known mediators of inflammation[189]. Its therefore suggested that there is possible binding of VEGFR1/2 and Tie-2 to ECs which may then drive increased calcification. Future studies could therefore be employed to study the relationship between Tie-2 in driving angiogenesis. In addition, it would be interesting to cross OPG mice with Tie-2 mice to further examine the specific effects of calcification on endothelial cells.

In Chapter 3, CM had differential effects on EC angiogenesis, where HIF-1α was upregulated with CM treatment, despite upregulation of calcification marker Runx2. Because of the role of Runx2 in its ability to increase HIF-1α expression, this provides a plausible

explanation for the regulation of HIF-1α . To fully understand this interaction, future studies performing siRNA knockdown for Runx2 in ECs following CM treatment could offset the possibility of early compensatory mechanisms for HIF-1α. Furthermore, it would be beneficial to measure intracellular calcium for internalisation into the cells, by measuring calcium sensing receptor activity. Other future directions for this study could involve performing ex-vivo experiments to study angiogenesis in OPG mice. This would involve performing aortic ring assays or Matrigel plug assays to assess angiogenic sprouting in mice with elevated calcium. In addition to this, ECs could be extracted from OPG deficient mice and cultured in vitro to perform angiogenic assays as previously done in this study.

7.7 Limitations

This thesis aimed to contribute to the current body of evidence on vascular calcification and its effects on angiogenesis both in vitro and in vivo. Physiologically, calcium serves many functions in the body and is ubiquitously available in biological fluids, whilst phosphate also serves as a common stimulus for molecular signalling pathways; thus, any shift in ion homeostasis for both Ca and phosphate can result in mineralisation. There are many cell and animal models to study the molecular processes of vascular calcification. Majority of cell lines do not calcify spontaneously in vitro and require stimuli to induce calcification. As mentioned in Chapter 3, this study utilised one stimulus for the induction of calcification in the cells, using calcium chloride and sodium phosphate as a form of calcification medium. Furthermore, while in vitro cell culture experiments are helpful in studying signalling pathways of calcification, tissue organisation of cells is lost and processes involving the ECM are not represented. Therefore, as an alternative, 3D cell culture models could be utilised in future as they mimic the direct physiological environment and thus provide a better understanding of mechanisms driving disease progression. There currently

exists one 3D model used to study calcific aortic valve disease which resembles human aortic calcification[196]. Based on this, it remains unclear of the most efficient way to stimulate VC in vitro and which limits our ability to fully study this in vitro. In Chapter 3, western blotting results demonstrated that hypoxia treatment with calcification medium decreased the levels of the housekeeping protein alpha-tubulin (loading control), and this may also contribute to the lack of significant in the data. Furthermore, the lack of statistical significance observed in this study could be due to the smaller sample size, thus future studies should include more n values to increase the statistical power.

Preclinical models using rats and mice are readily used to study vascular calcification in vivo as they provide a better physiological context. Currently, there are 4 approaches of inducing calcification in mice, including models that are naturally occurring, induction of VC by operation, substance application/feeding or by genetic modification[196]. The most commonly used models for calcification are genetically modified mouse models, whereby medial calcification is induced by disrupting protective mechanisms by inhibiting calcification inhibitors. These knockout models include deficiency in MGP, Fetuin-A, OPN and OPG[196]. Furthermore, calcification can be induced by increasing hormonal regulation of phosphate, by affecting serum phosphate concentration. This method involves supplementation with vitamin D and is often used to study calcification in the setting of chronic kidney disease. This model however is not suitable to study angiogenesis as vitamin D administration causes physical impairment and promotes weight loss.

In this study, I utilised the OPG knockout mice as a calcification model to mimic high calcific environment. It is therefore important to note that the absence of OPG could be responsible for the results obtained in vivo and this requires further investigation. Data from Chapter 4 confirmed that our OPG knockout mice indeed had increased circulating calcium

levels as measured using a calcium assay. Furthermore, in a different study, osteoprotegerin inactivation accelerated atherosclerotic plaque lesion progression and calcification in older ApoE$^{-/-}$ mice compared to controls[149]. Overall, the pre-clinical models used in this thesis provide mechanistic insight into how calcification may drive angiogenesis, particularly in the context of high calcium.

Finally, OPG levels in humans are gender specific with women having higher levels of OPG than men[234]. In mice, oestrogen has been shown to increase OPG expression[240]. Therefore, this study utilised male mice only to eliminate the effect of oestrogen on our doppler perfusion and inflammatory data. However, this study should be performed using both male and female mice to fully understand the effect on calcification milieu in OPG mice on angiogenesis.

7.8 Conclusion:

This study demonstrates that calcification may dampen physiological angiogenesis while having no effect on inflammatory-driven angiogenesis. These data suggest that high calcium mediates angiogenesis in part by activating endothelial cells and driving increased expression of calcification markers.

CHAPTER 8:

REFERENCES

1. Tong B and Stevenson C. *Comorbidity of cardiovascular disease, diabetes and chronic kidney disease in Australia*: Australian Institute of Health and Welfare; 2007.
2. Balakumar P, Maung-U K and Jagadeesh G. Prevalence and prevention of cardiovascular disease and diabetes mellitus. *Pharmacological Research*. 2016;113:600-609.
3. Ouriel K. Peripheral arterial disease. *Lancet (London, England)*. 2001;358:1257-64.
4. Ross R. Atherosclerosis — An Inflammatory Disease. *New England Journal of Medicine*. 1999;340:115-126.
5. Akers Emma J, Mulangala J, Psaltis Peter J, Bursill C, Nicholls Stephen J and Di Bartolo Belinda A. Abstract 169: Lipoproteins and their Modified Forms Regulate Smooth Muscle Cell Calcification. *Arteriosclerosis, Thrombosis, and Vascular Biology*. 2018;38:A169-A169.
6. Steinl DC and Kaufmann BA. Ultrasound imaging for risk assessment in atherosclerosis. *International journal of molecular sciences*. 2015;16:9749-9769.
7. Lahoz C and Mostaza JM. Atherosclerosis As a Systemic Disease. *Revista Española de Cardiología (English Edition)*. 2007;60:184-195.
8. Conte SM and Vale PR. Peripheral Arterial Disease. *Heart, Lung and Circulation*. 2018;27:427-432.
9. Criqui MH, Denenberg JO, Langer RD and Fronek A. The epidemiology of peripheral arterial disease: importance of identifying the population at risk. *Vascular medicine (London, England)*. 1997;2:221-6.
10. Golomb BA, Dang TT and Criqui MH. Peripheral arterial disease: morbidity and mortality implications. *Circulation*. 2006;114:688-99.
11. Krishna SM, Moxon JV and Golledge J. A review of the pathophysiology and potential biomarkers for peripheral artery disease. *International journal of molecular sciences*. 2015;16:11294-322.
12. Criqui MH and Aboyans V. Epidemiology of peripheral artery disease. *Circulation research*. 2015;116:1509-26.
13. Criqui Michael H and Aboyans V. Epidemiology of Peripheral Artery Disease. *Circulation Research*. 2015;116:1509-1526.
14. Muller MD, Reed AB, Leuenberger UA and Sinoway LI. Physiology in medicine: peripheral arterial disease. *Journal of applied physiology (Bethesda, Md : 1985)*. 2013;115:1219-26.
15. Ho CY and Shanahan CM. Medial Arterial Calcification: An Overlooked Player in Peripheral Arterial Disease. *Arterioscler Thromb Vasc Biol*. 2016;36:1475-82.
16. Salem S, Bruck H, Bahlmann FH, Peter M, Passlick-Deetjen J, Kretschmer A, Steppan S, Volsek M, Kribben A, Nierhaus M, Jankowski V, Zidek W and Jankowski J. Relationship between Magnesium and Clinical Biomarkers on Inhibition of Vascular Calcification. *American Journal of Nephrology*. 2012;35:31-39.
17. Serrano Hernando FJ and Martín Conejero A. Peripheral Artery Disease: Pathophysiology, Diagnosis and Treatment. *Revista Española de Cardiología (English Edition)*. 2007;60:969-982.
18. Ouriel K. Peripheral arterial disease. *The Lancet*. 358:1257-1264.
19. Palmer-Kazen U and Wahlberg E. Arteriogenesis in peripheral arterial disease. *Endothelium : journal of endothelial cell research*. 2003;10:225-32.
20. Rocha-Singh KJ, Zeller T and Jaff MR. Peripheral arterial calcification: prevalence, mechanism, detection, and clinical implications. *Catheterization and cardiovascular interventions : official journal of the Society for Cardiac Angiography & Interventions*. 2014;83:E212-20.
21. Wahlberg E. Angiogenesis and arteriogenesis in limb ischemia. *Journal of Vascular Surgery*. 2003;38:198-203.
22. Ghidei W and Collins TC. African Americans and Peripheral Arterial Disease: A Review Article. *ISRN Vascular Medicine*. 2012;2012:9.

23. Hiatt WR. Medical Treatment of Peripheral Arterial Disease and Claudication. *New England Journal of Medicine*. 2001;344:1608-1621.
24. Muir RL. Peripheral arterial disease: Pathophysiology, risk factors, diagnosis, treatment, and prevention. *Journal of Vascular Nursing*. 2009;27:26-30.
25. Hankey GJ, Norman PE and Eikelboom JW. Medical treatment of peripheral arterial disease. *Jama*. 2006;295:547-53.
26. Arain FA and Cooper LT, Jr. Peripheral arterial disease: diagnosis and management. *Mayo Clinic proceedings*. 2008;83:944-49; quiz 949-50.
27. Lewis CD. Peripheral Arterial Disease of the Lower Extremity. *Journal of Cardiovascular Nursing*. 2001;15.
28. Leng G, Fowler B and Ernst E. Exercise for intermittent claudication (Cochrane Review). *The Cochrane Library*. 2004;4.
29. Gebauer K and Reinecke H. PCSK9 inhibition for LDL lowering and beyond - implications for patients with peripheral artery disease. *VASA Zeitschrift fur Gefasskrankheiten*. 2018;47:165-176.
30. Bonaca MP, Nault P, Giugliano RP, Keech AC, Pineda AL, Kanevsky E, Kuder J, Murphy SA, Jukema JW, Lewis BS, Tokgozoglu L, Somaratne R, Sever PS, Pedersen TR and Sabatine MS. Low-Density Lipoprotein Cholesterol Lowering With Evolocumab and Outcomes in Patients With Peripheral Artery Disease: Insights From the FOURIER Trial (Further Cardiovascular Outcomes Research With PCSK9 Inhibition in Subjects With Elevated Risk). *Circulation*. 2018;137:338-350.
31. A randomised, blinded, trial of clopidogrel versus aspirin in patients at risk of ischaemic events (CAPRIE). *The Lancet*. 1996;348:1329-1339.
32. Steffel J, Eikelboom John W, Anand Sonia S, Shestakovska O, Yusuf S and Fox Keith AA. The COMPASS Trial. *Circulation*. 2020;142:40-48.
33. Guzman RJ. Clinical, cellular, and molecular aspects of arterial calcification. *Journal of Vascular Surgery*. 2007;45:A57-A63.
34. Guzman RJ, Brinkley DM, Schumacher PM, Donahue RMJ, Beavers H and Qin X. Tibial Artery Calcification as a Marker of Amputation Risk in Patients With Peripheral Arterial Disease. *Journal of the American College of Cardiology*. 2008;51:1967.
35. Everhart JE, Pettitt DJ, Knowler WC, Rose FA and Bennett PH. Medial arterial calcification and its association with mortality and complications of diabetes. *Diabetologia*. 1988;31:16-23.
36. Kamenskiy A, Poulson W, Sim S, Reilly A, Luo J and MacTaggart J. Prevalence of Calcification in Human Femoropopliteal Arteries and its Association with Demographics, Risk Factors, and Arterial Stiffness. *Arteriosclerosis, Thrombosis, and Vascular Biology*. 2018;38:e48-e57.
37. Zettervall SL, Marshall AP, Fleser P and Guzman RJ. Association of arterial calcification with chronic limb ischemia in patients with peripheral artery disease. *Journal of Vascular Surgery*. 2018;67:507-513.
38. Wong NKP, Solly EL, Bursill CA, Tan JTM and Ng MKC. Pathophysiology of Angiogenesis and Its Role in Vascular Disease. In: R. Fitridge, ed. *Mechanisms of Vascular Disease: A Textbook for Vascular Specialists* Cham: Springer International Publishing; 2020: 89-116.
39. Johnson T, Zhao L, Manuel G, Taylor H and Liu D. Approaches to therapeutic angiogenesis for ischemic heart disease. *Journal of molecular medicine (Berlin, Germany)*. 2019;97:141-151.
40. Iyer SR and Annex BH. Therapeutic Angiogenesis for Peripheral Artery Disease: Lessons Learned in Translational Science. *JACC Basic Transl Sci*. 2017;2:503-512.
41. Ferrara N and Kerbel RS. Angiogenesis as a therapeutic target. *Nature*. 2005;438:967-974.

42. Mitsos S, Katsanos K, Koletsis E, Kagadis GC, Anastasiou N, Diamantopoulos A, Karnabatidis D and Dougenis D. Therapeutic angiogenesis for myocardial ischemia revisited: basic biological concepts and focus on latest clinical trials. *Angiogenesis*. 2012;15:1-22.
43. Henry TD, Rocha-Singh K, Isner JM, Kereiakes DJ, Giordano FJ, Simons M, Losordo DW, Hendel RC, Bonow RO and Eppler SM. Intracoronary administration of recombinant human vascular endothelial growth factor to patients with coronary artery disease. *American heart journal*. 2001;142:872-880.
44. Stegmann TJ, Hoppert T, Schneider A, Gemeinhardt S, Köcher M, Ibing R and Strupp G. Induction of myocardial neoangiogenesis by human growth factors. A new therapeutic approach in coronary heart disease. *Herz*. 2000;25:589-599.
45. Schumacher B, Stegmann T and Pecher P. The stimulation of neoangiogenesis in the ischemic human heart by the growth factor FGF: first clinical results. *Journal of Cardiovascular Surgery*. 1998;39:783.
46. Carmeliet P and Jain RK. Angiogenesis in cancer and other diseases. *Nature*. 2000;407:249-57.
47. Wahlberg E. Angiogenesis and arteriogenesis in limb ischemia. *J Vasc Surg*. 2003;38:198-203.
48. Lapergue B, Mohammad A and Shuaib A. Endothelial progenitor cells and cerebrovascular diseases. *Progress in Neurobiology*. 2007;83:349-362.
49. Simons M. Angiogenesis: where do we stand now? *Circulation*. 2005;111:1556-66.
50. Carmeliet P. Mechanisms of angiogenesis and arteriogenesis. *Nature medicine*. 2000;6:389-95.
51. Min JK, Cho YL, Choi JH, Kim Y, Kim JH, Yu YS, Rho J, Mochizuki N, Kim YM, Oh GT and Kwon YG. Receptor activator of nuclear factor (NF)-kappaB ligand (RANKL) increases vascular permeability: impaired permeability and angiogenesis in eNOS-deficient mice. *Blood*. 2007;109:1495-502.
52. Scholz D, Cai W-j and Schaper W. Arteriogenesis, a new concept of vascular adaptation in occlusive disease. *Angiogenesis*. 4:247-257.
53. van Royen N, Piek JJ, Buschmann I, Hoefer I, Voskuil M and Schaper W. Stimulation of arteriogenesis; a new concept for the treatment of arterial occlusive disease. *Cardiovascular research*. 2001;49:543-553.
54. Ross MH, Kaye GI and Pawlina W. Histology : a text and atlas with cell and molecular biology. 2003.
55. Gornik HL and Beckman JA. Cardiology patient page. Peripheral arterial disease. *Circulation*. 2005;111:e169-72.
56. Igari K, Kudo T, Toyofuku T and Inoue Y. The Relationship between Endothelial Dysfunction and Endothelial Cell Markers in Peripheral Arterial Disease. *PLOS ONE*. 2016;11:e0166840.
57. Rajendran P, Rengarajan T, Thangavel J, Nishigaki Y, Sakthisekaran D, Sethi G and Nishigaki I. The vascular endothelium and human diseases. *International journal of biological sciences*. 2013;9:1057-69.
58. Zhang K, Yin F and Lin L. Circulating Endothelial Cells and Chronic Kidney Disease. *BioMed Research International*. 2014;2014:364738.
59. Sumpio BE, Riley JT and Dardik A. Cells in focus: endothelial cell. *The international journal of biochemistry & cell biology*. 2002;34:1508-12.
60. Collinson DJ and Donnelly R. Therapeutic angiogenesis in peripheral arterial disease: can biotechnology produce an effective collateral circulation? *European journal of vascular and endovascular surgery : the official journal of the European Society for Vascular Surgery*. 2004;28:9-23.

61. Johnson RC, Leopold JA and Loscalzo J. Vascular calcification: pathobiological mechanisms and clinical implications. *Circ Res*. 2006;99:1044-59.
62. Collett GD and Canfield AE. Angiogenesis and pericytes in the initiation of ectopic calcification. *Circ Res*. 2005;96:930-8.
63. Cola C, Almeida M, Li D, Romeo F and Mehta JL. Regulatory role of endothelium in the expression of genes affecting arterial calcification. *Biochem Biophys Res Commun*. 2004;320:424-7.
64. Ridiandries A, Tan JTM and Bursill CA. The Role of CC-Chemokines in the Regulation of Angiogenesis. *International journal of molecular sciences*. 2016;17:1856.
65. Liu T, Zhang L, Joo D and Sun SC. NF-κB signaling in inflammation. *Signal transduction and targeted therapy*. 2017;2:17023-.
66. Szade A, Grochot-Przeczek A, Florczyk U, Jozkowicz A and Dulak J. Cellular and molecular mechanisms of inflammation-induced angiogenesis. *IUBMB Life*. 2015;67:145-159.
67. Tan JT, Ng MK and Bursill CA. The role of high-density lipoproteins in the regulation of angiogenesis. *Cardiovascular research*. 2015;106:184-93.
68. Holmes DI and Zachary I. The vascular endothelial growth factor (VEGF) family: angiogenic factors in health and disease. *Genome biology*. 2005;6:209.
69. Ferrara N, Carver-Moore K, Chen H, Dowd M, Lu L, O'Shea KS, Powell-Braxton L, Hillan KJ and Moore MW. Heterozygous embryonic lethality induced by targeted inactivation of the VEGF gene. *Nature*. 1996;380:439-442.
70. Karamysheva AF. Mechanisms of angiogenesis. *Biochemistry Biokhimiia*. 2008;73:751-62.
71. Olszewska-Pazdrak B, Hein TW, Olszewska P and Carney DH. Chronic hypoxia attenuates VEGF signaling and angiogenic responses by downregulation of KDR in human endothelial cells. *American Journal of Physiology-Cell Physiology*. 2009;296:C1162-C1170.
72. Cannizzo CM, Adonopulos AA, Solly EL, Ridiandries A, Vanags LZ, Mulangala J, Yuen SCG, Tsatralis T, Henriquez R, Robertson S, Nicholls SJ, Di Bartolo BA, Ng MKC, Lam YT, Bursill CA and Tan JTM. VEGFR2 is activated by high-density lipoproteins and plays a key role in the proangiogenic action of HDL in ischemia. *The FASEB Journal*. 2018;32:2911-2922.
73. Formiga FR, Tamayo E, Simon-Yarza T, Pelacho B, Prosper F and Blanco-Prieto MJ. Angiogenic therapy for cardiac repair based on protein delivery systems. *Heart failure reviews*. 2012;17:449-73.
74. Park MH and Hong JT. Roles of NF-kappaB in Cancer and Inflammatory Diseases and Their Therapeutic Approaches. *Cells*. 2016;5.
75. Galkina E and Ley K. Vascular Adhesion Molecules in Atherosclerosis. *Arteriosclerosis, Thrombosis, and Vascular Biology*. 2007;27:2292-2301.
76. Mohammadpour AH, Falsoleiman H, Shamsara J, Allah Abadi G, Rasooli R and Ramezani M. Pentoxifylline decreases serum level of adhesion molecules in atherosclerosis patients. *Iran Biomed J*. 2014;18:23-27.
77. Krieglstein CF and Granger DN. Adhesion molecules and their role in vascular disease*. *American Journal of Hypertension*. 2001;14:44S-54S.
78. Lin J, Kakkar V and Lu X. Impact of MCP-1 in atherosclerosis. *Current pharmaceutical design*. 2014;20:4580-8.
79. Lee SJ, Lee IK and Jeon JH. Vascular Calcification-New Insights Into Its Mechanism. *International journal of molecular sciences*. 2020;21.
80. Demer LL and Tintut Y. Vascular calcification: pathobiology of a multifaceted disease. *Circulation*. 2008;117:2938-48.
81. Madhavan MV, Tarigopula M, Mintz GS, Maehara A, Stone GW and Genereux P. Coronary artery calcification: pathogenesis and prognostic implications. *J Am Coll Cardiol*. 2014;63:1703-14.

82. Zhu D, Mackenzie NCW, Farquharson C and MacRae VE. Mechanisms and Clinical Consequences of Vascular Calcification. *Frontiers in Endocrinology*. 2012;3:95.
83. Mustapha J and Diaz-Sandoval LJ. Arterial Deposition of Calcium and Outcomes of Peripheral Interventions: Is It Time to Redefine the "Gold Standard?". *VASCULAR DISEASE MANAGEMENT*. 2013;10:E208-E211.
84. Guzman RJ, Bian A, Shintani A and Stein CM. Association of foot ulcer with tibial artery calcification is independent of peripheral occlusive disease in type 2 diabetes. *Diabetes research and clinical practice*. 2013;99:281-286.
85. O'Neill WC, Han KH, Schneider TM and Hennigar RA. Prevalence of nonatheromatous lesions in peripheral arterial disease. *Arteriosclerosis, thrombosis, and vascular biology*. 2015;35:439-47.
86. Reynolds JL, Joannides AJ, Skepper JN, McNair R, Schurgers LJ, Proudfoot D, Jahnen-Dechent W, Weissberg PL and Shanahan CM. Human vascular smooth muscle cells undergo vesicle-mediated calcification in response to changes in extracellular calcium and phosphate concentrations: a potential mechanism for accelerated vascular calcification in ESRD. *Journal of the American Society of Nephrology : JASN*. 2004;15:2857-67.
87. Shanahan CM, Cary NR, Salisbury JR, Proudfoot D, Weissberg PL and Edmonds ME. Medial localization of mineralization-regulating proteins in association with Monckeberg's sclerosis: evidence for smooth muscle cell-mediated vascular calcification. *Circulation*. 1999;100:2168-76.
88. Mizobuchi M, Towler D and Slatopolsky E. Vascular calcification: the killer of patients with chronic kidney disease. *Journal of the American Society of Nephrology : JASN*. 2009;20:1453-64.
89. Shanahan CM. Inflammation Ushers in Calcification. *Circulation*. 2007;116:2782-2785.
90. Dhore Cherida R, Cleutjens Jack PM, Lutgens E, Cleutjens Kitty BJM, Geusens Piet PM, Kitslaar Peter JEHM, Tordoir Jan HM, Spronk Henri MH, Vermeer C and Daemen Mat JAP. Differential Expression of Bone Matrix Regulatory Proteins in Human Atherosclerotic Plaques. *Arteriosclerosis, Thrombosis, and Vascular Biology*. 2001;21:1998-2003.
91. Tintut Y, Patel J, Parhami F and Demer Linda L. Tumor Necrosis Factor-α Promotes In Vitro Calcification of Vascular Cells via the cAMP Pathway. *Circulation*. 2000;102:2636-2642.
92. Wallin R, Wajih N, Greenwood GT and Sane DC. Arterial calcification: a review of mechanisms, animal models, and the prospects for therapy. *Medicinal research reviews*. 2001;21:274-301.
93. Mizobuchi M, Towler D and Slatopolsky E. Vascular Calcification: The Killer of Patients with Chronic Kidney Disease. *Journal of the American Society of Nephrology*. 2009;20:1453.
94. Durham AL, Speer MY, Scatena M, Giachelli CM and Shanahan CM. Role of smooth muscle cells in vascular calcification: implications in atherosclerosis and arterial stiffness. *Cardiovascular research*. 2018;114:590-600.
95. Lehto S, Niskanen L, Suhonen M, Ronnemaa T and Laakso M. Medial artery calcification. A neglected harbinger of cardiovascular complications in non-insulin-dependent diabetes mellitus. *Arterioscler Thromb Vasc Biol*. 1996;16:978-83.
96. Lehto S, Niskanen L, Suhonen M, Rönnemaa T and Laakso M. Medial Artery Calcification. *Arteriosclerosis, Thrombosis, and Vascular Biology*. 1996;16:978-983.
97. Shanahan CM, Crouthamel MH, Kapustin A and Giachelli CM. Arterial calcification in chronic kidney disease: key roles for calcium and phosphate. *Circulation research*. 2011;109:697-711.
98. Reynolds JL, Joannides AJ, Skepper JN, McNair R, Schurgers LJ, Proudfoot D, Jahnen-Dechent W, Weissberg PL and Shanahan CM. Human Vascular Smooth Muscle Cells Undergo Vesicle-Mediated Calcification in Response to Changes in Extracellular Calcium

and Phosphate Concentrations: A Potential Mechanism for Accelerated Vascular Calcification in ESRD. *Journal of the American Society of Nephrology*. 2004;15:2857.
99. Malhotra A and Habibovic P. Calcium Phosphates and Angiogenesis: Implications and Advances for Bone Regeneration. *Trends in biotechnology*. 2016;34:983-992.
100. Shanahan CM, Crouthamel MH, Kapustin A and Giachelli CM. Arterial calcification in chronic kidney disease: key roles for calcium and phosphate. *Circ Res*. 2011;109:697-711.
101. Kestenbaum B, Sampson JN, Rudser KD, Patterson DJ, Seliger SL, Young B, Sherrard DJ and Andress DL. Serum phosphate levels and mortality risk among people with chronic kidney disease. *Journal of the American Society of Nephrology : JASN*. 2005;16:520-8.
102. Rogers MA, Aikawa M and Aikawa E. Macrophage Heterogeneity Complicates Reversal of Calcification in Cardiovascular Tissues. *Circulation research*. 2017;121:5-7.
103. New SEP, Goettsch C, Aikawa M, Marchini JF, Shibasaki M, Yabusaki K, Libby P, Shanahan CM, Croce K and Aikawa E. Macrophage-derived matrix vesicles: an alternative novel mechanism for microcalcification in atherosclerotic plaques. *Circulation research*. 2013;113:72-77.
104. Nakahara T, Dweck MR, Narula N, Pisapia D, Narula J and Strauss HW. Coronary Artery Calcification: From Mechanism to Molecular Imaging. *JACC Cardiovascular imaging*. 2017;10:582-593.
105. Giachelli CM. Vascular Calcification Mechanisms. *Journal of the American Society of Nephrology*. 2004;15:2959.
106. Lok Zoe Shin Y and Lyle Alicia N. Osteopontin in Vascular Disease. *Arteriosclerosis, Thrombosis, and Vascular Biology*. 2019;39:613-622.
107. Qin X, Corriere MA, Matrisian LM and Guzman RJ. Matrix metalloproteinase inhibition attenuates aortic calcification. *Arterioscler Thromb Vasc Biol*. 2006;26:1510-6.
108. Lee GS, Salazar HF, Joseph G, Lok ZSY, Caroti CM, Weiss D, Taylor WR and Lyle AN. Osteopontin isoforms differentially promote arteriogenesis in response to ischemia via macrophage accumulation and survival. *Laboratory Investigation*. 2019;99:331-345.
109. Luo G, Ducy P, McKee MD, Pinero GJ, Loyer E, Behringer RR and Karsenty G. Spontaneous calcification of arteries and cartilage in mice lacking matrix GLA protein. *Nature*. 1997;386:78-81.
110. Yao Y, Nowak S, Yochelis A, Garfinkel A and Boström KI. Matrix GLA protein, an inhibitory morphogen in pulmonary vascular development. *The Journal of biological chemistry*. 2007;282:30131-42.
111. Glienke J, Schmitt AO, Pilarsky C, Hinzmann B, Weiß B, Rosenthal A and Thierauch KH. Differential gene expression by endothelial cells in distinct angiogenic states. *European journal of biochemistry*. 2000;267:2820-2830.
112. Sharma B and Albig AR. Matrix Gla protein reinforces angiogenic resolution. *Microvasc Res*. 2013;85:24-33.
113. Ketteler M, Bongartz P, Westenfeld R, Wildberger JE, Mahnken AH, Böhm R, Metzger T, Wanner C, Jahnen-Dechent W and Floege J. Association of low fetuin-A (AHSG) concentrations in serum with cardiovascular mortality in patients on dialysis: a cross-sectional study. *Lancet (London, England)*. 2003;361:827-33.
114. Vervloet MG, Adema AY, Larsson TE and Massy ZA. The Role of Klotho on Vascular Calcification and Endothelial Function in Chronic Kidney Disease. *Seminars in Nephrology*. 2014;34:578-585.
115. Kuro-o M, Matsumura Y, Aizawa H, Kawaguchi H, Suga T, Utsugi T, Ohyama Y, Kurabayashi M, Kaname T, Kume E, Iwasaki H, Iida A, Shiraki-Iida T, Nishikawa S, Nagai R and Nabeshima YI. Mutation of the mouse klotho gene leads to a syndrome resembling ageing. *Nature*. 1997;390:45-51.

116. Villa-Bellosta R and Egido J. Phosphate, pyrophosphate, and vascular calcification: a question of balance. *European Heart Journal*. 2015;38:1801-1804.
117. Hah YS, Jun JS, Lee SG, Park BW, Kim DR, Kim UK, Kim JR and Byun JH. Vascular endothelial growth factor stimulates osteoblastic differentiation of cultured human periosteal-derived cells expressing vascular endothelial growth factor receptors. *Molecular biology reports*. 2011;38:1443-50.
118. Huang J, Deng F, Wang L, Xiang XR, Zhou WW, Hu N and Xu L. Hypoxia induces osteogenesis-related activities and expression of core binding factor alpha1 in mesenchymal stem cells. *The Tohoku journal of experimental medicine*. 2011;224:7-12.
119. Komori T, Yagi H, Nomura S, Yamaguchi A, Sasaki K, Deguchi K, Shimizu Y, Bronson RT, Gao YH, Inada M, Sato M, Okamoto R, Kitamura Y, Yoshiki S and Kishimoto T. Targeted disruption of Cbfa1 results in a complete lack of bone formation owing to maturational arrest of osteoblasts. *Cell*. 1997;89:755-64.
120. Zelzer E, Glotzer DJ, Hartmann C, Thomas D, Fukai N, Soker S and Olsen BR. Tissue specific regulation of VEGF expression during bone development requires Cbfa1/Runx2. *Mechanisms of Development*. 2001;106:97-106.
121. Kwon TG, Zhao X, Yang Q, Li Y, Ge C, Zhao G and Franceschi RT. Physical and functional interactions between Runx2 and HIF-1alpha induce vascular endothelial growth factor gene expression. *Journal of cellular biochemistry*. 2011;112:3582-93.
122. Lee S-H, Che X, Jeong J-H, Choi J-Y, Lee Y-J, Lee Y-H, Bae S-C and Lee Y-M. Runx2 Protein Stabilizes Hypoxia-inducible Factor-1α through Competition with von Hippel-Lindau Protein (pVHL) and Stimulates Angiogenesis in Growth Plate Hypertrophic Chondrocytes. *Journal of Biological Chemistry*. 2012;287:14760-14771.
123. Sun L, Vitolo M and Passaniti A. Runt-related gene 2 in endothelial cells: inducible expression and specific regulation of cell migration and invasion. *Cancer research*. 2001;61:4994-5001.
124. Valdivielso JM. [Vascular calcification: types and mechanisms]. *Nefrologia : publicacion oficial de la Sociedad Espanola Nefrologia*. 2011;31:142-7.
125. Yao Y, Jumabay M, Ly A, Radparvar M, Cubberly MR and Bostrom KI. A role for the endothelium in vascular calcification. *Circulation research*. 2013;113:495-504.
126. Li X, Yang HY and Giachelli CM. BMP-2 promotes phosphate uptake, phenotypic modulation, and calcification of human vascular smooth muscle cells. *Atherosclerosis*. 2008;199:271-7.
127. Proudfoot D and Shanahan MC. Biology of Calcification in Vascular Cells: Intima versus Media. *Herz*. 26:245-251.
128. Kaden JJ, Bickelhaupt S, Grobholz R, Haase KK, Sarikoc A, Kilic R, Brueckmann M, Lang S, Zahn I, Vahl C, Hagl S, Dempfle CE and Borggrefe M. Receptor activator of nuclear factor kappaB ligand and osteoprotegerin regulate aortic valve calcification. *Journal of molecular and cellular cardiology*. 2004;36:57-66.
129. Baud'huin M, Lamoureux F, Duplomb L, Redini F and Heymann D. RANKL, RANK, osteoprotegerin: key partners of osteoimmunology and vascular diseases. *Cellular and molecular life sciences : CMLS*. 2007;64:2334-50.
130. Lanzer P, Boehm M, Sorribas V, Thiriet M, Janzen J, Zeller T, St Hilaire C and Shanahan C. Medial vascular calcification revisited: review and perspectives. *European heart journal*. 2014;35:1515-25.
131. Papadopouli AE, Klonaris CN and Theocharis SE. Role of OPG/RANKL/RANK axis on the vasculature. *Histology and histopathology*. 2008;23:497-506.
132. Neven E and D'Haese PC. Vascular Calcification in Chronic Renal Failure What Have We Learned From Animal Studies? *Circulation research*. 2011;108:249-264.

133. Özkalaycı F, Gülmez Ö, Uğur-Altun B, Pandi-Perumal SR and Altun A. The Role of Osteoprotegerin as a Cardioprotective Versus Reactive Inflammatory Marker: the Chicken or the Egg Paradox. *Balkan Med J*. 2018;35:225-232.
134. Kiechl S, Schett G, Wenning G, Redlich K, Oberhollenzer M, Mayr A, Santer P, Smolen J, Poewe W and Willeit J. Osteoprotegerin Is a Risk Factor for Progressive Atherosclerosis and Cardiovascular Disease. *Circulation*. 2004;109:2175-2180.
135. Benslimane-Ahmim Z, Heymann D, Dizier B, Lokajczyk A, Brion R, Laurendeau I, Bieche I, Smadja DM, Galy-Fauroux I, Colliec-Jouault S, Fischer AM and Boisson-Vidal C. Osteoprotegerin, a new actor in vasculogenesis, stimulates endothelial colony-forming cells properties. *Journal of thrombosis and haemostasis : JTH*. 2011;9:834-43.
136. Vorkapic E, Kunath A and Wågsäter D. Effects of osteoprotegerin/TNFRSF11B in two models of abdominal aortic aneurysms. *Mol Med Rep*. 2018;18:41-48.
137. Cross SS, Yang Z, Brown NJ, Balasubramanian SP, Evans CA, Woodward JK, Neville-Webbe HL, Lippitt JM, Reed MW, Coleman RE and Holen I. Osteoprotegerin (OPG)--a potential new role in the regulation of endothelial cell phenotype and tumour angiogenesis? *International journal of cancer*. 2006;118:1901-8.
138. Heymann M-F, Herisson F, Davaine J-M, Charrier C, Battaglia S, Passuti N, Lambert G, Gouëffic Y and Heymann D. Role of the OPG/RANK/RANKL triad in calcifications of the atheromatous plaques: Comparison between carotid and femoral beds. *Cytokine*. 2012;58:300-306.
139. Jono S, Otsuki S, Higashikuni Y, Shioi A, Mori K, Hara K, Hashimoto H and Ikari Y. Serum osteoprotegerin levels and long-term prognosis in subjects with stable coronary artery disease. *Journal of Thrombosis and Haemostasis*. 2010;8:1170-1175.
140. Lieb W, Gona P, Larson MG, Massaro JM, Lipinska I, Keaney JF, Jr., Rong J, Corey D, Hoffmann U, Fox CS, Vasan RS, Benjamin EJ, O'Donnell CJ and Kathiresan S. Biomarkers of the osteoprotegerin pathway: clinical correlates, subclinical disease, incident cardiovascular disease, and mortality. *Arterioscler Thromb Vasc Biol*. 2010;30:1849-54.
141. Anand DV, Lahiri A, Lim E, Hopkins D and Corder R. The relationship between plasma osteoprotegerin levels and coronary artery calcification in uncomplicated type 2 diabetic subjects. *J Am Coll Cardiol*. 2006;47:1850-7.
142. Schoppet M, Al-Fakhri N, Franke FE, Katz N, Barth PJ, Maisch B, Preissner KT and Hofbauer LC. Localization of osteoprotegerin, tumor necrosis factor-related apoptosis-inducing ligand, and receptor activator of nuclear factor-kappaB ligand in Mönckeberg's sclerosis and atherosclerosis. *The Journal of clinical endocrinology and metabolism*. 2004;89:4104-12.
143. Pedersen S, Mogelvang R, Bjerre M, Frystyk J, Flyvbjerg A, Galatius S, Sørensen TB, Iversen A, Hvelplund A and Jensen JS. Osteoprotegerin predicts long-term outcome in patients with ST-segment elevation myocardial infarction treated with primary percutaneous coronary intervention. *Cardiology*. 2012;123:31-8.
144. Lis GJ, Czubek U, Jasinska M, Jasek E, Loboda A, Dulak J, Nessler J, Sadowski J and Litwin JA. Elevated serum osteoprotegerin is associated with decreased osteoclastic differentiation in stenotic aortic valves. *Journal of physiology and pharmacology : an official journal of the Polish Physiological Society*. 2014;65:377-82.
145. Bucay N, Sarosi I, Dunstan CR, Morony S, Tarpley J, Capparelli C, Scully S, Tan HL, Xu W, Lacey DL, Boyle WJ and Simonet WS. osteoprotegerin-deficient mice develop early onset osteoporosis and arterial calcification. *Genes Dev*. 1998;12:1260-1268.
146. Min H, Morony S, Sarosi I, Dunstan CR, Capparelli C, Scully S, Van G, Kaufman S, Kostenuik PJ, Lacey DL, Boyle WJ and Simonet WS. Osteoprotegerin Reverses Osteoporosis by Inhibiting Endosteal Osteoclasts and Prevents Vascular Calcification by

Blocking a Process Resembling Osteoclastogenesis. *Journal of Experimental Medicine*. 2000;192:463-474.
147. Ozaki Y, Koide M, Furuya Y, Ninomiya T, Yasuda H, Nakamura M, Kobayashi Y, Takahashi N, Yoshinari N and Udagawa N. Treatment of OPG-deficient mice with WP9QY, a RANKL-binding peptide, recovers alveolar bone loss by suppressing osteoclastogenesis and enhancing osteoblastogenesis. *PloS one*. 2017;12:e0184904-e0184904.
148. Zhang L, Liu M, Zhou X, Liu Y, Jing B, Wang X, Zhang Q and Sun Y. Role of Osteoprotegerin (OPG) in Bone Marrow Adipogenesis. *Cellular Physiology and Biochemistry*. 2016;40:681-692.
149. Bennett BJ, Scatena M, Kirk EA, Rattazzi M, Varon RM, Averill M, Schwartz SM, Giachelli CM and Rosenfeld ME. Osteoprotegerin inactivation accelerates advanced atherosclerotic lesion progression and calcification in older ApoE-/- mice. *Arterioscler Thromb Vasc Biol*. 2006;26:2117-24.
150. Kim YM, Kim YM, Lee YM, Kim HS, Kim JD, Choi Y, Kim KW, Lee SY and Kwon YG. TNF-related activation-induced cytokine (TRANCE) induces angiogenesis through the activation of Src and phospholipase C (PLC) in human endothelial cells. *The Journal of biological chemistry*. 2002;277:6799-805.
151. Wong BR, Josien R, Lee SY, Sauter B, Li HL, Steinman RM and Choi Y. TRANCE (tumor necrosis factor [TNF]-related activation-induced cytokine), a new TNF family member predominantly expressed in T cells, is a dendritic cell-specific survival factor. *The Journal of experimental medicine*. 1997;186:2075-80.
152. Min JK, Kim YM, Kim YM, Kim EC, Gho YS, Kang IJ, Lee SY, Kong YY and Kwon YG. Vascular endothelial growth factor up-regulates expression of receptor activator of NF-kappa B (RANK) in endothelial cells. Concomitant increase of angiogenic responses to RANK ligand. *The Journal of biological chemistry*. 2003;278:39548-57.
153. McGonigle JS, Giachelli CM and Scatena M. Osteoprotegerin and RANKL differentially regulate angiogenesis and endothelial cell function. *Angiogenesis*. 2009;12:35-46.
154. Benslimane-Ahmim Z, Poirier F, Delomenie C, Lokajczyk A, Grelac F, Galy-Fauroux I, Mohamedi A, Fischer A-M, Heymann D, Lutomski D and Boisson-Vidal C. Mechanistic study of the proangiogenic effect of osteoprotegerin. *Angiogenesis*. 2013;16:575-593.
155. Malyankar UM, Scatena M, Suchland KL, Yun TJ, Clark EA and Giachelli CM. Osteoprotegerin is an alpha vbeta 3-induced, NF-kappa B-dependent survival factor for endothelial cells. *The Journal of biological chemistry*. 2000;275:20959-62.
156. Wang DS, Miura M, Demura H and Sato K. Anabolic effects of 1,25-dihydroxyvitamin D3 on osteoblasts are enhanced by vascular endothelial growth factor produced by osteoblasts and by growth factors produced by endothelial cells. *Endocrinology*. 1997;138:2953-62.
157. Guzman RJ. Clinical, Cellular, and Molecular Aspects of Arterial Calcification. *Journal of vascular surgery : official publication, the Society for Vascular Surgery [and] International Society for Cardiovascular Surgery, North American Chapter*. 2007;45:A57-A63.
158. Deckers MML, van Bezooijen RL, van der Horst G, Hoogendam J, van der Bent C, Papapoulos SE and Löwik CWGM. Bone Morphogenetic Proteins Stimulate Angiogenesis through Osteoblast-Derived Vascular Endothelial Growth Factor A. *Endocrinology*. 2002;143:1545-1553.
159. Langenfeld EM and Langenfeld J. Bone morphogenetic protein-2 stimulates angiogenesis in developing tumors. *Molecular cancer research : MCR*. 2004;2:141-9.
160. Nadra I, Boccaccini AR, Philippidis P, Whelan LC, McCarthy GM, Haskard DO and Landis RC. Effect of particle size on hydroxyapatite crystal-induced tumor necrosis factor alpha secretion by macrophages. *Atherosclerosis*. 2008;196:98-105.
161. Nadra I, Mason Justin C, Philippidis P, Florey O, Smythe Cheryl DW, McCarthy Geraldine M, Landis Robert C and Haskard Dorian O. Proinflammatory Activation of Macrophages by

Basic Calcium Phosphate Crystals via Protein Kinase C and MAP Kinase Pathways. *Circulation Research*. 2005;96:1248-1256.
162. Limbourg A, Korff T, Napp LC, Schaper W, Drexler H and Limbourg FP. Evaluation of postnatal arteriogenesis and angiogenesis in a mouse model of hind-limb ischemia. *Nature protocols*. 2009;4:1737-46.
163. Brenes RA, Jadlowiec CC, Bear M, Hashim P, Protack CD, Li X, Lv W, Collins MJ and Dardik A. Toward a mouse model of hind limb ischemia to test therapeutic angiogenesis. *Journal of vascular surgery*. 2012;56:1669-1679.
164. Ridiandries A, Tan JTM, Ravindran D, Williams H, Medbury HJ, Lindsay L, Hawkins C, Prosser HCG and Bursill CA. CC-chemokine class inhibition attenuates pathological angiogenesis while preserving physiological angiogenesis. *The FASEB Journal*. 2017;31:1179-1192.
165. Proudfoot D and Shanahan CM. Biology of Calcification in Vascular Cells: Intima versus Media. *Herz*. 2001;26:245-251.
166. Boström K, Watson KE, Horn S, Wortham C, Herman IM and Demer LL. Bone morphogenetic protein expression in human atherosclerotic lesions. *Journal of Clinical Investigation*. 1993;91:1800-1809.
167. Callegari A, Coons ML, Ricks JL, Rosenfeld ME and Scatena M. Increased calcification in osteoprotegerin-deficient smooth muscle cells: Dependence on receptor activator of NF-kappaB ligand and interleukin 6. *Journal of vascular research*. 2014;51:118-31.
168. Collin-Osdoby P. Regulation of vascular calcification by osteoclast regulatory factors RANKL and osteoprotegerin. *Circ Res*. 2004;95:1046-57.
169. Kohli SS and Kohli VS. Role of RANKL–RANK/osteoprotegerin molecular complex in bone remodeling and its immunopathologic implications. *Indian Journal of Endocrinology and Metabolism*. 2011;15:175-181.
170. Ndip A, Williams A, Jude EB, Serracino-Inglott F, Richardson S, Smyth JV, Boulton AJ and Alexander MY. The RANKL/RANK/OPG signaling pathway mediates medial arterial calcification in diabetic Charcot neuroarthropathy. *Diabetes*. 2011;60:2187-96.
171. Panizo S, Cardus A, Encinas M, Parisi E, Valcheva P, Lopez-Ongil S, Coll B, Fernandez E and Valdivielso JM. RANKL increases vascular smooth muscle cell calcification through a RANK-BMP4-dependent pathway. *Circ Res*. 2009;104:1041-8.
172. Hamid HE, Azlina A, Khamis MF, Rahman RA, Abdul Razak NH, Mutum SS and Samsudin AR. Effect of Biphasic Calcium Phosphate Treated with Vascular Endothelial Growth Factor on Osteogenesis and Angiogenesis Gene Expression In Vitro. In: J. Goh, ed. *The 15th International Conference on Biomedical Engineering: ICBME 2013, 4th to 7th December 2013, Singapore* Cham: Springer International Publishing; 2014: 239-242.
173. Jono S, McKee MD, Murry CE, Shioi A, Nishizawa Y, Mori K, Morii H and Giachelli CM. Phosphate regulation of vascular smooth muscle cell calcification. *Circ Res*. 2000;87:E10-7.
174. Yang H, Curinga G and Giachelli CM. Elevated extracellular calcium levels induce smooth muscle cell matrix mineralization in vitro. *Kidney international*. 2004;66:2293-9.
175. Arnould T, Michiels C, Alexandre I and Remacle J. Effect of hypoxia upon intracellular calcium concentration of human endothelial cells. *Journal of cellular physiology*. 1992;152:215-21.
176. Moccia F, Negri S, Shekha M, Faris P and Guerra G. Endothelial Ca(2+) Signaling, Angiogenesis and Vasculogenesis: just What It Takes to Make a Blood Vessel. *International journal of molecular sciences*. 2019;20.
177. Michaelis UR. Mechanisms of endothelial cell migration. *Cellular and Molecular Life Sciences*. 2014;71:4131-4148.
178. Munaron L. Intracellular calcium, endothelial cells and angiogenesis. *Recent patents on anti-cancer drug discovery*. 2006;1:105-19.

179. Namba K, Abe M, Saito S, Satake M, Ohmoto T, Watanabe T and Sato Y. Indispensable role of the transcription factor PEBP2/CBF in angiogenic activity of a murine endothelial cell MSS31. *Oncogene*. 2000;19:106-114.
180. Zuo WH, Zeng P, Chen X, Lu YJ, Li A and Wu JB. Promotive effects of bone morphogenetic protein 2 on angiogenesis in hepatocarcinoma via multiple signal pathways. *Scientific reports*. 2016;6:37499.
181. Tseng WP, Yang SN, Lai CH and Tang CH. Hypoxia induces BMP-2 expression via ILK, Akt, mTOR, and HIF-1 pathways in osteoblasts. *Journal of cellular physiology*. 2010;223:810-8.
182. Di Bartolo BA, Schoppet M, Mattar MZ, Rachner TD, Shanahan CM and Kavurma MM. Calcium and osteoprotegerin regulate IGF1R expression to inhibit vascular calcification. *Cardiovascular research*. 2011;91:537-545.
183. Benslimane-Ahmim Z, Heymann D, Dizier B, Lokajczyk A, Brion R, Laurendeau I, BiÈChe I, Smadja DM, Galy-Fauroux I, Colliec-Jouault S, Fischer AM and Boisson-Vidal C. Osteoprotegerin, a new actor in vasculogenesis, stimulates endothelial colony-forming cells properties. *Journal of Thrombosis and Haemostasis*. 2011;9:834-843.
184. Rochette L, Meloux A, Rigal E, Zeller M, Cottin Y and Vergely C. The role of osteoprotegerin in the crosstalk between vessels and bone: Its potential utility as a marker of cardiometabolic diseases. *Pharmacology & therapeutics*. 2018;182:115-132.
185. Benslimane-Ahmim Z, Poirier F, Delomenie C, Lokajczyk A, Grelac F, Galy-Fauroux I, Mohamedi A, Fischer AM, Heymann D, Lutomski D and Boisson-Vidal C. Mechanistic study of the proangiogenic effect of osteoprotegerin. *Angiogenesis*. 2013;16:575-93.
186. Mokas S, Larivière R, Lamalice L, Gobeil S, Cornfield DN, Agharazii M and Richard DE. Hypoxia-inducible factor-1 plays a role in phosphate-induced vascular smooth muscle cell calcification. *Kidney International*. 2016;90:598-609.
187. Stempien-Otero A, Karsan A, Cornejo CJ, Xiang H, Eunson T, Morrison RS, Kay M, Winn R and Harlan J. Mechanisms of Hypoxia-induced Endothelial Cell Death: ROLE OF p53 IN APOPTOSIS. *Journal of Biological Chemistry*. 1999;274:8039-8045.
188. Lee MN, Hwang H-S, Oh S-H, Roshanzadeh A, Kim J-W, Song JH, Kim E-S and Koh J-T. Elevated extracellular calcium ions promote proliferation and migration of mesenchymal stem cells via increasing osteopontin expression. *Experimental & Molecular Medicine*. 2018;50:1-16.
189. Shroff R, Long DA and Shanahan C. Mechanistic insights into vascular calcification in CKD. *Journal of the American Society of Nephrology : JASN*. 2013;24:179-89.
190. Yu XJ, Xiao CJ, Du YM, Liu S, Du Y and Li S. Effect of hypoxia on the expression of RANKL/OPG in human periodontal ligament cells in vitro. *International journal of clinical and experimental pathology*. 2015;8:12929-35.
191. Tang Z-N, Zhang F, Tang P, Qi X-W and Jiang J. Hypoxia induces RANK and RANKL expression by activating HIF-1α in breast cancer cells. *Biochemical and Biophysical Research Communications*. 2011;408:411-416.
192. Langenfeld EM and Langenfeld J. Bone Morphogenetic Protein-2 Stimulates Angiogenesis in Developing Tumors¹1NIH K22 grant CA91919-01A1 and UMDNJ Foundation to J. Langenfeld. *Molecular Cancer Research*. 2004;2:141.
193. Bouletreau PJ, Warren SM, Spector JA, Peled ZM, Gerrets RP, Greenwald JA and Longaker MT. Hypoxia and VEGF up-regulate BMP-2 mRNA and protein expression in microvascular endothelial cells: implications for fracture healing. *Plastic and reconstructive surgery*. 2002;109:2384-97.

194. Di Bartolo BA, Cartland SP, Harith HH, Bobryshev YV, Schoppet M and Kavurma MM. TRAIL-deficiency accelerates vascular calcification in atherosclerosis via modulation of RANKL. *PloS one*. 2013;8:e74211.
195. Ducy P, Zhang R, Geoffroy V, Ridall AL and Karsenty G. Osf2/Cbfa1: a transcriptional activator of osteoblast differentiation. *Cell*. 1997;89:747-54.
196. Herrmann J, Babic M, Tölle M, van der Giet M and Schuchardt M. Research Models for Studying Vascular Calcification. *International journal of molecular sciences*. 2020;21:2204.
197. Bishop PD, Feiten LE, Ouriel K, Nassoiy SP, Pavkov ML, Clair DG and Kashyap VS. Arterial Calcification Increases in Distal Arteries in Patients with Peripheral Arterial Disease. *Annals of Vascular Surgery*. 2008;22:799-805.
198. Ozaki Y, Koide M, Furuya Y, Ninomiya T, Yasuda H, Nakamura M, Kobayashi Y, Takahashi N, Yoshinari N and Udagawa N. Treatment of OPG-deficient mice with WP9QY, a RANKL-binding peptide, recovers alveolar bone loss by suppressing osteoclastogenesis and enhancing osteoblastogenesis. *PLOS ONE*. 2017;12:e0184904.
199. Nakamura M, Udagawa N, Matsuura S, Mogi M, Nakamura H, Horiuchi H, Saito N, Hiraoka BY, Kobayashi Y, Takaoka K, Ozawa H, Miyazawa H and Takahashi N. Osteoprotegerin Regulates Bone Formation through a Coupling Mechanism with Bone Resorption. *Endocrinology*. 2003;144:5441-5449.
200. Giallauria F, Vigorito C, Ferrara N and Ferrucci L. Cardiovascular Calcifications in Old Age: Mechanisms and Clinical Implications. *Current Translational Geriatrics and Experimental Gerontology Reports*. 2013;2:255-267.
201. Tintut Y, Patel J, Territo M, Saini T, Parhami F and Demer Linda L. Monocyte/Macrophage Regulation of Vascular Calcification In Vitro. *Circulation*. 2002;105:650-655.
202. Pazár B, Ea H-K, Narayan S, Kolly L, Bagnoud N, Chobaz V, Roger T, Lioté F, So A and Busso N. Basic Calcium Phosphate Crystals Induce Monocyte/Macrophage IL-1β Secretion through the NLRP3 Inflammasome In Vitro. *The Journal of Immunology*. 2011;186:2495.
203. Rokosova B and Peter Bentley J. Effect of calcium on cell proliferation and extracellular matrix synthesis in arterial smooth muscle cells and dermal fibroblasts. *Experimental and Molecular Pathology*. 1986;44:307-317.
204. Gross P, Six I, Kamel S and Massy ZA. Vascular Toxicity of Phosphate in Chronic Kidney Disease
– Beyond Vascular Calcification –. *Circulation Journal*. 2014;78:2339-2346.
205. Rochette L, Meloux A, Rigal E, Zeller M, Cottin Y and Vergely C. The Role of Osteoprotegerin and Its Ligands in Vascular Function. *International journal of molecular sciences*. 2019;20:705.
206. Ledebur HC and Parks TP. Transcriptional regulation of the intercellular adhesion molecule-1 gene by inflammatory cytokines in human endothelial cells. Essential roles of a variant NF-kappa B site and p65 homodimers. *The Journal of biological chemistry*. 1995;270:933-43.
207. van de Stolpe A and van der Saag PT. Intercellular adhesion molecule-1. *Journal of molecular medicine (Berlin, Germany)*. 1996;74:13-33.
208. Shu HB, Agranoff AB, Nabel EG, Leung K, Duckett CS, Neish AS, Collins T and Nabel GJ. Differential regulation of vascular cell adhesion molecule 1 gene expression by specific NF-kappa B subunits in endothelial and epithelial cells. *Mol Cell Biol*. 1993;13:6283-9.
209. Deshmane SL, Kremlev S, Amini S and Sawaya BE. Monocyte chemoattractant protein-1 (MCP-1): an overview. *J Interferon Cytokine Res*. 2009;29:313-326.
210. Carr MW, Roth SJ, Luther E, Rose SS and Springer TA. Monocyte chemoattractant protein 1 acts as a T-lymphocyte chemoattractant. *Proc Natl Acad Sci U S A*. 1994;91:3652-3656.
211. New SEP and Aikawa E. Molecular imaging insights into early inflammatory stages of arterial and aortic valve calcification. *Circulation research*. 2011;108:1381-1391.

212. New Sophie EP and Aikawa E. Role of Extracellular Vesicles in De Novo Mineralization. *Arteriosclerosis, Thrombosis, and Vascular Biology*. 2013;33:1753-1758.
213. McCarthy GM, Augustine JA, Baldwin AS, Christopherson PA, Cheung HS, Westfall PR and Scheinman RI. Molecular mechanism of basic calcium phosphate crystal-induced activation of human fibroblasts. Role of nuclear factor kappab, activator protein 1, and protein kinase c. *The Journal of biological chemistry*. 1998;273:35161-9.
214. Buendía P, Montes de Oca A, Madueño JA, Merino A, Martín-Malo A, Aljama P, Ramírez R, Rodríguez M and Carracedo J. Endothelial microparticles mediate inflammation-induced vascular calcification. *The FASEB Journal*. 2014;29:173-181.
215. Sánchez-Duffhues G, García de Vinuesa A, van de Pol V, Geerts ME, de Vries MR, Janson SG, van Dam H, Lindeman JH, Goumans MJ and Ten Dijke P. Inflammation induces endothelial-to-mesenchymal transition and promotes vascular calcification through downregulation of BMPR2. *The Journal of pathology*. 2019;247:333-346.
216. Ding J, Ghali O, Lencel P, Broux O, Chauveau C, Devedjian JC, Hardouin P and Magne D. TNF-alpha and IL-1beta inhibit RUNX2 and collagen expression but increase alkaline phosphatase activity and mineralization in human mesenchymal stem cells. *Life sciences*. 2009;84:499-504.
217. Gilbert L, He X, Farmer P, Rubin J, Drissi H, van Wijnen AJ, Lian JB, Stein GS and Nanes MS. Expression of the Osteoblast Differentiation Factor RUNX2 (Cbfa1/AML3/Pebp2αA) Is Inhibited by Tumor Necrosis Factor-α. *Journal of Biological Chemistry*. 2002;277:2695-2701.
218. Ye X, Huang H, Zhao N, Zhang J and Yang P. Inhibition of Runx2 signaling by TNF-α in ST2 murine bone marrow stromal cells undergoing osteogenic differentiation. *In Vitro Cell Dev Biol Anim*. 2016;52:1026-1033.
219. Zhang B, Ouyang P, Chen Y, Lai WY, Xie JG and Xu DL. [Tumor necrosis factor-alpha regulates the proliferation and syndecan-4 expression of human umbilical vein endothelial-like cells cultured in vitro]. *Nan fang yi ke da xue xue bao = Journal of Southern Medical University*. 2007;27:496-8.
220. Chinetti-Gbaguidi G, Daoudi M, Rosa M, Vinod M, Louvet L, Copin C, Fanchon M, Vanhoutte J, Derudas B, Belloy L, Haulon S, Zawadzki C, Susen S, Massy ZA, Eeckhoute J and Staels B. Human Alternative Macrophages Populate Calcified Areas of Atherosclerotic Lesions and Display Impaired RANKL-Induced Osteoclastic Bone Resorption Activity. *Circ Res*. 2017;121:19-30.
221. New Sophie EP, Aikawa E and Towler Dwight A. Molecular Imaging Insights Into Early Inflammatory Stages of Arterial and Aortic Valve Calcification. *Circulation Research*. 2011;108:1381-1391.
222. Aikawa E, Nahrendorf M, Figueiredo J-L, Swirski Filip K, Shtatland T, Kohler Rainer H, Jaffer Farouc A, Aikawa M and Weissleder R. Osteogenesis Associates With Inflammation in Early-Stage Atherosclerosis Evaluated by Molecular Imaging In Vivo. *Circulation*. 2007;116:2841-2850.
223. Demer Linda L and Tintut Y. Inflammatory, Metabolic, and Genetic Mechanisms of Vascular Calcification. *Arteriosclerosis, Thrombosis, and Vascular Biology*. 2014;34:715-723.
224. Byon CH, Sun Y, Chen J, Yuan K, Mao X, Heath JM, Anderson PG, Tintut Y, Demer LL, Wang D and Chen Y. Runx2-upregulated receptor activator of nuclear factor κB ligand in calcifying smooth muscle cells promotes migration and osteoclastic differentiation of macrophages. *Arteriosclerosis, thrombosis, and vascular biology*. 2011;31:1387-1396.
225. O'Neill WC, Han KH, Schneider TM and Hennigar RA. Prevalence of Nonatheromatous Lesions in Peripheral Arterial Disease. *Arteriosclerosis, Thrombosis, and Vascular Biology*. 2015;35:439-447.

226. Ohtake T, Oka M, Ikee R, Mochida Y, Ishioka K, Moriya H, Hidaka S and Kobayashi S. Impact of lower limbs' arterial calcification on the prevalence and severity of PAD in patients on hemodialysis. *Journal of Vascular Surgery*. 2011;53:676-683.
227. Kohn EC, Alessandro R, Spoonster J, Wersto RP and Liotta LA. Angiogenesis: role of calcium-mediated signal transduction. *Proceedings of the National Academy of Sciences of the United States of America*. 1995;92:1307-11.
228. Yao Y, Jumabay M, Ly A, Radparvar M, Cubberly MR and Boström KI. A role for the endothelium in vascular calcification. *Circulation research*. 2013;113:495-504.
229. Feno S, Butera G, Vecellio Reane D, Rizzuto R and Raffaello A. Crosstalk between Calcium and ROS in Pathophysiological Conditions. *Oxidative Medicine and Cellular Longevity*. 2019;2019:9324018.
230. Kim HW, Lin A, Guldberg RE, Ushio-Fukai M and Fukai T. Essential role of extracellular SOD in reparative neovascularization induced by hindlimb ischemia. *Circ Res*. 2007;101:409-19.
231. Kim Y-W and Byzova TV. Oxidative stress in angiogenesis and vascular disease. *Blood*. 2014;123:625-631.
232. Pescatore Luciana A, Gamarra Lionel F and Liberman M. Multifaceted Mechanisms of Vascular Calcification in Aging. *Arteriosclerosis, Thrombosis, and Vascular Biology*. 2019;39:1307-1316.
233. Byon CH, Javed A, Dai Q, Kappes JC, Clemens TL, Darley-Usmar VM, McDonald JM and Chen Y. Oxidative stress induces vascular calcification through modulation of the osteogenic transcription factor Runx2 by AKT signaling. *Journal of Biological Chemistry*. 2008;283:15319-15327.
234. Szulc P, Hofbauer LC, Heufelder AE, Roth S and Delmas PD. Osteoprotegerin Serum Levels in Men: Correlation with Age, Estrogen, and Testosterone Status1. *The Journal of Clinical Endocrinology & Metabolism*. 2001;86:3162-3165.
235. Zannettino ACW, Holding CA, Diamond P, Atkins GJ, Kostakis P, Farrugia A, Gamble J, To LB, Findlay DM and Haynes DR. Osteoprotegerin (OPG) is localized to the Weibel-Palade bodies of human vascular endothelial cells and is physically associated with von Willebrand factor. *Journal of cellular physiology*. 2005;204:714-723.
236. Tsapournioti S, Mylonis I, Hatziefthimiou A, Ioannou MG, Stamatiou R, Koukoulis GK, Simos G, Molyvdas PA and Paraskeva E. TNFα induces expression of HIF-1α mRNA and protein but inhibits hypoxic stimulation of HIF-1 transcriptional activity in airway smooth muscle cells. *Journal of cellular physiology*. 2013;228:1745-53.
237. Jung Y, Isaacs JS, Lee S, Trepel J, Liu ZG and Neckers L. Hypoxia-inducible factor induction by tumour necrosis factor in normoxic cells requires receptor-interacting protein-dependent nuclear factor kappa B activation. *The Biochemical journal*. 2003;370:1011-7.
238. Cai J, Pardali E, Sánchez-Duffhues G and ten Dijke P. BMP signaling in vascular diseases. *FEBS Letters*. 2012;586:1993-2002.
239. Collett GDM and Canfield AE. Angiogenesis and Pericytes in the Initiation of Ectopic Calcification. *Circulation Research*. 2005;96:930-938.
240. Jia J, Zhou H, Zeng X and Feng S. Estrogen stimulates osteoprotegerin expression via the suppression of miR-145 expression in MG-63 cells. *Mol Med Rep*. 2017;15:1539-1546.